

Thesis for the
Master's degree in Chemistry

Åsmund Kaupang

**Intramolecular
C-H Insertion Reactions
of α -Bromodiazacetamides**

60 study points

DEPARTMENT OF CHEMISTRY
Faculty of mathematics and natural sciences
UNIVERSITY OF OSLO 07/2010



to all
who share
their knowledge

I would like to take this opportunity to record here my belief that one should take a minimum of care and preparation over first experiments. If they are unsuccessful one is not then discouraged since many possible reasons for failure can be thought of, and improvements can be made. Much can often be learned by the repetition under different conditions, even if the desired result is not obtained. If every conceivable precaution is taken at first, one is often too discouraged to proceed at all.

Biochemist and Nobel Laureate in chemistry for his contribution to the invention of partition chromatography, Archer John Porter Martin (1910 – 2002) in his Nobel Prize Lecture, 1952.

Contents

Contents	vii
Abstract	xiii
Abbreviations and acronyms	xv
I Introduction	1
1 Diazo compounds as precursors for carbenes/carbenoids	3
1.1 Electrophilic diazoalkane substitution	5
1.2 Halogenation of diazo compounds	6
1.3 Halogenation of α -diazoacetamides	7
2 The carbene/carbenoid route to β-lactams	11
2.1 Carbene types and philicities	11
2.2 Metal carbene complexes and transition metal catalysis of diazo compounds	14
2.3 Dirhodium(II) catalysts - morphologies and syntheses	15
2.4 The C–H insertion reaction - mechanism and selectivity	18
II Experimental Results and Discussion	25
3 Synthesis of α-diazoacetamides	27
3.1 The choice of synthetic strategy	28
3.2 Experimental results	31
3.3 Modifications to the Toma procedure	33
3.4 Results of the modifications	34
3.5 The precipitated TMG · HO ₂ S–C ₆ H ₄ CH ₃ /TMG · HO ₃ S–C ₆ H ₄ CH ₃	35

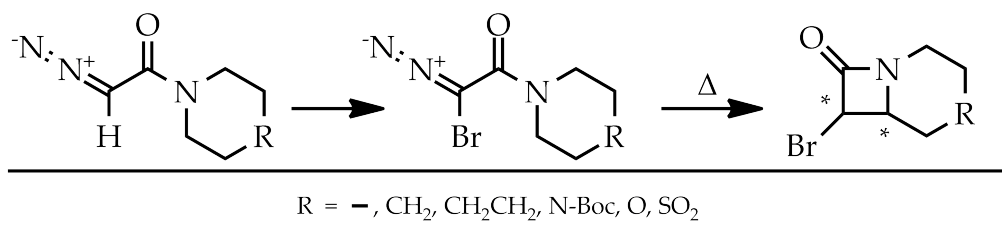
3.6	Previously unreported α -diazoacetamides	37
4	The synthesis and reactivity of α-halodiazoacetamides	41
4.1	First impressions	41
4.2	Optimization studies	43
4.3	Results of the thermolysis of 1d-6d and 8d	44
4.4	A comparison of the thermolytic and catalytic reactions, employing three prototypical transition metal catalysts	49
4.5	Synthesis and thermolysis of α -chloro- and α -iodo- 4c	50
4.6	The scope of the thermolysis reaction beyond the intramolecular C-H insertions	51
5	A synthetic outlook for the α-bromo-β-lactams	53
5.1	Polymer-supported <i>N</i> -halo reagents	53
5.2	Coupling with indole structures	54
III	Experimental Procedures and Physical Data	57
6	General introduction to the experimental section	59
7	Synthesis of <i>N</i>-bromo compounds and <i>N,N'</i>-ditosylhydrazine	61
7.1	<i>N</i> -bromo-2-pyrrolidone	61
7.2	<i>N</i> -bromosuccinimide	62
7.3	<i>N</i> -bromophthalimide	63
7.4	<i>N</i> -bromosaccharin	64
7.5	<i>N,N'</i> -ditosylhydrazine	65
8	α-bromoacetamides	69
8.1	2-bromo-1-(pyrrolidin-1-yl)ethanone (1b)	69
8.2	2-bromo-1-(piperidin-1-yl)ethanone (2b)	70
8.3	1-(azepan-1-yl)-2-bromoethanone (3b)	72
8.4	<i>tert</i> -butyl 4-(2-bromoacetyl)piperazine-1-carboxylate (4b)	73
8.5	<i>N,N'</i> -bis(2-bromoacetyl)piperazine (5b)	74
8.6	2-bromo-1-morpholinoethanone (6b)	75
8.7	2-bromo-1-thiomorpholinoethanone (7b)	76

8.8	2-bromo-1-(1,1-dioxidothiomorpholino)ethanone (8b)	77
9	α-diaoacetamides	79
9.1	2-diazo-1-(pyrrolidin-1-yl)ethanone (1c)	79
9.2	2-diazo-1-(piperidin-1-yl)ethanone (2c)	82
9.3	1-(azepan-1-yl)-2-diazoethanone (3c)	85
9.4	<i>tert</i> -butyl 4-(2-diazoacetyl)piperazine-1-carboxylate (4c)	87
9.5	<i>N,N'</i> -bis(2-diazoacetyl)piperazine (5c)	90
9.6	2-diazo-1-morpholinoethanone (6c)	93
9.7	2-diazo-1-(1,1-dioxido-4-thiomorpholinyl)ethanone (8c)	95
9.8	1,1,3,3-tetramethylguanidine <i>p</i> -toluenesulfinate	97
9.9	1,1,3,3-tetramethylguanidine <i>p</i> -toluenesulfonate	98
10	β-lactams	99
10.1	6-bromo-1-azabicyclo[3.2.0]heptan-7-one (1e)	101
10.2	7-bromo-1-azabicyclo[4.2.0]octan-8-one (2e)	101
10.3	8-bromo-1-azabicyclo[5.2.0]nonan-9-one (3e)	102
10.4	<i>tert</i> -butyl 7-bromo-8-oxo-1,4-diazabicyclo[4.2.0]octane-4-carboxylate (4e)	104
10.5	7-bromo-4-oxa-1-azabicyclo[4.2.0]octan-8-one (6e)	104
10.6	7-bromo-4-thia-1-azabicyclo[4.2.0]octan-8-one 4,4-dioxide (8e) . .	105
11	Synthesis of the methacrylonitrile copolymers	107
11.1	General experimental procedure for the free radical suspension copolymerization reactions	107
12	Synthesis of the dirhodium(II) catalysts	109
12.1	Tetrakis μ -caprolactamato dirhodium(II)	109
12.2	<i>cis-M/P</i> -Rh ₂ (μ -O ₂ CCH ₃) ₂ [Ph ₂ P(C ₆ H ₄)] ₂ (CH ₃ CN) ₂	110
13	Purification of the dirhodium(II) catalysts	113
13.1	The application of methacrylonitrile copolymer beads in the purification of dirhodium(II) catalysts	114
	References & Notes	119

IV Appendix	127
Contents of Appendix	129
14 NMR Spectra	135
14.1 <i>N</i> -bromo-2-pyrrolidone	136
14.2 <i>N</i> -bromophthalimide	138
14.3 <i>N,N'</i> -ditosylhydrazine	139
14.4 2-bromo-1-(pyrrolidin-1-yl)ethanone	141
14.5 2-bromo-1-(piperidin-1-yl)ethanone	143
14.6 1-(azepan-1-yl)-2-bromoethanone	145
14.7 <i>tert</i> -butyl 4-(2-bromoacetyl)piperazine-1-carboxylate	148
14.8 <i>N,N'</i> -bis(2-bromoacetyl)piperazine	150
14.9 2-bromo-1-morpholinoethanone	152
14.10 2-bromo-1-(1,1-dioxidothiomorpholino)ethanone	154
14.11 2-diazo-1-(pyrrolidin-1-yl)ethanone	156
14.12 2-diazo-1-(piperidin-1-yl)ethanone	159
14.13 1-(azepan-1-yl)-2-diazoethanone	162
14.14 <i>tert</i> -butyl 4-(2-diazoacetyl)piperazine-1-carboxylate	165
14.15 <i>N,N'</i> -bis(2-diazoacetyl)piperazine	167
14.16 2-diazo-1-morpholinoethanone	169
14.17 2-diazo-1-(1,1-dioxido-4-thiomorpholinyl)ethanone	172
14.18 1,1,3,3-tetramethylguanidine sulfinate (and sulfonate)	174
14.19 Crude 6-bromo-1-azabicyclo[3.2.0]heptan-7-one	175
14.20 Crude 7-bromo-1-azabicyclo[4.2.0]octan-8-one - NBS	176
14.21 Crude 7-bromo-1-azabicyclo[4.2.0]octan-8-one - NBP	177
14.22 Crude 8-bromo-1-azabicyclo[5.2.0]nonan-9-one	178
14.23 Crude <i>tert</i> -butyl 7-bromo-8-oxo-1,4-diazabicyclo[4.2.0]octane-4-carboxylate	179
14.24 Crude 7-bromo-4-oxa-1-azabicyclo[4.2.0]octan-8-one	180
14.25 Crude 7-bromo-4-thia-1-azabicyclo[4.2.0]octan-8-one 4,4-dioxide .	181

14.26	Crude; carbene dimer from catalytic decomposition of 2d with Cu(acac) ₂	182
14.27	7-bromo-1-azabicyclo[4.2.0]octan-8-one	183
14.28	1-(piperidin-1-yl)-2-tosylethanone	184
14.29	2,2-dibromo-1-(piperidin-1-yl)ethanone	186
14.30	<i>cis</i> -8-bromo-1-azabicyclo[5.2.0]nonan-9-one	188
14.31	<i>trans</i> -8-bromo-1-azabicyclo[5.2.0]nonan-9-one	190
14.32	<i>cis</i> -2,2-Tetrakis μ -caprolactamato dirhodium(II)	192
14.33	<i>cis</i> - <i>M/P</i> -Rh ₂ (μ -O ₂ CCH ₃) ₂ [Ph ₂ P(C ₆ H ₄)] ₂ (CH ₃ CN) ₂	193
14.34	Crude; thermolysis of α -Br-EDA in neat styrene	197
14.35	Thermolysis product of α -Br-EDA in neat styrene (w/ internal standard)	198
14.36	Crude; thermolysis of (4d) in neat styrene	199
15	X-ray Diffraction Data	201
15.1	<i>N,N'</i> -bis(2-diazoacetyl)piperazine (5c)	202
15.2	2-diazo-1-(1,1-dioxido-4-thiomorpholinyl)ethanone (8c)	203
15.3	TMG <i>p</i> -toluenesulfinate	204
15.4	TMG <i>p</i> -toluenesulfonate	205
15.5	<i>tert</i> -butyl 4-(2-diazoacetyl)piperazine-1-carboxylate (4c)	206

Abstract



A synthesis of α -bromodiazacetamides derived from cyclic, symmetric amines is presented. The brominated α -diazacetamides constitute a new entry to the range of known α -diazacetamides. Their thermolysis, at ambient temperature, produce α -bromocarbene amides which undergo intramolecular C-H insertion to form α -bromo bicyclic β -lactams.

The synthesis of the α -bromodiazacetamides has been optimized with respect to base and halogen source, and the scope of the intramolecular C-H insertion reaction investigated by varying the ring size and substitution pattern of the cyclic amine precursors.

Abbreviations and acronyms

AMBN	2,2'-Azobis-(2-methylbutyronitrile)
AN	Acrylonitrile
CCD	Charge-coupled device
DABCO	1,4-Diazobicyclooctane
DBU	1,8-Diazabicyclo-[5.4.0]-undec-7-ene
DCC	Dicyclohexylcarbodiimide
DCU	Dicyclohexylurea
DEPT	Distortionless Enhancement by Polarization Transfer
DFT	Density Functional Theory
DIPEA	<i>N,N'</i> -Diisopropylethylamine
DMSO	Dimethyl Sulfoxide
DVB	Divinylbenzene
EDA	Ethyl Diazoacetate
EI	Electron Impact Ionization
ESI	Electrospray Ionization
FID	Free Induction Decay
FT-ICR	Fourier Transform Ion Cyclotron Resonance
FT-IR	Fourier Transform Infrared Spectroscopy
FTMS	Fourier Transform Mass Spectroscopy
GPCR	G-Protein Coupled Receptor
HMQC	Heteronuclear Multiple Quantum Coherence
HPLC	High-performance Liquid Chromatography
HRMS	High Resolution Mass Spectrometry
LDA	Lithium diisopropylamide
MAN	Methacrylonitrile
MS	Mass Spectrometry
NBP	<i>N</i> -Bromophthalimide
NBPy	<i>N</i> -Bromo-2-pyrrolidone
NBS	<i>N</i> -Bromosuccinimide
NBSa	<i>N</i> -Bromosaccharin
NMR	Nuclear Magnetic Resonance
<i>p</i>-ABSA	<i>p</i> -Acetamidobenzenesulfonyl hydrazide
PTFE	Polytetrafluoroethylene
rpm	Revolutions Per Minute
TBD	1,5,7-Triazabicyclo[4.4.0]dec-1-ene
THF	Tetrahydrofuran
TLC	Thin Layer Chromatography
TMG	1,1,3,3-Tetramethylguanidine
TOF	Time Of Flight
XRD	X-Ray Diffraction

Part I.

Introduction

1. Diazo compounds as precursors for carbenes/carbenoids

The first preparation and isolation of ethyl diazoacetate by Theodor Curtius (1857–1928) a little over 125 years ago, marked the beginning of the era of diazo compounds as reagents in synthetic organic chemistry.^{1a,2} It would, however, take another 50 years to merely determine that the structure of the N_2-CR_2 moiety was indeed linear.^{1b} A more thorough study of the electron density distribution behind this geometry and the non-integral C–N and N–N bonds was first made possible by modern spectroscopic methods and quantum-mechanical theory.

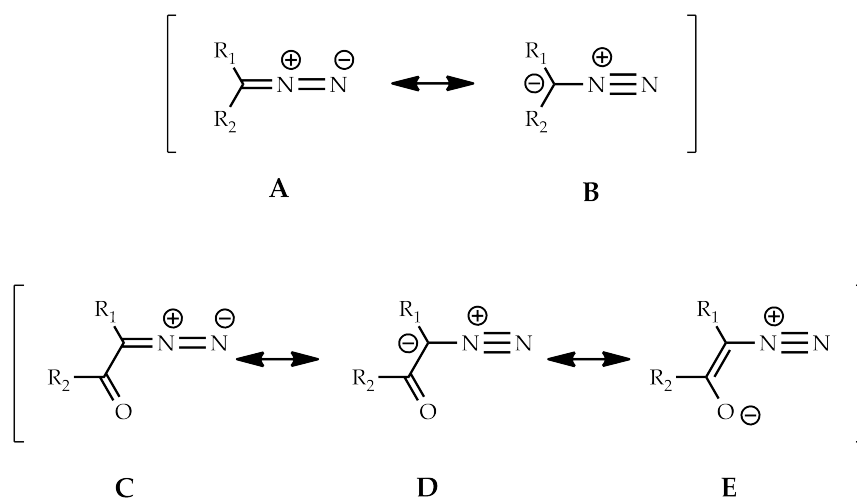


Figure 1.1.: Electron distribution of α -diazocarbonyl compounds

The resonance hybrid of the diazo group is best described by the structures **A** and **B** in figure 1.1, in which the largest contribution is made by **B**. In a similar

manner, the diazocarbonyl compounds have three major resonance forms **C**, **D** and **E**, here represented by their (*Z*)-rotamer. The contribution of structure **E** is major for α -diazocarbonyl compounds^{1b} ($R_1 = H$) and is larger for amides ($R_2 = NR_2$) than for esters ($R_2 = OR$).^{1c}

Contrary to this, the most common way of depicting diazo compounds in the literature is by means of structures of the type **A** or **C**, and most often for α -diazocarbonyl compounds, they are drawn as the (*E*)-rotamer. For α -diazoacetic esters in $CDCl_3$ -solution, the (*Z*)/(*E*)-ratio at 223 K was found to be ~1.2:1.^{1d} Moreover, the α -diazoacetamides characterized by X-ray crystallography in this work, crystallized as their (*Z*)-rotamers. As such, the α -diazoacetamides will be represented by their (*Z*)-rotamer and, for the sake of congruence with the literature, the resonance forms **A/C** will be used throughout this text.

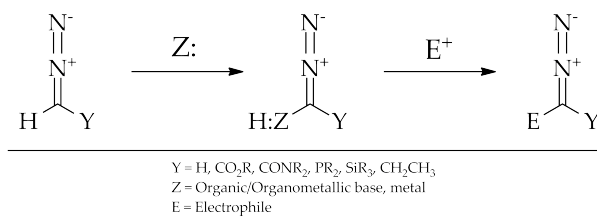
Diazo compounds have gained popularity as nitrogenous precursors of carbenes/carbenoids in synthetic organic chemistry. The potent reactivity of carbenic species provides access to a host of transformations from diazo precursors which are often relatively stable and easy to handle. Historically, a common use of diazo compounds is in the formation of methyl esters from acids with diazomethane. Apart from the advantage of the reaction being highly selective, the lability of diazomethane and the occurrence of explosions^{1e} have possibly swayed workers from considering the use of any diazo compound when designing their synthetic schemes. This lability, the propensity towards dediazotization, is however influenced by the substituents on the carbon bearing the diazo group to such an extent that the commercially available ethyl diazo acetate, has been deemed safe by rigorous testing^{1f,1g} and is frequently employed by today's workers. As well as imparting stability against nitrogen extrusion, the carbonyl group broadens the range of transformations relevant to α -diazocarbonyl compounds as compared to diazomethane.

More generally, the reactions in which diazo compounds take part can be categorized on the basis of whether or not the reaction pathway involves the extrusion of dinitrogen and subsequent formation of a carbene/carbenoid. For α -diazocarbonyl compounds, reactions of the type where dinitrogen is lost include: β -hydride elimination, ylide formation and subsequent pathways,

aromatic C–H insertion, aromatic cycloaddition (Büchner reaction), cycloprope-
nation, cyclopropanation, C–H and Y–H insertion (Y = O, N, S, Si) and
Wolff-rearrangement and subsequent pathways.³ On the other hand, among
the reactions of the type that does not involve the loss of dinitrogen, the most
important are 1,3-dipolar cycloadditions (diazo compounds are among the major
classes of known 1,3-dipoles) and electrophilic substitution reactions (*vide infra*).

Although most of the above mentioned transformations are relevant to
 α -diazoacetamides as a substance class, this work is primarily concerned with
the intramolecular C–H insertion reactions of the α -bromodiazoacetamides
prepared from the corresponding α -diazoacetamides. The investigated method
of preparation of the α -halodiazoacetamides is an example of electrophilic
diazoalkane substitution,⁴ which is the topic of the next section.

1.1. Electrophilic diazoalkane substitution



The $\text{N}_2\text{—CHR}$ group take part in reactions with a wide range of electrophiles
in which the diazo function remains intact.⁴ Among the transformations are
substitutions of the diazomethyl hydrogen atom for electrophiles based on
silicon,⁵ phosphorous,⁶ boron,⁷ nitrogen (NO_2^+),⁸ sulfur⁹ or halogens,¹⁰ as well
as carbon in aldol reactions with aldehydes,¹¹ ketones¹² and imines.¹³

An organic or organometallic base is usually required to generate an acid-base
complex or metallated derivative suitable for a given reaction. In aldol reactions
the use of catalytic or substoichiometric amounts of base (catalyst) is commonly
achieved, in some cases with recycling of the catalyst.^{13e}

Bases of several strengths have been applied successfully, among them
members of the amine, amidine and guanidine families, as well as alkyl lithium,

lithium amide and hydroxide bases *e.g.* diisopropylethyl amine (DIPEA),^{5f} 1,8-diazabicyclo-[5.4.0]-undec-7-ene (DBU),^{11d,13a} tetramethyl guanidine (TMG),^{11e} lithium diisopropyl amide (LDA),^{12c} *n*-butyl lithium (*n*-BuLi)^{5a,12a} and rubidium hydroxide (RbOH).^{11c}

α -Diazoacetamides are, under similar conditions, reported to undergo electrophilic substitutions with silicon^{5c} and carbon in aldol reactions with aldehydes^{11a} and imines,^{13b,13c} in reminiscence to the reactions reported for diazoacetates, attesting to the similar electronic properties if the two in this reaction.

1.2. Halogenation of diazo compounds

Historically, the direct substitution of the diazomethyl hydrogen atom for a halogen atom is only scarcely reported. The low temperature ($-100\text{ }^{\circ}\text{C}$) chlorination and bromination of diazomethane^{10a,10b} and diazopropane^{10e} were accomplished with the corresponding *t*-butyl halides. The resulting α -halodiazoalkanes were sensitive compounds, decomposing photolytically in visible light above $-65\text{ }^{\circ}\text{C}$ and thermolytically above $-40\text{ }^{\circ}\text{C}$.

The first syntheses of α -halodiazoacetic esters were reported by Gerhart and Schöllkopf *et al.* in the late 1960s, who reacted the mercury derivative of ethyl diazoacetate (EDA) with sources of electrophilic halogen (SO_2Cl_2 , Br_2 or I_2). This route allowed the workers to study the properties of the α -halo ethyl diazoacetates and the reactivity of their photolytically derived carbenes.^{10c,10d,10f}

Some ten years later Regitz *et al.* reported the syntheses of α -halodiazomethyl phosphonic acid dimethyl ester and an α -halodiazomethyl diphenyl phosphoxide, employing a similar strategy, starting from the silver derivatives of the respective diazoaceto compounds.^{10g}

More recently, a direct halogenation of ethyl diazoacetate at $0\text{ }^{\circ}\text{C}$ was published by Bonge *et al.*,^{10h} which employs the amidine base 1,8-diazabicyclo-[5.4.0]-undec-7-ene (DBU) and *N*-bromosuccinimide (NBS) as the halogen source. The reaction proceeds to completion within minutes of the addition of the halogen source to a solution of EDA and DBU in dichloromethane. The work-up yielded the α -halo EDA in dichloromethane solution, which could be used directly in

further reactions or the solvent could be changed to a higher boiling solvent appropriate for the chemistry to follow. In the publication, toluene was added and the dichloromethane evaporated at 0 °C using a rotary evaporator, before submitting the α -halo EDA to dirhodium(II) catalyzed cyclopropanation with styrene. The halogenation of higher esters using this method has not been reported, but is currently being studied in our group.

1.3. Halogenation of α -diazacetamides

There are to date no reports in the literature¹⁵ of α -halodiazoacetamides as a substance class, suggesting that the electrophilic halogenation of a α -diazacetamide has not been investigated. Thus, to create an extension of the current methodology to encompass the halogenation of α -diazacetamides, it seemed prudent to investigate the effect of alternative bases and sources of halogen, alongside the reported combination, on the formation of the α -halodiazoacetamides.

1.3.1. Bases

Base	p <i>K_a</i>	Solvent
DABCO	8.5	DMSO ^{14a}
TMG	15.5	THF ^{14d}
DBU	16.9	THF ^{14d}
TBD	21.0	THF ^{14d}

Looking at the bases employed in aldol reactions with α -diazocarbonyl compounds, the guanidine base 1,1,3,3-tetramethylguanidine (TMG)^{11e} is a base of similar structure and base strength. What also makes TMG an interesting alternative, is the postulated intermediacy, in bromolactonization reactions, of an *N*-bromo-TMG cation as the active catalyst.^{16c} This notion was substantiated some time later by the isolation and crystallographic characterization of an *N*-bromo amidine which proved to be an active catalyst in the same reaction.^{17a} In this vein, the diamine base 1,4-diazabicyclooctane (DABCO) should also be of interest as it is reported to form a stable adduct with *N*-bromosuccinimide^{16b} which in turn can be used for mild oxidations^{17b} (halogenation probably involved). Another highly basic member of the guanidine family, which is also bicyclic,

is 1,5,7-triazabicyclo[4.4.0]dec-1-ene (TBD). The bases are listed in order of increasing strength in table 1.1 on the previous page.

1.3.2. Halogenating agents

The halogenating agents that have been employed in the halogenation of diazo compounds are: molecular halogen,^{10c,10d} bromocyan,^{10g} *t*-butyl halides^{10b,10a,10e} and *N*-halo succinimides.^{10h} The *N*-halo succinimides are widely employed in organic synthesis as sources of electrophilic halogen as they present advantages like straightforward syntheses, ease of handling, storage stability and enhanced chemoselectivity over that of molecular halogen in certain transformations.^{18e} Many of these favourable characteristics can be extended to other *N*-halo imides, such as *N*-bromophthalimide (NBP), as well as to other sources of electrophilic halogen such as *N*-halo amides, *N*-halo sulfonamides, *N*-halo saccharins and *N*-halo disulfonimides.^{18f,18d} None of the latter have been investigated in the halogenation of diazo compounds.¹⁵

The activity of *N*-halo reagents in heterolytic (polar) reactions can reasonably be related to the stability of the resulting amide, imide or sulfonimide anion, resulting from the heterolytic cleavage of the N–halogen bond.^{18a,18c} In bromolactonization reactions, such a trend was observed, although it was not reflected in the yield of all the entries.^{18b} The authors proposed that the acid dissociation constant of the corresponding amide, imide or sulfonimide can indicate the polarity of the N–halogen bond and thus the propensity of a given reagent towards furnishing a halonium ion in a heterolytic reaction pathway. The acidities of relevant scaffolds from which to make *N*-halo reagents, have been listed in table 1.2.

Amide	pK_a (DMSO)	The ease with which the α -halodiazoacetates extrude nitrogen, reflected in their thermal lability (they decompose over hours at 0 °C), ^{10c,10h} is also an indicator of their lability towards acids. ¹⁹ The protonation of the basic, negatively charged carbon bearing the diazo group, is an expedient way to effect nitrogen
2-pyrrolidone	24.2 ^{14b}	
Succinimide	14.6 ^{14b}	
Phthalimide	13.4 ^{14c}	
Saccharin	4.0 ^{14b}	

Table 1.2.: Amide acidities

extrusion. This is indeed the intended pathway in acid-catalyzed cyclizations of diazoketones.^{27d} Not knowing the stability of α -halodiazoacetamides as a chemical species, raises the question of whether weak acids like the amides, imides and sulfonimides corresponding to the *N*-halo reagents, would have a detrimental effect on the produced α -halodiazoacetamides.

The results of the investigation of different bases and *N*-halo reagents in the halogenation of α -diazoacetamides, can be found in chapter 4 on page 41. The next chapter introduces carbenes/carbenoids, and discusses the position of the carbenic species derived from halogenated diazo compounds, before introducing transition metal catalysis and selectivity considerations in C-H insertion reactions.

2. The carbene/carbenoid route to β -lactams

2.1. Carbene types and philicities

A carbene is a divalent carbon atom with 6 electrons in its valence shell. For most carbenes this means an sp^2 -type hybridization, where two of the sp^2 hybrids are occupied by the substituents. The last electron pair can be distributed in the remaining non-bonding sp^2 hybrid and the p_y orbital. Carbenes thus possess the possibility of ground state spin multiplicity. There are four possible distributions of the two electrons with two possible spins in the two non-bonding orbitals. Of these four, the one which has two spin paired electrons in the sp^2 orbital, the orbital in plane with the substituents, and an empty p_y orbital, is the unexcited singlet carbene, which is most relevant to this work.²⁰ⁱ The sp^2 and p_y orbitals will be referred to as the σ and p_π orbitals in the rest of this text.

It has been shown that the interactions of the substituents with the carbene carbon σ and π orbitals, dictate which electronic state will be its ground state. In evaluating the carbenic species involved in this work, α -halocarbenes- and carbenoids, the conclusion is reached that they should be singlet carbenes. This is because the singlet state is favoured by a large energy difference between the p_π and the σ orbital. The π -donating interaction of the lone electron pairs on the halogen atom to the vacant p_π orbital is destabilizing, which increases the energy of the p_π orbital and thus the $p_\pi - \sigma$ gap.

Substituents of high electronegativity are found to stabilize the electron pair in the σ orbital through σ -electron withdrawal, which increases the orbitals s -character, thus lowering its energy. More importantly, the carbonyl (amide) group can stabilize the lone pair in the carbene σ orbital by an overlap with

the vacant p orbital of the carbonyl carbon which is in plane with the carbene σ orbital.²⁰ⁱ Similarly, the conclusion was reached by others, about the related α -halocarboethoxycarbenes derived from α -halodiazoacetic esters, that they are also singlet carbenes.^{10f} The stabilizing effect of the vacant p orbital of the carbonyl carbon on the electron pair in the carbene σ orbital, should be stronger in esters than in amides, owing to the presence of the lone electron pair on the amide nitrogen. This would indicate that the α -halocarbene esters are more stabilized than their corresponding α -halocarbene amides.

The electronic distribution of singlet carbenes make them inherent ambiphiles; one orbital has a nucleophilic non-bonding electron pair and the other is vacant and thus electrophile. One of the first carbenes known - methylene - is intensely electrophile (*vide infra*) and it was long believed that this was the only reactivity mode of the carbenes.^{20j} The much wider range of carbene philicities is the topic of the next section.

2.1.1. Reactivity and selectivity of carbenes

Some 50 years ago the simplest of the carbenes, methylene, was described by William von Eggers Doering as "... the most indiscriminate reagent known in organic chemistry." This description owed to the near statistical product ratio obtained upon photolysis of diazomethane in 2,3-dimethylbutane, with respect to 1° *vs.* 2° *vs.* 3° C–H insertion. A similar absence of chemoselectivity was observed upon photolysis of diazomethane in cyclohexene, with respect to cyclopropanation *vs.* 2° homoallylic *vs.* 2° allylic *vs.* vinylic C–H insertion.^{20b} The latter result was much unlike the selectivity with which :CCl₂ and :CBr₂ would cyclopropanate the double bond in cyclohexene,^{20a} let alone the observation that the rates of reaction of :CBr₂ increased with increasing olefin substitution.^{20c,20d} In other words, the substitution of the diazomethyl hydrogens for halogens, had a tremendous impact on the selectivity of the resulting carbene towards the available "nucleophiles" (olefins and C–H bonds). Over the next five decades several workers, among them Robert A. Moss,²¹ studied a number of heterocarbenes (carbenes with substituents other than H) and their relative rates of cyclopropanation of a standard set of olefins in order to quantitate the selectivity with which they reacted. Many of the works in question have

been reviewed by Moss.^{20j} Today, these results constitute a cornerstone in a more general understanding of the diverse reactivity profile of carbenes - from electrophilic through ambiphilic to nucleophilic.

Moss' scale of carbene philicity was based on the cyclopropanation of increasingly electron-rich olefins with electrophilic carbenes. The scale was later extended to include electron-poor olefins, as it became clear that carbenes like :C(OMe)_2 behave as nucleophiles, reacting at increasing rates with increasingly electron-deficient olefins. Many nucleophilic carbenes are known today, and in analogy to the cyclopropanation of electron-deficient olefins, selecting the correct substrate has made C–H insertion of nucleophilic carbenes possible.^{20h} The further discoveries of Arduengo^{20g} and Bertrand²⁰ⁱ of stable, isolable carbenes add to the impressive width of carbene reactivity. In summary, the diversity of transformations in which the divalent 6-electron carbon can take part, reinforces its fundamental importance in chemistry alongside carbanions and carbocations.

Carbenes can now be characterized in terms of either electrophilic selectivity or nucleophilic selectivity of which the former, for now, is the most frequently used. The above discussion delineates the context in which the α -halocarbonylcarbenes reside. As for the electrophilic selectivity of α -bromocarboethoxycarbene compared to the halocarbenes and bromophenylcarbene, it has been shown that it is among the least selective, which means it is among the most reactive. It is, however, more selective and less reactive than carboethoxycarbene.^{20f} Given that a C–H bond is a much poorer "nucleophile" than a double bond, the need for a correspondingly electrophilic carbene can possibly make use of this trait, given that other pathways are not available to the less discriminate carbene.

The carbenes that are complexed with other atoms during reaction, have gained the name carbenoids, owing to the influence of the complexation on their "natural" reactivity. The discussion around what is a real or "free" carbene is outside the scope of this text, but has been probed with interesting experimental techniques elsewhere.^{20e,20k} In carbenoids, the complexed atom is most often a transition metal. The transition metal carbene complexes and especially the dirhodium(II) complexes, are the topics of the next section.

2.2. Metal carbene complexes and transition metal catalysis of diazo compounds

The extrusion of nitrogen from a diazo compound, to generate a carbenic intermediate, can be effected thermally, photolytically, by protonation by a Brønsted acid or by coordination to a Lewis acid.¹⁹ The Lewis acid is often a transition metal, e.g. the powdered metal, a salt such as CuSO_4 , but more often, and of greater synthetic potential, a ligated transition metal catalyst.

The metal carbene complexes, are referred to as metal carbenoids, or simply carbenoids, to indicate their similar yet distinct reactivity as compared to that of the "free" carbenes, generated by photolysis or thermolysis. Through experimentation and computational studies, this reactivity difference has been observed and rationalized in terms of properties of the carbene and its precursor, and importantly, in terms of the properties of the metal and its ligands.^{25i,23a,23c}

The potential for strategically modulating the reactivity of a metal carbene complex, by the variation of the ligands bound to the metal, has inspired the input of considerable efforts to investigate and rationally design competent catalysts. The result of these efforts is a broadening of the synthetic utility of a given carbene precursor, e.g. a diazo compound, through the possibility to almost exclusively induce a given reaction path based on the choice of catalyst.^{22c,23b}

By today, the synthetic potential of carbene transfer reactions involving transition metal catalysts, has been demonstrated in most facets of carbene chemistry. Only in the area of C–H insertion reactions, impressive examples exist in which excellent chemo-, regio- and enantioselectivity has been achieved.^{22b,22f}

Members from nearly all the periodic groups of transition metals are featured in catalysts for carbenoid transformations, and a number of metals and catalyst morphologies have been employed in catalysts that are competent in carbene transfer reactions.^{22a} Among the catalysts that have had the greatest success to date, are those derived from ligated Cu^{2+} - and Rh_2^{4+} -cores.

The morphologies of the copper(II) catalysts depend on the structure, bite and number of ligands. Among the many notable copper(II) complexes are those

ligated by box-type ligands, which have found special utility in intermolecular N-H insertion reactions, where they have yielded α -carbonyl amines with excellent enantiomeric excesses.^{22e} Still, the catalysts that have received the most attention to this day with respect to carbenoid chemistry, are the dirhodium(II) catalysts. This work will attempt to employ prototypical dirhodium(II) catalysts in the intramolecular C-H insertion of α -halodiazoacetamides. Therefore, the following sections will discuss the morphology and synthesis of dirhodium(II) catalysts, before moving on to a discussion of selectivity in carbene/carbenoid C-H insertion reactions, with relevance to the ones attempted in this work.

2.3. Dirhodium(II) catalysts - morphologies and syntheses

A large diversity of dirhodium(II) complexes are reported in the literature,^{22d} and far from all have found use in catalysis involving diazo compounds. A collection of three prototypical dirhodium(II) catalysts relevant to catalytic reactions with diazo compounds, are shown in figure 2.1 on the following page. The homoleptic complexes share the common structural feature of four chemically equal ligands bridging the Rh-Rh bond, the bridging unit being typically a monoanionic three-atom bidentate group. The $\text{Rh}_2(\text{tfa})_4$ and the $\text{Rh}_2(\text{cap})_4$ are both examples of this. Complexes like $\text{Rh}_2(\text{OAc})_2(\text{pc})_2$ found use as catalysts in carbenoid chemistry years after the domains of the other families were established, although the complex had been known for some time.

The paddlewheel-like dirhodium(II) complexes, are neutral, 14 electron complexes with free coordination seats axially. These seats are made up of the $4d_z^2$ orbitals on the outer face of each rhodium atom, in the axis of the Rh-Rh single bond.^{24e} The Lewis acidities of the axial seats are influenced by the electronic properties of the bridging ligands as well as those of a ligand coordinated to one of the axial seats. Bridging ligands that are electron withdrawing increase the Lewis acidity, thus making $\text{Rh}_2(\text{tfa})_4$ a stronger Lewis acid than $\text{Rh}_2(\text{OAc})_4$, which in turn is more acidic than $\text{Rh}_2(\text{OAc})_2(\text{pc})_2$ (pc = orthometalated PPh_3) and $\text{Rh}_2(\text{cap})_4$.

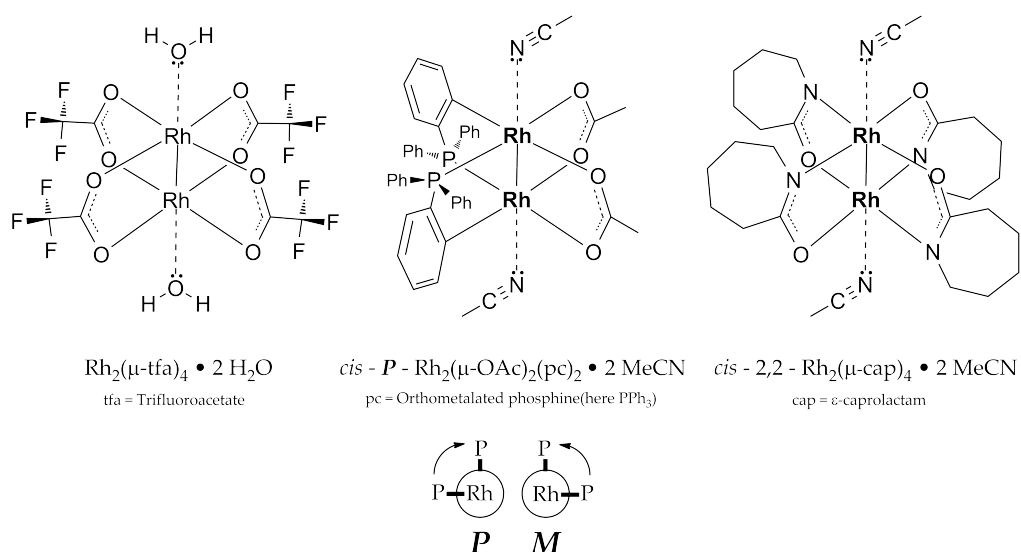


Figure 2.1.: Representatives from three dirhodium(II) catalyst families. Decreasing Lewis acidity from left to right.

The axial seats coordinate most Lewis bases, even weak ones like H_2O , which will be coordinated if the complex is exposed to air over longer periods of time. The more acidic $\text{Rh}_2(\text{tfa})_4$ and $\text{Rh}_2(\text{OAc})_4$ will even coordinate olefins in solution, whereas the remaining two will not.^{23a} The coordination of one axial ligand, decreases the rate at which the second seat is occupied.^{25g,25m} The Rh-L bond (L = axial ligand) is fairly labile with weaker donors, which are easily displaced. In example, axially coordinated acetonitrile molecules can be displaced by dissolving the complex in a weakly coordinating solvent like CH_2Cl_2 . Stronger donors are conversely not easily displaced, and since the axial seats are the site of reaction with the Lewis basic diazo carbon, strong Lewis bases will poison the catalyst, as they competitively inhibit the coordination of the diazo compound. Another distinct characteristic of axial ligation in dirhodium(II) complexes, is the colour the presence or absence of different axial ligands will impart on the complex - from brown through red and green to blue.

Historically the dirhodium(II) complexes have been synthesized either by the concomitant construction of the dirhodium core with ligands, or by the substitution of the ligands on an existing dirhodium(II) core. The reaction of $\text{RhCl}_3 \cdot 2\text{H}_2\text{O}$ with NaOAc in $\text{CH}_3\text{CO}_2\text{H}/\text{EtOH}$ yields $\text{Rh}_2(\text{OAc})_4$ ^{25a} – which together with $\text{Rh}_2(\text{tfa})_4$ are the most common substrates for ligand exchange

reactions. These exchange reactions are normally driven to completion utilizing azeotropic distillation from chlorobenzene or toluene in which the azeotrope with $\text{CH}_3\text{CO}_2\text{H}$ is distilled out of the flask or captured by a base in a Soxhlet-extractor thimble.^{25f,25n}

As alternatives to the removal the released acetic acid, the reaction of $\text{Rh}_2(\text{OAc})_4$ with an alkali metal salt of the ligand, as in the synthesis of $\text{Rh}_2(\text{py})_4$ (py = pyrazole),^{25b} or the reaction of $\text{Na}_4\text{Rh}_2(\text{CO}_3)_4$ and the ligand as a free carboxylic acid, will yield a tetraligated Rh_2^{4+} -core. The latter method was employed by McKerverey *et al.* to synthesize a series of dirhodium(II) carboxylates, both monodentate and bidentate.^{25e}

Another, perhaps surprising method, considering that in the starting material the Rh_2^{4+} -core is ligated by acetate groups, is to run the ligand exchange reaction in acetic acid. This technique was reported in the ligand exchange with arylphosphines^{25c,25d} and 1,8-naphthyridine.^{25k}

In the synthesis of the complex $\text{Rh}_2(\text{OAc})_2(\text{pc})_2$, by orthometalation of PPh_3 , only two acetates are exchanged and the phosphine ligands become positioned in a head-to-tail arrangement, that is, the phosphorous atoms are bound to each their rhodium atom. The resulting *cis*-configuration will, although the ligands are achiral, yield an axially chiral complex. The syntheses of orthometalated arylphosphine complexes thus afford racemic mixtures of enantiomers *M* and *P* (cf. figure 2.1 on the preceding page). If desirable, the remaining acetate ligands can be exchanged for monochiral carboxylate ligands (e.g. proline derivatives) yielding diastereomers, which can then be separated on common chromatographic media. To obtain the pure enantiomers *M* and *P*, the proline groups are then exchanged for acetate groups.^{25h} If the orthometalation is carried out with chiral phosphines, diastereomers result as well.^{25j}

In this work, the syntheses of $\text{Rh}_2(\text{OAc})_2(\text{pc})_2 \cdot 2 \text{MeCN}$ and $\text{Rh}_2(\text{cap})_4 \cdot 2 \text{MeCN}$ have been carried out so that these catalysts can be employed, in addition to the commercially available $\text{Rh}_2(\text{tfa})_4$, in the intramolecular C–H insertion reactions of α -halodiazoacetamides. The catalysts have been purified by a novel method which is described in detail in chapter 13 on page 113 in the experimental section.

In the next sections, the focus is turned to the mechanism and later the selectivity of C–H insertion reactions with carbenes and carbenoids.

2.4. The C–H insertion reaction - mechanism and selectivity

The experimental results that form the basis for Moss' selectivity concept for the heterocarbenes, have a parallel in the literature on the metal carbenoids. The dirhodium(II) catalysts possess an important feature; their ability to donate electron density to suitable orbitals on the carbon atom with which they are complexed. The result of this donation is a modulation of the selectivity inherent to a given carbene, in contrast to its "free" carbene behaviour. In order to discuss this concept it is prudent to look at the general electronic trends among the families of dirhodium(II) complexes. The electron withdrawal of the ligands, that is, the electronegativity of the elements in the bridging group and the rest of the ligand, and more rarely the electron withdrawal of a group in resonance with the Rh_2^{4+} -core, decrease the electron density available for donation. The dirhodium(II) perfluorocarboxylates are thus the most electron deficient, and those least capable of donation of electron density. Moving in the opposite direction, we find the carboxylates e.g. those derived from proline,^{24d} the orthometalated arylphosphines and finally the carboxamidates.

There are several occasions in which the varying electron-richness of a dirhodium(II) complex needs to be considered in the context of catalysis: The diazo compounds are Lewis bases and will more easily form Lewis acid-base complexes with the more acidic catalysts. The formation of these complexes is the first step in the catalytic cycle, as it has recently been described by computational methods (DFT) for aliphatic C–H insertion reactions of methyl diazoacetate.^{24e}

The second step involves nitrogen extrusion and formation of the metal carbene complex. During this step, electron density moves from the $4d_{xz}$ orbitals on Rh atom to which the diazo carbon is coordinated, into the σ^* orbital of the C–N bond in the complexed diazo group, helping to drive off dinitrogen.

Upon formation of the the metal carbene complex, the donation from the Rh-atom can be found in the p_π orbital on the carbene carbon. This added electron density will exercise a modulation of the electrophilic selectivity of the metal carbene complex (*vide infra*). Interestingly, at this point, the carbonyl group π bond of methyl diazoacetate is found to be in conjugation with the Rh–C σ bond, in analogy to the free carbene, where it is in conjugation with the electron pair of the non-bonding σ orbital (cf. section 2.1 on page 11).

In the step in which the C–H insertion takes place, a transfer of a hydride from the substrate to the carbene p_π orbital precedes the C–C bond formation.^{24e} It has been observed, that in substrates with activated C–H bonds, the hydride transfer tends to be further advanced in relation to the C–C bond formation.^{26c}

An additional consequence of the differential ability of the dirhodium(II) catalyst to donate electron density, from here referred to as back-donation, should be considered. The trends of Lewis acidity and back-donative ability are roughly opposite. This could imply that there is a balance between the frequency of Lewis acid-base complex formation (given that it is reversible) and the frequency with which such a complex proceeds to the rate determining step, which is the nitrogen extrusion aided by back-donation from the catalyst. Certainly, the fact that back-donation is involved, does not necessarily mean that nitrogen extrusion depends on it. Still, it may well be that the less Lewis acidic catalysts maintain their apparent reactivity with the help of back-donation, to a larger extent than those more Lewis acidic.

The influence of the catalyst ligands on the selectivity in reactions where multiple pathways are possible, have been compiled from the yields of the different products. The amount of back-donation exercised by a given catalyst, has been shown to be important for the electrophilic selectivity with which the dirhodium(II) carbenoid reacts with both olefins and C–H bonds. The consequence of increased electron population in the carbene p_π , should as it is for the carbenes (cf. section 2.1 on page 11), be an increase in energy of the p_π orbital and subsequently a larger $\sigma - p_\pi$ energy gap, which in turn leads to a stabilization of the metal carbene complex.^{23c} This is linked to an increasingly late transition state in a given reaction of the metal carbene complex,^{23a,23b,22f} which is expressed in the chemoselectivity and regioselectivity trends seen in figure 2.2 on the next page.

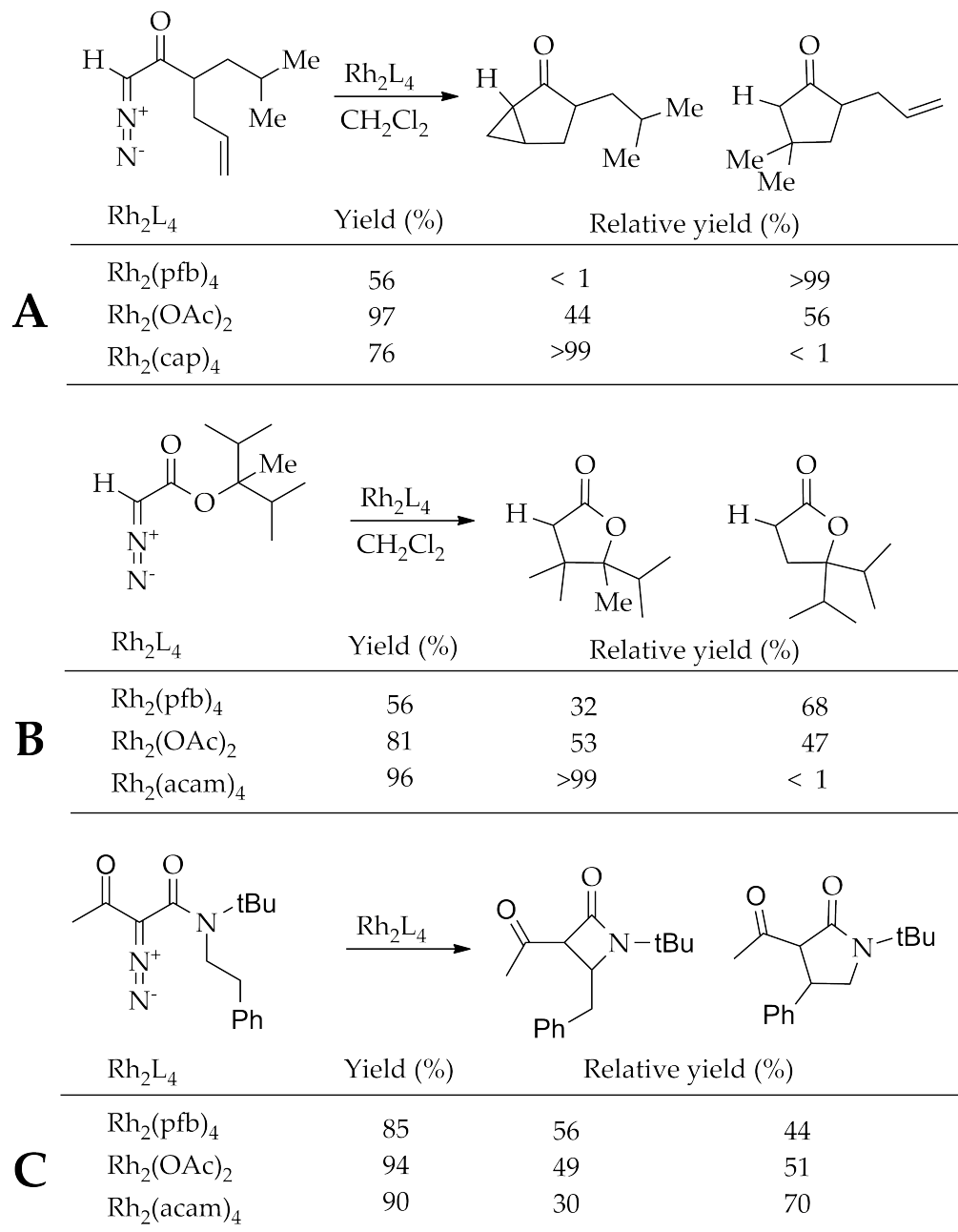


Figure 2.2.: Empirical selectivities in C-H insertion by dirhodium(II) carbenoids

As can be seen in figure 2.2, the selectivity for the better nucleophile and for the reaction with the later transition state increases with the increasing back-donating capability of the catalyst. The order of preferential reactivity in the different systems are:

A ^{24b} Olefin cyclopropanation > 3° C–H insertion

B ^{23a} 3° C–H insertion > 1° C–H insertion

C ^{24b} 5-membered ring formation > 4-membered ring formation

In relation to entry **C**, it is clear that the differentiation between the pathways to the 4- or 5-membered rings, given that both the α - and β -positions are methylenes, is governed by the stability of the carbenoid. The formation of the 4-membered ring thus proceeds through an earlier transition state. Still, selectivity is not very high when both insertion points are relatively unhindered.

Additionally, not shown in the figure, is the phenomenon of α -activation by heteroatoms^{24a,24d} and the α - and sometimes β -deactivation^{24a} by electron withdrawing substituents. These trends are rationalized by the stabilizing or destabilizing electronic effect of the heteroatom or the electron withdrawing group, on the build-up of positive charge during the C–H insertion transition state (involving hydride transfer).^{24e} The β -deactivation, however, does not always appear to exercise regiocontrol.^{24c} In relevance to this work, a concept that apparently has not been investigated in the same way as shown in figure 2.2, is how back-donation and subsequent stabilization of the metal carbene complex, affects the outcome of a reaction where the number of productive pathways is restricted and in which the C–H insertion is conformationally difficult.

In this perspective, the carbene dimerization reaction should be mentioned. Dimerization to yield the olefinic formal carbene dimer, is thought to occur either by the combination of two carbenes, or by the electrophilic attack of a carbene on the nucleophilic carbon of a neighbouring diazo compound, consequently effecting nitrogen extrusion and dimer formation. Apparently not reported,¹⁵ is whether increased back-donation increases the selectivity for the dimerization processes relative to other productive pathways.

Being a common by-product in many reactions of carbenes/carbenoids, it

appears there is a disregard for the dimeric species, and it is considered by many workers in diazo chemistry, as a product without further synthetic value. In contrast, and possibly following a pathway similar to that of dimerization, is the formation of alleged syndiotactic (e.g. highly ordered, almost crystalline) high molecular weight polymers from EDA using a Rh(I) catalyst.^{24f} This example indicates that carbene self-coupling processes can indeed be of synthetic value, as well as it emphasizes that carbene self-coupling processes not always lead to the olefinic dimer. The possibility that a by-product observed in the reactions performed in this work could stem from a self-coupling process is discussed in section 4.3 on page 46.

The next section focuses on the formation of bicyclic β -lactams and strategies involving carbenes that have had success in their preparation

2.4.1. β -lactam formation

The ability of carbenes and carbenoids derived from α -diazoacetamides to insert into C–H bonds α and β to the amide nitrogen, has been exploited in the preparation of both β - and γ -lactams. Focusing on the formation of β -lactams, and especially on the efforts to establish bicyclic systems, most of the reactions reported in the literature¹⁵ were carried out to prepare nuclear analogues of penicillin and cephalosporin antibiotics. More specifically, *p*-tosylhydrazones were treated with a strong base, or the corresponding α -diazoamides subjected to photolysis or thermolysis to yield carbenoids/carbenes which in all cases underwent C–H insertion to afford β -lactams in moderate to excellent yields.²⁷ About two decades after the earliest publications, reports of dirhodium(II)-catalyzed reactions appeared, also providing chemoselectivity and high yields.

Most of the α -diazoamides (or hydrazones) in question, had substituents other than H on the carbon bearing the diazo group. Still, examples of successful application of α -diazoacetamides have been reported using photolysis,^{27b,27c} thermolysis,^{27b} and dirhodium(II) catalysis.^{27f,37h} In the aforementioned publications, the second substituent on the diazo carbon is frequently a phenyl^{27a,27b,27h} or a carbonyl group,^{27c} but examples of an arylsulfonyl group^{27e} and dialkylphosphono groups^{27g} can also be found. All of the above mentioned substituents

are commonly employed in synthesis with α -diazoamides in non-cyclic systems. In general, the C–H insertions with the disubstituted carbenic species have been more successful than the monosubstituted, both in terms of yield and diastereoselectivity.

Having the possibility to insert into C–H bonds on either face of the cyclic amide residue, the most abundant diastereomer obtained in the bulk of these reactions is the one in which the second carbene substituent and the ring residue are in a *trans*-relationship, leaving them on opposite sides of the β -lactam plane.

As stated above, the bicyclic β -lactams are nuclear analogues of penicillin and cephalosporin antibiotics. However, as one of the publications states, the obtained bicyclic β -lactams showed no antibacterial activity.^{27c} For the β -lactams fused with 6-membered rings, this can be correlated with their lower reactivity towards hydrolysis as compared to the β -lactams fused with 5-membered rings.^{27b}

The α -halo- β -lactams (halo = Cl, Br) derived from piperidine, *cis/trans*-7-halo-1-azabicyclo[4.2.0]octan-8-one, as well as a few other α -halo- β -lactams more closely resembling antibiotics, were prepared some 30 years ago and their synthesis was indeed accomplished by a carbene/carbenoid route.²⁸ This reaction was based upon Seyferth's discovery that halomethylphenylmercury compounds readily fragment to phenylmercury halides and halocarbenes.²⁹ Thus, the thermal decomposition of *N,N'*-dihalophenylmercury amides yielded phenylmercury halides and α -halocarbene amides which underwent intramolecular C–H insertion to form the bicyclic β -lactams. The diastereomers of the α -halo- β -lactams derived from piperidine were separated and characterized by NMR, MS and elemental analysis. The stereochemical assignments were made by NMR in correlation to previously published β -lactam structures,²⁸ and are the background for the assignments made in this work (cf. the experimental section)

In this work, the intramolecular C–H insertion reactions of α -halodiazoacetamides will be investigated for a set of α -diazoacetamides derived from cyclic amines (see figure 3.2 on page 28). If the reactions are successful, they will afford α -halo- β -lactams. The presence of a halogen in the α -position of the β -lactam should render it a good electrophile and possibly a viable cross-coupling partner. In

such a reaction scheme, the relative hydrolytic stability of the β -lactams fused with 6-membered rings, can prove itself a valuable trait. The latter statement assumes that the presence of the halogen does not increase the propensity towards hydrolysis. A brief discussion of possible coupling conditions can be found in chapter 5 on page 53.

The syntheses and applications of the α -halodiazoacetamides are treated in chapter 4 on page 41. The next chapter is concerned with the preparation of the α -diazoacetamides to be halogenated.

Part II.

**Experimental Results and
Discussion**

3. Synthesis of α -diazoacetamides

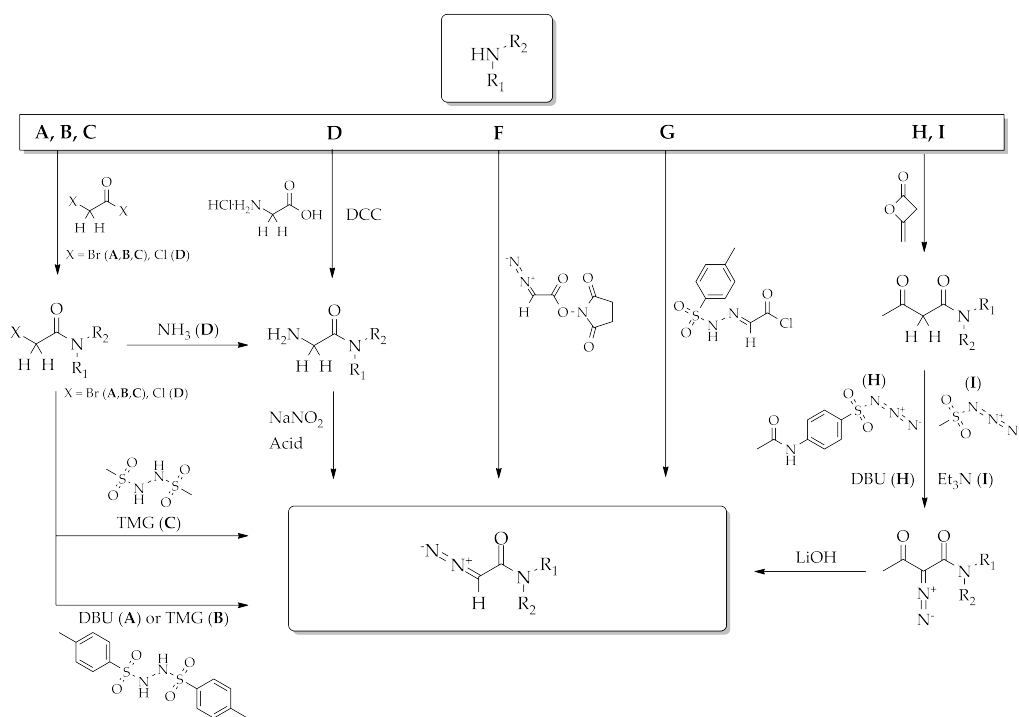


Figure 3.1.: Routes of synthesis of α -diazoacetamides labelled A-I.

Over the last decade, since the first syntheses of ethyl diazoacetate^{30a} and diazomethane,^{30b} the number of synthetic methods that form a diazo group within a molecule has grown continuously.^{30c} The discoveries of a wide range of precursor moieties suited for transformation into a diazo group, create ample possibilities for the inclusion of diazo chemistry in a synthetic strategy. Such structural flexibilities aside, only a few of the newer approaches can outperform the two longest standing methods, alkaline cleavage of *N*-alkyl-*N*-nitrosoureas and amine diazotization, with respect to two general drawbacks in the synthesis of the diazo group: atom economy and cost. Moreover, not all of the known

routes are applicable in the synthesis of α -diazoacetamides. The possible synthetic approaches are depicted in figure 3.1 on the preceding page.

One goal of this work was the synthesis of α -diazoacetamides from readily available cyclic, symmetric amines. As such a collection of amines was purchased. Their names and indexes, which will be used throughout the rest of this work, are shown in figure 3.2. The structures appearing in the coming synthetic steps will gain their indexes from an alphabetical increment in the letter, so that the synthetic products derived from e.g. piperidine are called **2b - 2e**.

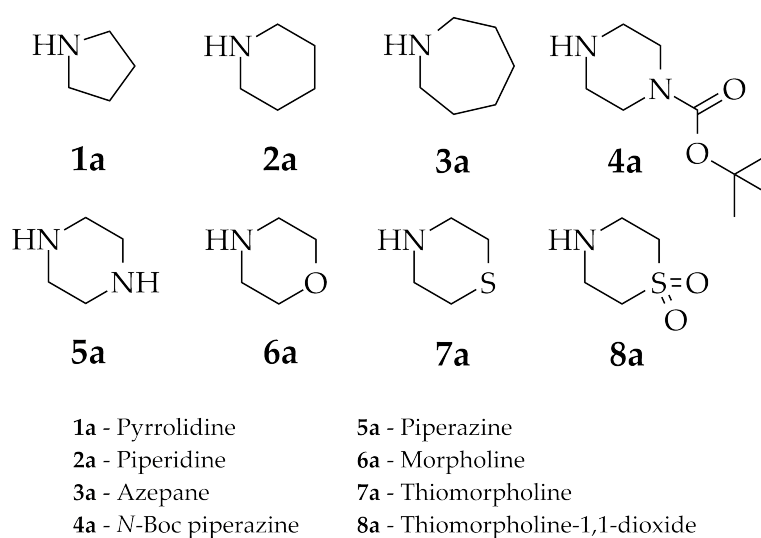


Figure 3.2.: Amines employed in the synthesis of α -diazoacetamides

3.1. The choice of synthetic strategy

In order to choose what synthetic strategy to employ, the routes marked A - I in figure 3.1 on the preceding page have been evaluated with respect to atom economy and cost, starting from an amine. In pathways where several reagents are suggested, the relevant reagents are marked with the letter corresponding to the route in question. A brief description of the synthetic routes corresponding to the letters A - I is given in table 3.1 on the next page.

Route	Description
A	The Toma procedure ^{31a} using <i>N,N'</i> -ditosylhydrazine and DBU
B	This work, the Toma procedure ^{31a} using <i>N,N'</i> -ditosylhydrazine and TMG
C	A hypothetical route, the Toma procedure ^{31a} using <i>N,N'</i> -dimesylhydrazine ^{31b} and TMG
D	A Gabriel-synthesis followed by Curtius diazotization ^{32a,32b}
E	A peptide coupling followed by Curtius diazotization ^{32a,32c}
F	Diazoacetyl transfer as published by Ouhia ^{33b}
G	The House/Blankley procedure. Acylation with glyoxylic acid chloride <i>p</i> -tosylhydrazone ^{15,34a,34b}
H	Regitz diazo transfer ^{35b} using <i>p</i> -acetamido benzenesulfonyl azide (<i>p</i> -ABSA) and DBU ^{35f}
I	Regitz diazo transfer ^{35b} as modified by Doyle using mesyl azide and triethylamine ^{35a,35c,35d,35e}

Table 3.1.: A short description of the possible synthetic routes to α -diazoacetamides

The concept of atom economy applied in this calculation is that of Barry Trost^{36a} and the following terminology^{36b} is used: The *Atom Economy* of the reaction sequence in question is the molecular weight of the introduced diazoacetyl group (MW 69 g/mole) divided by the sum of the molecular weights of the reagents used to introduce it. As an extension of this term, the *Experimental Atom Economy* is similarly the molecular weight of the introduced group divided by the molecular weights of the reagents, which this time, is multiplied by their respective molar equivalents. Finally, the term *Experimental Atom Economy* \times *Yield* provides an overall impression of how many moles of reagents are spent compared to how many moles of product that can be isolated. The last of these terms, is the most informative and is thus the only one included in table 3.2 on the following page.

The costs are calculated in accordance to the reagent equivalents and overall yields given in the cited procedures (see table 3.1) for structures similar to the ones in this work. Therefore, the cost calculation is not generally applicable in principle, although in all the described procedures the amines function as nucleophiles and there is little doubt that most cyclic amines are capable reagents as such. All the necessary reagents are included in the calculation, also those needed to prepare the key nitrogen containing reagents. Solvents are not included. Reagent prices are representative of the least expensive option for each item (often larger quantities) available to the Department of Chemistry at the University of Oslo, through the Sigma-Aldrich web site, in June 2010. Hence, they do not necessarily reflect industrial production prices, and must at best be regarded as indicative.

As can be observed in table 3.2 on the following page, the overall efficiency in

Table 3.2.: Cost in € and atom economy calculations per mole of diazoacetamide for different synthetic strategies. Cost figures are rounded off to the nearest tenth.

Synthetic strategy	€/mole product ^a	Yield ^b	Yield × Experimental Atom Economy
A	920	73%	2.6%
B	530	60%	2.0%
C	280	60%	2.3%
D	120	53%	1.8%
E	120	36%	5.2%
F	500	98%	9.7%
G	470	75%	6.4%
H	400	88%	3.6%
I	90	48%	5.3%

^a Calculated using currency conversion rates dated 14.07.2010

^b Overall yield from the point of introduction of the amine

the preparation of diazoacetamides, starting from an amine, is quite low. Worthy of note, is the fact that the largest differences between the atom economies of the various routes, is no more than fivefold (cf. entry F vs. D), compared to the tenfold difference in cost between the routes A and I. As well, the most atom efficient route is among the top three in cost, while the least expensive route is the third most atom efficient route (Route I). This owes much to the fact that the modified Regitz^{35b} diazo transfer route, using diketene and mesyl azide/Et₃N comes at a surprisingly low cost considering the extra step (cf. figure 3.1 on page 27). It is also more efficient than the diazo transfer with *p*-ABSA and DBU, even though the reported yield in the latter procedure is higher. It is also worth noting that the preparation of succinimidyl diazoacetate (route F) and glyoxylic acid chloride *p*-tosylhydrazone (route G), are one and two step processes respectively, which are not necessarily convenient or easy to perform (*vide infra*). The route F is, however, the most desirable strategy to employ if the amine is either costly or in shortage as a function of synthetic steps needed to prepare it.

Included in the table 3.2 is the result of the same cost and atom economy calculation with respect to this work (Route B). The numbers show that the modifications made to the original procedure (Route A) had some positive

impact on the cost, although the yields were slightly lower (*vide infra*). A further hypothetical improvement to this strategy using *N,N'*-dimesylhydrazine instead of *N,N'*-ditosylhydrazine, would if the yields were equal, improve the cost efficiency even further (Route C).

3.2. Experimental results

Apart from atom economy and cost, a trait of useful synthetic transformations is scalability. Given that the investigation of the halogenation of the α -diazoacetamides would require access to ample amounts of the diazo compounds, it was desirable to prepare the α -diazoacetamides at a 10 - 50 millimole scale.

Starting out, both routes G and F were explored due to their widespread use in the literature. These routes intercept each other at the point of the glyoxylic acid *p*-tosylhydrazone (which is easily prepared by the reaction of glyoxylic acid and *p*-tosyl hydrazide).^{34b} As has been reported by others,^{34b,33a} the preparation of the corresponding acid chloride (route G) was difficult, also in our hands, in terms of its synthesis and purification.

Succinimidyl diazoacetate on the other hand (Route F), is reported to be a shelf stable reagent which can be prepared by the dicyclohexyl carbodiimide (DCC)-mediated coupling of *N*-hydroxysuccinimide and glyoxylic acid *p*-tosylhydrazone,^{33b} a reaction which simultaneously dehydrogenates the hydrazone to form the diazo group. However, this procedure was not successful owing to the difficult chromatographic separation of the dicyclohexylurea (DCU) produced in the coupling and the succinimidyl diazoacetate. Succinimidyl diazoacetate has been prepared by Doyle^{33c} on a large scale (40 g) by the acylation of *N*-hydroxysuccinimide with glyoxylic acid chloride *p*-tosylhydrazone. This route was not pursued by us in consequence of our difficulties in preparing the glyoxylic acid chloride *p*-tosylhydrazone. Interestingly, succinimidyl diazoacetate has recently been used in enantioselective cyclopropanations of olefins with chiral cobalt(II)-porphyrin catalysts, establishing asymmetry *before* introducing the amide function.^{37b}

Our next attempt focused on a publication by Toma *et al.*^{31a} in which the diazo group was introduced by a novel reaction between *N,N'*-ditosylhydrazine and several α -bromo esters (Route A). The mechanism, although not fully elucidated, appears to involve an S_N2 reaction followed by steps reminiscent of those found in the dehydrogenation of hydrazones. A short mechanistic proposal based on what is described in the publication is shown in figure 3.3. In the step in which the intermediate is a tautomer of a hydrazone, the hydrazone is shown in parentheses.

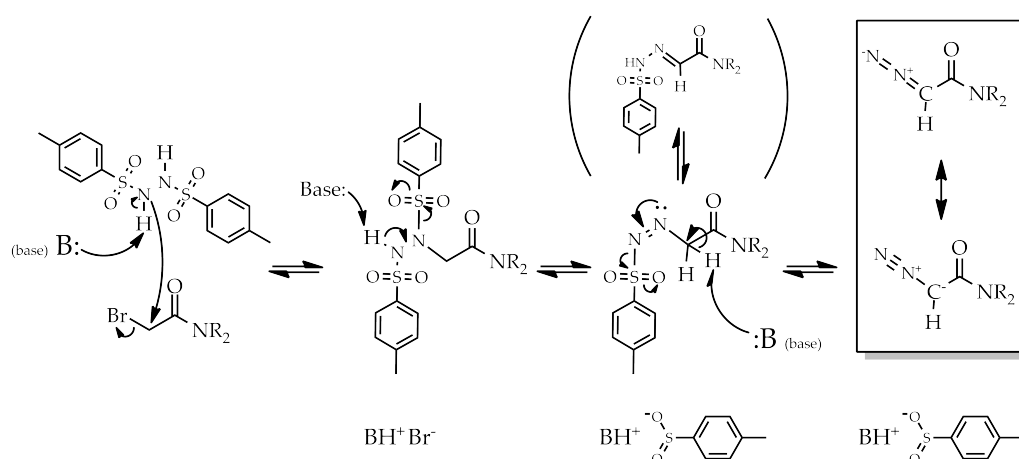


Figure 3.3.: A tentative mechanism for the base-induced introduction of the diazo group with *N,N'*-ditosylhydrazine

Although this approach had not been reported for the preparation of α -diazoacetamides, it seemed likely that it would be compatible, given that the α -bromo amides would react similarly to the α -bromo esters. Thus, the amines **1a-8a** were bromoacetylated in high yields with bromoacetyl bromide and tribasic K_3PO_4 , as shown in figure 3.4 on the facing page. The use of K_3PO_4 instead of Na_2CO_3 , as in the original publication, was founded on the results of an optimization study of the acylation of amines with respect to different bases, which concluded that K_3PO_4 was optimal for this type of reaction.^{31c} Indeed, the reaction was clean, and no purification besides the work-up was needed to provide compounds pure enough to be used directly in the subsequent step (cf. the crude NMR spectra in the appendix).

Unfortunately, the analogue **7b** became a brittle lacquer upon evaporation of the solvent, which was completely insoluble in solvents suited for the next step.

This was possibly due to a reaction between the thioether and a neighbouring α -bromoamide, forming a salt. The compound was not included in further synthesis.

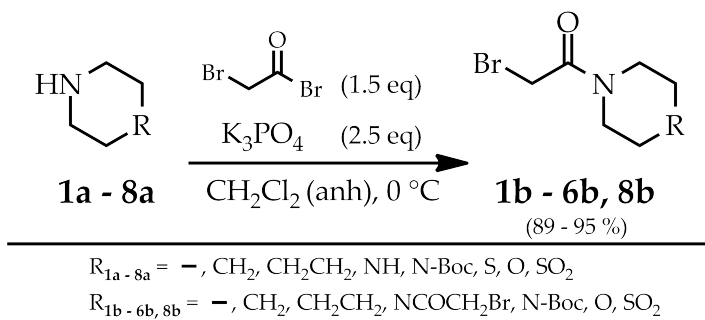


Figure 3.4.: First synthetic step

3.3. Modifications to the Toma procedure

In the second step, the original procedure (Route A) used the amidine base DBU to deprotonate the *N,N'*-ditosylhydrazine and subsequently the adduct with the amide, that resulted from the nucleophilic attack of the hydrazine anion on the α -carbon (cf. figure 3.3 on the preceding page). The similar base strength of TMG (cf. table 1.1 on page 7) and its properties as a nucleophilic catalyst,^{37a} made it an interesting alternative to DBU. The route employing TMG is route B in figure 3.1 on page 27.

In the original procedure, the crude reaction mixture was quenched with $\text{NaHCO}_3(\text{aq})$ and then extracted with Et_2O . In our experience - assuming that the mechanistic proposal is accurate - it was problematic to perform a clean extraction due to the presence of the 4 molar equivalents of $\text{DBU-HO}_2\text{S-C}_6\text{H}_4\text{CH}_3$ and 1 equivalent of DBU-HBr . This situation manifested itself more gravely on a reaction scale > 5 mmol. The problem could lie in the intermediate solubility of the $\text{DBU-HO}_2\text{S-C}_6\text{H}_4\text{CH}_3$ complex between the aqueous phase and the ether phase. What further complicated the matter of an aqueous extraction procedure, was the aqueous solubility of the obtained α -diazoacetamides. The aqueous phases had to be thoroughly extracted to obtain decent yields, which

also increased the solvent expenditure. Yields of 50 - 60 % were obtained over two steps, however the reaction mixtures were discoloured and the number of extractions imposed limitations of the reaction scale.

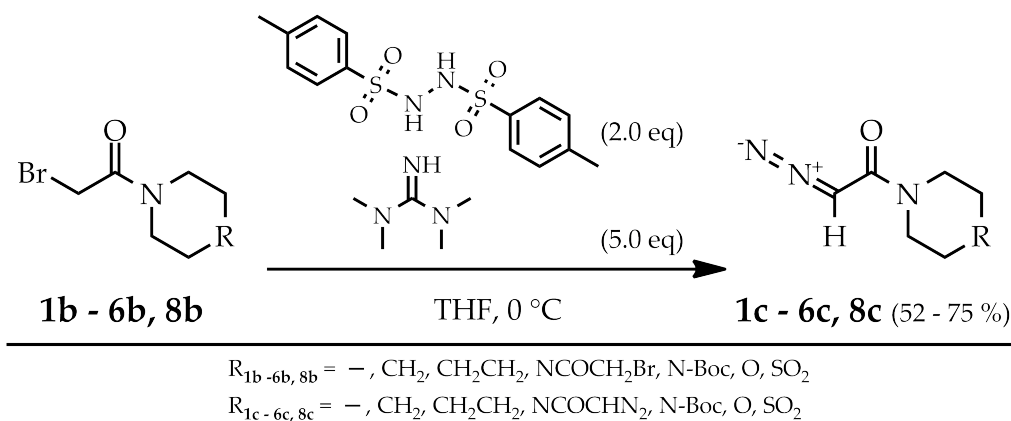


Figure 3.5.: Second synthetic step

3.4. Results of the modifications

When the reaction was run with TMG instead of DBU, a quick, clean reaction was observed and after stirring for a period of approximately 60 minutes, a heavy precipitate formed, which settled to reveal a bright yellow solution when stirring was stopped. The THF was then removed under reduced pressure and Et_2O added. Vigorous stirring left a suspension which could then be filtered with suction to give transparent bright yellow solution, leaving behind an almost white filter cake. By NMR the filtrate consisted chiefly of the product (cf. crude NMR of **1c** in the appendix).

To obtain the α -diazoacetamides with sufficient purity for an investigation of their halogenation, chromatography was carried out on silica gel. Chromatography on alumina, both neutral and basic, appeared to be detrimental to the compounds, based on observed surges of bubbles from within the column in the middle of elution. Worthy of note, is the effect of the almost complete removal of the produced $\text{TMG} \cdot \text{HO}_2\text{S-C}_6\text{H}_4\text{CH}_3$ by filtration of the precipitate. This simplified the chromatography considerably, allowing the columns to be fairly heavily loaded, e.g. 2.6 g of **3c** was isolated from an 8.5×3.5 cm column

of standard silica gel. The elution needed to be slow in order to achieve separation from a common by-product with a slightly lower R_f value, which is the α -tosylacetamide. This compound was also observed in the publication by Toma *et al.*^{31a} and its formation can be rationalized by the nucleophilic attack on the α carbon of the unreacted α -bromo amide by the sulfur atom in the sulfinate group. A reaction summary is presented in figure 3.5 on the facing page and the experimental details for all the compounds can be found in the experimental section (section 9 on page 79)

3.5. The precipitated

TMG · HO₂S-C₆H₄CH₃/TMG · HO₃S-C₆H₄CH₃

The precipitated TMG · HO₂S-C₆H₄CH₃ merits further discussion. The salt is a free-flowing white powder, which becomes hygroscopic as the sulfinic acid is oxidized to sulfonic acid in air. A sample left exposed to air, became a sludge after about a month, presumably due to water solvation. The salt is highly soluble in H₂O, CH₂Cl₂, CHCl₃, MeOH and MeCN, but has limited solubility in THF and almost none in Et₂O. The composition of the salt was probed by mass spectrometry (ESI) and by growing crystals suitable for X-ray diffraction studies. The MS sample was isolated from a freshly filtered batch, and dried and stored under argon until the spectra could be recorded. Already at this point, some sulfonic acid could be detected. This, most likely owes to the reaction being conducted in an air atmosphere.

The crystals of TMG · HO₂S-C₆H₄CH₃ grew while storing a MeCN solution at 4 °C overnight, whereas the TMG · HO₃S-C₆H₄CH₃ were grown by exposing a sample of TMG · HO₂S-C₆H₄CH₃ to air for several days before submitting it to crystallization from CH₂Cl₂/Et₂O. The molecular arrangement is similar in both crystals and involve two molecules of base and two of acid. This was corroborated by the observation of the TMG · TMG · HO₂S-C₆H₄CH₃ and TMG · TMG · HO₃SC₆H₄CH₃ fragments in the mass spectrometer (MS-ESI). The structures are shown in figures 3.6 and 3.7 on the following page.

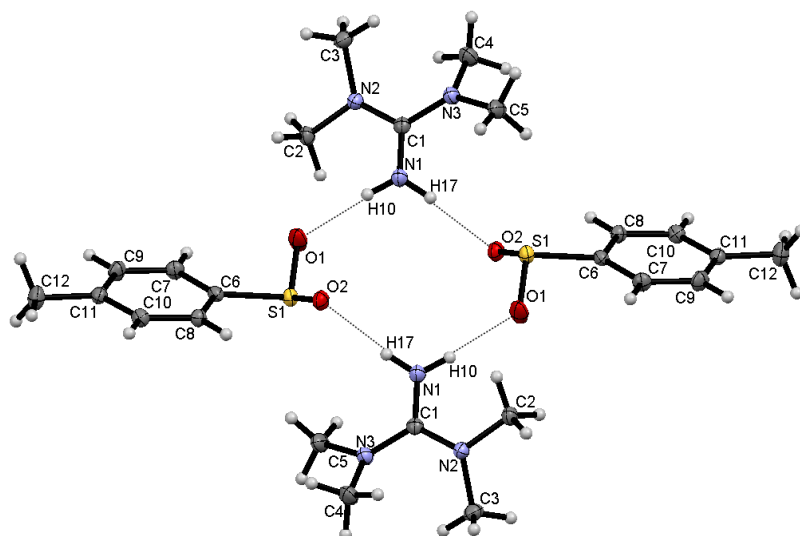


Figure 3.6.: Structure showing intermolecular hydrogen bonding in the crystal of 1,1,3,3-tetramethylguanidine sulfinate. The data were recorded at 105 K. Displacement ellipsoids are shown at the 50 % probability level with hydrogen atoms as spheres of arbitrary size.

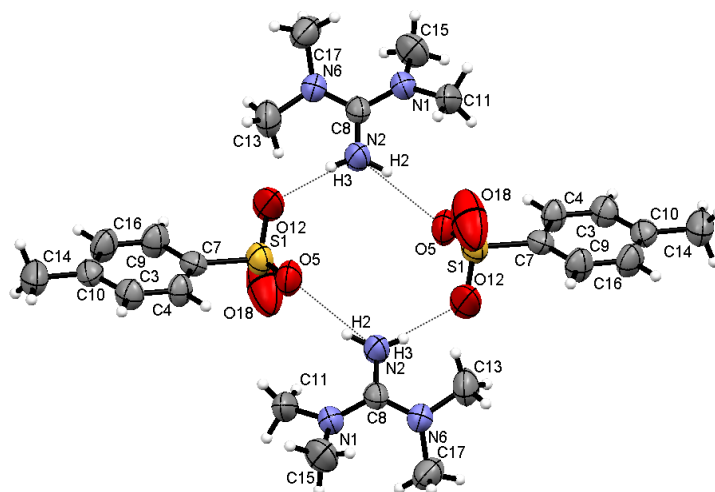


Figure 3.7.: Structure showing intermolecular hydrogen bonding in the crystal of 1,1,3,3-tetramethylguanidine sulfonate. The data were recorded at 296 K. Displacement ellipsoids are shown at the 50 % probability level with hydrogen atoms as spheres of arbitrary size.

3.6. Previously unreported α -diazoacetamides

Of the α -diazoacetamides that were prepared, some were described in the literature, but the experimental details concerning their preparation were rather scarce. Most frequently, the compounds had been prepared by the reaction of the amine with succinimidyl diazoacetate. Of the known compounds were **1c**,^{37b,37i} **2c**,^{27b,32a,33b,37c,37d,37e,37f,37h} **3c**,^{37h} and **6c**.^{32a,33b,37j}

Since the three remaining analogues were unknown,¹⁵ crystals suitable for X-ray crystallography were grown and low temperature diffraction data (105 K) recorded to unequivocally determine the structures of **4c**, **5c** and **8c**. The structures and intermolecular bonding present in the crystals are shown in figure 3.8 and in 3.9 and 3.10 on page 39, respectively.

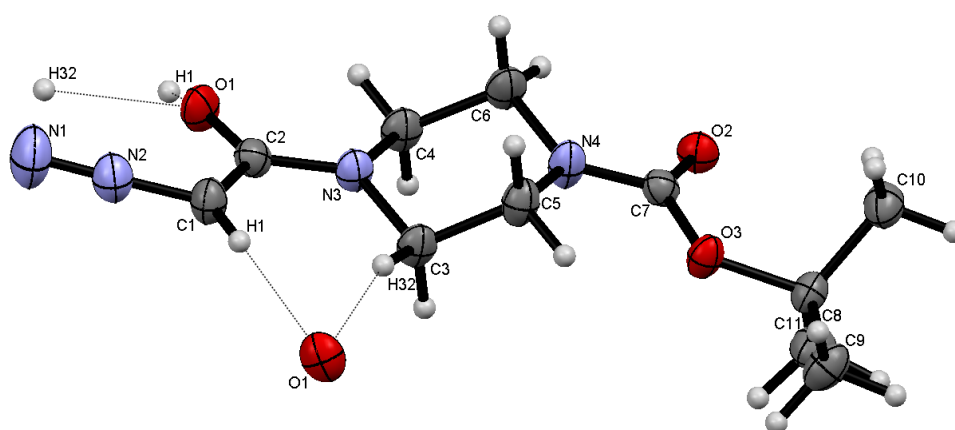


Figure 3.8.: Structure showing intermolecular hydrogen bonding in the crystal of *tert*-butyl 4-(2-diazoacetyl)piperazine-1-carboxylate (**4c**). The data were recorded at 105 K. Displacement ellipsoids are shown at the 50 % probability level with hydrogen atoms as spheres of arbitrary size

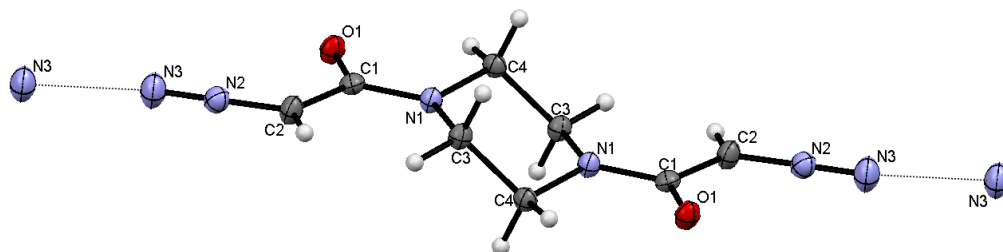


Figure 3.9.: Structure showing intermolecular bonding in the crystal of *N,N'*-bis(2-diazoacetyl)piperazine (**5c**). The data were recorded at 105 K. Displacement ellipsoids are shown at the 50 % probability level with hydrogen atoms as spheres of arbitrary size

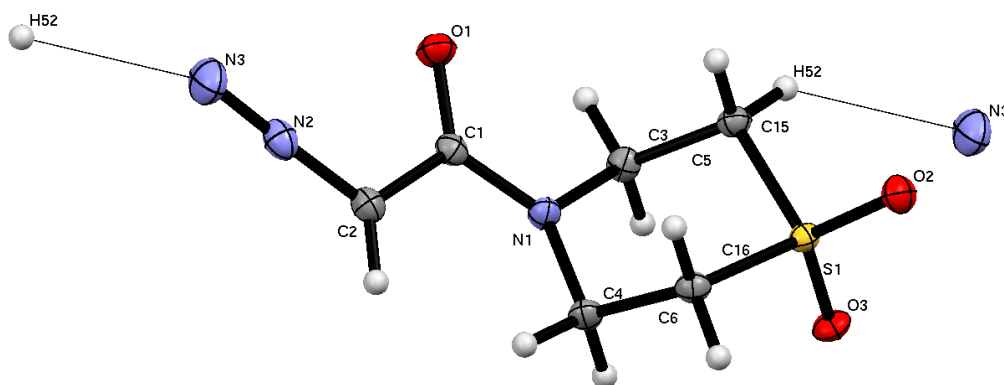


Figure 3.10.: Structure showing intermolecular hydrogen bonding in the crystal of 2-diazo-1-(1,1-dioxido-4-thiomorpholinyl)ethanone (**8c**). The data were recorded at 105 K. Displacement ellipsoids are shown at the 50 % probability level with hydrogen atoms as spheres of arbitrary size

4. The synthesis and reactivity of α -halodiazoacetamides

α -halodiazoacetic esters have been utilized in dirhodium(II) catalyzed cyclopropanations, C–H and Si–H insertions, showing that they are indeed competent reactants in reactions common in the field of metal carbenoids.^{26a,10h} Additionally, they have been photolyzed to give the corresponding carbenes which underwent cyclopropanation and C–H insertion reactions.^{10f} They are reported to be highly kinetically active, when used in rhodium catalyzed reactions.^{26a,10h} This can be interpreted as an expression of the low energy barrier towards the rate-limiting nitrogen extrusion step. It should also indicate that their ground state lies quite high in energy. Thus, for the first attempts to synthesize the α -halodiazoacetamides, we decided to direct our attention to the brominated analogue, as it was expected to be a slightly more chemically stable compound than the chlorinated analogue.^{10d}

4.1. First impressions

Our first attempts to synthesize the α -bromodiazoacetamide derived from **2c**, were carried out using the reported methodology.^{10h} The reaction itself proceeded in the expected way; the colour change from bright yellow to bright red upon adding the halogen source is complete within a few minutes. It was observed, however, that a lower temperature and less handling (washing, transferring) was necessary to assure the reproducibility. As measures to achieve this, a cryostat was employed to secure a reaction temperature of $-5\text{ }^{\circ}\text{C}$, quenching ($\text{Na}_2\text{S}_2\text{O}_3(\text{aq})$) and drying (MgSO_4) were omitted, and the short column used to separate the brominated α -diazoacetamide from the base and remaining scaffold of the *N*-bromo source, was built into a holder which could

be filled with CO₂(s), giving a temperature of approximately -80 °C during the quick chromatographic step. The results of these modifications appeared satisfactory, judging by the colour of the solution eluted from the column (bright red). It was also possible to analyze the reaction by thin layer chromatography (TLC) in a cooled chamber. Judging by the plate, the conversion of **2c** to **2d** was high, if not complete.

The first attempts to cyclize **2d** were carried out with dirhodium(II) catalysis using commercial Rh₂(esp)₂ and the synthesized Rh₂(OAc)₂(pc)₂ · 2MeCN (pc = orthometalated PPh₃). To our satisfaction, the product was visible by ¹H-NMR, but the yields were low (10 - 30 %). In the ¹H-NMR, carbene dimerization products, but also the corresponding α, α' -Br₂-piperidine acetamide, were the other major species.

The fact that the product had formed, was interesting as previous attempts by others,^{37h} although with the essentially different **2c**, catalyzed by chiral dirhodium(II) carboxamidates, did not yield any product. The workers in the mentioned publication, did however obtain high yields of the β -lactam derived from **3c**, which held promise for our later attempts with this substrate. Although the substituents are sterically and electronically distinct, the formation of the β -lactam indicated that the halogen substituent was comparable to a phenyl group, at least in the sense that their carbenes/carbenoids in fact achieve the cyclization (cf. discussion in section 2.4.1 on page 22). The electronic effects of the halogen substituents on α -halodiazoacetic esters in comparison to other common substituents in the context of dirhodium(II) catalyzed cyclopropanations, has been investigated computationally by our group.^{26b}

Incidentally, the rest of an incompletely eluted short column was left on the bench in ambient temperature, out of curiosity to see what would happen if the α -bromodiazoacetamide was allowed to “decompose” by itself. Our expectation to obtain a crude reaction mixture which would not contain any product, was confused by the fact that although thermolysis of diazo compounds is indeed a common route to synthetically competent carbenes, it had not before been done with the heat available at ambient temperature. What the ¹H-NMR showed, was ironical to anyone working with transition metal catalysis; Complete conversion, with almost complete chemoselectivity for the intramolecular β -lactam formation, had occurred. A subsequent trial

was immediately set up and a few hours later the result was reproduced. The chemoselectivity of the C–H insertion reaction, was marginally compromised by the formation of carbene dimerization products and a small amount of the α, α' -Br₂–amide.

4.2. Optimization studies



Figure 4.1. – 2 mmoles of **2d** undergoing thermolysis. The septum is perforated with a cannula and is only present to avoid evaporation.

With this reaction in hand, we could pursue the optimization of the conditions of formation of the α -bromodiazoacetamide **2d** from **2c**. We had learned from the first attempts and from the syntheses of the α -diazoacetamides, that alumina was too active to be used as a chromatographic medium. We proceeded to investigate the effect of dilution on the reaction of **2d** \rightarrow **2e**. The results, which can be seen in table 4.1, indicate that within the concentration range we examined, there was no good reason to increase the solvent expenditure.

Table 4.1.: Yields^a of *trans*-7-bromo-1-azabicyclo[4.2.0]octan-8-one obtained by varying the reaction concentration in the thermolysis of **2d**

Reaction volume (mL)	Concentration (mM)	Yield (%)
50	10	50
100	5	51
300	1 $\frac{2}{3}$	54

^a Determined by ¹H-NMR,³⁸ 0.5 mmol reaction scale

We then investigated the effects of different bases and bromine sources, as discussed in section 1.3 on page 7. The reaction conditions are shown in figure 4.2 on the next page and the results can be found in table 4.2 beneath the figure. The reaction times were not optimized, which could mean that e.g. TMG may serve as well as DBU with longer reaction times. In general, the yields were uplifting, considering the results from the dirhodium(II) catalyzed reactions.

4.3. Results of the thermolysis of 1d-6d and 8d

Under the reaction conditions, both NBS and NBP provided clean products, according to spectral analysis. It was, however, possible to trace both succinimido and pththalimido species by $^1\text{H-NMR}$ (cf. the crude spectra corresponding to NBS and NBP in the appendix), and this caused some worry as to whether the failure of the dirhodium(II) catalysis might be attributed to an inhibition of the catalyst active site by these species. By TLC analyses however, it seems probable that these species are unreacted NBS or NBP, given the relatively high R_f of the α -bromodiazoacetamide **2d** with which they coelute. Fortunately, they do not seem to have a negative impact on the intramolecular C–H insertion reaction, by what must be presumed to be the “free” α -bromocarbene amide.^{20k} With this reasoning, the conditions providing the highest yields (DBU/NBP), were applied to the analogues **1c** - **6c** and **8c**. A reaction scheme can be seen in figure 4.3 on page 46 and the results are displayed in table 4.3 on page 47.

As can be seen in table 4.3 on page 47, the reaction is apparently more difficult for rings with less conformational freedom. The total yield thus decreases with decreasing ring size, especially when moving from the six-membered to the five-membered ring, plausibly reflecting the increasing strain in the bicyclic system (cf. the yields of **1e** vs. **2e** vs. **3e** and note *d* below the table). Focusing on the six-membered rings, the introduction of a heteroatom clearly restrains the conformational freedom, as thus the ease with which the carbene is able to form the β -lactam. Additionally, comparing the higher yield of **4e** vs. **6e** and **8e**, it seems possible that other carbenic pathways may be operating. The ether oxygen in **6e** and the sulfonyl oxygens in **8e** could possibly take part in ylide formations, which would lower the yield of the β -lactam products. Crude spectra from the

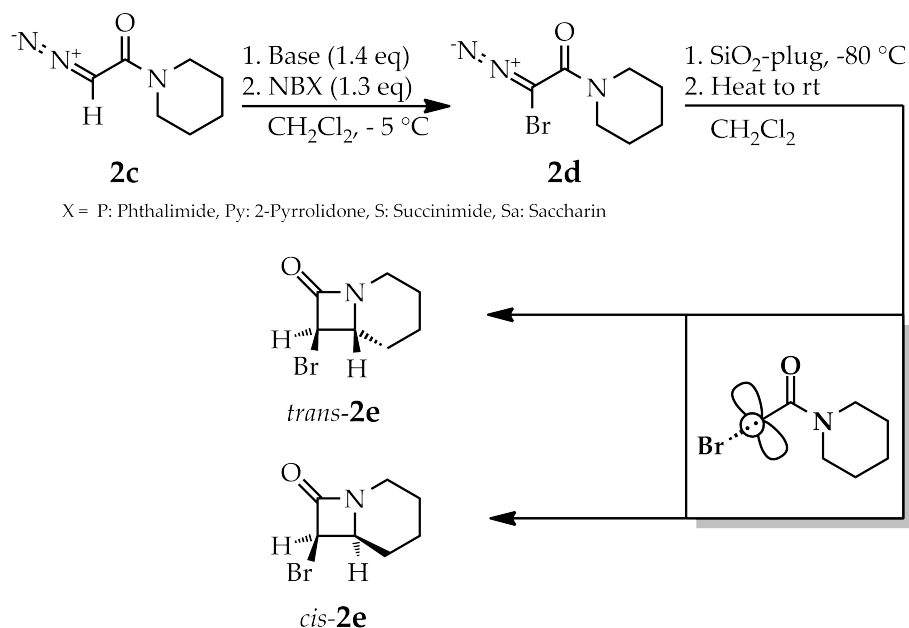


Figure 4.2.: The reaction conditions in the bromination of the α -diazoacetamides

Table 4.2.: Yields^a in % of *trans*-7-bromo-1-azabicyclo[4.2.0]octan-8-one (**2e**), obtained by varying the base and bromine source

	NBPy	NBS	NBP	NBSa
DABCO ^b	- ^d	43	37	- ^e
TMG ^c	33	41	51	- ^e
DBU ^c	65	56	73	- ^f
TBD ^c	- ^e	- ^f	- ^f	- ^f

^a Determined by ¹H-NMR,³⁸ 0.5 mmol reaction scale

^b The reaction time was 30 minutes

^c The reaction time was 5 minutes

^d No appreciable reaction progress was observed after 30 minutes

^e Rapid gas evolution and loss of colour were interpreted as signs of decomposition

^f The reaction was not carried out as the reagent combination was considered unsuitable based on the related results

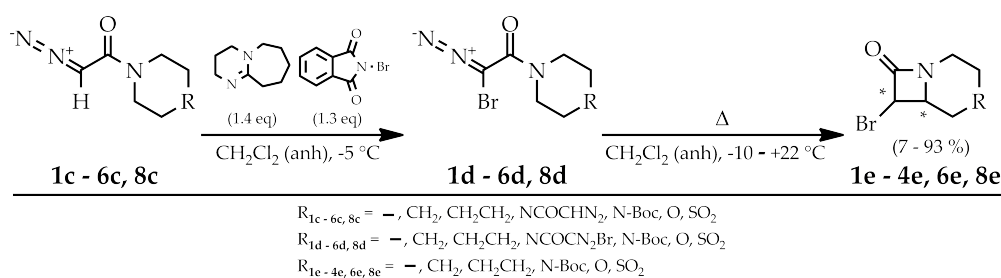


Figure 4.3.: The reaction sequence from α -diazoacetamide to α -bromodiazoacetamide to β -lactam

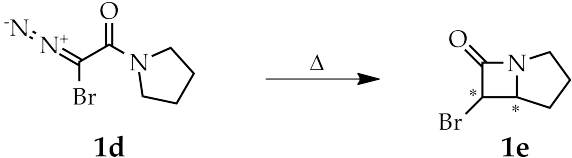
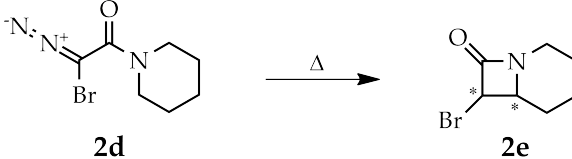
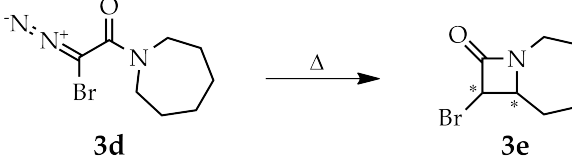
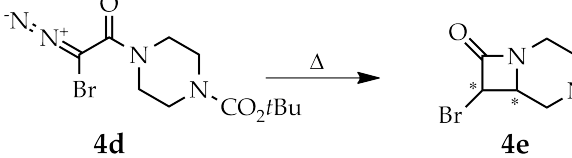
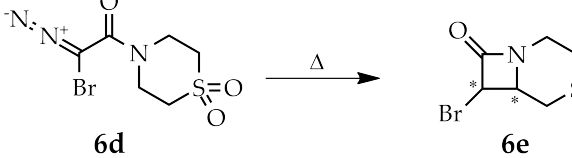
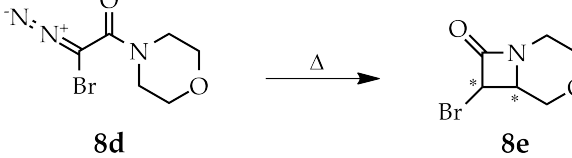
six reactions are shown in the appendix, and it is notable that the more highly functionalized analogues, do not react as cleanly as **2d** and **3d**.

Nonetheless, the reaction **3d** \rightarrow **3e** shows how well the α -bromocarbene amide C–H inserts in the absence of steric or conformational hindrance. A larger scale reaction of **3c** \rightarrow **3e** (2 mmoles of **3c**) was undertaken successfully. The yield after chromatography (used to separate the diastereomers) is reported in parentheses in table 4.3 on the next page. The spectra of the crude and chromatographed products, as well as other pertinent details, are found in the appendix and the experimental section (section 10.3 on page 102).

The doubly diazoacetylated analogue **5c** was also brominated and thermolyzed using the same conditions. It appeared that the compound could be brominated similarly to the other analogues, judging by the colour change, but the $^1\text{H-NMR}$ and the mass spectrometry data (ESI) of the crude reaction mixture, were largely uninterpretable. Given the variety of products that could result from one or two intramolecular C–H insertions, let alone dimerization reactions and intermolecular reactions, this result was not unexpected.

Finally, a variation which is difficult to justify is that of the yields of the α, α' - Br_2 -amides. They are known products from the reactions of diazo compounds and molecular halogen,¹⁵ yet here it seems unlikely that they are formed in the bromination step; The large variation in their yield and the inverse covariation with the product yield ($R^2 = 0.84$, see figure 4.4 on page 48), could suggest that they are somehow derived from the α -bromocarbene amides or their α -bromodiazoacetamide precursors. The α, α' - Br_2 -amide of piperidine has been characterized by $^1\text{H-NMR}$ (cf. section 10.2.1 on page 102 and the spectrum in the appendix).

Table 4.3.: Yields^a in % of β -lactam obtained from the thermolysis of the α -bromodiazooacetamides

Reaction	<i>trans/cis</i>		α, α' -Br ₂ - Total Amide		
	<i>trans</i>	<i>cis</i>		ratio ^b	
 1d $\xrightarrow{\Delta}$ 1e	7	- ^c	n/a	7 ^d	34
 2d $\xrightarrow{\Delta}$ 2e	73	11	6:1	84	2
 3d $\xrightarrow{\Delta}$ 3e	77 (81) ^e	16 (13) ^e	5:1 (6:1) ^e	93 (94) ^e	trace (-)
 4d $\xrightarrow{\Delta}$ 4e	34	2	17:1	36	21
 6d $\xrightarrow{\Delta}$ 6e	12	1	6:1	13	20
 8d $\xrightarrow{\Delta}$ 8e	14	3	5:1	17	12

^a Determined by ¹H-NMR³⁸^b Rounded off to the nearest whole number^c Not detected by ¹H-NMR^d Upon taking a new ¹H-NMR spectrum of the reaction mixture after approximately 48 hours (as has been done routinely to verify the yield measurements),³⁸ the characteristic doublet used to measure the yield was no longer present, indicating that the compound had decomposed; possibly by hydrolysis.^{27b}^e Isolated yield after chromatography. The α -bromodiazooacetamide precursor was prepared using DBU and NBS (cf. table 4.2 on page 45)

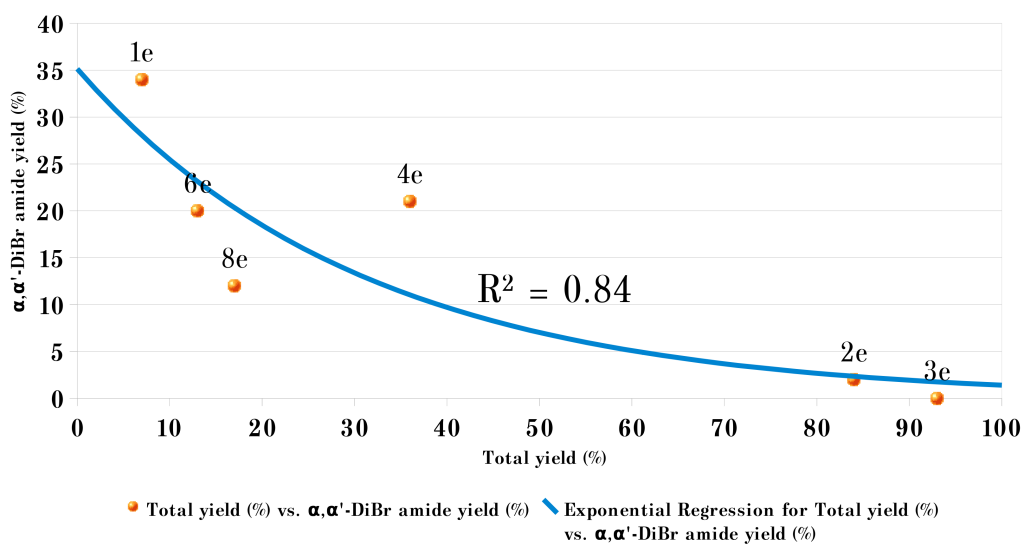
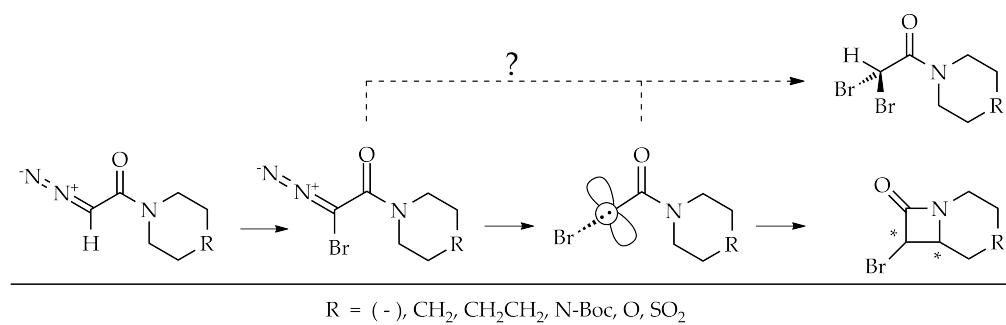


Figure 4.4.: A plot of the yield of the α, α' -Br₂-amides vs. the total yield of the β -lactams for each analogue.

4.4. A comparison of the thermolytic and catalytic reactions, employing three prototypical transition metal catalysts

Having obtained the thermolysis results, we turned back to verify the results with the dirhodium(II) catalysts. This time we chose two dirhodium(II) catalysts from two entirely different families; $\text{Rh}_2(\text{tfa})_4$, one of the most Lewis acidic catalysts available and its extreme opposite, the $\text{Rh}_2(\text{cap})_4$. A copper(II) catalyst $\text{Cu}(\text{acac})_2$ was also included in the interest of exploring the reactivity of the α -bromodiazacetamides with this family of catalysts. Finally, the best result with the $\text{Rh}_2(\text{OAc})_2(\text{pc})_2 \cdot 2 \text{MeCN}$ (pc = orthometalated PPh_3) and with thermolysis using the DBU/NBS conditions, were included for comparison (an average of 5 such thermolysis reactions are included in parentheses). The results of the catalytic dediazotization of **2d** are shown in table 4.4 on the following page.

A methodological problem arises, when it is known that the α -bromodiazacetamides selectively form the desired product upon thermolysis, and the reported optimal conditions for catalysis with α -bromodiazacetic ethyl ester^{26b} (used here as a guideline), involve letting the solution of the α -bromodiazacetic ethyl ester warm up to room temperature before injecting a solution of the catalyst. Fortunately, studying table 4.4 on the next page, reveals that the result with the copper(II) catalyst, disappointing nonetheless, serves to inform of a bottom line which hardly contains any product. The crude $^1\text{H-NMR}$ spectrum shows a near complete conversion to the formal carbene dimer (cf. spectrum in the appendix), a result which attests to the efficiency of the catalyst, although not in the desired pathway. In spite of this, there is in principle no way of rigorously excluding the possibility that the thermolysis pathway is operational under the described conditions.

The other three catalysts produce the product in low yields alongside dimeric products. It is interesting to see the small difference, in this reaction, between the two catalysts $\text{Rh}_2(\text{tfa})_4$ and $\text{Rh}_2(\text{cap})_4$, that show such distinct reactivity with other substrates. $\text{Rh}_2(\text{tfa})_4$ is reported to give results in selectivity experiments, that indicate that it, to some extent, releases the free carbene.^{23a} In such a situation, the yield produced by the "free" carbene would add to the yield

produced by the metal carbene complex, the consequence being that the noted yield with $\text{Rh}_2(\text{tfa})_4$ becomes higher than it should. If this is the case, it is tempting to propose, at the risk of being mistaken about the time scales on which the reaction operates, that the higher yield using $\text{Rh}_2(\text{cap})_4$, can be attributed to a carbene complex which is sufficiently stabilized to experience a higher number of viable conformations in which to C–H insert. This proposition, however, goes unsubstantiated (cf. discussion in 2.4 on page 21).

Table 4.4. Yields^a in % of *trans/cis*-7-bromo-1-azabicyclo[4.2.0]octan-8-one obtained from the catalytic dediazotization of **2d**. Thermolysis result is shown for comparison.

Catalyst	Nominal catalyst loading (% mol)	<i>trans/cis</i>			Total	α, α' – Br ₂ - Amide
		<i>trans</i>	<i>cis</i>	ratio		
$\text{Cu}(\text{acac})_2^b$	3	2	- ^c	n/a	2	2
$\text{Rh}_2(\text{tfa})_4^b$	3	22	6	3.7:1	28	25
$\text{Rh}_2(\text{OAc})_2(\text{pc})_2^b$	1	30	4	7.5:1	34	10
$\text{Rh}_2(\text{cap})_4^b$	3	38	6	6.3:1	44	14
None (thermolysis) ^b	n/a	57 (55) ^d	10	5.7:1	67	3

^a Determined by ¹H-NMR³⁸

^b DBU/NBS bromination conditions

^c Not detected by ¹H-NMR

^d Averaged over 5 reactions under nearly equal conditions

4.5. Synthesis and thermolysis of α -chloro- and α -iodo-**4c**

It was desirable to investigate whether the reaction of the α -bromodiazoacetamide, could be extended to its chlorine and iodine analogues. **4d** was chosen as the model compound, because its insertion reaction with bromine gave a moderate to low yield, which provided an opportunity for its chlorine and iodine analogues to expose their differential reactivity. The halogenation reactions were carried out using DBU/NXS (X = Cl, Br, I) and proceeded similarly to the bromination reactions.

Table 4.5: Yields^a in % of *trans/cis-tert-butyl* 7-halo-8-oxo-1,4-diazabicyclo[4.2.0]octane-4-carboxylate **X-4e** (X = Cl, Br, I) obtained from the thermolysis of α -chloro-, α -bromo- and α -iodo-*tert-butyl* 4-(2-diazoacetyl)piperazine-1-carboxylate

Compound	<i>trans/cis</i>			Total
	<i>trans</i>	<i>cis</i>	ratio	
Cl-4e	10	2	5:1	12
Br-4e ^b	34	2	17:1	36
I-4e	2	- ^c	n/a	2

^a Determined by ¹H-NMR³⁸

^b This run is independent of the run in table 4.3 on page 47

^c Not detected by ¹H-NMR

As can be observed from the table 4.5, the bromine analogue appears to be the most efficient of the substituents for this reaction. The lower yields with both the other analogues are unexpected, based on the results with the three halogen analogues in cyclopropanation reactions.^{10h} Additionally, the result with the iodine analogue might not be representative; During the preparation of the α -iodo-**4d**, the coloured solution assumed to contain the α -iododiazacetamide, eluted from the short column as normal, but did not lose its colour upon standing in ambient temperature for a period of 24 hours. After this time, the solvent was evaporated to give the result seen in table 4.5. Normally, the intense red colour of the α -bromodiazacetamides disappears to leave a transparent solution within ~ 60 minutes. This could indicate that the result of thermolysis of **I-4d** is not valid.

4.6. The scope of the thermolysis reaction beyond the intramolecular C-H insertions

It seemed of interest to substantiate whether the thermolysis reactions of α -halodiazacetic esters and amides have a potential outside the scope in which they have been used in this work. Thus, EDA was brominated following the published procedure,^{10h} styrene was added and the CH₂Cl₂ evaporated to give

the α -bromo-EDA dissolved in styrene. The solution was left to thermolyze for a few hours at ambient temperature. Then, one crystal of the radical inhibitor hydroquinone was added to keep the styrene from polymerizing, while evaporating the styrene under reduced pressure at 30 °C. The residue was run through a plug of silica gel before determining by $^1\text{H-NMR}$ ³⁸ that the reaction had afforded a 42 % yield of ethyl 1-bromo-2-phenylcyclopropanecarboxylate (*trans:cis*/1.2:1). Although not the excellent yield (91 %, *trans:cis*/9:1) obtained with dirhodium(II) catalysis,^{10h} the result holds promise for the development of a catalyst-free route to the racemic cyclopropanes in question.

In the same vein, **4d** was thermolyzed in styrene and although the reaction outcome was not quantified, the cyclopropane signals in the recorded $^1\text{H-NMR}$ spectrum are clearly visible. A trace amount of β -lactam can also be seen. The $^1\text{H-NMR}$ spectra for both of these reactions are included in the appendix. A further exploration of the range of carbenic transformations in which the α -bromocarbene esters and amides will take part, is a natural extension of this work.

5. A synthetic outlook for the α -bromo- β -lactams

Below are two brief discussions on ideas that were conceived during the planning of this work. One seeks to improve the methodology of synthesis and ease of isolation of the thermolabile halogenated diazo compounds, while the other brings the α -bromo- β -lactams further by making use of the structural complexity created by the C–H insertion reaction.

5.1. Polymer-supported *N*-halo reagents

Given the lability of the α -halodiazocarbonyl compounds, their method of preparation and isolation could benefit from the use of immobilized reagents. In the halogenation reaction described in this work, the exchange of the monomeric *N*-halo reagent for a solid phase reagent would likely be the most beneficial modification. Of the *N*-halo reagent scaffolds mentioned in section 1.3.2 on page 8, several have been immobilized on polymer supports, among them amides, imides and sulfonamides. Commonly, this is achieved by copolymerization of feedstock monomers like methacrylamide with a crosslinker and suitable comonomers. Many of these preparations have been reviewed.^{18f,16a} The polymeric material thus obtained, must then be treated with e.g. aqueous hypohalites to give the *N*-halo polymers. Given that the halogenation reaction with a given solid phase reagent proceeds similarly to the reaction with the monomeric reagents, the work-up procedure would be simplified, requiring only to separate the highly polar base from the produced α -halodiazocarbonyl compound, after filtering off the polymeric material. This separation could be achieved using a cooled short column, as done in this work.

5.2. Coupling with indole structures

Assuming that the α -halo- β -lactams are fairly hydrolytically stable, and not active inhibitors of β -lactamase, they would seem to have little future as penicillin analogues. Consequently, the employment of their structural features must be reviewed. In the beginning of this work, the idea was conceived that the amide nitrogen in the α -halo- β -lactams could be used as a source of a "biogenic amine" in the synthesis new compounds similar to known neurotransmitters in the tryptamine family (including serotonin), by the coupling of the α -halo- β -lactams and the 3-position of substituted indole structures. The coupling can be accomplished using the potential coupling point, constituted by the α -halocarbonyl moiety, which is presumably a potent electrophile with respect to the α carbon.

The coupling ideally establishes a two carbon distance between an indole aromatic system and the amide nitrogen, which upon either reduction of the carbonyl group, or hydrolysis, becomes an amine. The resulting structures contain highly conserved motifs that are found in many endogenous and synthetic agonists and inverse agonists of class A G-protein coupled receptors (GPCRs) throughout the body (e.g. the serotonin receptors).

To create variation in the side chain, while maintaining the "privileged" indole moiety in its endogenous form, is sensible because it is the aromatic moiety, together with the amine nitrogen itself, which are the most highly conserved elements, and that confer the general compatibility with this class of receptors. Variations in the side chain and its substituents, are in turn thought to confer selectivity through interactions with residues in the binding pocket whose arrangement is subtype-specific. The utilization of motifs that are highly conserved, can also be a route to multipotent drugs (dirty drugs), that is compounds with activity in more than one receptor subtype.³⁹

The necessary coupling can be achieved through a polar pathway,^{28e} or perhaps more likely, a radical pathway.⁴⁰ There is also the possibility of using transition metal catalyzed cross-coupling methodology.

An outlook to target compounds in the proposed coupling strategy and

beyond is shown in figure 5.1 on the next page. In the figure, two pathways to render the free amine after coupling are proposed, as well as an alternative use of the amine, resulting in structural analogues of ergoline:

- A** A hydrolytic pathway
(to *beta*-tryptophan analogues)

- B** A hydrolytic pathway followed by Buchwald-Hartwig amination
(to 10-azaergoline derivatives)

- C** A reductive pathway
(to caged-amine analogues of tryptamine and serotonin)

Of the compounds listed in figure 5.1 on the following page, very few are reported.¹⁵

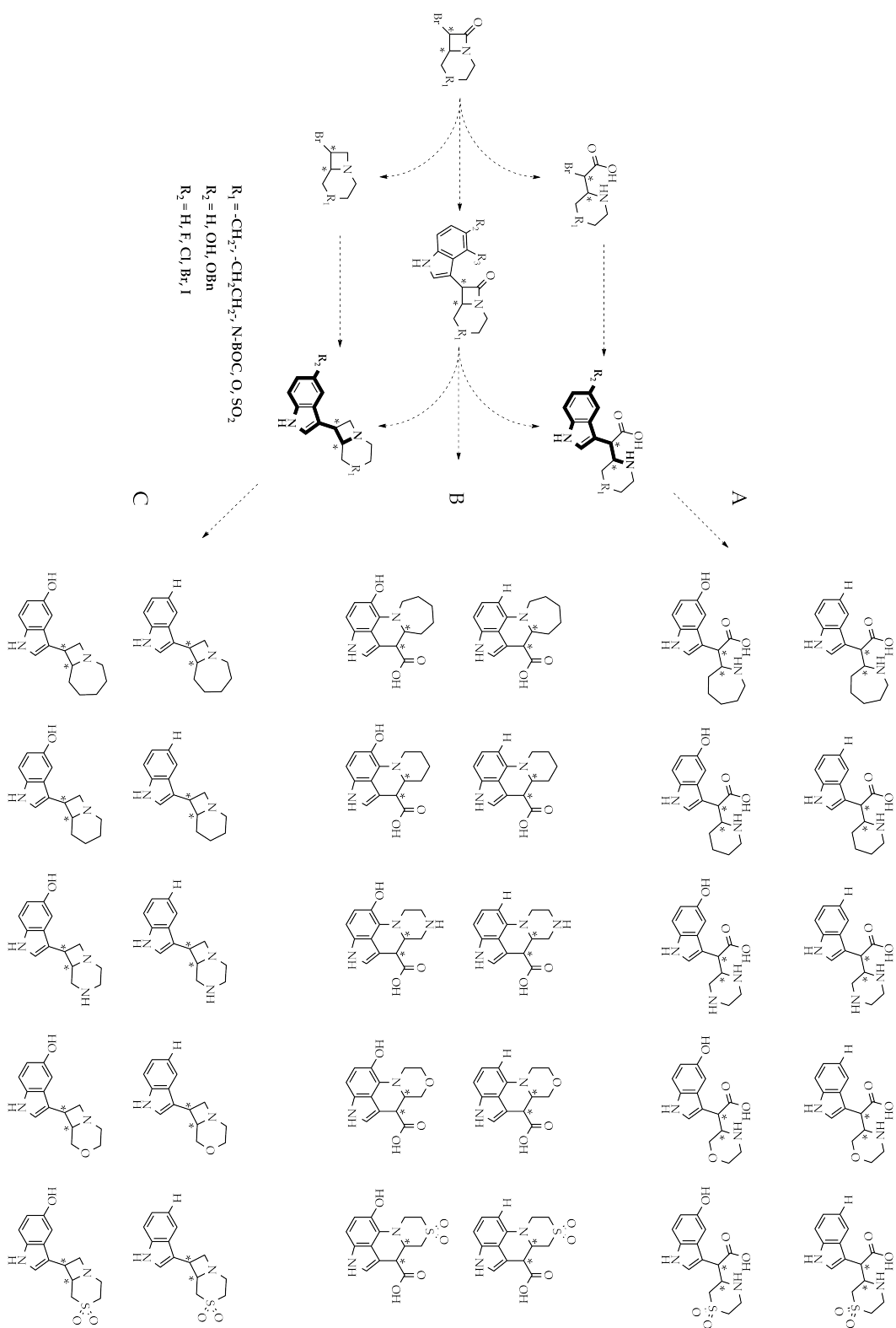


Figure 5.1.: Target compounds following the proposed coupling strategy and beyond

Part III.

**Experimental Procedures and
Physical Data**

6. General introduction to the experimental section

All commercially available reagents and solvents were used as received except in the cases where purification was necessary to ensure the purity of a reagent. The CH_2Cl_2 used in the acylation of the amines and in the dediazotization reactions was obtained from an MBraun MB SPS-800 solvent purification system and is dry, but more importantly free of alcoholic stabilizers. Regular, stabilized CH_2Cl_2 does not inhibit the reactions in question, but traces of ethyl esters (O-acylation) and ethyl ethers (carbene O-H insertion product) have been observed spectroscopically when running the reactions in stabilized CH_2Cl_2 .

The prepared *N*-bromo compounds and diazo compounds were stored in a freezer at $-20\text{ }^\circ\text{C}$ to ensure their integrity and were left in ambient temperature for about 5 minutes before exposing them to air in order to minimize weighing errors caused by condensed water.

Except for the above stated routine, no special precautions were taken to exclude air or airborne moisture at any point during the syntheses described in this work, except in the acylation reactions where it was clearly detrimental. Inert atmosphere (Ar or N_2) is used only where stated specifically (acylations, catalyzed reactions and free radical polymerization reactions). Stirring refers to magnetic stirring in all the procedures. Heating was performed with fluoropolymer-coated all-metal heating mantles.

Chromatography was performed on silica gel (Merck 60, 40-63 μm) and thin layer chromatography (TLC) on aluminium sheets coated with silica gel (Fluka 6607780, 20 mm, fluorescent coating for 254 nm) or neutral alumina (Macherey Nagel Alugram Alox N, 0.20 mm, unactivated, no fluorescent coating). The plates were visualized with KMnO_4 , K_2CO_3 and NaOH in water

for the α -bromo amides (alumina) and UV-light and/or a solution of *p*-anisaldehyde, concentrated H₂SO₄ and glacial CH₃CO₂H in 96% EtOH for the α -diazoacetamides (silica gel), followed by heating with a heat gun for both. The β -lactams (alumina) were visualized with a solution of ninhydrin and pyridine in absolute EtOH followed by heating or with a solution containing AgNO₃, H₂O, 2-phenoxyethanol, acetone and H₂O₂ (30 %, aq) followed by exposing the plate to UV-light for about 10 minutes.

Nuclear magnetic resonance (NMR) spectroscopy was performed on Bruker DXP200/DXP300 spectrometers operating at 200/300 MHz for ¹H and 75/50 MHz for ¹³C, and on a Bruker DXP200 operating at 81 MHz for ³¹P. The chemical shifts are reported in parts per million (δ) relative to the residual solvent signal in general accordance with the literature:⁴¹ δ -¹H/ δ -¹³C (Solvent); 7.26/77.00 (CDCl₃), 5.32/53.80 (CD₂Cl₂), 2.50/39.52 (DMSO-*d*₆) and 1.94/118.26 (CD₃CN). Chemical shifts are given in the section for physical data for each compound. Additionally, the spectra for the reported compounds are included in the appendix where their signals are assigned to numbered structures appearing on each spectrum, based on the information gained from the performed NMR experiments. The NMR data were processed with ACD/Labs NMR Processor Academic Edition.

Mass spectrometry experiments were carried out with a Fisons VG ProSpec for electron impact ionization (EI) and a Micromass Q-TOF 2 or a Bruker Apex FTMS (FT-ICR, 4.7 T) for electrospray ionization (ESI). The results from the two instruments are marked (ESI, Q-TOF) and (ESI, FT-ICR), respectively. The solvent used and other essential details are noted in each case.

Melting points were taken a Stuart SMP10 (Barloworld Scientific Ltd., UK).

X-ray diffraction crystallography was performed using a Bruker axs Smart Apex II CCD D8 diffractometer with an installed temperature control system. Coordinates were refined for H-atoms involved in H-bonding. Other H-atoms were positioned with idealized geometry. The available crystallographic data for the unpublished structures are included in the appendix, as well as the publication of the structure of **4c**.

7. Synthesis of *N*-bromo compounds and *N,N'*-ditosylhydrazine

7.1. *N*-bromo-2-pyrrolidone

N-bromo-2-pyrrolidone was prepared by extending a procedure published by Souza *et. al*⁴² for the preparation of *N*-chloro- and *N*-bromosaccharin. The original procedure is modified by an additional 0.25 eq of Na₂CO₃.

2-pyrrolidone is freely soluble in water and the reaction proceeds with only barely visible yellow/orange colour of free bromine upon addition of the oxidant (see the synthesis of *N*-Bromosaccharin for some general details about the reaction).

The *N*-bromo-2-pyrrolidone was recrystallized from EtOAc/Et₂O (2:1). It is apparently stable in the dark at -20 °C and no appreciable yellowing occurred over months of storage, however at 4 °C this occurs over weeks, which is in coherence with the literature.⁴³ The IR spectrum is in accordance with that published by Parsons.⁴⁴

7.1.1. Experimental procedure

2-pyrrolidone (17.50 g, 205.7 mmol, 1.0 eq), Na₂CO₃ (16.36 g, 154.3 mmol, 0.75 eq) and KBr (24.47 g, 205.7 mmol, 1.0 eq) were added to a 1000 mL round bottom flask followed by H₂O (Type II, 300 mL). The flask was cooled on an ice/water bath for 5 minutes, after which potassium peroxydisulfate (as its triple salt 2 KHSO₅ · KHSO₄ · K₂SO₄, oxone®) (126.5 g, 205.7 mmol, 1.0 eq)

suspended in H₂O (Type II, 200 mL) was added in small aliquots, with vigorous stirring (700 pm), over a period of 10 minutes. The colour change towards yellow for each addition was minimal and the solution rapidly turned back into a white suspension. Care was taken towards the end of the addition, as the white suspension frothed and increased its volume for each addition. The cooling bath was removed and the flask wrapped in aluminium foil, allowing the suspension to stir in the dark for period of 19 hours. The light yellow suspension was extracted with CH₂Cl₂ (8 × 50 mL), and the combined organic phases evaporated under reduced pressure, at or below ambient temperature, leaving a white solid. The solid was dissolved in EtOAc (100 mL) and Et₂O (50 mL) was added without the solution becoming turbid. Upon standing overnight the solution deposited 10.87 g (32 %) of clear prisms (1 × 1 mm – 3 × 3 mm).

7.1.2. Physical data

- ¹H-NMR (300 MHz, CDCl₃) δ 3.58 – 3.00 (m, 2H), 2.36 – 2.26 (m, 2H), 2.24 – 2.09 (m, 2H)
- ¹³C-NMR (75 MHz, CDCl₃) δ 174.2, 53.3, 26.5, 19.8
- Melting point: 95 – 100 °C (EtOAc/Et₂O, melting, then decomposition) (lit. 95 °C⁴³)
- FTIR (KBr) $\tilde{\nu}/\text{cm}^{-1}$ (intensity); 3320 (w), 2986 (m), 2963 (m), 2925 (m), 2894 (m), 1685 (vs), 1653 (vs), 1486 (m), 1451 (m), 1383 (s), 1258 (s), 1223 (m), 1204 (m), 1174 (m), 1122 (m), 1015 (m), 923 (w), 817 (m), 708 (m), 623 (m), 553 (w), 530 (m)

7.2. N-bromosuccinimide

N-bromosuccinimide was purchased from Sigma-Aldrich and recrystallized from boiling water to give thin transparent plates in accordance with the literature.⁴⁵

7.3. *N*-bromophthalimide

N-bromophthalimide was prepared from phthalimide by extending a procedure published by Souza *et. al*⁴² for the preparation of *N*-chloro- and *N*-bromosaccharin. The original procedure is modified by an additional 0.25 eq of Na₂CO₃ (see the synthesis of *N*-Bromosaccharin for some general details about the reaction).

The reaction proceeds noticeably slower than in the case of sodium saccharin or 2-pyrrolidone, possibly due to the fairly low solubility of phthalimide even in basic water. Another consequence of this is a prolonged and more visible release of bromine. As the consumption of the released bromine is slower than with saccharin, it is necessary to close the reaction vessel with a glass stopper to contain the evolution of bromine gas. The yield was 65 %, comparable to the yield of *N*-bromosaccharin. The obtained spectroscopic data were in correspondence to published data, although with a lower melting point, possibly owing to the fact that the recrystallization from toluene left a slightly amorphous crystal mass.

7.3.1. Experimental procedure

Phthalimide (7.36 g, 50.0 mmol, 1.0 eq), Na₂CO₃ (3.98 g, 37.6 mmol, 0.75 eq) and KBr (5.95 g, 50.0 mmol, 1.0 eq) were added through a solid addition funnel to a 500 mL round bottom flask followed by H₂O (Type II, 200 mL). The flask was cooled on an ice/water bath for 10 minutes, after which potassium peroxymonosulfate (as its triple salt 2 KHSO₅ · KHSO₄ · K₂SO₄, oxone®) (30.8 g, 50.1 mmol, 1.0 eq) suspended in H₂O (Type II, 75 mL) was added in small aliquots, with vigorous stirring (700 rpm), over a period of 10 minutes. The addition of the oxidant resulted in vigorous release of bromine gas, and thus the flask was capped with a glass stopper between additions. The mixture quickly turned into an orange spongelike suspension with visible bromine gas above it. The suspension was left to stir for 24 hours, at which point it had become a yellow solution with a white precipitate. Stirring was continued another 24 hours, until the solution above the precipitate was almost clear. The suspension

was filtered on a Büchner-funnel and the filter cake sucked dry for a period of 30 minutes. The white precipitate was dissolved in boiling toluene (150 mL), hot filtered into a beaker and left to cool slowly to ambient temperature, covered with an aluminium foil. Upon reaching ambient temperature, precipitation had begun and the beaker was placed in a refrigerator at 4 °C for a period of 17 hours, before filtering the precipitate on a Büchner-funnel. The filter cake was washed with *n*-pentane (30 mL) to give 6.52 g (57 %) of small white crystals. The mother liquor was concentrated, filtered and the filter cake washed with toluene (5 mL) and *n*-pentane (10 mL) to give 0.91 g (8 %). Both crops were of equal purity by ¹H-NMR. The total yield was 65%.

7.3.2. Physical data

- ¹H-NMR (200 MHz, CDCl₃) δ 7.95 – 7.81 (m, 2H), 7.81 – 7.68 (m, 2H) (Ref. ⁴⁶)
- Melting point: 176 – 184 °C (C₆H₅CH₃, decomposition)
(lit. 199 – 200 °C, ⁴⁶ CH₂Cl₂)

7.4. N-bromosaccharin

N-bromosaccharin was prepared in 55 % yield following a procedure published by Souza *et. al*⁴² in which bromine is generated *in situ* by oxidation of KBr in water. The spectroscopic data obtained was in accordance with that published.

7.4.1. Experimental procedure

Sodium-saccharin (8.21 g, 40.0 mmol, 1.0 eq), Na₂CO₃ (2.12 g, 20.0 mmol, 0.5 eq) and KBr (4.77 g, 40.1 mmol, 1.0 eq) were added through a solid addition funnel to a 250 mL round bottom flask followed by H₂O (Type II, 100 mL). The flask was cooled on an ice/water bath for 10 minutes, after which potassium peroxymonosulfate (as its triple salt 2KHSO₅ · KHSO₄ · K₂SO₄, oxone®) (24.6 g, 40.0 mmol, 1.0 eq) suspended in H₂O (Type II, 80 mL) was added in small

aliquots, with vigorous stirring (700 rpm), over a period of 10 minutes, and the flask loosely capped with a glass stopper. During the addition the clear solution turned to a yellow and then orange voluminous suspension. The colour returned to light yellow as the released bromine was consumed. The cooling bath was allowed to melt and stirring was continued for period of 23 hours. The suspension was filtered on a Büchner-funnel and the filter cake washed with H₂O (Type II, 2 × 100 mL), leaving a white powder. The powder was dried in the dark in a fume hood for 24 hours after which it weighed 5.77 g (55 %)

7.4.2. Physical data

- Melting point: 174 – 180 °C
(lit. 165 – 167 °C,⁴² 170 – 172 °C⁴⁷)
- FTIR (KBr) $\tilde{\nu}/\text{cm}^{-1}$ (intensity); 3404 (w), 3094 (m), 3072(w), 1709 (vs), 1671 (m), 1637 (m), 1588 (m), 1465 (m), 1456 (m), 1352 (s), 1287 (s), 1231 (s), 1191 (s), 1168 (s), 1136 (s), 1121 (s), 949 (s), 784 (s), 748 (s), 722 (m), 671 (s), 657 (m), 574 (s), 525 (m), 496 (s)

7.5. *N,N'*-ditosylhydrazine

7.5.1. Synthesis route and comments

N,N'-ditosylhydrazine was synthesized in 92 % yield in one step by the reaction of tosylhydrazine with tosyl chloride in the presence of pyridine, as described by Toma *et al.*,^{31a} albeit with a slight modification of the work-up procedure. The modified procedure requires less methanol than in the original procedure, making the work-up easier and safer to perform on a preparative scale (~ 100 g), without compromising the purity of the isolated product.

The reaction has been performed once following the original procedure, with a yield comparable to that reported. The procedure was originally performed on a 50 mmol scale and employed a recrystallization from 400 mL of boiling MeOH as the final purification step. The yield was 15 g (85 %).

In the modified work-up procedure, the crude precipitate (see experimental details below) is simply slurried in methanol at reflux, lowering the expenditure of MeOH considerably.

The reaction could thus be performed at various scales with a low methanol expenditure:

Scale (mmol)	MeOH volume (mL)	Yield (g)	Yield (%)
100	400	31	92
192	500	61	93
300	800	95	93
350	900	109	92

The $^1\text{H-NMR}$ and $^{13}\text{C-NMR}$ spectra of the obtained products were identical to those of the product obtained using the original procedure, and are in accordance with the published spectroscopic data. An X-ray structure can also be found in the literature.⁴⁸

7.5.2. Experimental procedure

Tosyl chloride (100.0 g, 524.5 mmol, 1.5 eq) and tosylhydrazide (65.12 g, 349.7 mmol, 1.0 eq) were added to a 1000 mL round-bottom flask through a solid addition funnel, and dissolved/suspended in anhydrous CH_2Cl_2 (250 mL), giving a concentration of approximately 1 M based on the limiting reactant. An oval stir bar (3.5 × 1.5 cm) was added and the suspension stirred (700 rpm) while cooling on an ice/water bath, until an internal temperature of 3 °C was reached. Addition of a solution of pyridine (41.49 g, 524.5 mmol, 1.5 eq) in anhydrous CH_2Cl_2 (80 mL) over a period of 10 minutes, in such a way that the internal temperature did not rise above 20 °C. This gave a transparent yellow solution which soon deposited a white precipitate, upon which stirring was increased to 1000 rpm, and continued for a period of 3 hours.

Et_2O (200 mL) was added and the suspension solidified. The heavy precipitation was broken up with a spatula and the suspension was transferred to a 1500 mL beaker, where it was stirred with a triangular stir bar (5 × 1 × 1 cm). H_2O

(Type II, 200 mL) and Et₂O (200 mL) was added in the given order. Stirring was continued for 10 minutes, before filtering the precipitate on a 13 cm Büchner-funnel, where it was left to air dry with suction for a period of 5 minutes.

The solid was transferred directly to a 2000 mL round bottom flask and suspended in MeOH (900 mL). The flask was equipped with a reflux-condenser and an oval stir bar (5 × 2 cm) before heating the suspension to reflux (mantle temperature 67 °C) and stirring for a period of 3 hours. The suspension, which at this point would separate to slightly yellow solution above a bright white precipitate, was allowed to cool before filtering on a 13 cm Büchner-funnel. The filter cake was washed with MeOH (300 mL) and Et₂O (300 mL). The filtrate was then concentrated on a rotary evaporator (bath temperature ~ 45 °C) to a volume of approximately 150 mL, before cooling the flask under running tap water. The precipitate was filtered on a Büchner-funnel, washed with MeOH (200 mL) and Et₂O (200 mL) giving a second crop. The first crop was a voluminous white powder, while the second more crystalline crop consists of short white needles. Both crops were dried in air in a fume hood over a period of 48 hours before determining the yield. Crop I: 97.60 g (81 %), crop II: 12.34 g (10 %). The total yield was 109.94 g (92 %). Both crops were of equal purity by NMR analysis and were subsequently mixed and stored in a screw-capped PTFE jar at ambient temperature.

7.5.3. Physical data

- ¹H-NMR (300 MHz, DMSO-d₆) δ 2.40 (s, 6H), 7.37 – 7.40 (m, 4H), 7.64 – 7.67 (m, 4H), 9.59 (s, 2H)
- ¹³C-NMR (75 MHz, DMSO-d₆) δ 21.0, 127.8, 129.4, 135.5, 143.4
- Melting point: 212 – 215 °C (decomposition)

8. α -bromoacetamides

8.0.4. Synthesis route and comments

The α -bromoacetamides were synthesized by the slow addition of the amine in CH_2Cl_2 (20 mmol/30 mL) to bromoacetyl bromide and tribasic potassium phosphate in CH_2Cl_2 . The procedure was based on a recent publication where the authors have optimized the formation of amides from amines and acid chlorides with respect to the base.^{31c}

8.1. 2-bromo-1-(pyrrolidin-1-yl)ethanone (1b)

8.1.1. Experimental procedure

A 250 mL round bottom flask was charged, in the given order, with bromoacetyl bromide (6.061 g, 30.02 mmol, 1.5 eq), anhydrous CH_2Cl_2 (20 mL) and K_3PO_4 (10.63 g, 50.05 mmol, 2.5 eq). An oval stir bar (3.5 × 1.5 cm) was added and the flask was fitted with a 100 mL addition funnel, containing pyrrolidine (1.423 g, 20.01 mmol, 1 eq) in anhydrous CH_2Cl_2 (30 mL). The flask was cooled on an ice/water bath, while purging the system with argon, for a period of 5 minutes. Stirring (500 rpm) was commenced and the amine solution added drop wise over a period of 30 minutes, after which the addition funnel was washed with anhydrous CH_2Cl_2 (5 mL). Stirring was then continued for a period of 165 minutes, before quenching the excess acid bromide with aqueous HCl (0.5 M, 30 mL). After stirring another 5 minutes, H_2O (10 mL) and brine (10 mL) were added and the now transparent two phases transferred to a separatory funnel and the organic phase drained off. The aqueous phase was extracted with CH_2Cl_2

(1 × 20 mL), before washing the joint organic phases with a mixture of aqueous KHCO_3 (10 %wt, 20 mL) and brine (10 mL), and then with brine (20 mL). Drying over MgSO_4 and evaporating under reduced pressure at 30 °C bath temperature, afforded 3.466 g (90 %) of a slightly brown oil which crystallized upon cooling to ambient temperature. The crude material was stored at –20 °C for period of approximately 70 days before being submitted to the next synthetic step.

8.1.2. Physical data

- $^1\text{H-NMR}$ (300 MHz, CDCl_3) δ 3.77 (s, 2H), 3.51 – 3.42 (m, 4H), 2.03 – 1.80 (m, 4H)
- $^{13}\text{C-NMR}$ (75 MHz, CDCl_3) δ 164.9, 46.9, 46.3, 27.3, 26.0, 24.2
- MS (EI) m/z (% rel. int.) 193/191 (M^+ , 16/16), 121/123 (4/4), 112 (100), 98 (81), 93/95 (6/6), 70 (48)
- HRMS (EI) Calcd. for $\text{C}_6\text{H}_{10}^{79}\text{BrNO}$ [M^+]: 190.9946; found 190.9950 (–2.2 ppm)
- TLC (Al_2O_3 (N), 1 × CH_2Cl_2) R_f : 0.35

8.2. 2-bromo-1-(piperidin-1-yl)ethanone (2b)

8.2.1. Experimental procedure

A 250 mL round bottom flask was charged, in the given order, with bromoacetyl bromide (12.162 g, 60.25 mmol, 1.5 eq), anhydrous CH_2Cl_2 (40 mL) and K_3PO_4 (21.248 g, 100.09 mmol, 2.5 eq). An oval stir bar (3.5 × 1.5 cm) was added and the flask was fitted with a 100 mL addition funnel, containing piperidine (3.407 g, 40.01 mmol, 1 eq) in anhydrous CH_2Cl_2 (60 mL). The flask was cooled on an ice/water bath, while purging the system with argon, for a period of 5 minutes. Stirring (500 rpm) was commenced and the amine solution added drop wise

over a period of 2.5 hours, after which the addition funnel was washed with anhydrous CH₂Cl₂ (5 mL). Stirring was then continued for a period of 4 hours, before quenching the excess acid bromide with aqueous HCl (0.5 M, 60 mL). After stirring another 5 minutes, the now transparent two phases were transferred to a separatory funnel and the organic phase drained off. The aqueous phase was extracted with CH₂Cl₂ (1 × 20 mL), before washing the joint organic phases with a mixture of aqueous KHCO₃ (10 %wt, 50 mL) and brine (20 mL). The aqueous phase was back-extracted with CH₂Cl₂ (1 × 20 mL) and the joint organic phases were washed with brine (40 mL). Drying over MgSO₄ and evaporating under reduced pressure at or below ambient temperature, afforded 7.750 g (94 %) of a slightly yellow oil. The crude material solidified to a peach crystalline solid upon storage at −20 °C.

8.2.2. Physical data

- ¹H-NMR (300 MHz, CDCl₃) δ 3.84 (s, 2H), 3.57 – 3.49 (m, 2H), 3.46 – 3.36 (m, 2H), 1.69 – 1.59 (m, 4H), 1.59 – 1.48 (m, 2H)
- ¹³C-NMR (75 MHz, CDCl₃) δ 165.0, 47.8, 43.2, 26.1, 26.1, 25.3, 24.2
- MS (EI) *m/z* (% rel. int.) 207/205 (M⁺, 4/4), 126 (100), 123/121 (3/4), 112 (20), 95/93 (2/2), 84 (18)
- MS (ESI, Q-TOF) (MeOH) *m/z* 230.0/228.0 [M + Na]⁺, 208.0/206.0 [M + H]⁺
- HRMS (EI) Calcd. for C₇H₁₂⁷⁹BrNO [M⁺]: 205.0102; found 205.0104 (−1.0 ppm)
- TLC (Al₂O₃ (N), 1 × CH₂Cl₂) R_f: 0.54

8.3. 1-(azepan-1-yl)-2-bromoethanone (3b)

8.3.1. Experimental procedure

A 250 mL round bottom flask was charged, in the given order, with bromoacetyl bromide (6.064 g, 30.04 mmol, 1.5 eq), anhydrous CH₂Cl₂ (20 mL) and K₃PO₄ (10.621 g, 50.03 mmol, 2.5 eq). An oval stir bar (3.5 × 1.5 cm) was added and the flask was fitted with a 100 mL addition funnel, containing azepane (hexamethyleneimine) (1.985 g, 20.01 mmol, 1 eq) in anhydrous CH₂Cl₂ (30 mL). The flask was cooled on an ice/water bath, while purging the system with argon, for a period of 5 minutes. Stirring (500 rpm) was commenced and the amine solution added drop wise over a period of 60 minutes, after which the addition funnel was washed with anhydrous CH₂Cl₂ (5 mL). Stirring was then continued for a period of 3.5 hours, before quenching the excess acid bromide with aqueous HCl (0.5 M, 30 mL). After stirring another 5 minutes, H₂O (10 mL) and brine (10 mL) were added and the now transparent two phases transferred to a separatory funnel and the organic phase drained off. The aqueous phase was extracted with CH₂Cl₂ (1 × 20 mL), before washing the joint organic phases with a mixture of aqueous KHCO₃ (10 %wt, 30 mL) and brine (10 mL), and then with brine (20 mL). Drying over MgSO₄ and evaporating under reduced pressure at 25 °C, afforded 4.151 g (94 %) of a transparent oil. The crude material was stored at -20 °C for period of approximately 30 days before being submitted to the following synthetic step.

8.3.2. Physical data

- ¹H-NMR (300 MHz, CDCl₃) δ 3.84 (s, 2H), 3.54 – 3.42 (m, 4H), 1.82 – 1.62 (m, 4H), 1.62 – 1.47 (m, 4H)
- ¹³C-NMR (75 MHz, CDCl₃) δ 166.3, 48.5, 46.3, 28.9, 27.2, 27.1, 26.4, 26.4
- MS (EI) *m/z* (% rel. int.) 221/219 (M⁺, 1/1), 140 (100), 126 (7), 123/121 (2/3), 98(8), 95/93 (2/2)

- HRMS (EI) Calcd. for C₈H₁₄⁷⁹BrNO) [M⁺]: 219.0259; found 219.0257 (0.6 ppm)
- TLC (Al₂O₃ (N), 1 × CH₂Cl₂) R_f: 0.45

8.4. *tert-butyl 4-(2-bromoacetyl)piperazine-1-carboxylate (4b)*

8.4.1. Experimental procedure

A 250 mL round bottom flask was charged, in the given order, with bromoacetyl bromide (6.099 g, 30.21 mmol, 1.5 eq), anhydrous CH₂Cl₂ (20 mL) and K₃PO₄ (10.632 g, 50.08 mmol, 2.5 eq). An oval stir bar (3.5 × 1.5 cm) was added and the flask was fitted with a 100 mL addition funnel, containing *tert-butyl piperazine-1-carboxylate* (3.725 g, 20.00 mmol, 1 eq) in anhydrous CH₂Cl₂ (30 mL). The flask was cooled on an ice/water bath, while purging the system with argon, for a period of 5 minutes. Stirring (500 rpm) was commenced and the amine solution added drop wise over a period of 30 minutes, after which the addition funnel was washed with anhydrous CH₂Cl₂ (5 mL). Stirring was then continued for a period of 2 hours, before quenching the excess acid bromide with aqueous HCl (0.5 M, 30 mL). After stirring another 5 minutes, H₂O (10 mL) and brine (10 mL) were added and the now transparent two phases transferred to a separatory funnel and the organic phase drained off. The aqueous phase was extracted with CH₂Cl₂ (1 × 20 mL), before washing the joint organic phases with a mixture of aqueous KHCO₃ (10 %wt, 20 mL) and brine (10 mL), and then with brine (20 mL). Drying over MgSO₄ and evaporating under reduced pressure at or below ambient temperature, left an oil which upon addition of Et₂O (10 mL) and reevaporation, afforded 5.885 g (95 %) of a white solid. The crude material was stored at –20 °C for period of approximately 70 days before being submitted to the following synthetic step.

8.4.2. Physical data

- ¹H-NMR (300 MHz, CDCl₃) δ 3.85 (s, 2H), 3.62 – 3.38 (m, 8H), 1.45 (s, 9H)
- ¹³C-NMR (75 MHz, CDCl₃) δ 165.4, 154.4, 80.4, 46.5 (2C), 41.9 (2C), 28.3 (3C), 25.6
- MS (EI) *m/z* (% rel. int.) 308/306 (M⁺, 4/4), 252/250 (9/9), 235/233 (9/9), 207/205 (2/1), 171 (22), 170 (37), 127 (16), 123/121 (3/3), 113 (14), 95/93 (1/2), (85 (35), 57 (100)
- HRMS (EI) Calcd. for C₁₁H₁₉⁷⁹BrN₂O₃ [M⁺]: 306.0579; found 306.0587 (–2.7 ppm)
- TLC (Al₂O₃ (N), 1 × CH₂Cl₂) R_f: 0.14

8.5. *N,N'*-bis(2-bromoacetyl)piperazine (5b)

8.5.1. Experimental procedure

A 250 mL round bottom flask was charged, in the given order, with bromoacetyl bromide (6.088 g, 30.16 mmol, 3 eq), anhydrous CH₂Cl₂ (20 mL) and K₃PO₄ (10.649 g, 50.16 mmol, 5 eq). An oval stir bar (3.5 × 1.5 cm) was added and the flask was fitted with a 100 mL addition funnel, containing piperazine (0.865 g, 10.05 mmol, 1 eq) in anhydrous CH₂Cl₂ (40 mL). The flask was cooled on an ice/water bath, while purging the system with argon, for a period of 5 minutes. Stirring (500 rpm) was commenced and the amine solution added drop wise over a period of 2.5 hours, after which the addition funnel was washed with anhydrous CH₂Cl₂ (3 × 5 mL). Stirring was then continued for a period of 5 hours, before quenching the excess acid bromide with aqueous HCl (0.5 M, 30 mL). After stirring another 5 minutes, H₂O (10 mL) and brine (10 mL) were added and the now transparent two phases transferred to a separatory funnel and the organic phase drained off. The aqueous phase was extracted with CH₂Cl₂ (1 × 20 mL), before washing the joint organic phases with a mixture of

aqueous KHCO_3 (10 %wt, 30 mL) and brine (10 mL), and then with brine (20 mL). Drying over MgSO_4 and evaporating under reduced pressure at or below ambient temperature afforded 2.746 g (83 %) of a white solid. The crude material was stored at $-20\text{ }^\circ\text{C}$ for period of approximately 15 days before being submitted to the following synthetic step.

8.5.2. Physical data

- $^1\text{H-NMR}$ (300 MHz, CDCl_3) δ 3.88 (s, 4H), 3.78 – 3.46 (m, 8H)
- $^{13}\text{C-NMR}$ (75 MHz, CDCl_3) δ 165.6 (2C), 46.3, 46.1, 41.8, 41.6, 25.3 (2C)
- MS (EI) m/z (% rel. int.) 330/328/326 (M^+ , 2/4/2), 249/247 (39/40), 248/246 (35/33), 235/233 (12/12), 207/205 (20/21), 168 (8), 127 (7), 123/121 (11/11), 113 (11), 95/93 (8/8), 85 (100)
- HRMS (EI) Calcd. for $\text{C}_8\text{H}_{12}\text{Br}_2^{79}\text{N}_2\text{O}_2$ [M^+]: 325.9266; found 325.9256 (3.1 ppm)
- TLC (Al_2O_3 (N), $1 \times \text{CH}_2\text{Cl}_2$) R_f : 0.20

8.6. 2-bromo-1-morpholinoethanone (6b)

8.6.1. Experimental procedure

A 250 mL round bottom flask was charged, in the given order, with bromoacetyl bromide (6.181 g, 30.62 mmol, 1.5 eq), anhydrous CH_2Cl_2 (20 mL) and K_3PO_4 (10.625 g, 50.05 mmol, 2.5 eq). An oval stir bar (3.5 \times 1.5 cm) was added and the flask was fitted with a 100 mL addition funnel, containing morpholine (1.7423 g, 20.00 mmol, 1 eq) in anhydrous CH_2Cl_2 (30 mL). The flask was cooled on an ice/water bath, while purging the system with argon, for a period of 5 minutes. Stirring (500 rpm) was commenced and the amine solution added drop wise over a period of 30 minutes, after which the addition funnel was

washed with anhydrous CH₂Cl₂ (5 mL). Stirring was then continued for a period of 2 hours, before quenching the excess acid bromide with aqueous HCl (0.5 M, 30 mL). After stirring another 5 minutes, H₂O (10 mL) and brine (10 mL) were added and the now transparent two phases transferred to a separatory funnel and the organic phase drained off. The aqueous phase was extracted with CH₂Cl₂ (1 × 20 mL), before washing the joint organic phases with a mixture of aqueous KHCO₃ (10 %wt, 20 mL) and brine (10 mL), and then with brine (20 mL). Drying over MgSO₄ and evaporating under reduced pressure at or below ambient temperature afforded 3.737 g (89 %) of a slightly brown oil which solidified upon refrigeration. The crude material was stored at -20 °C for period of approximately 60 days before being submitted to the following synthetic step.

8.6.2. Physical data

- ¹H-NMR (300 MHz, CDCl₃) δ 3.83 (s, 2H), 3.75 – 3.64 (m, 4H), 3.64 – 3.56 (m, 2H), 3.54 – 3.47 (m, 2H)
- ¹³C-NMR (75 MHz, CDCl₃) δ 165.3, 66.5, 66.3, 47.1, 42.3, 25.4
- MS (EI) *m/z* (% rel. int.) 209/207 (M⁺, 21/21), 194/192 (14/15), 128 (100), 123/121 (14/14), 114 (16), 95/93 (5/5), 86 (79)
- HRMS (EI) Calcd. for C₆H₁₀⁷⁹BrNO₂ [M⁺]: 206.9895; found 206.9888 (3.5 ppm)
- TLC (Al₂O₃ (N), 1 × CH₂Cl₂) R_f: 0.37

8.7. 2-bromo-1-thiomorpholinoethanone (7b)

Upon evaporation of the dichloromethane used for extraction, the became an insoluble lacquer, possibly caused by an intermolecular reaction between the thioether and the *α*-bromo amide to form a salt (it slowly dissolved in HCl (aq, 0.5 M))

8.7.1. Experimental procedure

A 250 mL round bottom flask was charged, in the given order, with bromoacetyl bromide (6.105 g, 30.24 mmol, 1.5 eq), anhydrous CH₂Cl₂ (20 mL) and K₃PO₄ (10.625 g, 50.05 mmol, 2.5 eq). An oval stir bar (3.5 × 1.5 cm) was added and the flask was fitted with a 100 mL addition funnel, containing thiomorpholine (2.068 g, 20.04 mmol, 1 eq) in anhydrous CH₂Cl₂ (30 mL). The flask was cooled on an ice/water bath, while purging the system with argon, for a period of 5 minutes. Stirring (500 rpm) was commenced and the amine solution added drop wise over a period of 30 minutes, after which the addition funnel was washed with anhydrous CH₂Cl₂ (5 mL). Stirring was then continued for a period of 100 minutes, before quenching the excess acid bromide with aqueous HCl (0.5 M, 30 mL). After stirring another 5 minutes, H₂O (10 mL) and brine (10 mL) were added and the now transparent two phases transferred to a separatory funnel. The aqueous phase was discarded and the organic phase washed with a mixture of aqueous KHCO₃ (10 %wt, 30 mL) and brine (10 mL), and then with brine (20 mL). Drying over MgSO₄ and evaporating under reduced pressure at 30 °C left 4.375 g (97 %) of a brittle golden solid. This solid would not dissolve in CH₂Cl₂, CHCl₃, MeOH, MeCN, Et₂O or THF, however it slowly dissolved in DMSO and HCl (aq, 0.5 M). Further synthesis with this compound was not attempted.

8.8. 2-bromo-1-(1,1-dioxidothiomorpholino)ethanone (8b)

The solubility of both the amine thiomorpholine-1,1-dioxide and the obtained amide is relatively poor in CH₂Cl₂. As such, the CH₂Cl₂ volume in which the amide was initially dissolved was increased in relationship to the other analogues (7 mmol/30 mL), as well as the extraction volume (150 mL). A longer reaction time was also needed to reach full conversion.

8.8.1. Experimental procedure

A 250 mL round bottom flask was charged, in the given order, with bromoacetyl bromide (2.309 g, 11.44 mmol, 1.5 eq), anhydrous CH₂Cl₂ (20 mL) and K₃PO₄ (3.934 g, 18.53 mmol, 2.5 eq). An oval stir bar (3.5 × 1.5 cm) was added and the flask was fitted with a 100 mL addition funnel, containing thiomorpholine-1,1-dioxide (1.001 g, 7.40 mmol, 1 eq) in anhydrous CH₂Cl₂ (30 mL). The flask was cooled on an ice/water bath, while purging the system with argon, for a period of 5 minutes. Stirring (500 rpm) was commenced and the amine solution added drop wise over a period of 1 hour, after which the addition funnel was washed with anhydrous CH₂Cl₂ (5 mL). Stirring was then continued for a period of 23 hours, before quenching the excess acid bromide with aqueous HCl (0.5 M, 30 mL). After stirring another 5 minutes, the mixture was diluted with CH₂Cl₂ (100 mL) to give two transparent phases which were transferred to a separatory funnel. The aqueous phase was discarded and the organic phase washed with a mixture of aqueous KHCO₃ (10 %wt, 20 mL) and brine (10 mL), and then with brine (20 mL). Drying over MgSO₄ and evaporating under reduced pressure at or below ambient temperature, afforded 1.7328 g (91 %) of a white crystalline solid. The crude material was stored at -20 °C for period of approximately 50 days before being submitted to the following synthetic step.

8.8.2. Physical data

- ¹H-NMR (300 MHz, CD₃CN) δ 4.06 (s, 2H), 4.01 – 3.86 (m, 4H), 3.20 – 2.96 (m, 4H)
- ¹³C-NMR (75 MHz, CD₃CN) δ 163.2, 52.3, 52.1, 45.7, 41.6, 27.8
- MS (EI) *m/z* (% rel. int.) 257/255 (M⁺, 1/1), 193/191 (1/1), 192/190 (2/2), 176 (41), 162 (9), 134 (45), 123/121 (14/14), 112 (100), 95/93 (8/9), 70 (44)
- HRMS (EI) Calcd. for C₆H₁₀⁷⁹BrNO₃S [M⁺]: 254.9565; found 254.9565 (-0.2 ppm)
- TLC (Al₂O₃ (N), 1 × CH₂Cl₂) R_f: 0.29

9. α -diazoacetamides

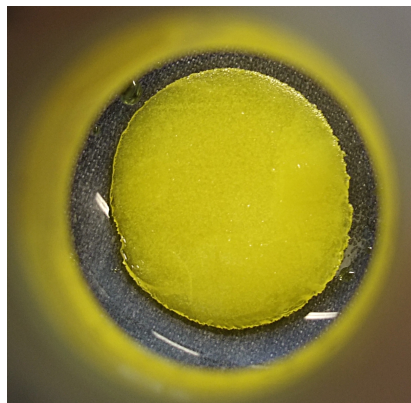
9.0.3. Synthesis route and comments

The α -diazoacetamides were synthesized by the procedure of Toma *et al.*,^{31a} modified as described in section 3.3 on page 33.

The solvent-dependent fragments observed in the mass spectrometry experiments (ESI) have (possibly) been noted by others.⁴⁹

9.1. 2-diazo-1-(pyrrolidin-1-yl)ethanone (1c)

The compound was obtained as a yellow oil at ambient temperature which solidified to a crystalline solid at -20 °C. Upon exposure to ambient temperature the solid melts within minutes. The yield was 67 % starting from 2-bromo-1-(pyrrolidin-1-yl)ethanone and 61 % starting from pyrrolidine.



The compound is previously reported in the literature.^{37b,37i}

9.1.1. Experimental procedure

To a 250 mL round bottom flask containing 2-bromo-1-(pyrrolidin-1-yl)ethanone (3.466 g, 18.05 mmol, 1 eq), were added through a solid addition funnel *N,N'*-ditosylhydrazine (12.290 g, 36.10 mmol, 2 eq), THF (35 mL) and an oval stir bar (3.5 × 1.5 cm). The suspension was cooled on an ice/water bath with stirring (400 rpm) for a period of 5 minutes, upon which a solution of 1,1,3,3-tetramethylguanidine (8.319 g, 72.23 mmol, 4 eq) in THF (5 mL) was added in aliquots using a pasteur pipette over a period of 2 minutes. During the addition the white suspension became yellow and at one point almost transparent, before depositing a white precipitate in a bright yellow solution. This suspension was stirred for a period of 60 minutes, before removing the THF under reduced pressure at or below ambient temperature. The resulting solid was treated with anhydrous Et₂O (150 mL) and vigorously stirred for 10 minutes, before being filtered on a Büchner-funnel. The filter cake was washed with anhydrous Et₂O (2 × 50 mL), leaving an almost white filter cake. The bright yellow filtrate was filtered again through a folded filter into a 500 mL round bottom flask. The Et₂O was then evaporated under reduced pressure at or below ambient temperature, to give 2.5632 g of yellow oil.

By ¹H-NMR, the oil chiefly consists of the desired product (~ 85 %wt) and the α -tosyl amide (~ 15 %wt), thus amounting to a crude yield of ~ 87 %. The oil was dissolved in Et₂O/Pet.Ether (1:1, 10 mL) and loaded onto a column (8.0 × 3.5 cm) of silica gel packed in Et₂O/Pet.Ether (1:1). Elution of one broad yellow band with Et₂O/Pet.Ether (1:1) afforded, after evaporation of the eluent, a bright yellow oil. The solvent expenditure was ~ 1.4 L. A ¹H-NMR showed that the separation of diazoacetamide from the α -tosyl amide was fairly successful, however other tosyl species, plausibly *p*-toluene sulfinic acid or *p*-toluene sulfonic acid, had eluted together with the product.

The oil was dissolved in Et₂O (100 mL), transferred to a separatory funnel and washed with a 5 %wt NaOH solution saturated with NaCl (4 × 25 mL), and then with brine (1 × 20 mL). The joint aqueous phases were placed in a beaker and saturated by adding NaCl in excess. This suspension was back-extracted by stirring vigorously with Et₂O (3 × 20 mL) and decanting the top phase into a separatory funnel, where the phases were separated. The joint organic phases were evaporated under reduced pressure, dissolved in CH₂Cl₂ and dried over Na₂SO₄. Filtration and evaporation of the solvent under reduced pressure, afforded 1.706

g (67 %) of a bright yellow oil.

9.1.2. Physical data

- $^1\text{H-NMR}$ (300 MHz, CD_2Cl_2) δ 4.92 (s, 1H), 3.54 – 2.98 (m, 4H), 2.06 – 1.64 (m, 4H)
- $^{13}\text{C-NMR}$ (75 MHz, CD_2Cl_2) δ 163.8, 46.4, 46.2 (2C), 26.1, 24.8
- MS (ESI, FT-ICR) (MeCN, no HCOOH) m/z 162.0 $[\text{M} + \text{Na}]^+$
- TLC (SiO_2 , 1 \times Et₂O) R_f : 0.13
- TLC (SiO_2 , 3 \times Et₂O) R_f : 0.30

9.2. 2-diazo-1-(piperidin-1-yl)ethanone (2c)

The compound was obtained as a yellow oil at ambient temperature which solidified to a crystalline solid at $-20\text{ }^{\circ}\text{C}$. Upon exposure to ambient temperature the solid melts over some ten minutes. The yield was 52 % starting from 2-bromo-1-(piperidin-1-yl)ethanone and 49 % starting from piperidine.



The compound is previously reported in several publications.^{27b,37h,32a,33b,37c,37d,37e,37f}

9.2.1. Experimental procedure

To a 250 mL round bottom flask containing 2-bromo-1-(piperidin-1-yl)ethanone (7.750 g, 37.61 mmol, 1 eq), were added through a solid addition funnel *N,N'*-ditosylhydrazine (25.619 g, 75.26 mmol, 2 eq), THF (85 mL) and an oval stir bar (3.5 × 1.5 cm). The suspension was cooled on an ice/water bath with stirring (400 rpm) for a period of 10 minutes, upon which a solution of 1,1,3,3-tetramethylguanidine (21.668 g, 188.12 mmol, 5 eq) in THF (20 mL) was added in aliquots using a pasteur pipette over a period of 5 minutes. During the addition the white suspension became yellow and at one point almost transparent, before depositing a white precipitate in a bright yellow solution. This suspension was stirred for a period of 90 minutes, before removing the THF under reduced pressure at or below ambient temperature. The resulting solid was treated with anhydrous Et₂O (150 mL) and vigorously stirred for 10 minutes, before being filtered on a Büchner-funnel. The filter cake was washed with anhydrous Et₂O (2 × 50 mL), leaving an almost white filter cake. The bright yellow filtrate was transferred to a separatory funnel and washed with a 5 %wt NaOH solution saturated with NaCl (3 × 50 mL). During washing, the aqueous phases had

become turbid and yellow, thus they were combined, brine (20 mL) was added and they were back-extracted with CH₂Cl₂ (3 × 30 mL). The CH₂Cl₂ was evaporated under reduced pressure and the residue extracted with Et₂O (2 × 30 mL), before combining the ethereal phases and drying over Na₂SO₄. Evaporation under reduced pressure at or below ambient temperature left 5.4 g of yellow oil (~ 90 % of theoretical maximum weight)

The oil was redissolved in Et₂O (50 mL) and TLC-grade silica gel (5 tablespoons) were added, before evaporating the Et₂O, leaving a yellow powder. This powder was placed over a column of alumina (B, 20 cm × 3 cm) packed in CH₂Cl₂ and then equilibrated with petroleum ether. Elution with petroleum ether (100 mL), Et₂O/Pet.Ether (1:1, 400 mL) and then Et₂O (600 mL) separated a yellow band. During elution, bubbling from within the column was observed possibly indicating some decomposition of the diazoacetamide on alumina (B). The total solvent expenditure was 1.1 L. The yield was 3.008 g (52 %)

9.2.2. Physical data

- ¹H-NMR (300 MHz, CD₂Cl₂) δ 5.16 (s, 1H), 3.30 (bs, 4H), 1.66 – 1.55 (m, 2H), 1.55 – 1.42 (m, 4H)
- ¹³C-NMR (75 MHz, CD₂Cl₂) δ 164.3, 46.1, 45.2 (2C), 26.2, 24.8 (2C)
- MS (EI) *m/z* (% rel. int.) 154 (5), 153 (M⁺, 25), 125 (19), 112 (11), 96 (45), 84 (38), 69 (53), 55 (71), 42 (100), 41 (79)
- MS (ESI, Q-TOF) (MeCN) *m/z* 167.1 [M + H – N₂ + MeCN]⁺
- MS (ESI, Q-TOF) (MeOH) *m/z* 180.1 [M + Na – N₂ + MeOH]⁺, 158.1 [M + H – N₂ + MeOH]⁺
- MS (ESI, FT-ICR) (MeCN, no HCOOH) *m/z* 176.1 [M + Na]⁺
- HRMS (EI) Calcd. for C₇H₁₁N₃O [M⁺]: 153.0902; found 153.0891 (7.2 ppm)
- TLC (SiO₂, 1 × Et₂O) R_f: 0.28

1-(piperidin-1-yl)-2-tosylethanone — a commonly observed by-product.^{31a}

- MS (EI) *m/z* (% rel. int.) 282 ($M^+ + 1$, 1), 217 (26), 155 (6), 127 (14), 126 (100), 112 (42), 110 (30), 97 (29), 91 (43), 84 (34)
- MS (ESI, Q-TOF) (MeCN) *m/z* 282.2 [$M + H$]⁺, 585.3 [$2M + Na$]⁺

9.3. 1-(azepan-1-yl)-2-diazoethanone (3c)

The compound was obtained as a soft yellow solid at ambient temperature. The yield was 66 % starting from 1-(azepan-1-yl)-2-bromoethanone and 63 % starting from azepane.

The compound is previously reported as a reagent,^{37h} however no details on its synthesis were disclosed.



9.3.1. Experimental procedure

To a 250 mL round bottom flask containing 1-(azepan-1-yl)-2-bromoethanone (4.151 g, 18.86 mmol, 1 eq), were added through a solid addition funnel *N,N'*-ditosylhydrazine (12.842 g, 37.72 mmol, 2 eq), THF (45 mL) and an oval stir bar (3.5 × 1.5 cm). The suspension was cooled on an ice/water bath with stirring (400 rpm) for a period of 8 minutes, upon which a solution of 1,1,3,3-tetramethylguanidine (10.864 g, 94.32 mmol, 5 eq) in THF (30 mL) was added using a pasteur pipette over a period of 6 minutes. At this point the bath temperature was 3 °C and the internal temperature was 12 °C. During the addition the white suspension became yellow and at one point almost transparent, before depositing a white precipitate in a bright yellow solution. This suspension was stirred for a period of 60 minutes, before removing the THF under reduced pressure at or below ambient temperature. The resulting solid was treated with anhydrous Et₂O (100 mL) and vigorously stirred for 10 minutes, before being filtered on a Büchner-funnel. The filter cake was washed with anhydrous Et₂O (3 × 50 mL), leaving an almost white filter cake. The bright yellow filtrate was filtered again through a folded filter into a 500 mL round bottom flask. The solution was then concentrated under reduced pressure to ~ 10 mL and loaded onto a column (8.5 × 3.5 cm) of silica gel packed in Et₂O. Elution of a yellow band with Et₂O left, upon evaporation of the solvent, 2.634 g (75 %) of a bright yellow waxy solid with an irritating smell. By ¹H-NMR the

solid chiefly consists of the product (~ 90 %wt) and the α -tosyl amide (~ 10 %wt). The solid was rechromatographed on a column (7.0 \times 3.5 cm) of silica gel packed in Et₂O/Pet.Ether (25:75). The compound was eluted isocratically with Et₂O/Pet.Ether (25:75), yielding 2.217 g (66 %) of a bright yellow solid, which was stored at -20 °C.

9.3.2. Physical data

- ¹H-NMR (300 MHz, CD₂Cl₂) δ 5.07 (s, 1H), 3.68 – 3.00 (m, 4H), 1.79 – 1.61 (m, 4H), 1.61 – 1.43 (m, 4H)
- ¹³C-NMR (75 MHz, CD₂Cl₂) δ 165.2, 47.8, 46.2 (2C), 28.8 (2C), 27.5, 27.3
- MS (EI) *m/z* (% rel. int.) 168 (7), 167 (M⁺, 16), 139 (7), 138 (15), 126 (8), 111 (9), 110 (21), 96 (61), 69 (64), 55 (65), 41 (100)
- MS (ESI, FT-ICR) (MeCN, no HCOOH) *m/z* 190.1 [M + Na]⁺
- HRMS (EI) Calcd. for C₈H₁₃N₃O [M⁺]: 167.1059; found 167.1060 (-0.6 ppm)
- TLC (SiO₂, 1 \times Et₂O) R_f: 0.39
- TLC (SiO₂, 5 \times Et₂O/Pet.Ether (1:1)) R_f: 0.45
- Melting point: 48 – 50 °C

Dimerization was observed in the mass spectrometer (EI) as has been noted by others.⁵⁰ The dimer radical cation had the following characteristics:

- MS (EI) *m/z* (% rel. int.) 279 (5), 278 (M⁺, 4), 181 (12), 180 (12), 152 (8), 149 (17), 110 (13), 98 (100)
- HRMS (EI) Calcd. for C₁₆H₂₆N₂O₂ [M⁺]: 278.1994; found 278.1984 (3.8 ppm)

1-(azepan-1-yl)-2-tosylethanone — a commonly observed by-product:^{31a}

- TLC (SiO₂, 5 \times Et₂O/Pet.Ether (1:1)) R_f: 0.17

9.4. *tert-butyl 4-(2-diazoacetyl)piperazine-1-carboxylate (4c)*

The compound was obtained as a yellow amorphous solid at ambient temperature. The yield was 60 % starting from *tert-butyl 4-(2-bromoacetyl)piperazine-1-carboxylate* and 56 % starting from *N-Boc-piperazine*.



The compound is previously unreported.¹⁵

9.4.1. Experimental procedure

To a 250 mL round bottom flask containing *tert-butyl 4-(2-bromoacetyl)piperazine-1-carboxylate* (5.885 g, 19.16 mmol, 1 eq) were added, through a solid addition funnel, *N,N'*-ditosylhydrazine (13.045 g, 38.32 mmol, 2 eq), THF (40 mL) and an oval stir bar (3.5 × 1.5 cm). The suspension was cooled on an ice/water bath with stirring (400 rpm) for a period of 10 minutes, upon which a solution of 1,1,3,3-tetramethylguanidine (11.043 g, 95.88 mmol, 5 eq) in THF (20 mL) was added using a pasteur pipette over a period of 2 minutes. During the addition the white suspension became yellow and at one point almost transparent, before depositing a white precipitate in a bright yellow solution. This suspension was stirred for a period of 70 minutes, before removing the THF under reduced pressure at or below ambient temperature.

The resulting solid was treated with anhydrous Et₂O (200 mL) and vigorously stirred for 10 minutes, before being filtered on a Büchner-funnel. The filter cake was washed with anhydrous Et₂O (5 × 50 mL), leaving an almost white filter cake. The bright yellow filtrate was filtered again through a folded filter into a 500 mL round bottom flask. The Et₂O was then evaporated under reduced pressure at or below ambient temperature to give a bright yellow solid. This solid was dissolved in Et₂O/CH₂Cl₂ (1:1, 10 mL) and loaded onto a column (10.0 × 3.5

cm) of silica gel and eluted with Et₂O/CH₂Cl₂ (1:1, 450 mL). TLC- and NMR-analyses of the eluted band show that a clean separation of the product and the *α*-tosyl amide had not been achieved.

Thus to the combined fractions was added silica gel (3 tablespoons), and the solvents evaporated under reduced pressure. The resulting yellow powder was placed on top of a column (10.0 × 3.5 cm) of silica gel packed in Et₂O/Pet.Ether (1:1). Elution with Et₂O/Pet.Ether (1:1, 400 mL), Et₂O/Pet.Ether (3:2, 500 mL) and then Et₂O/Pet.Ether (3:1, 350 mL) afforded 2.938 g (60 %) of a bright yellow solid, which could be broken up to fine yellow powder with a spatula. The solvent expenditure was 1.25 L.

XRD crystal growth

A 2.5 ml vial containing *tert*-butyl 4-(2-diazoacetyl)piperazine-1-carboxylate (10.8 mg) and dichloromethane (1000 μL) was capped and a pinhole (0.5 mm) was made in the cap to allow for vapour diffusion of solvents. This vial was placed inside a 25 ml vial containing *n*-pentane (8 ml) that was subsequently capped and stored in the dark at ambient temperature for approximately 48 hours, affording bright yellow plate-shaped crystals.

The first dataset recorded at ambient temperature and showed severe distortion of the ring carbon electron densities. When a new dataset was recorded at 105 K, the ring was in a well defined chair conformation. The structure was recently published.⁵¹

9.4.2. Physical data

- ¹H-NMR (300 MHz, CD₂Cl₂) δ 5.13 (s, 1H), 3.47 – 3.21 (m, 8H), 1.42 (s, 9H)
- ¹³C-NMR (75 MHz, CD₂Cl₂) δ 165.0, 154.6, 80.1, 46.5, 43.9 (br, 4C), 28.4
- MS (EI) *m/z* (% rel. int.) 255 (1), 254 (M⁺, 10), 198 (11), 181 (6), 170 (64), 128 (8), 125 (6), 97 (10), 85 (31), 69 (20), 57 (100), 41 (32)

- MS (ESI, Q-TOF) (MeCN) m/z 308.2 $[M-N_2 + 2 MeCN]^+$, 268.2 $[M + H-N_2 + MeCN]^+$, 212.1 $[M + H-N_2-56 (iso-butene) + MeCN]^+$
- MS (ESI, Q-TOF) (MeOH) m/z 539.3 $[2 M + Na-2 N_2 + 2 MeOH]^+$, 281.1 $[M + Na-N_2 + MeOH]^+$, 203.1 $[M + H-N_2-56 (iso-butene) + MeOH]^+$
- MS (ESI, Q-TOF) (MeCN, no HCOOH) m/z 277.1 $[M + Na]^+$
- HRMS (EI) Calcd. for $C_{11}H_{18}N_4O_3$ $[M^+]$: 253.1379; found 254.1374 (2.1 ppm)
- TLC (SiO_2 , $1 \times Et_2O$) R_f : 0.20
- Melting point: 108 – 111 °C

9.5. *N,N'*-bis(2-diazoacetyl)piperazine (5c)

The compound was obtained as a yellow amorphous solid at ambient temperature. The yield was 58 % starting from *N,N'*-bis(2-bromoacetyl)piperazine and 48 % starting from piperazine.



The compound is generally poorly soluble in common solvents, and is previously unreported.¹⁵

9.5.1. Experimental procedure

To a 250 mL round bottom flask containing *N,N'*-bis(2-bromoacetyl)piperazine (2.746 g, 8.37 mmol, 1 eq) were added, through a solid addition funnel, *N,N'*-ditosylhydrazine (11.401 g, 33.49 mmol, 4 eq), THF (50 mL) and an oval stir bar (3.5 × 1.5 cm). The suspension was cooled on an ice/water bath with stirring (400 rpm) for a period of 10 minutes, upon which a solution of 1,1,3,3-tetramethylguanidine (9.650 g, 83.78 mmol, 10 eq) in THF (10 mL) was added in bulk. After the addition the white suspension slowly became yellow and a white precipitate was deposited in a dark yellow solution. This suspension was stirred for a period of 60 minutes, before removing the THF under reduced pressure at or below ambient temperature.

The resulting solid was treated with anhydrous Et₂O (100 mL) and then THF (100 mL) as it would not dissolve/suspend in only Et₂O. The mixture was vigorously stirred for 10 minutes, before being filtered on a Büchner-funnel. The filter cake was washed with THF/Et₂O (1:1, 100 mL) and then THF (2 × 50 mL). The filtrate was set aside and the filter cake washed with MeCN (2 × 100 mL) as it was not completely decolourized by the THF. The addition of MeCN caused a noticeable colour change, and a dark yellow filtrate and an almost white filter cake resulted. TLC-analyses indicated that the product was present in both filtrates, and they were thus combined. Addition of silica gel (4

tablespoons) and subsequent evaporation of the solvents under reduced pressure at 20 °C, gave a light yellow powder. The powder was placed on top of a column (9.0 × 3.5 cm) of silica gel packed in THF/CH₂Cl₂/Et₂O (1:1:2) and eluted with THF/CH₂Cl₂/Et₂O (1:1:2, 600 mL) and then THF/CH₂Cl₂/Et₂O (1:1:1, 600 mL) affording a light yellow fraction. A TLC-analysis showed the presence of the same contamination in all the fractions, possibly due to a low solubility of the contaminant when Et₂O was used in the eluent. The solvent expenditure was 1.2 L.

The fractions were combined and adsorbed on silica gel (3 tablespoons) by evaporation of the solvents. The resulting powder was placed on top of a column (10.0 × 3.5 cm) of silica gel packed in CH₂Cl₂ and eluted with THF/CH₂Cl₂ (5:95, 300 mL), THF/CH₂Cl₂ (6:94, 900 mL), until a pale yellow band started eluting, and then with THF/CH₂Cl₂ (10:90, 100 mL), THF/CH₂Cl₂ (15:85, 400 mL) and THF/CH₂Cl₂ (20:80, 600 mL). Solvent expenditure was 2.3 L. The combined fractions were analysed by TLC and ¹H-NMR, and found to be of acceptable purity. The yield was 1.089 g (48 %).

XRD crystal growth

Crystals suitable for X-ray crystallography were grown by slow evaporation of a solution of 4.0 mg of the compound in 500 μL of MeCN, placed in a vial measuring 30 × 6 mm. After 48 hours in the dark at ambient temperature yellow needles had grown. A crystal measuring 1.4 × 0.2 × 0.2 mm was selected and the data were recorded at 105 K. The available crystallographic data are included in the appendix.

9.5.2. Physical data

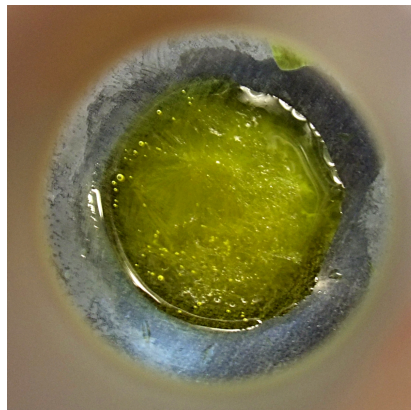
- ¹H-NMR (300 MHz, CDCl₃) δ 4.99 (s, 2H), 3.44 (bs, 8H)
- ¹³C-NMR (75 MHz, CDCl₃) δ 165.0 (2C), 46.7 (2C), 43.4 (br, 4C)
- MS (EI) *m/z* (% rel. int.) 223 (1), 222 (M⁺, 7), 194 (1), 166 (28), 137 (6), 125 (8), 123 (39), 110 (9), 96 (21), 85 (64), 69 (100)

- MS (ESI) (MeCN, no HCOOH) m/z 245.0 [M + Na]⁺
- HRMS (EI) Calcd. for C₈H₁₀N₆O₂ [M⁺]: 222.0865; found 222.0865 (0.3 ppm)
- TLC (SiO₂, 3 × THF/CH₂Cl₂ (2:8)) R_f: 0.25
- Melting point: 109 °C (decomposition)

9.6. 2-diazo-1-morpholinoethanone (6c)

The compound was obtained as a dark yellow oil at ambient temperature, which barely solidified at $-20\text{ }^{\circ}\text{C}$. The yield was 60 % starting from 2-bromo-1-morpholinoethanone and 54 % starting from morpholine.

The compound is previously reported in several publications.^{32a,33b,37j}



9.6.1. Experimental procedure

To a 250 mL round bottom flask containing 2-bromo-1-morpholinoethanone (3.7369 g, 17.97 mmol, 1 eq), were added through a solid addition funnel *N,N'*-ditosylhydrazine (12.333 g, 36.23 mmol, 2 eq), THF (40 mL) and an oval stir bar (3.5 × 1.5 cm). The suspension was cooled on an ice/water bath with stirring (400 rpm) for a period of 5 minutes, upon which a solution of 1,1,3,3-tetramethylguanidine (10.353 g, 30.41 mmol, 5 eq) in THF (30 mL) was added using a pasteur pipette over a period of 4 minutes. During the addition the white suspension became yellow and at one point almost transparent, before depositing a white precipitate in a bright yellow solution. This suspension was stirred for a period of 80 minutes, before removing the solvent under reduced pressure at or below ambient temperature. The resulting solid was treated with anhydrous Et_2O (200 ml) and swirled before filtering on a Büchner-funnel. The filter cake was washed with anhydrous Et_2O (4 × 100 mL), leaving an almost white filter cake. The bright yellow filtrate was evaporated under reduced pressure at or below ambient temperature, during which time the residue became dark yellow, then red and then dark brown. A TLC-analysis showed that the diazoacetamide was still present.

The residue was shaken with Et_2O (2 × 10 mL) and loaded onto a column (5.5 × 2.0 cm) of silica gel packed in Et_2O . Elution with Et_2O presented one yellow band, leaving behind the dark tar at the top of the column. Evaporation under

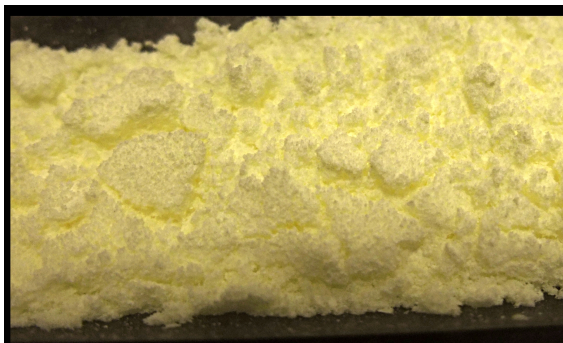
reduced pressure at or below ambient temperature, afforded 1.677 g (54 %) of yellow oil. The oil was pure by TLC and by $^1\text{H-NMR}$, and solidified after three days of storage at $-20\text{ }^\circ\text{C}$.

9.6.2. Physical data

- $^1\text{H-NMR}$ (300 MHz, CD_2Cl_2) δ 5.05 (s, 1H), 3.68 – 3.56 (m, 4H), 3.37 – 3.23 (m, 4H)
- $^{13}\text{C-NMR}$ (75 MHz, CD_2Cl_2) δ 165.1, 66.9 (2C), 46.3, 44.4 (2C)
- MS (EI) m/z (% rel. int.) 156 (10), 155 (M^+ , 74), 140 (13), 127(8), 114 (6), 98 (22), 86 (25), 69 (65), 56 (81), 41 (100)
- MS (ESI, FT-ICR) (MeCN, no HCOOH) m/z 178.0 [$\text{M} + \text{Na}$] $^+$
- HRMS (EI) Calcd. for $\text{C}_6\text{H}_9\text{N}_3\text{O}_2$ [M^+]: 155.0695; found 155.0693 (1.1 ppm)
- TLC (SiO_2 , $1 \times \text{Et}_2\text{O}$) R_f : 0.15

9.7. 2-diazo-1-(1,1-dioxido-4-thiomorpholinyl)ethanone (8c)

The compound was obtained as a light yellow powder at ambient temperature. The yield was 64 % starting from 2-bromo-1-(1,1-dioxidothiomorpholino)ethanone and 58 % starting from thiomorpholine-1,1-dioxide.



The compound is generally poorly soluble in common solvents, and is previously unreported¹⁵

9.7.1. Experimental procedure

To a 250 mL round bottom flask containing 2-bromo-1-(1,1-dioxidothiomorpholino)ethanone (1.928 g, 7.53 mmol, 1 eq), were added through a solid addition funnel *N,N'*-ditosylhydrazine (5.129 g, 15.07 mmol, 2 eq), THF (50 mL) and an oval stir bar (3.5 × 1.5 cm). The suspension was cooled on an ice/water bath with stirring (400 rpm) for a period of 15 minutes, upon which a solution of 1,1,3,3-tetramethylguanidine (4.337 g, 37.65 mmol, 5 eq) in THF (10 mL) was added in bulk. The white suspension quickly became yellow, and was then stirred for a period of 70 minutes, before adding Et₂O (100 mL) causing the disappearance of the yellow colour from the THF/Et₂O phase, as the product was no longer soluble. Removal of some of the Et₂O under reduced pressure, brought the yellow colour back to the liquid phase in the suspension. The mixture was filtered on a Büchner-funnel and the filter cake washed with THF/Et₂O (2:1, 75 mL) and THF (30 mL), leaving an almost white filter cake.

A preliminary purification was performed by adding Celite (3 tablespoons) to the filtrate, and evaporating the solvents under reduced pressure at 20 °C. The resulting slightly sticky powder, was suspended in CH₂Cl₂ (15 mL) and loaded on top of 1 cm of sea-sand covering a column (8.0 × 3.5 cm) of silica gel packed in

CH₂Cl₂. A yellow band was eluted with MeOH/CH₂Cl₂ (5:95). To this fraction was added silica gel (2 tablespoons) and the solvents evaporated, leaving a pale yellow powder. The powder was loaded on top of a column (5.5 × 3.5 cm) of silica gel packed in CH₂Cl₂, and the product slowly eluted with CH₂Cl₂ and from the point of elution CHCl₃. The solvent expenditure was 1.6 L. The solvents were evaporated under reduced pressure at or below room temperature affording 0.987 g (64 %) of a pale yellow powder which was stored at –20 °C.

XRD crystal growth

Crystals suitable for X-ray crystallography were grown by slow evaporation of a solution of 4.0 mg of the compound in 500 μ L of CH₂Cl₂ placed in a 2.5 ml vial which was capped and a pinhole (0.5 mm) made in the cap to allow for slow evaporation. After approximately 48 hours in the dark at ambient temperature a head of yellow needles had grown. A crystal measuring 0.8 × 0.3 × 0.2 mm was selected and the data were recorded at 105 K. The available crystallographic data are included in the appendix.

9.7.2. Physical data

- ¹H-NMR (300 MHz, CD₂Cl₂) δ 5.13 (s, 1H), 3.94 – 3.80 (m, 4H), 3.07 – 2.97 (m, 4H)
- ¹³C-NMR (75 MHz, CD₂Cl₂) δ 165.1, 52.4 (2C), 47.2, 42.8 (2C)
- MS (EI) *m/z* (% rel. int.) 205 (1), 204 (2), 203 (M⁺, 19), 175 (2), 162 (5), 134 (21), 118 (6), 111 (5), 83 (100), 70 (30), 69 (94)
- HRMS (EI) Calcd. for C₆H₉N₃O₃S [M⁺]: 203.0365; found 203.0366 (–0.7 ppm)
- TLC (SiO₂, 5 × CH₂Cl₂) R_f: 0.33
- Melting point: 165 – 176 °C (decomposition)

9.8. 1,1,3,3-tetramethylguanidine *p*-toluenesulfinate

9.8.1. Experimental procedure and XRD crystal growth

The precipitation of this salt formed during the preparations of the α -diazoacetamides as described in their experimental procedures. In one instance the precipitate was weighed dry and it accounted for 98 %w of the theoretical amount. A small amount of the precipitation was immediately dried and stored under an argon atmosphere to ensure a low degree of oxidation before submitting the sample to mass spectrometry (ESI).

The crystal mass was isolated by filtration of an acetonitrile solution also containing 2-diazo-1-(1,1-dioxido-4-thiomorpholinyl)ethanone, where thick needles had formed overnight at 4 °C. A small crystal measuring 0.6 × 0.4 × 0.3 mm was selected for X-ray crystallography, and the data recorded at 105 K. The available crystallographic data are included in the appendix. See figure 3.6 on page 36 for the structure.



9.8.2. Physical data

Mixture of 1,1,3,3-tetramethylguanidine *p*-toluenesulfinate and 1,1,3,3-tetramethylguanidine *p*-toluenesulfonate (a complete tentative assignment of the peaks can be found on the spectrum in the appendix):

- $^1\text{H-NMR}$ (200 MHz, CDCl_3) δ 8.92 (bs), 7.72 (m), 7.53 (m), 7.11 (m), 7.08 (m), 3.87 (bs), 2.80 (s), 2.28 (s)
- MS (ESI) (Argon then H_2O) (ES+) m/z 510/508/506 [2 TMG + 2 HBr + H] $^+$, 403.4 [2 TMG + $p\text{-Ts-SO}_3\text{H}$ + H] $^+$, 387.5 [2 TMG + $p\text{-Ts-SO}_2\text{H}$ + H] $^+$, 313/311 [2 TMG + HBr] $^+$, 231.3 [2 TMG + H] $^+$, 116.2 [TMG + H] $^+$
- MS (ESI) (Argon then H_2O) (ES-) m/z 171 [$p\text{-Ts-SO}_3$] $^-$, 155 [$p\text{-Ts-SO}_2$] $^-$

9.9. 1,1,3,3-tetramethylguanidine *p*-toluenesulfonate

9.9.1. Experimental procedure and XRD crystal growth

The precipitate isolated as described above, was exposed to air for approximately 72 hours before being submitted to crystallization. Then, a 2.5 ml vial containing the crude precipitation (4.8 mg) and anhydrous dichloromethane (500 μL) was capped and a pinhole (0.3 mm) was made in the cap to allow for vapour diffusion of solvents. This vial was placed inside a 25 ml vial containing Et_2O (5 ml) that was subsequently capped and stored in the dark at ambient temperature for approximately 48 hours, affording thin transparent needles. A crystal was selected and the data recorded at 296 K. The structure can be seen in 3.7 on page 36.

9.9.2. Physical data

This compounds appears as a minor component in a mixture with 1,1,3,3-tetramethylguanidine *p*-toluenesulfinate and its spectroscopic details are included in the data given above.

10. β -lactams

The reported stability of the halogenated α -bromodiazooacetic ethyl esters was “day-long stability at 0 °C”^{10f} In our experience the 2 – 5 °C temperatures, obtainable with a common ice/water bath, were not sufficiently low to work with the halogenated α -diazooacetamides with high reproducibility. Therefore, all the procedures were carried out at –5 °C using an acetone bath in which the temperature was controlled by a cryostat.

In the summaries from the mass spectrometry experiments, the R-group in α, α' -Br₂-NR₂ refers to the cyclic amine moiety of the respective compound.

10.0.3. General experimental procedure

The diazoacetamide (0.5 mmol, 1.0 eq) was weighed out in a 25 mL pear shaped flask, the base (0.7 mmol, 1.4 eq) in a 10 mL beaker and the *N*-halo compound (0.65 mmol, 1.3 eq) in a weighing funnel. The flask was charged with a small magnetic stir bar (10 × 2 mm) and CH₂Cl₂ (2 mL, ambient temperature), and was subsequently mounted alongside a 250 mL round bottom flask containing CH₂Cl₂ (250 mL) in an acetone bath cooled by a cryostat to –5 °C (measured with an alcohol thermometer at the surface). Stirring (300 RPM) was commenced and after 2 minutes the base in CH₂Cl₂ (2 mL, ambient temperature) was added. After 2 minutes the *N*-halo compound was added in bulk through the funnel and the funnel rinsed with CH₂Cl₂ (1 mL, ambient temperature). The addition effected a colour change from bright yellow to bright red. While stirring, a short plug of silica gel (2 × 2 cm) was packed in CH₂Cl₂ (ambient temperature) in a fritted flash chromatography column (15 × 2 cm) and mounted inside a holder which allows for the filling of dry ice around the column (covering ~ 300°, leaving an observation window, see figure 10.1 on page 106 in the appendix).

After stirring for 5 minutes, the thermometer was placed in the 250 mL flask and $\text{CO}_2(\text{s})$ was added to the bath until the internal temperature of the CH_2Cl_2 had reached $-15\text{ }^\circ\text{C}$. The space around the column was filled with dry ice, and the column equilibrated with CH_2Cl_2 ($-15\text{ }^\circ\text{C}$, 20 mL). The reaction mixture was then poured directly onto the column, and the flask rinsed with two pipette volumes of CH_2Cl_2 ($-15\text{ }^\circ\text{C}$). The reaction mixture was run into the column using pressurized air (ambient temperature), and the column filled up with CH_2Cl_2 ($-15\text{ }^\circ\text{C}$). The column was then run with CH_2Cl_2 ($-15\text{ }^\circ\text{C}$, $\sim 200\text{ mL}$) under air pressure to completely elute a bright red band into a 250 mL flask in the cooling bath. The eluted solution is bright red-pink in colour.

Catalyzed reactions: The flask was charged with a stir bar, capped with a septum and maintained in the cooling bath at approximately -15 while degassing with argon (5 minutes). The flask was then taken out of the cooling bath and a degassed solution of the catalyst in CH_2Cl_2 (2 mL) was added via syringe under vigorous stirring. The solution was then left to heat towards room temperature.

Thermolysis: The flask was placed on the bench without stirring while the temperature rose from $-15\text{ }^\circ\text{C}$ towards ambient temperature. The solution became clear in approximately 60 minutes. For the more polar analogues it was necessary to add Et_2O (5 mL) to the last 50 mL of the eluent to completely collect the red band. It should be noted that Et_2O has a much higher elution strength than CH_2Cl_2 under these conditions, and fortunately, it does not seem to interfere with the C-H insertion reaction at this concentration.

Yield measurement using an internal standard: The reactions were left to expire overnight, before evaporating the solvent under reduced pressure at $20\text{ }^\circ\text{C}$. 0.5 molar equivalents of 2-naphthaldehyde was then added and the weight noted, before dissolving the entire crude material in CDCl_3 . The solution was transferred to an NMR-tube and a ^1H -NMR spectrum recorded.

The $\text{CO}_2(\text{s})$ -cooled column used in this procedure, has been illustrated at the end of this chapter. See figure 10.1 on page 106.

10.1. 6-bromo-1-azabicyclo[3.2.0]heptan-7-one (1e)

The compound was prepared following the general procedure for thermolysis given above and apparently decomposed at some point before a second ¹H-NMR spectrum was recorded, 48 hours after the first. This is consistent with the rapid hydrolysis of β-lactams fused with 5-membered rings.^{27b}

10.1.1. Physical data

Crude reaction mixture from thermolysis:

- Partial ¹H-NMR (300 MHz, CDCl₃) δ 4.395 (d, *J* = 1.7 Hz, 1H)
- MS (ESI, FT-ICR) (MeCN) *m/z* 274/272/270 [α, α' -Br₂-NR₂ + H]⁺, 210/208 [M + H₂O + H]⁺ (hydrolysis)

10.2. 7-bromo-1-azabicyclo[4.2.0]octan-8-one (2e)

The compound was prepared following the general procedure for thermolysis given above.

10.2.1. Physical data

Crude reaction mixture from thermolysis, mixture of *cis/trans*-isomers:

- ¹H-NMR (300 MHz, CDCl₃) δ 4.945 (dd, *J* = 4.43, 1.60 Hz, 1H, *cis*), 4.395 (d, *J* = 1.13 Hz, 1H, *trans*), 3.805 (dd, *J* = 13.19, 4.52 Hz, 1H), 3.50 (ddd, *J* = 10.69, 4.47, 1.04 Hz, 1H), 2.735 (ddd, *J* = 13.47, 11.77, 4.33 Hz, 1H), 2.10 (m, 1H), 1.95 – 1.10 (comp, 5H)

Crude reaction mixture from dirhodium(II) catalysis:

- MS (ESI, Q-TOF) (MeOH) m/z 433/431/429 [$C_{17}H_{20}Br_2N_2O_2 + Na$]⁺ (formal carbene dimer), 288/286/284 [α, α' -Br₂-NR₂ + H]⁺, 206/204 [M + H]⁺

Isolated by preparative TLC:

- TLC (SiO₂, 1 × Et₂O) R_f trans: 0.29, cis: 0.19
- MS (EI) m/z (% rel. int.) 205/203 (M⁺, 6/6), 134/132 (22/22), 124 (100), 121/119 (7/7), 96 (8), 84 (11), 81 (22), 69 (9)
- HRMS (EI) Calcd. for C₇H₁₀⁷⁹BrNO [M⁺]: 202.9946; found 202.9938 (3.6 ppm)

α, α' -Br₂-piperidine acetamide — a common by-product:

The free induction decay (FID) of this compound in ¹H-NMR, had an interesting undulate shape. The FID is included in the appendix.

- TLC (SiO₂, 1 × Et₂O) R_f 0.54
- ¹H-NMR (300 MHz, CDCl₃) δ 6.21 (s, HCB₂-NR₂), 6.14 (s, HCB₂-NR₂), 3.75 – 3.50 (m, 4H), 1.80 – 1.50 (m, 6H)
- MS (EI) m/z (% rel. int.) 287/285/283 (M⁺, 6/13/6), 206/204 (56/57), 175/173/171 (4/9/4), 122/120 (6/6), 112 (100), 84 (21), 69 (69)

10.3. 8-bromo-1-azabicyclo[5.2.0]nonan-9-one (3e)

The compound was prepared following the general procedure for thermolysis given above.

10.3.1. Chromatographic procedure

The diastereomers *trans*-**3e** and *cis*-**3e** were separated on a column of alumina (N, 10 × 2.5 cm), using Et₂O as the eluent.

10.3.2. Physical data

Isolated by chromatography:

trans-8-bromo-1-azabicyclo[5.2.0]nonan-9-one

- ¹H-NMR (300 MHz, CDCl₃) δ 4.255 (dd, *J* = 1.13, 1.13 Hz, 1H), 3.765 (ddd, *J* = 9.61, 2.83, 1.70 Hz, 1H), 3.45 – 3.23 (m, 2H), 2.15 – 2.05 (m, 1H), 1.95 – 1.70 (m, 3H), 1.60 – 1.25 (m, 4H)
- ¹³C-NMR (75 MHz, CDCl₃) δ 162.5, 64.6, 45.7, 43.4, 33.7, 29.2, 27.2, 26.6

cis-8-bromo-1-azabicyclo[5.2.0]nonan-9-one

- ¹H-NMR (300 MHz, CDCl₃) δ 4.905 (ddd, *J* = 4.62, 1.79, 0.75 Hz, 1H), 3.85 (ddd, *J* = 10.13, 4.66, 2.17 Hz, 1H), 3.40 – 3.25 (m, 2H), 2.00 – 1.75 (m, 5H), 1.60 – 1.20 (m, 5H)
- ¹³C-NMR (75 MHz, CDCl₃) δ 163.2, 57.1, 47.9, 43.5, 33.3, 28.9, 28.1, 26.7

Crude reaction mixture from thermolysis, mixture of *cis/trans*-isomers:

- MS (ESI, FT-ICR) (MeCN) *m/z* 220/218 [M + H]⁺
- TLC (SiO₂, 1 × Et₂O) R_f *trans*: 0.49, *cis*: 0.36, α, α'-Br₂-NR₂: 0.65

10.4. *tert*-butyl 7-bromo-8-oxo-1,4-diazabicyclo[4.2.0]octane-4-carboxylate (4e)

The compound was prepared both following the general procedure for thermolysis and catalysis given above.

10.4.1. Physical data

Crude reaction mixture from thermolysis:

- Partial ¹H-NMR (300 MHz, CDCl₃) δ 4.935 (dd, *J* = 4.52, 1.13 Hz, 1H, *cis*), 4.495 (d, *J* = 1.32 Hz, 1H, *trans*)
- MS (ESI, FT-ICR) (MeCN) *m/z* 325/323 [M + H₂O + H]⁺ (hydrolysis), 251/249 [M – 56 (*iso*-butene) + H]⁺ (Boc-degradation pathway to carboxylate)

10.5. 7-bromo-4-oxa-1-azabicyclo[4.2.0]octan-8-one (6e)

The compound was prepared following the general procedure for thermolysis given above.

10.5.1. Physical data

Crude reaction mixture from thermolysis:

- Partial ¹H-NMR (300 MHz, CDCl₃) δ 4.935 (dd, *J* = 4.52, 1.32 Hz, 1H, *cis*), 4.485 (d, *J* = 1.32 Hz, 1H, *trans*)

- MS (ESI, FT-ICR) (MeCN) m/z 415/413/411 [$C_{12}H_{16}Br_2N_2O_4 + H$]⁺
(formal carbene dimer), 208/206 [M + H]⁺

10.6. 7-bromo-4-thia-1-azabicyclo[4.2.0]octan-8-one 4,4-dioxide (8e)

The compound was prepared following the general procedure for thermolysis given above.

10.6.1. Physical data

Crude reaction mixture from thermolysis:

- Partial ¹H-NMR (300 MHz, CDCl₃) δ 5.20 (dd, $J = 4.71, 1.32$ Hz, 1H, *cis*),
4.70 (d, $J = 1.51$ Hz, 1H, *trans*)
- MS (ESI, FT-ICR) (MeCN) m/z 274/272 [M + H₂O + H]⁺ (hydrolysis)

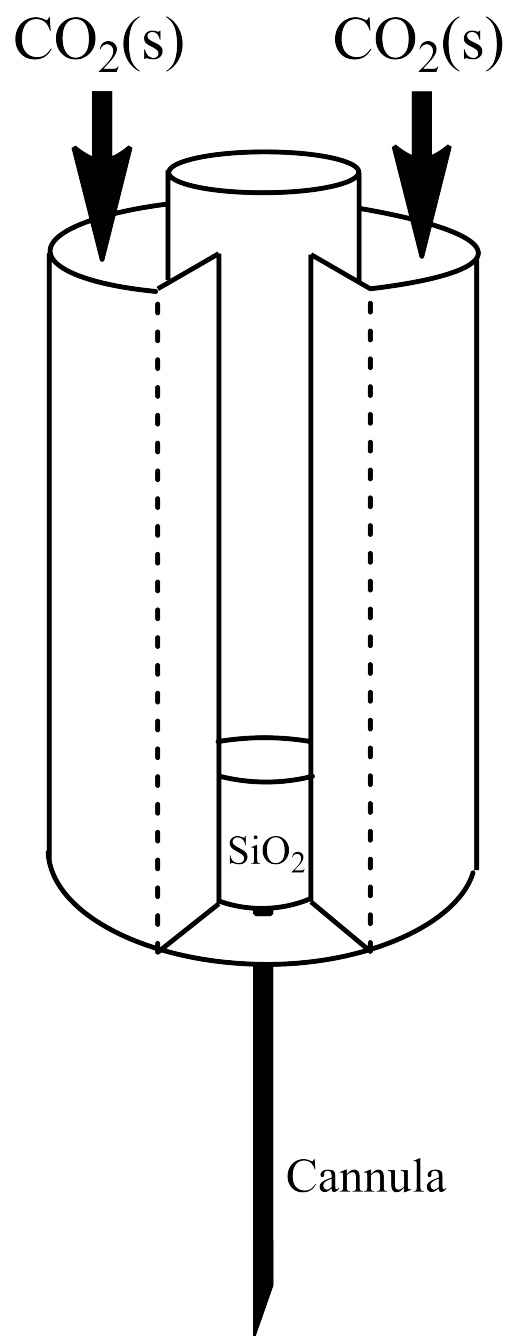


Figure 10.1.: An illustration of the column with a compartment for $\text{CO}_2(\text{s})$

11. Synthesis of the methacrylonitrile copolymers

11.1. General experimental procedure for the free radical suspension copolymerization reactions

A 250 mL three-necked round bottom flask was charged with an oval stir bar (3.5 × 1.5 cm), potassium iodide (40 mg, aqueous phase polymerization inhibitor) and 0.5 %wt aqueous polyvinyl alcohol ($M_w \approx 205\ 000$ and 88 % hydrolysis, 130 mL). All the monomers S/MAN/DVB or MAN/DVB were weighed out in a beaker, 2,2'-Azobis-(2-methylbutyronitrile) (AMBN) (200 mg, 1 %wt in relation to all the monomers) was added followed by the diluent mixture (toluene, cyclohexanol or 2-ethylhexanol) and the beaker swirled until everything had dissolved. This mixture was gently added to aqueous phase through a funnel while stirring (700 rpm). The flask was flushed with nitrogen for a period of 5 minutes, before heating to 75 °C (mantle temperature) and stirring for a period of 19 hours.

The heat was turned off and stirring reduced (500 rpm) while cooling. The mixture was then poured into MeOH (250 mL) in a beaker and the mixture vigorously swirled. When the material had settled the MeOH was decanted and another portion of MeOH (250 mL) added. The mixture was swirled, left to settle, most of the MeOH was decanted and the material filtered on a Büchner funnel. The filter cake was washed with H₂O (3 × 800 mL) and acetone (1 × 200 mL) before being spread out in a bowl to dry in air. After 24 hours, the now free-flowing beads weighed 95 – 99 % of the starting material. The obtained beads were stored in glass jars with PTFE caps, protected from direct sunlight. The beads from II (see table 13.1) are displayed in figure 13.2 on page 117.

12. Synthesis of the dirhodium(II) catalysts

12.1. Tetrakis μ -caprolactamato dirhodium(II)

12.1.1. Experimental procedure

An oven dried 50 mL round bottom flask containing 40 mL of chlorobenzene was degassed for a period of 5 minutes under stirring before adding anhydrous $\text{Rh}_2(\text{OAc})_4$ (0.199 g, 0.45 mmol, 1.0 eq) and ϵ -caprolactam (1.028 g, 9.08 mmol, 20.2 eq) under stream of argon. The addition of the lactam caused a colour change from deep green to deep blue. The flask was fitted with an oven dried, degassed Soxhlet extraction apparatus in which the thimble was charged with an oven dried mixture of Na_2CO_3 and sand (5 g, 3:1 ratio). A degassed reflux condenser was fitted on top of the Soxhlet apparatus and the mixture was vigorously stirred while heating to 160 °C (mantle temperature) When the first extraction cycle was observed, the temperature was reduced to 155 °C (mantle temperature) and the mixture stirred for a period of 46 hours yielding a dark turquoise solution. The solvent was then evaporated under reduced pressure at 40 °C to give dark purple solid. This solid was dissolved in MeOH (10 mL) and loaded onto a 13 × 1.5 cm column of the methacrylonitrile copolymer beads from run II described in section 13.1 on page 114 and prepared following the general procedure given above. Elution with MeOH (50 mL) separated an almost clear first fraction, which was discarded. The next 50 mL separated a purple band, which eluted, and the eluent was again colourless. Elution with MeCN/MeOH (100 mL, 1:4) gave a purple fraction which turned to a blue solid

upon evaporation under reduced pressure at 40 °C. The weight was 0.238 g (71 %, assuming the formula $\text{Rh}_2(\text{cap})_4 \cdot 2 \text{MeCN}$)

12.1.2. Physical data

- $^1\text{H-NMR}$ (300 MHz, CD_3CN) δ 2.46 (d, $J = 2.1$ Hz, 30H), 2.025 (q, $J = 2.2$ Hz), 2.02 (s, 6H)

12.2. *cis-M/P*- $\text{Rh}_2(\mu\text{-O}_2\text{CCH}_3)_2[\text{Ph}_2\text{P}(\text{C}_6\text{H}_4)]_2(\text{CH}_3\text{CN})_2$

12.2.1. Experimental procedure

A 50 mL round bottom flask was charged with $\text{Rh}_2(\text{OAc})_4 \cdot 2 \text{H}_2\text{O}$ (0.200 g, 0.42 mmol, 1.0 eq) and acetic acid (30 mL) and fitted with a reflux condenser capped by a rubber septum. PPh_3 (0.238 g, 0.91 mmol, 2.2 eq) was weighed out on a weighing paper. The deep green solution was degassed with argon for a period of 10 minutes and the triphenylphosphine was added under a continuous flow of argon, giving a bright red suspension. This suspension was heated to reflux in a heating mantle and stirred at 125 °C (mantle temperature) for a period of 3 hours. The heat was turned off and the now purple suspension was allowed to cool while stirring for 17 hours. The suspension was concentrated under reduced pressure to approximately 10 mL and filtered on a Büchner funnel. The filter cake was washed with a few drops of acetic acid, to give 0.245 g (60 %) a light purple powder with some dark purple needles. The mother liquor was concentrated under reduced pressure to a volume of approximately 5 mL and placed in a freezer at -15 °C until frozen. The frozen cake was divided into pieces, placed on a Büchner funnel, where it subsequently melted leaving a purple powder. This powder was washed with a few drops of acetic acid to give a second crop of 0.067 g (16 %). Both crops were pure by $^1\text{H-NMR}$ and $^{31}\text{P-NMR}$, and were subsequently mixed and stored in a capped glass jar in an air atmosphere. The total yield was 77 %.

12.2.2. Physical data

- ¹H-NMR (300 MHz, CD₂Cl₂) δ 7.80 – 6.50 (comp, 28H), 2.21 (s, 6H), 2.14 (s, 6H)
- ¹³C-NMR (75 MHz, CD₂Cl₂) δ 182.1, 182.1, 145.6, 140.3, 140.1, 134.6, 134.5, 134.4, 133.9, 133.8, 133.6, 133.2, 133.0, 129.4, 129.4, 128.8, 128.4, 127.8, 127.7, 127.5, 127.4, 120.5, 120.5, 116.0, 22.8, 3.4
- ³¹P-NMR (75 MHz, CD₂Cl₂) δ 19.3 (d, J = 156.3 Hz)

13. Purification of the dirhodium(II) catalysts

The method of choice for the work-up and purification of dirhodium(II) complexes, depend on the solubility, crystallinity, stability and, linked to all of the aforementioned, what axial ligands are present in the product complex. In general, the members of each catalyst family (cf. figure 2.1 on page 16) are worked up and purified in a similar way, owing to their similar synthesis protocols and chemical properties. Each catalyst family will thus present a set of axial ligands, or a lack thereof, after work-up depending on the method applied. Recrystallization is often only practically possible if the axial seats are occupied. A complex with volatile axial ligands e.g. acetonitrile can be heated under high vacuum to remove these, given that the complex is sufficiently thermally stable, or they may be displaced in a weakly coordinating solvent (cf. discussion in section 2.3 on page 15).

The use of column chromatography on silica gel has been employed in the purification of all three families, but is most commonly reported for dirhodium(II) carboxylates and orthometalated phosphines. The preferred methods for the preparative purification of dirhodium(II) carboxamides are recrystallization or cation exchange-type chromatography on a column packed with J.T. Baker BAKERBOND Cyano 40 um prep LC packIng medium.⁵² This column packing medium is an amorphous silica gel whose free Si-OH groups have been capped by a reaction with (4-trichlorosilyl) butanenitrile and chlorotrimethylsilane. Thus, when the reaction mixture is applied to the column, the free nitrile groups bind to the dirhodium(II) carboxamidate through its axial seats (cf. discussion in section 2.3). This near permanently retards the complex. Taking advantage of this coordination, the excess ligand from the ligand exchange reaction could be eluted using MeOH, leaving behind only

dirhodium(II) species capable of axial coordination. The pure catalyst could then be eluted by the addition of MeCN to the eluent, as the nitrile groups on the stationary phase are outcompeted by those in the mobile phase. Having followed the reaction to completion by HPLC, the eluted substance could safely be assumed to consist solely of the *cis*-2,2 dirhodium(II) carboxamidate.²⁵¹

Most dirhodium(II) complexes will bind nitrile groups axially from a ligand-free state or in favour of weaker donors e.g. the axially hydrogen bonded acetic acid molecules in the products obtained from the reaction of dirhodium(II) tetraacetate dihydrate and arylphosphines in refluxing acetic acid. The strength of the coordination should vary with the Lewis acidity of the complex, but given that the technique works for the least Lewis acidic family of the dirhodium(II) catalysts used in diazo chemistry, there is promise of some generality to this method. In contrast to this, the use of this method of purification has not been reported for members from other dirhodium(II) catalyst families. Possibly this owes to the cost of the BAKERBOND Cyano medium. We hypothesized that the inclusion nitrile groups in macroporous copolymer beads could be achieved using free radical suspension copolymerization based on feedstock monomers like acrylonitrile/methacrylonitrile and divinylbenzene. The preparation of macroporous methacrylonitrile-divinylbenzene beads and the purification of the synthesized dirhodium(II) catalysts using the obtained beads, is the topic of the next section.

13.1. The application of methacrylonitrile copolymer beads in the purification of dirhodium(II) catalysts

A survey of the literature showed that the suspension copolymerization of styrene (S) – divinylbenzene (DVB), acrylonitrile (AN) – divinylbenzene (DVB) or all three had been investigated with respect to the sorption properties, porosity and specific surface area obtained with respect to the monomer fractions, crosslinking degree and porogens (diluent).⁵³ Additionally, the use of S/AN/DVB and AN/DVB copolymer beads as supports for transition metal catalysts has been reported.⁵⁴ The joint results of the authors were used to adjust our starting parameters. Due to the AN monomer being carcinogenic, we

opted for methacrylonitrile (MAN).

Run	S (%wt)	MAN (%wt)	DVB	Porogen (diluent)	$X_{v/v}$
I	58	42	0.25 %mol	Toluene/Cyclohexanol	5:5
II	-	50	50 %wt	Toluene/2-Ethylhexanol	9:1
III	-	50	50 %wt	Toluene/2-Ethylhexanol	5:5

Figure 13.1.: Variations in monomer ratios and porogens(diluents)

Three batches of polymers were prepared using the conditions give in table 13.1. The experimental details of the suspension polymerization reactions can be found in the experimental section. In all the runs, the suspension polymerization gave round beads of even size (the size was not measured). The beads from the first run were glass-like and almost transparent. The beads from the subsequent runs were white and opaque. To our satisfaction, the beads functioned as one should expect from reading about the use of the BAKERBOND Cyano medium. It appears therefore that that the nitrile groups are sufficiently available within the crosslinked network, although they are located at a shorter distance from the “backbone” than in the post-modified silica gel. The material obtained in the first run was not suited as a chromatographic medium, because it needed to be pre-swelled in either THF or CH_2Cl_2 prior to use, in order to function. This was not the case for the, presumably more macroporous beads from the last two runs. The retention of the of dirhodium(II) catalyst, which was used for testing the beads between the runs, was also somewhat higher on the material II and III, as compared to I. The handling of the beads was most convenient with I and II, presumably due to the increase in the fraction of 2-ethylhexanol in the porogen mixture, which left the beads from III more sensitive to static electricity and with a slightly more amorphous appearance.

The beads II were put to a real-life test in the purification of $\text{Rh}_2(\text{cap})_4$. The reported procedure uses 35 g of the BAKERBOND Cyano chromatography medium per gram of catalyst, and the catalyst could be eluted in MeOH. In our case, 42 grams of II per gram catalyst, in a column (13×1.5 cm) was used, and the catalyst band was eluted by adding MeCN to the eluent, after having eluted the column with a few column volumes of MeOH. Upon adding MeCN to the eluent, a colour change was observed, possibly owing to the coordination of free nitrile groups replacing the ones in the stationary phase.

In figure 13.2 on the next page the colour change is shown for the complex $\text{Rh}_2(\text{OAc})_2(\text{pc})_2 \cdot \text{CH}_3\text{COOH}$ (pc = orthometalated PPh_3), recently loaded in MeOH (A), and at the beginning of the elution with MeOH/MeCN (B).

As has been discussed, the interaction with the nitrile group is stronger for the more Lewis acidic catalysts. Thus, the challenge with this system is the sufficient retention of the more weakly Lewis acidic catalysts. The result with one of the weaker Lewis acids among the dirhodium(II) catalysts utilized in diazo chemistry ($\text{Rh}_2(\text{cap})_4$), were positive. Worthy of note, is the fact that in the reported procedures for the purification of other dirhodium(II) carboxamidates on the BAKERBOND Cyano medium, MeCN needs to be added to elute the catalysts. The same was the case with the $\text{Rh}_2(\text{OAc})_2(\text{pc})_2 \cdot \text{CH}_3\text{COOH}$ used in the testing of obtained copolymer beads. In conclusion, the preliminary results with this system, hold promise of a low-cost, widely applicable system for the purification of the dirhodium(II) catalysts.

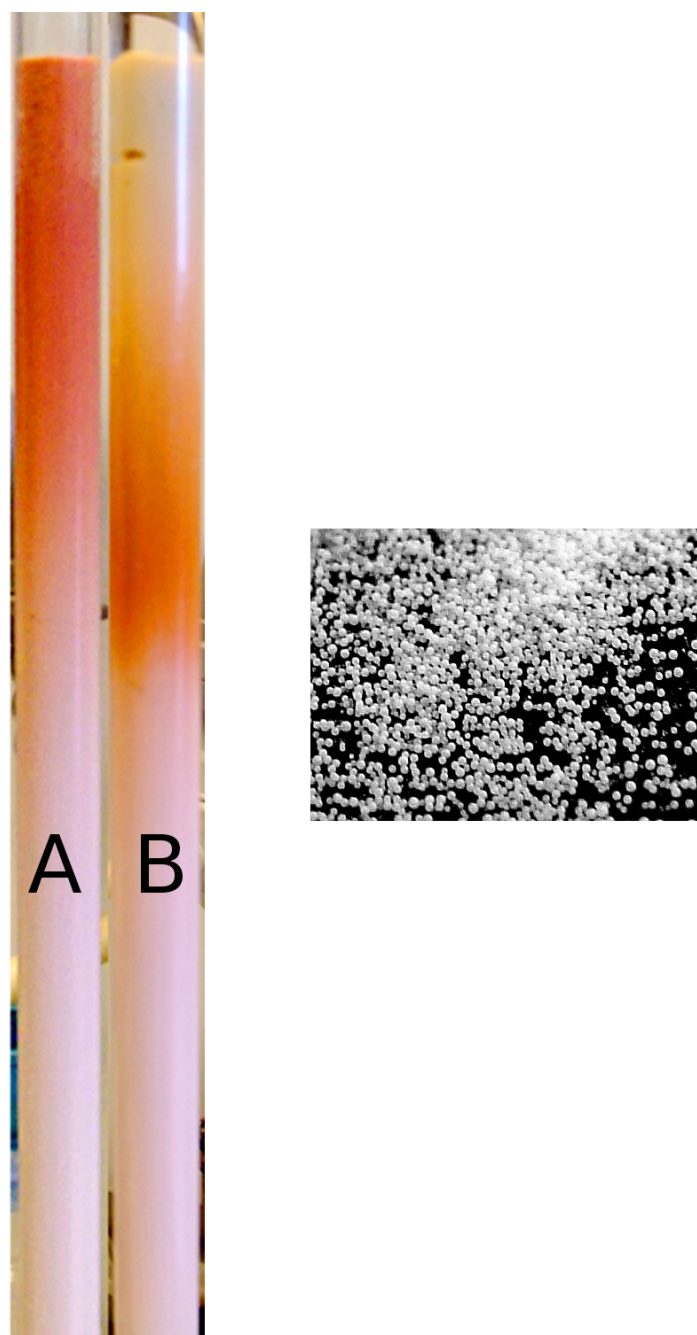


Figure 13.2.: The methacrylonitrile beads in action (left) and under the camera (right)

References & Notes

- [1] a) H. Zollinger, *Diazo Chemistry II - Aliphatic, Inorganic and Organometallic Compounds, Vol. 2 of 2*, VCH Verlagsgesellschaft mbH, Weinheim, Germany, **1995**
b) O. P. Studzinskii, I. K. Korobitsyna, *Russ. Chem. Rev.* **1970**, *39*, 834 – 843
c) A. Fersner, J. M. Karty, Y. Mo, *J. Org. Chem.* **2009**, *74*, 7245–7253
d) F. Kaplan, G. K. Meloy, *J. Am. Chem. Soc.* **1966**, *88*, 950–956
e) J. A. Moore, D. E. Reed, *Org. Synth.* **1961**, *41*, 16
f) J. D. Clark, A. S. Shah, J. C. Peterson, L. Patelis, R. J. A. Kersten, A. H. Heemskerck, M. Grogan, S. Camden, *Thermochim. Acta* **2002**, *386*, 65 – 72
g) J. D. Clark, A. S. Shah, J. C. Peterson, L. Patelis, R. J. A. Kersten, A. H. Heemskerck, *Thermochim. Acta* **2002**, *386*, 73 – 79
- [2] As Heinrich Zollinger notes in his book on diazo chemistry^{1a}: [... The beginning of diazo chemistry is generally dated to 1858 when Peter Griess discovered and identified the first aromatic diazo compound. Transient diazonium ions had been obtained, however, ten years before the discovery of Griess, but it took many years until their formation was established. In 1848 [Raffaele] Piria treated two aliphatic amines with nitrosating reagents in water and found that the amino group was replaced by a hydroxy group ...]
- [3] T. Ye, M. A. McKervey, *Chem. Rev.* **1994**, *94*, 1091–1160
- [4] J. Fink, M. Regitz, *Synthesis* **1985**, *1985*, 569–585
- [5] a) U. Schöllkopf, H. Frasnelli, *Angew. Chem. Int. Ed. Engl.* **1970**, *9*, 301–302
b) R. Brückmann, G. Maas, *Chem. Ber.* **1987**, *120*, 635–641
c) R. Brückmann, K. Schneider, G. Maas, *Tetrahedron* **1989**, *45*, 5517 – 5530
d) P. Müller, F. Lacrampe, G. Bernardinelli, *Tetrahedron: Asymmetry* **2003**, *14*, 1503 – 1510
e) P. Müller, F. Lacrampe, *Helv. Chim. Acta* **2004**, *87*, 2848 – 2859
f) W. F. Austina, Y. Zhanga, R. L. Danheiser, *Tetrahedron* **2008**, *64*, 915 – 925
- [6] a) H. J. Nees, H. Keller, T. Facklam, A. Herrmann, J. Welsch, U. Bergstraesser, H. Heydt, M. Regitz, *J. Prakt. Chem.* **1993**, *335*, 589–598

- b) J. Krysiak, C. Lyon, A. Baceiredo, H. Gornitzka, M. Mikolajczyk, G. Bertrand, *Chem. Eur. J.* **2004**, *10*, 1982 – 1986
- [7] a) M.-P. Arthur, A. Baceiredo, G. Bertrand, *J. Am. Chem. Soc.* **1991**, *113*, 5856 – 5857
b) L. Weber, H. B. Wartig, H.-G. Stammer, B. Neumann, *Organometallics* **2001**, *20*, 5248 – 5250
- [8] a) U. Schöllkopf, H. Schaefer, *Angew. Chem.* **1965**, *77*, 379
b) U. Schöllkopf, P. Tonne, H. Schaefer, P. Markusch, *Justus Liebigs Ann. Chem.* **1969**, *722*, 45–51
c) P. E. O'Bannon, W. P. Dailey, *Tetrahedron Lett.* **1989**, *30*, 4197 – 4200
d) O. A. Ivanova, N. V. Yashin, E. B. Averina, Y. K. Grishin, T. S. Kuznetsova, N. S. Zefirov, *Russ. Chem. Bull.* **2001**, *50*, 2101 – 2105
- [9] E. Cuevas-Yañez, J. M. Muchowski, R. Cruz-Almanza, *Tetrahedron Lett.* **2004**, *45*, 2417 – 2419
- [10] a) G. L. Closs, J. J. Coyle, *J. Am. Chem. Soc.* **1962**, *84*, 4350
b) G. L. Closs, J. J. Coyle, *J. Am. Chem. Soc.* **1965**, *87*, 4270 – 4279
c) F. Gerhart, U. Schöllkopf, H. Schumacher, *Angew. Chem.* **1967**, *79*, 50
d) U. Schöllkopf, F. Gerhart, M. Reetz, H. Frasnelli, H. Schumacher, *Justus Liebigs Ann. Chem.* **1968**, *716*, 204–206
e) R. J. Bussey, R. C. Neuman, Jr., *J. Org. Chem.* **1969**, *34*, 1323 – 1327
f) U. Schöllkopf, M. Reetz, *Tetrahedron Lett.* **1969**, *20*, 1541–1544
g) M. Regitz, B. Weber, U. Eckstein, *Liebigs Ann. Chem.* **1979**, *7*, 1002–1009
h) H. T. Bonge, B. Pintea, T. Hansen, *Org. Biomol. Chem.* **2008**, *6*, 3670 – 3672
- [11] a) M. Ma, L. Peng, C. Li, X. Zhang, J. Wang, *J. Am. Chem. Soc.* **2005**, *127*, 15016 – 15017
b) R. Varala, R. Enugala, S. Nuvula, S. R. Adapa, *Tetrahedron Lett.* **2006**, *47*, 877 – 880
c) K. Hasegawa, S. Arai, A. Nishida, *Tetrahedron* **2006**, *62*, 1390 – 1401
d) F. Xiao, Y. Liu, J. Wang, *Tetrahedron Lett.* **2007**, *48*, 1147 – 1149
e) P. R. Likhar, S. Roy, M. Roy, M. S. Subhas, M. L. Kantam, *Synlett* **2008**, *2008*, 1283–1286
f) B. M. Trost, S. Malhotra, B. A. Fried, *J. Am. Chem. Soc.* **2009**, *131*, 1674 – 1675
- [12] a) U. Schöllkopf, B. Bánhidai, H. Frasnelli, R. Meyer, H. Beckhaus, *Justus Liebigs Ann. Chem.* **1974**, *11*, 1767–1783
b) F. Benfatti, S. Yilmaz, P. G. Cozzi, *Adv. Synth. Catal.* **2009**, *351*, 1763 – 1767
c) A. Gioiello, F. Venturoni, B. Natalini, R. Pellicciari, *J. Org. Chem.* **2009**, *74*, 3520 – 3523

- [13] a) N. Jiang, J. Wang, *Tetrahedron Lett.* **2002**, *43*, 1285 – 1287
b) N. Jiang, Z. Ma, Z. Qu, X. Xing, L. Xie, J. Wang, *J. Org. Chem.* **2003**, *68*, 893 – 900
c) Y. Zhao, Z. Ma, X. Zhang, Y. Zou, X. Jin, J. Wang, *Angew. Chem. Int. Ed.* **2004**, *43*, 5977 – 5980
d) Y. Zhao, N. Jiang, S. Chen, C. Peng, X. Zhang, Y. Zou, S. Zhang, J. Wang, *Tetrahedron* **2005**, *61*, 6546 – 6552
e) M. L. Kantam, V. Balasubrahmanyam, K. B. S. Kumar, G. T. Venkanna, F. Figueras, *Adv. Synth. Catal.* **2007**, *349*, 1887 – 1890
- [14] a) R. L. Benoit, D. Lefebvre, M. Fréchet, *Can. J. Chem.* **1987**, *65*, 996 – 1001
b) F. G. Bordwell, *Acc. Chem. Res.* **1988**, *21*, 456–463
c) L. M. Huffman, S. S. Stahl, *J. Am. Chem. Soc.* **2008**, *130*, 9196–9197
d) I. Leito, *Acidity-Basicity Data (pKa Values) in Nonaqueous Solvents*, http://tera.chem.ut.ee/~ivo/HA_UT/
- [15] *Chemical Abstracts Service*, **2008**, accessed July, 2010.
- [16] a) C. Varkey, PhD thesis, Faculty of Science, Mahatma Ghandi University, **1998**
b) E. H. Crowston, A. M. Lobo, S. Parbhakar, H. S. Rzepa, D. J. Williams, *J. Chem. Soc. Chem. Commun.* **1984**, *5*, 276 – 278
c) S. M. Ahmad, D. C. Braddock, G. Cansell, S. A. Hermitage, *Tetrahedron Lett.* **2007**, *48*, 915 – 918
- [17] a) S. M. Ahmad, D. C. Braddock, G. Cansell, S. A. Hermitage, J. M. Redmond, A. J. White, *Tetrahedron Lett.* **2007**, *48*, 5948 – 5952
b) K. K. Davood Azarifar, R. A. Veisi, *ARKIVOC* **2010**, *ix*, 178 – 184
- [18] a) J. R. Shelton, T. Kasuga, *J. Org. Chem.* **1963**, *28*, 2841–2843
b) S.-s. Jew, *Arch. Pharmacol Res.* **1982**, *5*, 97 – 101
c) C. M. Das, P. Indrasenan, *Int. J. Food Sci. Technol.* **1987**, *22*, 339 – 344
d) I. V. Koval, *Russ. J. Org. Chem.* **2001**, *37*, 297 – 317
e) I. V. Koval, *Russ. J. Org. Chem.* **2002**, *38*, 301 – 337
f) E. Kolvari, A. Ghorbani-Choghamarani, P. Salehi, F. Shirini, M. A. Zolfigol, *J. Iran. Chem. Soc.* **2007**, *4*, 126 – 174
- [19] M. Regitz, G. Maas, *Diazo compounds: properties and synthesis*, Orlando: Academic Press, **1986**
- [20] a) W. v. E. Doering, A. K. Hoffmann, *J. Am. Chem. Soc.* **1954**, *76*, 6162–6165
b) W. v. E. Doering, R. G. Buttery, R. G. Laughlin, N. Chaudhuri, *J. Am. Chem. Soc.* **1956**, *78*, 3224

- c) P. S. Skell, A. Y. Garner, *J. Am. Chem. Soc.* **1956**, *78*, 3409–3411
- d) P. S. Skell, A. Y. Garner, *J. Am. Chem. Soc.* **1956**, *78*, 5430–5433
- e) J. M. Fox, J. E. G. Scacheri, K. G. L. Jones, M. Jones, Jr., P. B. Shevlin, B. Armstrong, R. Szyrbicka, *Tetrahedron Lett.* **1992**, *33*, 5021–5024
- f) R. A. Moss, C. B. Mallon, C.-T. Ho, *J. Am. Chem. Soc.* **1977**, *99*, 4105 – 4110
- g) A. J. Arduengo, *Acc. Chem. Res.* **1999**, *32*, 913–921
- h) A. J. Arduengo, III, J. Calabrese, F. Davidson, H. Rasika Dias, J. R. Goerlich, R. Krafczyk, W. J. Marshall, M. Tamm, R. Schmutzler, *Helv. Chim. Acta* **1999**, *82*, 2348–2364
- i) D. Bourissou, O. Guerret, F. P. Gabbaï, G. Bertrand, *Chem. Rev.* **2000**, *100*, 39 – 91
- j) R. A. Moss, *Carbene Philicity*, FontisMedia S.A. and Marcel Dekker, Inc., **2002**, pp. 57–96
- k) E. M. Tippmann, M. S. Platz, I. B. Svir, O. V. Klymenko, *J. Am. Chem. Soc.* **2004**, *126*, 5750–5762
- [21] At first under the supervision of G.L. Closs. See references to his work on the halogenation of diazomethane^{10b,10a}
- [22] a) A. B. Charette, H. Lebel, *Cyclopropanation and C-H Insertion with metals other than Cu and Rh*, Vol. 2, Springer, 1st ed., **1999**, pp. 581–603
- b) P. Gois, C. Afonso, *Eur. J. Org. Chem.* **2004**, *2004*, 3773–3788
- c) D. J. Timmons, M. P. Doyle in *Multiple Bonds Between Metal Atoms* (Eds.: F. A. Cotton, C. A. Murillo, R. A. Walton), Springer Science and Business Media, Inc., 3rd ed., **2005**, pp. 591–632
- d) *Multiple bonds between metal atoms*, (Eds.: F. A. Cotton, C. A. Murillo, R. A. Walton), Springer Science and Business Media, Inc., 3rd ed., **2005**
- e) B. Liu, S.-F. Zhu, W. Zhang, C. Chen, Q.-L. Zhou, *J. Am. Chem. Soc.* **2007**, *129*, 5834–5835
- f) M. P. Doyle, R. Duffy, M. Ratnikov, L. Zhou, *Chem. Rev.* **2010**, *110*, 704 – 724
- [23] a) M. C. Pirrung, A. T. Morehead, Jr., *J. Am. Chem. Soc.* **1994**, *116*, 8991 – 9000
- b) M. P. Doyle, T. Ren in *Progress in Inorganic Chemistry* (Ed.: K. D. Karlin), **2001**, pp. 113–168
- c) J. Lloret, J. J. Carbo, C. Bo, A. Lledos, J. Perez-Prieto, *Organometallics* **2008**, *27*, 2873 – 2876
- [24] a) G. Stork, N. Kazuhiko, *Tetrahedron Lett.* **1988**, *29*, 2283 – 2286
- b) A. Padwa, D. J. Austin, A. T. Price, M. A. Semones, M. P. Doyle, M. N. Protopopova, W. R. Winchester, A. Tran, *J. Am. Chem. Soc.* **1993**, *115*, 8669–8680
- c) N. Watanabe, M. Anada, S.-i. Hashimoto, S. Ikegami, *Synlett* **1994**, *1994*,

1031–1033

d) H. M. L. Davies, C. Venkataramani, T. Hansen, D. W. Hopper, *J. Am. Chem. Soc.* **2003**, *125*, 6462–6468

e) E. Nakamura, N. Yoshikai, M. Yamanaka, *J. Am. Chem. Soc.* **2002**, *124*, 7181–7192

f) D. G. H. Hetterscheid, C. Hendriksen, W. I. Dzik, J. M. M. Smits, E. R. H. van Eck, A. E. Rowan, V. Busico, M. Vacatello, V. Van Axel Castelli, A. Segre, E. Jellema, T. G. Bloemberg, B. de Bruin, *J. Am. Chem. Soc.* **2006**, *128*, 9746–9752

- [25] a) G. A. Rempel, P. Legzdins, H. Smith, G. Wilkinson, D. A. Ucko, *Inorg. Synth.* **1972**, *13*, 90–91
- b) A. R. Barron, G. Wilkinson, M. Motevalli, M. B. Hursthouse, *Polyhedron* **1985**, *4*, 1131 – 1134
- c) A. R. Chakravarty, F. A. Cotton, D. A. Tocher, J. H. Tocher, *Organometallics* **1985**, *4*, 8–13
- d) P. Lahuerta, J. Paya, M. A. Pellinghelli, A. Tiripicchio, *Inorg. Chem.* **1992**, *31*, 1224–1232
- e) G. H. P. Roos, M. A. McKerverey, *Synth. Commun.* **1992**, *22*, 1751–1756
- f) M. P. Doyle, L. J. Westrum, W. N. E. Wolthuis, M. M. See, W. P. Boone, V. Bagheri, M. M. Pearson, *J. Am. Chem. Soc.* **1993**, *115*, 958–964
- g) M. C. Pirrung, A. T. Morehead, Jr., *J. Am. Chem. Soc.* **1996**, *118*, 8162 – 8163
- h) D. F. Taber, S. C. Malcolm, K. Bieger, P. Lahuerta, M. Sanaú, S.-E. Stiriba, J. Pérez-Prieto, M. A. Monge, *J. Am. Chem. Soc.* **1999**, *121*, 860–861
- i) T. Ren, C. Lin, E. J. Valente, J. D. Zubkowski, *Inorg. Chim. Acta* **2000**, *297*, 283 – 290
- j) F. Estevan, P. Krueger, P. Lahuerta, E. Moreno, J. Pérez-Prieto, M. Sanaú, H. Werner, *Eur. J. Inorg. Chem.* **2001**, *2001*, 105–109
- k) M. Basato, A. Biffis, G. Martinati, C. Tubaro, C. Graiff, A. Tiripicchio, L. A. Aronica, A. M. Caporusso, *J. Organomet. Chem.* **2006**, *691*, 3464 – 3471
- l) C. J. Welch, Q. Tu, T. Wang, C. Raab, P. Wang, X. Jia, X. Bu, D. Bykowski, B. Hohenstaufen, M. P. Doyle, *Adv. Synth. Catal.* **2006**, *348*, 821–825
- m) P. Hirva, J. Esteban, J. Lloret, P. Lahuerta, J. Pérez-Prieto, *Inorg. Chem.* **2007**, *46*, 2619–2626
- n) J. M. Nichols, PhD thesis, University of Maryland, **2008**
- [26] a) H. T. Bonge, T. Hansen, *Synthesis* **2009**, *1*, 91 – 96
- b) H. T. Bonge, T. Hansen, *J. Org. Chem.* **2010**, *75*, 2309–2320
- c) H. T. Bonge, T. Hansen, *Eur. J. Org. Chem.* **2010**, *2010*, 4355–4359
- [27] a) E. J. Corey, A. M. Felix, *J. Am. Chem. Soc.* **1965**, *87*, 2518–2519
- b) R. H. Earle, Jr., D. T. Hurst, M. Viney, *J. Chem. Soc. C* **1969**, 2093 – 2098

- c) D. M. Brunwin, G. Lowe, J. Parker, *J. Chem. Soc. D* **1971**, 865 – 867
- d) S. D. Burke, P. A. Grieco, *Org. React. (N.Y.)* **1979**, 26, 361 – 475
- e) D. D. Ridley, G. W. Simpson, *Aust. J. Chem.* **1986**, 39, 687 – 698
- f) M. P. Doyle, M. S. Shanklin, S. M. Oon, H. Q. Pho, F. R. V. der Heide, W. R. Veal, *J. Org. Chem.* **1988**, 53, 3384 – 3386
- g) Y. Okada, T. Minami, M. Miyamoto, T. Otaguro, S. Sawasaki, J. Ichikawa, *Heteroat. Chem.* **1995**, 6, 195 – 210
- h) J. M. Axten, L. Krim, H. F. Kung, J. D. Winkler, *J. Org. Chem.* **1998**, 63, 9628–9629
- [28] a) N. G. Johansson, B. Åkermark, *Acta. Chem. Scand. B* **1971**, 25, 1927 – 1929
- b) N. G. Johansson, B. Åkermark, *Tetrahedron Lett.* **1971**, 12, 4785–4786
- c) B. Åkermark, I. Lagerlund, J. Lewandowska, *Acta. Chem. Scand. B* **1974**, 28, 1238 – 1239
- d) B. Åkermark, S. Bystrøm, E. Florin, N. G. Johansson, I. Lagerlund, *Acta. Chem. Scand. B* **1974**, 28, 375 – 376
- e) I. Lagerlund, *Acta. Chem. Scand. B* **1976**, 30, 318 – 322
- [29] D. Seyferth, J. M. Burlitch, H. Dertouzos, H. D. Simmons, *J. Organomet. Chem.* **1967**, 7, 405 – 413
- [30] a) J. W. T. Curtius, *Ber. Dtsch. Chem. Ges.* **1883**, 16, 2230–2231
- b) H. V. Pechmann, *Ber. Dtsch. Chem. Ges.* **1894**, 27, 1888–1891
- c) G. Maas, *Angew. Chem. Int. Ed.* **2009**, 48, 8186–8195
- [31] a) T. Toma, J. Shimokawa, T. Fukuyama, *Org. Lett.* **2007**, 9, 3195 – 3197
- b) A. G. Newcombe, *Can. J. Chem.* **1955**, 33, 1250 – 1255
- c) L. Zhang, X. jun Wang, J. Wang, N. Grinberg, D. Krishnamurthy, C. H. Senanayake, *Tetrahedron Lett.* **2009**, 50, 2964 – 2966
- [32] a) N. P. Peet, S. Sunder, *J. Heterocycl. Chem.* **1975**, 12, 1191–1197
- b) J.-M. Contreras, I. Parrot, W. Sippl, Y. M. Rival, C. G. Wermuth, *J. Med. Chem.* **2001**, 44, 2707–2718
- c) X.-M. e. a. Zheng, *Yingyong Huaxue* **2007**, 24, 850–852
- [33] a) A. Ouhia, L. René, B. Badet, *Tetrahedron Lett.* **1992**, 33, 5509 – 5510
- b) A. Ouhia, L. Rene, J. Guilhem, C. Pascard, B. Badet, *J. Org. Chem.* **1993**, 58, 1641 – 1642
- c) M. P. Doyle, A. V. Kalinin, *J. Org. Chem.* **1996**, 61, 2179–2184
- [34] a) H. O. House, C. J. Blankley, *J. Org. Chem.* **1968**, 33, 53 – 60
- b) F. J. Sauter, C. J. Blankley, O. House, *Org. Synth.* **1969**, 49, 22

- [35] a) J. H. Boyer, C. H. Mack, N. Goebel, L. R. Morgan, Jr., *J. Org. Chem.* **1958**, *23*, 1051–1053
b) A. Liedhegener, M. Regitz, *Ber. Dtsch. Chem. Ges.* **1966**, *99*, 3128–3147
c) M. P. Doyle, R. J. Pieters, J. Taunton, H. Q. Pho, A. Padwa, D. L. Hertzog, L. Precedo, *J. Org. Chem.* **1991**, *56*, 820 – 829
d) M. P. Doyle, R. L. Dorow, J. W. Terpstra, R. A. Rodenhouse, *J. Org. Chem.* **1985**, *50*, 1663 – 1666
e) D. F. Taber, R. E. Ruckle, Jr., M. J. Hennessy, *J. Org. Chem.* **1986**, *51*, 4077 – 4078
f) C. P. Park, A. Nagle, C. H. Yoon, C. Chen, K. W. Jung, *J. Org. Chem.* **2009**, *74*, 6231 – 6236
- [36] a) B. Trost, *Science* **1991**, *254*, 1471 – 1477
b) M. C. Cann, *A Green Chemistry Module: ATOM ECONOMY: A Measure of the Efficiency of a Reaction*, Web page, **2010**,
<http://academic.scranton.edu/faculty/cannm1/organicmodule.html>
- [37] a) R. S. Grainger, N. E. Leadbeater, A. M. Pàmies, *Catal. Commun.* **2002**, *3*, 449 – 452
b) J. V. Ruppel, T. J. Gauthier, N. L. Snyder, J. A. Perman, X. P. Zhang, *Org. Lett.* **2009**, *11*, 2273–2276
c) M. Regitz, J. Hocker, A. Liedhegener, *Org. Prep. Proced.* **1969**, *1*, 99–104
d) G. Lowe, J. Parker, *J. Chem. Soc. D* **1971**, *18*, 1135–1136
e) J. S. Wiering, H. Wynberg, *J. Org. Chem.* **1976**, *41*, 1574–1578
f) K. Bott, *Chem. Ber.* **1987**, *120*, 1867–1871
g) A. Skiebe, A. Hirsch, *J. Chem. Soc. Chem. Commun.* **1994**, *3*, 335–336
h) M. P. Doyle, A. V. Kalinin, *Synlett* **1995**, *1995*, 1075–1076
i) V. K. Aggarwal, P. Blackburn, R. Fieldhouse, R. V. H. Jones, *Tetrahedron Lett.* **1998**, *39*, 8517 – 8520
j) A. Saghatelian, J. Buriak, V. S. Y. Lin, M. R. Ghadiri, *Tetrahedron* **2001**, *57*, 5131 – 5136
- [38] Using 0.5 eq 2-Naphthaldehyde as an internal standard. ^{10h} See section 10.0.3 on page 100 in the experimental section for details
- [39] a) R. P. Bywater, *J. Mol. Recognit.* **2005**, *18*, 60 – 72
b) R. P. Bywater in *GPCRs: From Deorphanization to Lead Structure Identification*, Springer Berlin Heidelberg, **2007**, pp. 75–92
- [40] J. M. Richter, B. W. Whitefield, T. J. Maimone, D. W. Lin, M. P. Castroviejo, P. S. Baran, *J. Am. Chem. Soc.* **2007**, *129*, 12857–12869
- [41] H. E. Gottlieb, V. Kotlyar, A. Nudelman, *J. Org. Chem.* **1997**, *62*, 7512–7515

- [42] S. P. L. de Souza, J. F. M. da Silva, M. C. S. de Mattos, *Synth. Commun.* **2003**, *33*, 935–939
- [43] J. Tafel, M. Stern, *Ber. Dtsch. Chem. Ges.* **1900**, *33*, 2224–2236
- [44] A. E. Parsons, *J. Mol. Spectrosc.* **1961**, *6*, 201 – 204
- [45] H. J. Dauben, Jr., L. L. McCoy, *J. Am. Chem. Soc.* **1959**, *81*, 4863 – 4873
- [46] J.-J. Kim, D.-H. Kweon, S.-D. Cho, H.-K. Kim, S.-G. Lee, Y.-J. Yoon, *Synlett* **2006**, *2*, 194 – 200
- [47] E. Sanchez, M. Fumarola, *Synthesis* **1976**, *11*, 736–737
- [48] S. K. Vasisht, P. Venugopalan, J. Kataria, A. Sharma, *Indian J. Chem.* **2002**, *41A*, 2054–2059
- [49] B. P. Axe, *J. Pharm. Biomed. Anal.* **2006**, *41*, 804 – 810
- [50] A. T. Lebedev, *Mass Spectrom. Rev.* **1991**, *10*, 91–132
- [51] Å. Kaupang, C. H. Görbitz, T. Hansen, *Acta Crystallogr. Sect. E: Struct. Rep. Online* **2010**, *66*, o1299
- [52] The chromatographic medium is registered to CAS # 126850-03-1, and is the product of a reaction between silica gel (CAS # 63231-67-4), (4-trichlorosilyl) butanenitrile (CAS # 1071-27-8) and chlorotrimethylsilane (CAS # 75-77-4)
- [53] a) M. Wojaczynska, B. N. Kolarz, *J. Chromatogr. A* **1980**, *196*, 75 – 83
b) B. N. Kolarz, P. P. Wieczorek, M. Wojaczynska, *Angew. Makromol. Chem.* **1981**, *96*, 193–200
c) M. Wojaczynska, B. N. Kolarz, *J. Chromatogr. A* **1986**, *358*, 129 – 136
d) I. C. Poinescu, C. Beldie, *Angew. Makromol. Chem.* **1988**, *164*, 45–58
e) M. Wojaczynska, B. N. Kolarz, D. Hlavata, J. Liesiene, A. Gorbunov, *Makromol. Chem.* **1992**, *193*, 2259–2264
f) B. N. Kolarz, M. Wojaczynska, J. Bryjak, B. Pawlów, *React. Polym.* **1994**, *23*, 123 – 130
- [54] Z. Michalska, B. Ostaszewski, J. Zientarska, B. Kolarz, M. Wojaczynska, *React. Polym.* **1992**, *16*, 213 – 221

Part IV.

Appendix

Contents of Appendix

Contents of Appendix	129
14 NMR Spectra	135
14.1 <i>N</i> -bromo-2-pyrrolidone	136
14.1.1 ¹ H-NMR	136
14.1.2 ¹³ C-NMR	137
14.2 <i>N</i> -bromophthalimide	138
14.2.1 ¹ H-NMR	138
14.3 <i>N,N'</i> -ditosylhydrazine	139
14.3.1 ¹ H-NMR	139
14.3.2 ¹³ C-NMR	140
14.4 2-bromo-1-(pyrrolidin-1-yl)ethanone	141
14.4.1 ¹ H-NMR	141
14.4.2 ¹³ C-NMR & DEPT-135	142
14.5 2-bromo-1-(piperidin-1-yl)ethanone	143
14.5.1 ¹ H-NMR	143
14.5.2 ¹³ C-NMR & DEPT-135	144
14.6 1-(azepan-1-yl)-2-bromoethanone	145
14.6.1 ¹ H-NMR	145
14.6.2 ¹³ C-NMR & DEPT-135	146
14.6.3 HMQC (¹ J _{13C,1H})	147

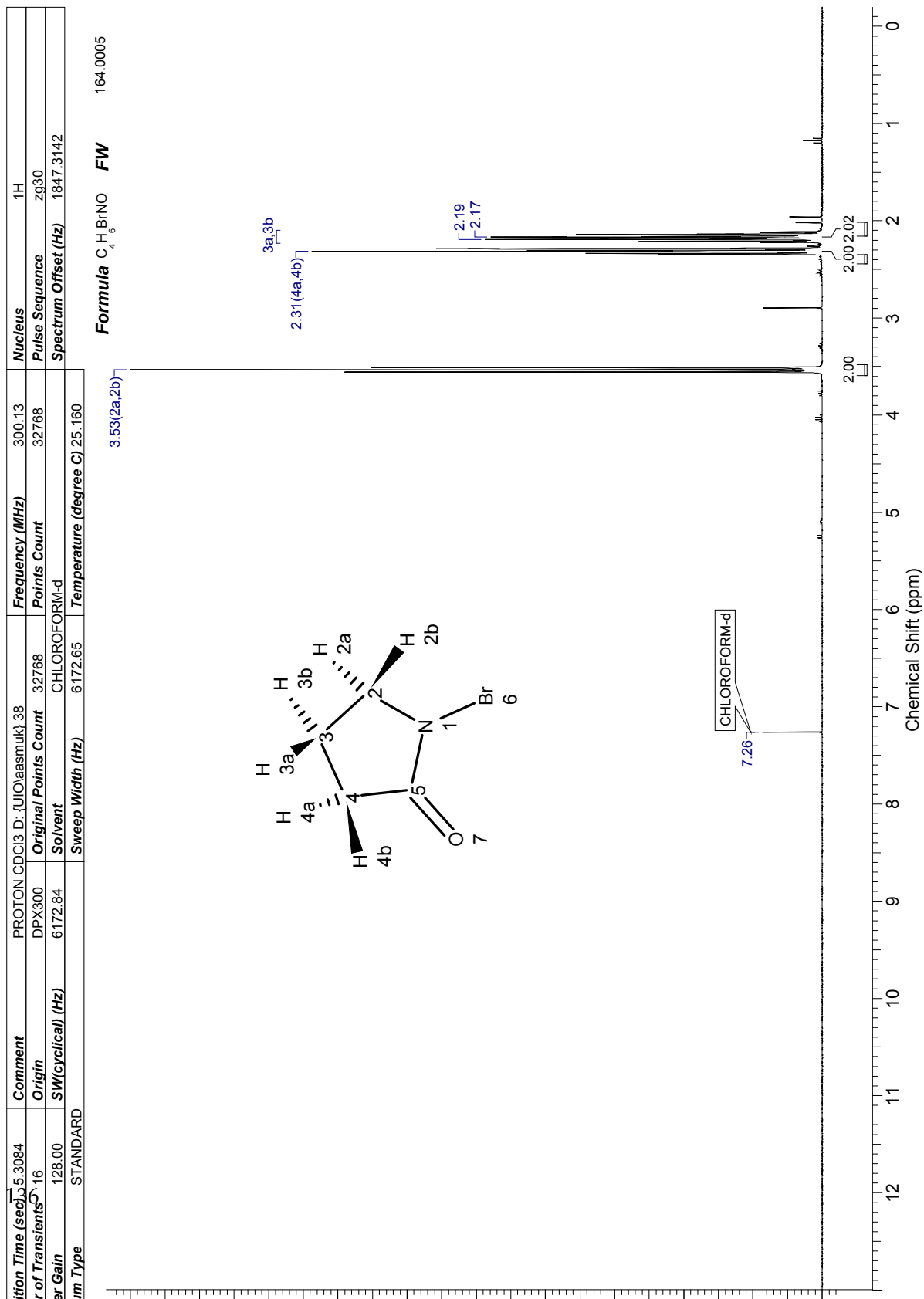
14.7	<i>tert</i> -butyl 4-(2-bromoacetyl)piperazine-1-carboxylate	148
14.7.1	¹ H-NMR	148
14.7.2	¹³ C-NMR & DEPT-135	149
14.8	<i>N,N'</i> -bis(2-bromoacetyl)piperazine	150
14.8.1	¹ H-NMR	150
14.8.2	¹³ C-NMR & DEPT-135	151
14.9	2-bromo-1-morpholinoethanone	152
14.9.1	¹ H-NMR	152
14.9.2	¹³ C-NMR & DEPT-135	153
14.10	2-bromo-1-(1,1-dioxidothiomorpholino)ethanone	154
14.10.1	¹ H-NMR	154
14.10.2	¹³ C-NMR & DEPT-135	155
14.11	2-diazo-1-(pyrrolidin-1-yl)ethanone	156
14.11.1	¹ H-NMR	156
14.11.2	¹³ C-NMR & DEPT-135	157
14.11.3	Crude ¹ H-NMR	158
14.12	2-diazo-1-(piperidin-1-yl)ethanone	159
14.12.1	¹ H-NMR	159
14.12.2	¹³ C-NMR & DEPT-135	160
14.12.3	HMQC (¹ <i>J</i> _{13C,1H})	161
14.13	1-(azepan-1-yl)-2-diazoethanone	162
14.13.1	¹ H-NMR	162
14.13.2	¹³ C-NMR & DEPT-135	163
14.13.3	HMQC (¹ <i>J</i> _{13C,1H})	164
14.14	<i>tert</i> -butyl 4-(2-diazoacetyl)piperazine-1-carboxylate	165
14.14.1	¹ H-NMR	165

14.14.2	¹³ C-NMR & DEPT-135	166
14.15	<i>N,N'</i> -bis(2-diazoacetyl)piperazine	167
14.15.1	¹ H-NMR	167
14.15.2	¹³ C-NMR	168
14.16	2-diazo-1-morpholinoethanone	169
14.16.1	¹ H-NMR	169
14.16.2	¹³ C-NMR & DEPT-135	170
14.16.3	HMQC (¹ J _{13C,1H})	171
14.17	2-diazo-1-(1,1-dioxido-4-thiomorpholinyl)ethanone	172
14.17.1	¹ H-NMR	172
14.17.2	¹³ C-NMR	173
14.18	1,1,3,3-tetramethylguanidine sulfinat (and sulfonate)	174
14.18.1	¹ H-NMR	174
14.19	Crude 6-bromo-1-azabicyclo[3.2.0]heptan-7-one	175
14.19.1	¹ H-NMR	175
14.20	Crude 7-bromo-1-azabicyclo[4.2.0]octan-8-one - NBS	176
14.20.1	¹ H-NMR	176
14.21	Crude 7-bromo-1-azabicyclo[4.2.0]octan-8-one - NBP	177
14.21.1	¹ H-NMR	177
14.22	Crude 8-bromo-1-azabicyclo[5.2.0]nonan-9-one	178
14.22.1	¹ H-NMR	178
14.23	Crude <i>tert</i> -butyl 7-bromo-8-oxo-1,4-diazabicyclo[4.2.0]octane-4-carboxylate	179
14.23.1	¹ H-NMR	179
14.24	Crude 7-bromo-4-oxa-1-azabicyclo[4.2.0]octan-8-one	180
14.24.1	¹ H-NMR	180

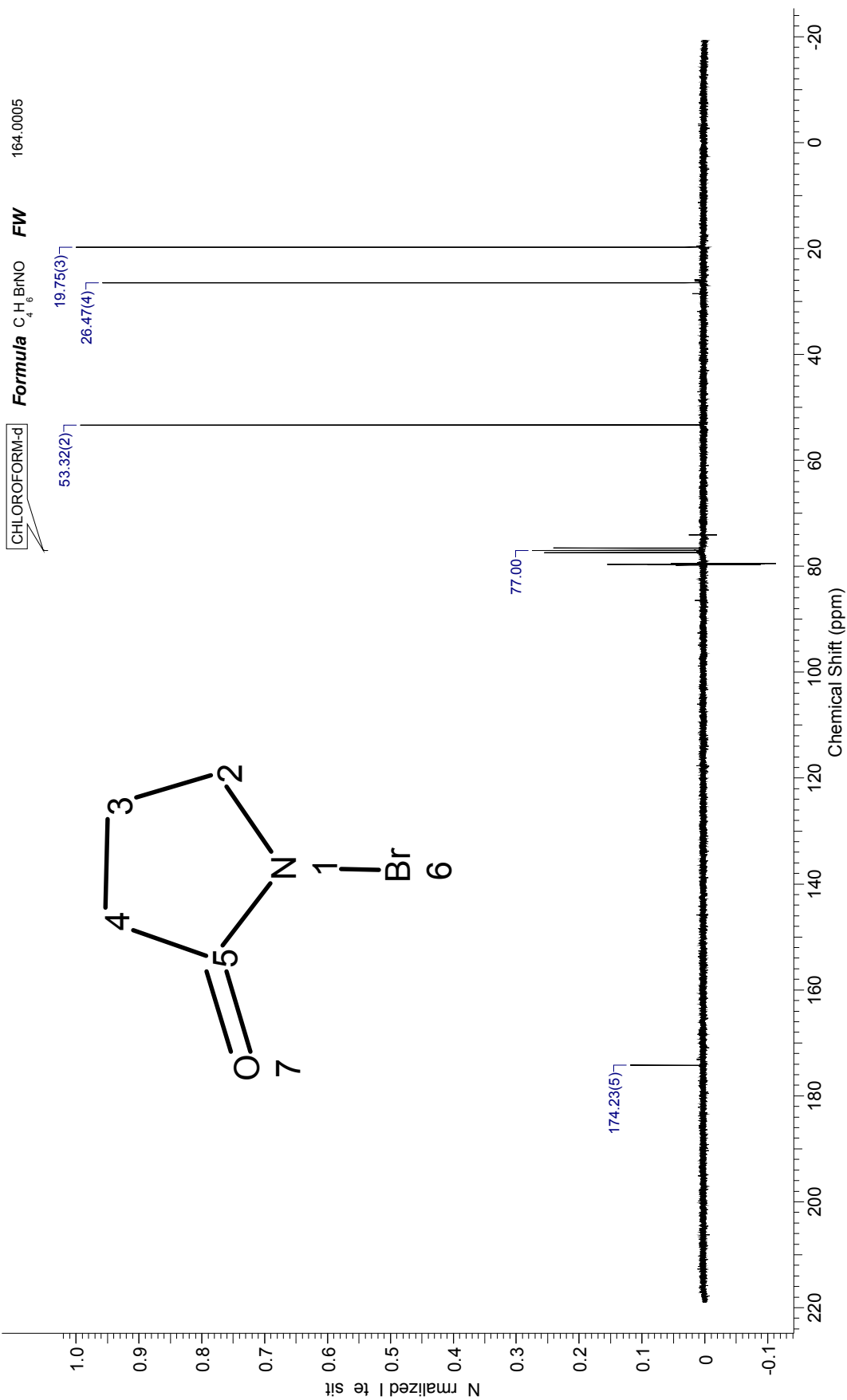
14.25	Crude 7-bromo-4-thia-1-azabicyclo[4.2.0]octan-8-one 4,4-dioxide .	181
14.25.1	¹ H-NMR	181
14.26	Crude; carbene dimer from catalytic decomposition of 2d with Cu(acac) ₂	182
14.26.1	¹ H-NMR	182
14.27	7-bromo-1-azabicyclo[4.2.0]octan-8-one	183
14.27.1	¹ H-NMR	183
14.28	1-(piperidin-1-yl)-2-tosylethanone	184
14.28.1	¹ H-NMR	184
14.28.2	¹³ C-NMR	185
14.29	2,2-dibromo-1-(piperidin-1-yl)ethanone	186
14.29.1	¹ H-NMR	186
14.29.2	FID	187
14.30	<i>cis</i> -8-bromo-1-azabicyclo[5.2.0]nonan-9-one	188
14.30.1	¹ H-NMR	188
14.30.2	¹³ C-NMR & DEPT-135	189
14.31	<i>trans</i> -8-bromo-1-azabicyclo[5.2.0]nonan-9-one	190
14.31.1	¹ H-NMR	190
14.31.2	¹³ C-NMR & DEPT-135	191
14.32	<i>cis</i> -2,2-Tetrakis μ -caprolactamato dirhodium(II)	192
14.32.1	¹ H-NMR	192
14.33	<i>cis</i> - <i>M/P</i> -Rh ₂ (μ -O ₂ CCH ₃) ₂ [Ph ₂ P(C ₆ H ₄)] ₂ (CH ₃ CN) ₂	193
14.33.1	¹ H-NMR	193
14.33.2	¹³ C-NMR	194
14.33.3	HMQC (¹ J _{13C,1H})	195
14.33.4	³¹ P-NMR	196

14.34	Crude; thermolysis of α -Br-EDA in neat styrene	197
14.34.1	$^1\text{H-NMR}$	197
14.35	Thermolysis product of α -Br-EDA in neat styrene (w/ internal standard)	198
14.35.1	$^1\text{H-NMR}$	198
14.36	Crude; thermolysis of (4d) in neat styrene	199
14.36.1	$^1\text{H-NMR}$	199
15	X-ray Diffraction Data	201
15.1	<i>N,N'</i> -bis(2-diazoacetyl)piperazine (5c)	202
15.1.1	XRD Data	202
15.2	2-diazo-1-(1,1-dioxido-4-thiomorpholiny)ethanone (8c)	203
15.2.1	XRD Data	203
15.3	TMG <i>p</i> -toluenesulfinate	204
15.3.1	XRD Data	204
15.4	TMG <i>p</i> -toluenesulfonate	205
15.4.1	XRD Data	205
15.5	<i>tert</i> -butyl 4-(2-diazoacetyl)piperazine-1-carboxylate (4c)	206
15.5.1	Publication in Acta Cryst. E	206

14. NMR Spectra



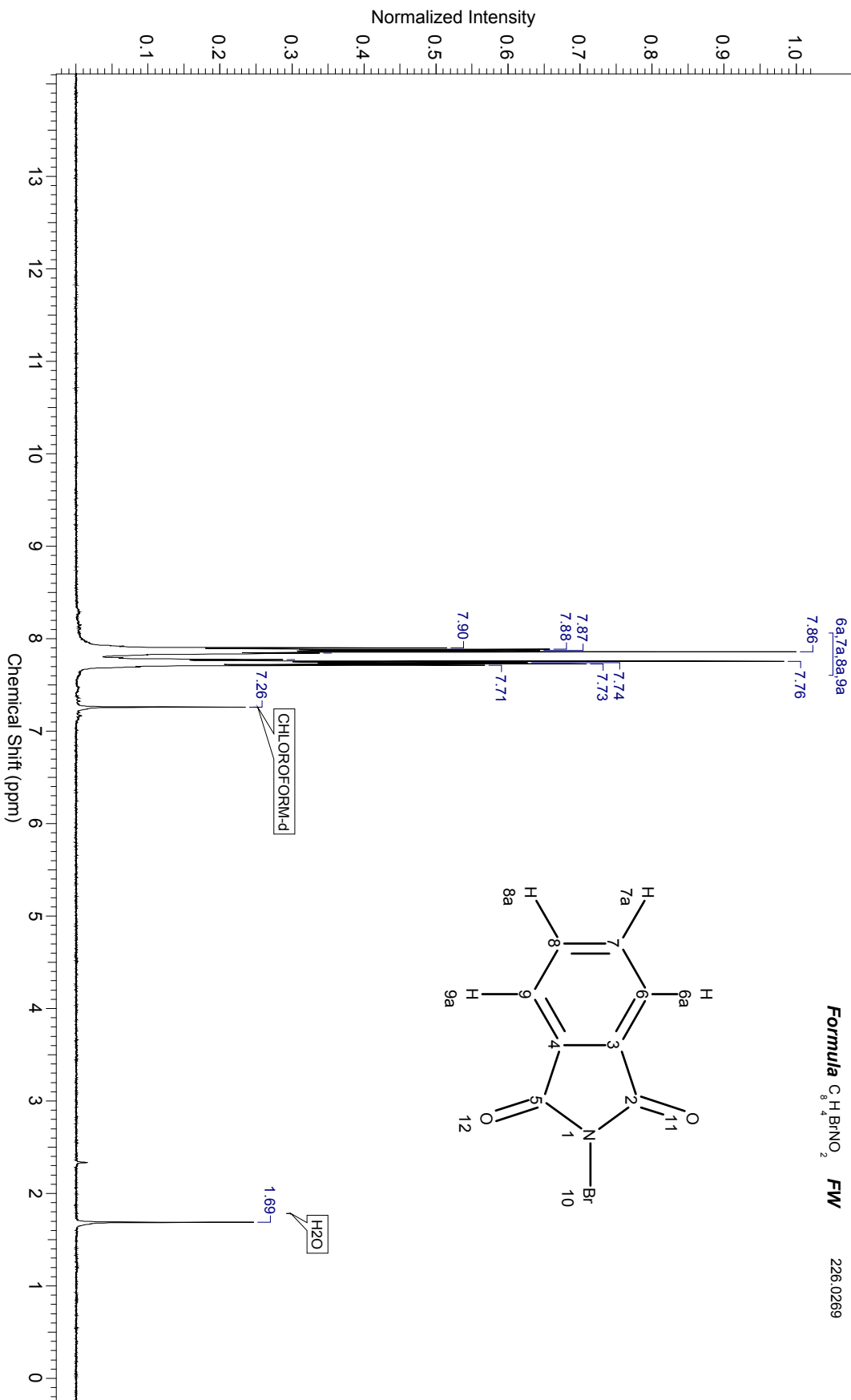
Acquisition Time (sec)	1.8219	Comment	C13CPD CDC13 D: (JIO\laasmuk)\38	Frequency (MHz)	75.48	Nucleus	¹³ C
Number of Transients	512	Origin	DPX300	Points Count	32768	Pulse Sequence	zgpg30
Receiver Gain	3251.00	SW(cyclical) (Hz)	17985.61	Original Points Count	32768	Spectrum Offset (Hz)	7533.1514
Spectrum Type	STANDARD	Solvent	CHLOROFORM-d	Sweep Width (Hz)	17985.06	Temperature (degree C)	25.160



¹H-NMR – N-bromophthalimide

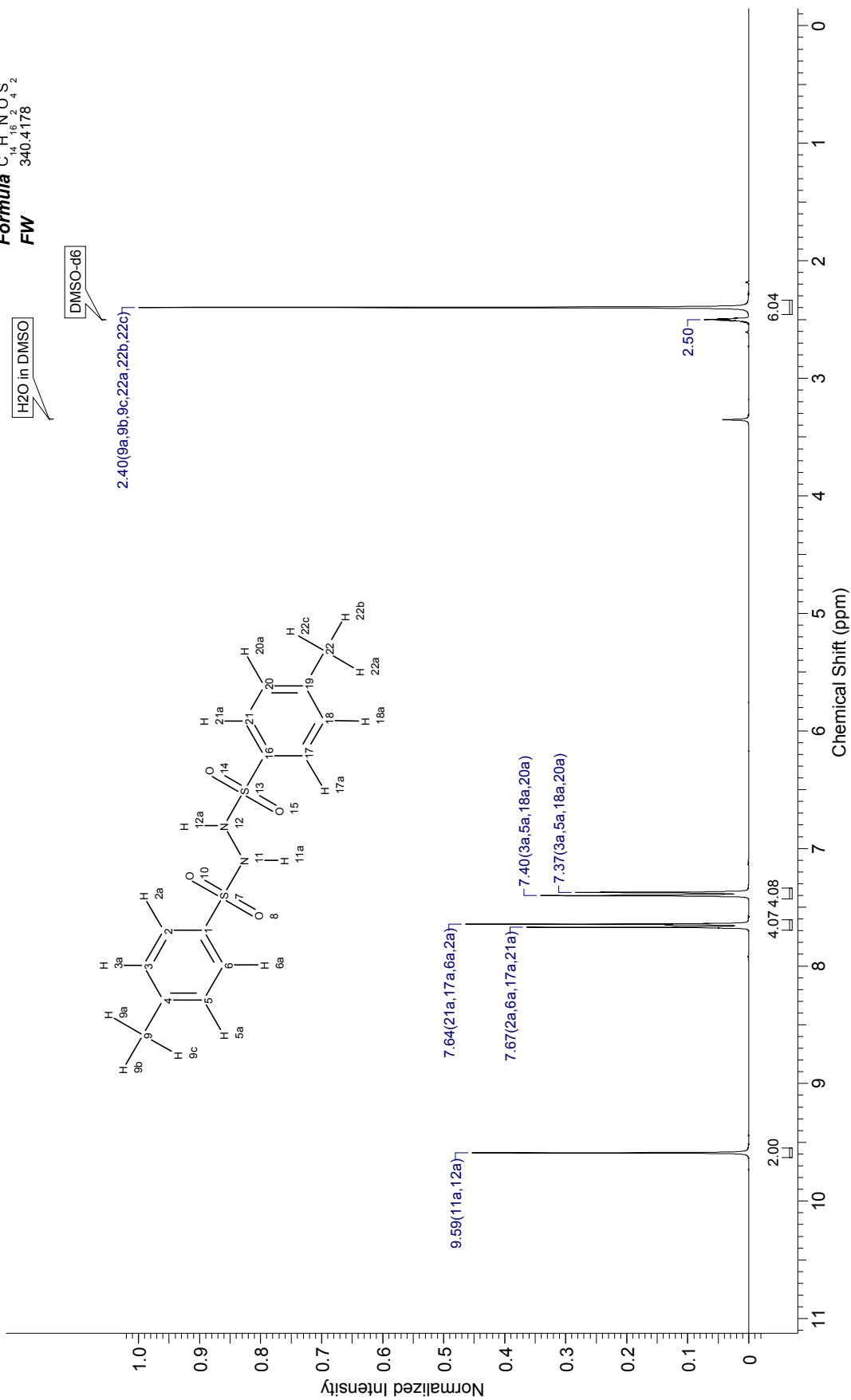
Acquisition Time (sec)	2.9999	Frequency (MHz)	200.13	Nucleus	¹ H	Number of Transients	16	Origin	DPX200
Original Points Count	12417	Points Count	16384	Pulse Sequence	zg30	Receiver Gain	1625.50	SW(cyclical) (Hz)	4139.07
Solvent	CHLOROFORM-d	Temperature (degree C)	25.160	Spectrum Offset (Hz)	1233.7882	Spectrum Type	STANDARD		
Sweep Width (Hz)	4138.82								

Formula C₈H₄BrNO₂ FW 226.0269



Acquisition Time (sec)	5.3084	Comment	PROTON DMSO D: (UIO\vaasmuk) 31	Frequency (MHz)	300.13	Nucleus	¹ H
Number of Transients	16	Origin	DPX300	Points Count	32768	Pulse Sequence	zg30
Receiver Gain	161.30	SW(cyclical) (Hz)	6172.84	Solvent	DMSO-d6	Spectrum Type	STANDARD
Sweep Width (Hz)	6172.65	Temperature (degree C)	25.160	Original Points Count	32768		
				Spectrum Offset (Hz)	1852.0708		

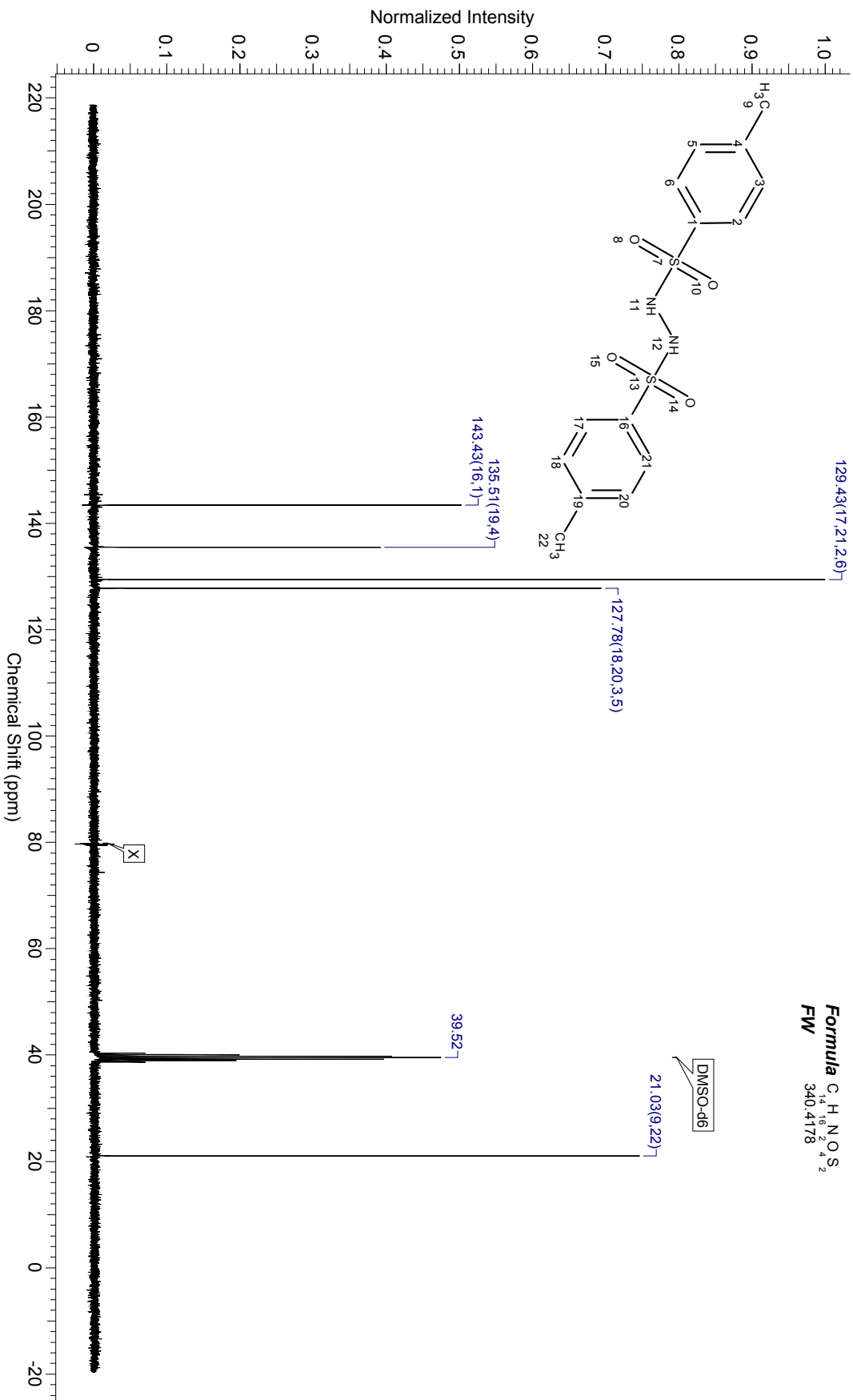
Formula C₁₄H₁₆N₂O₄S₂
FW 340.4178



¹³C-NMR – N,N'-ditosylhydrazine

Acquisition Time (sec)	1.8219	Comment	C13CPD DMSO-D: (UO)aasmuk\31	Frequency (MHz)	75.48	Nucleus	13C
Number of Transients	512	Origin	DPX300	Points Count	32768	Pulse Sequence	ZPD930
Receiver Gain	3649.10	SW(Cyclical) (Hz)	17985.61	Spectrum Offset (Hz)	7511.2959	Spectrum Type	STANDARD
Sweep Width (Hz)	17985.06	Temperature (degree C)	25.160				

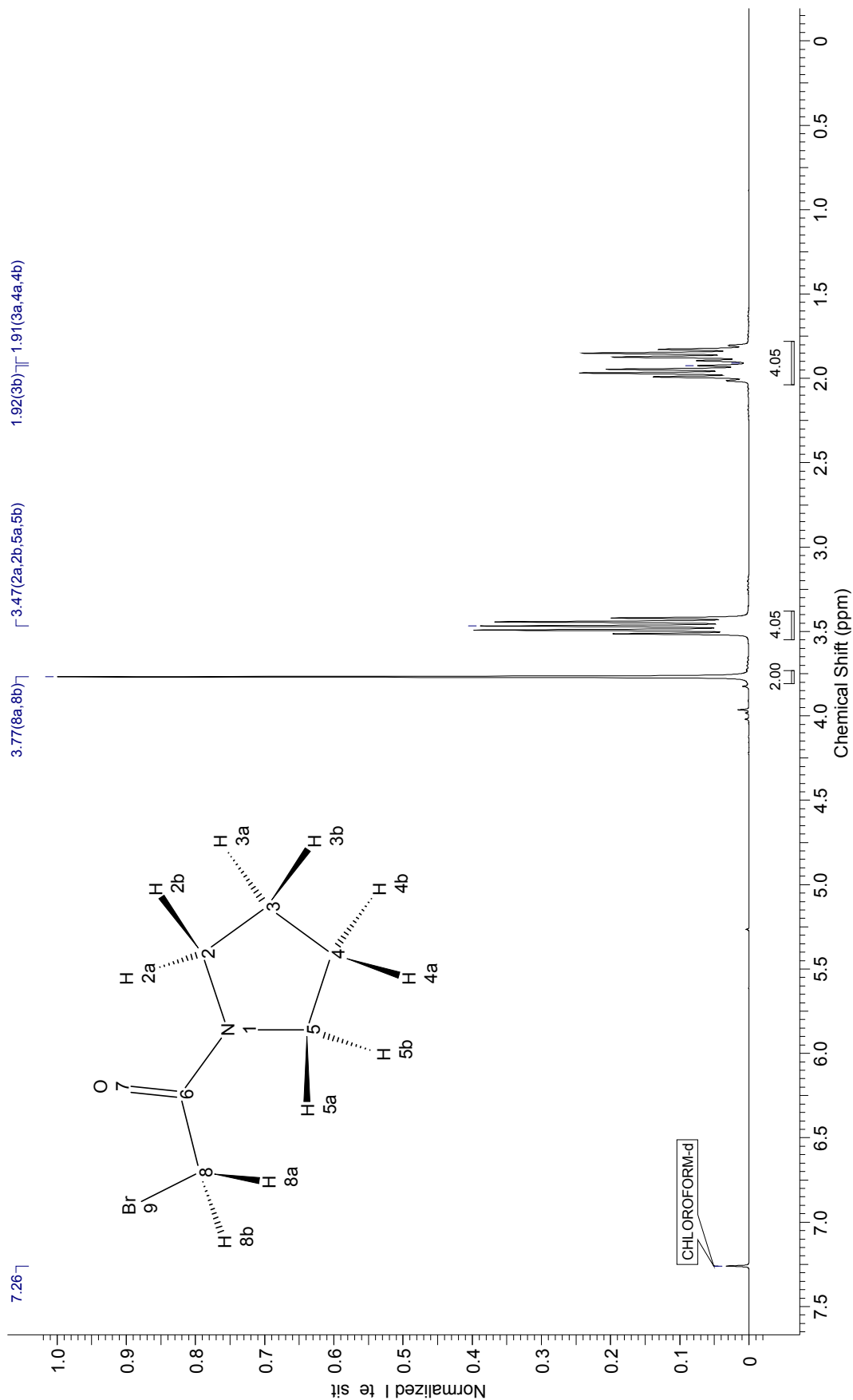
Formula C₁₄H₁₆N₂O₄S₂
FW 340.4178



2-bromo-1-(pyrrolidin-1-yl)ethanone – ¹H-NMR

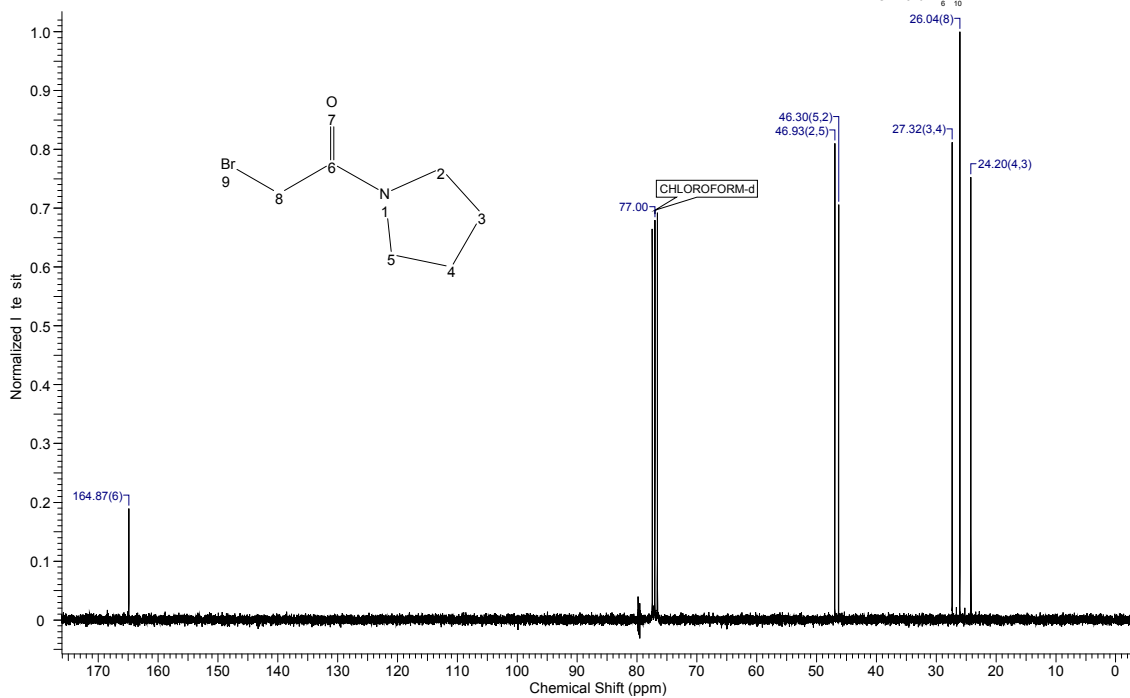
Acquisition Time (sec)	15.3084	Frequency (MHz)	300.13	Nucleus	¹ H	Origin	Original Points Count	32768	Points Count	65536
Pulse Sequence	ZG30	Spectrum Offset (Hz)	1847.2621			Spectrum Type	STANDARD		Sweep Width (Hz)	6172.84

Formula C₆H₁₀BrNO FW 192.0537

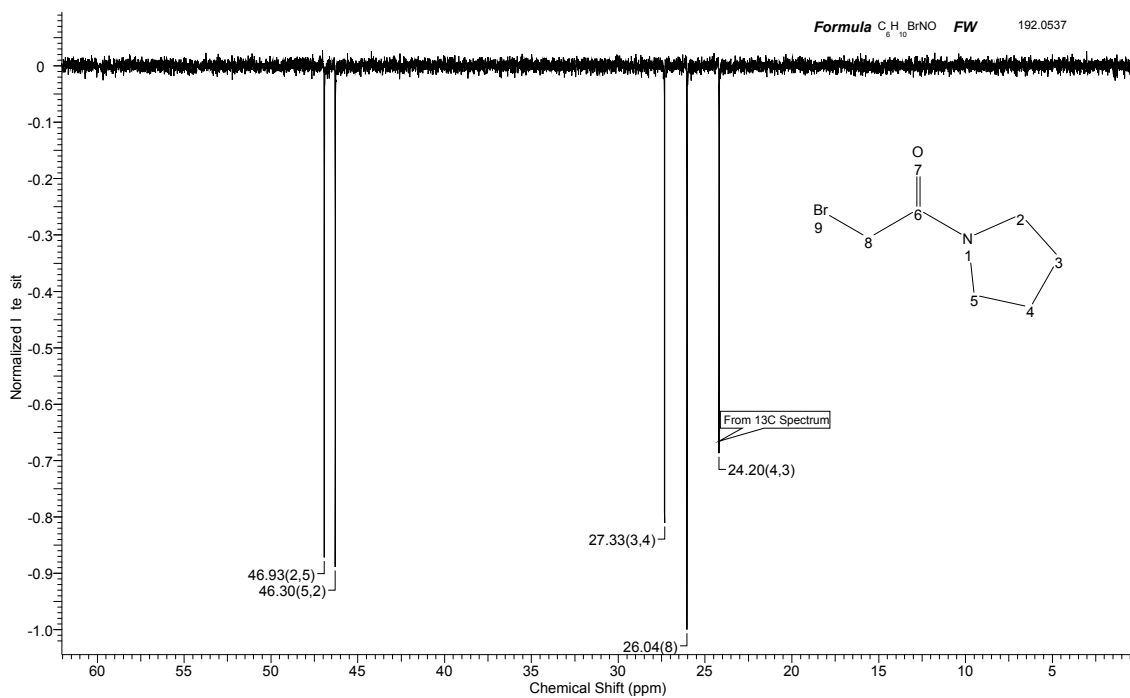


¹³C-NMR & DEPT-135 – 2-bromo-1-(pyrrolidin-1-yl)ethanone

Acquisition Time (sec)	1.8219	Comment	C13CPD CDCI3 D: (UIO)aasmuk) 50	Frequency (MHz)	75.48	Nucleus	13C
Number of Transients	1024	Origin	DPX300	Original Points Count	32768	Points Count	32768
Receiver Gain	11585.20	SW(cyclical) (Hz)	17985.61	Solvent	CHLOROFORM-d	Spectrum Offset (Hz)	7538.0913
Spectrum Type	STANDARD	Sweep Width (Hz)	17985.06	Temperature (degree C)	25.160	Formula	C ₆ H ₁₀ BrNO FW 192.0537



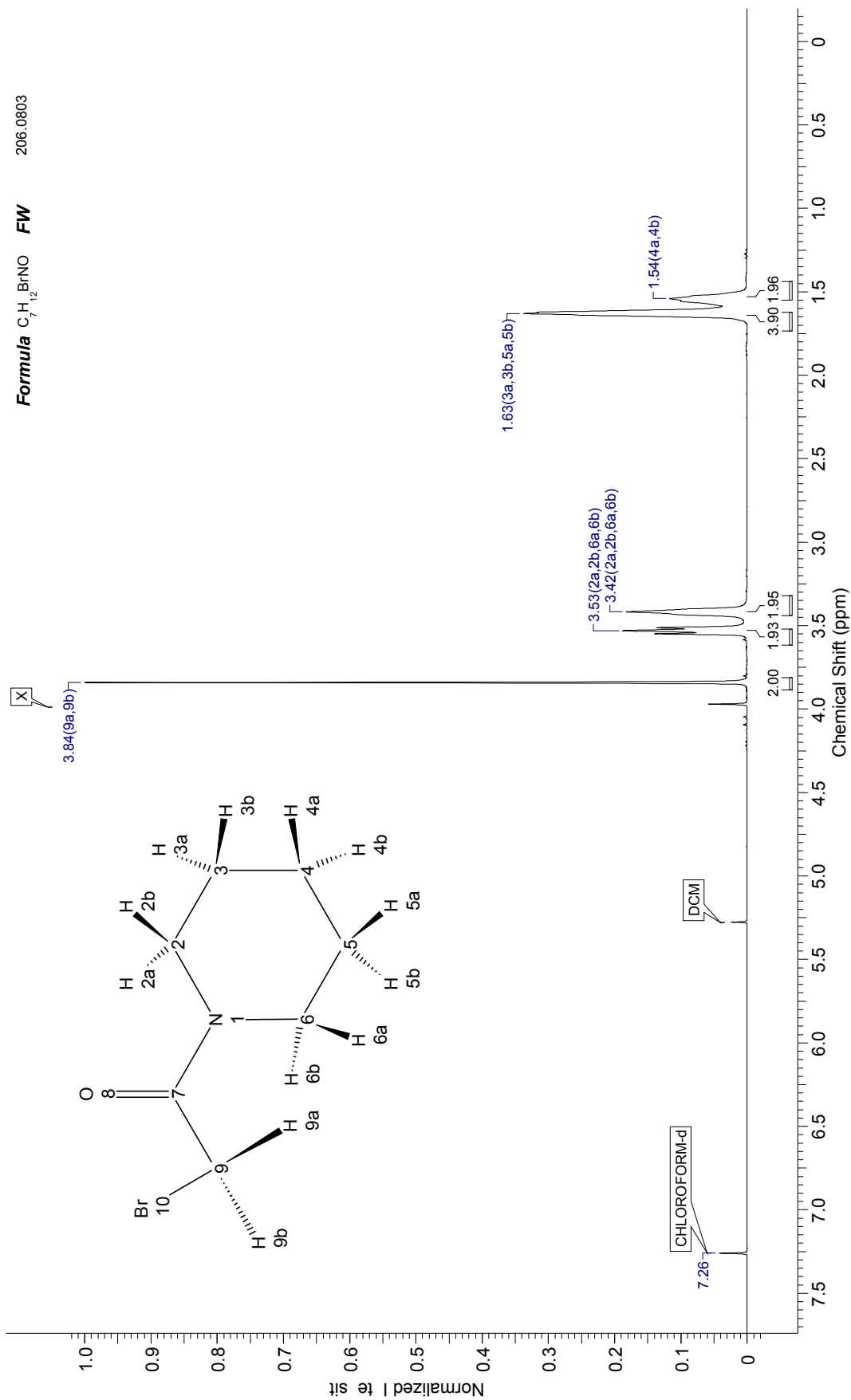
Acquisition Time (sec)	1.8219	Comment	C13DEPT135 CDCI3 D: (UIO)aasmuk) 50	Frequency (MHz)	75.48	Nucleus	13C
Number of Transients	256	Origin	DPX300	Original Points Count	32768	Points Count	32768
Receiver Gain	16384.00	SW(cyclical) (Hz)	17985.61	Solvent	CHLOROFORM-d	Spectrum Offset (Hz)	7538.3940
Spectrum Type	DEPT135	Sweep Width (Hz)	17985.06	Temperature (degree C)	25.160	Formula	C ₆ H ₁₀ BrNO FW 192.0537



2-bromo-1-(piperidin-1-yl)ethanone – ¹H-NMR

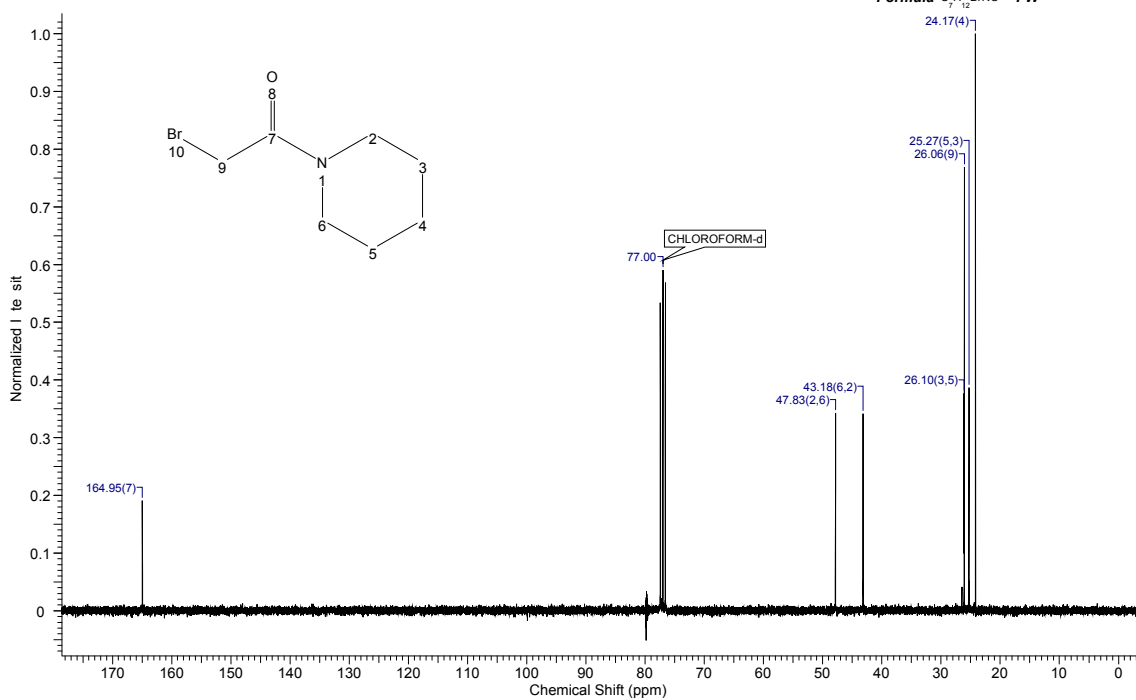
Acquisition Time (sec)	5.3084	Comment	PROTON CDCl3 D: {UOlaasmuk} 51	Frequency (MHz)	300.13	Nucleus	¹ H
Number of Transients	128	Origin	DPX300	Original Points Count	32768	Pulse Sequence	zg30
Receiver Gain	143.70	SW(cyclical) (Hz)	6172.84	Solvent	CHLOROFORM-d	Spectrum Offset (Hz)	1847.1259
Spectrum Type	STANDARD			Sweep Width (Hz)	6172.65	Temperature (degree C)	25.160

Formula C₇H₁₂BrNO FW 206.0803

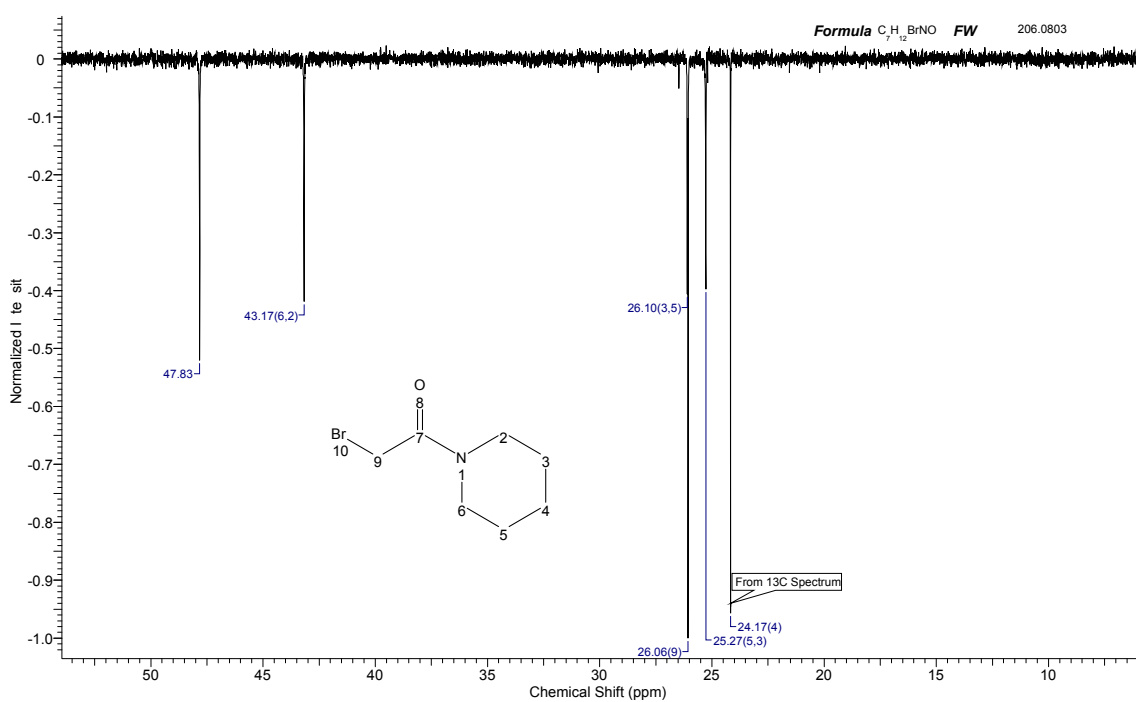


¹³C-NMR & DEPT-135 – 2-bromo-1-(piperidin-1-yl)ethanone

Acquisition Time (sec)	1.8219	Comment	C13CPD CDCI3 D: (UIO)aasmuk) 51	Frequency (MHz)	75.48	Nucleus	13C
Number of Transients	1024	Origin	DPX300	Original Points Count	32768	Points Count	32768
Receiver Gain	11585.20	SW(cyclical) (Hz)	17985.61	Solvent	CHLOROFORM-d	Spectrum Offset (Hz)	7540.2866
Spectrum Type	STANDARD	Sweep Width (Hz)	17985.06	Temperature (degree C)	25.160	Formula	C ₇ H ₁₂ BrNO FW 206.0803

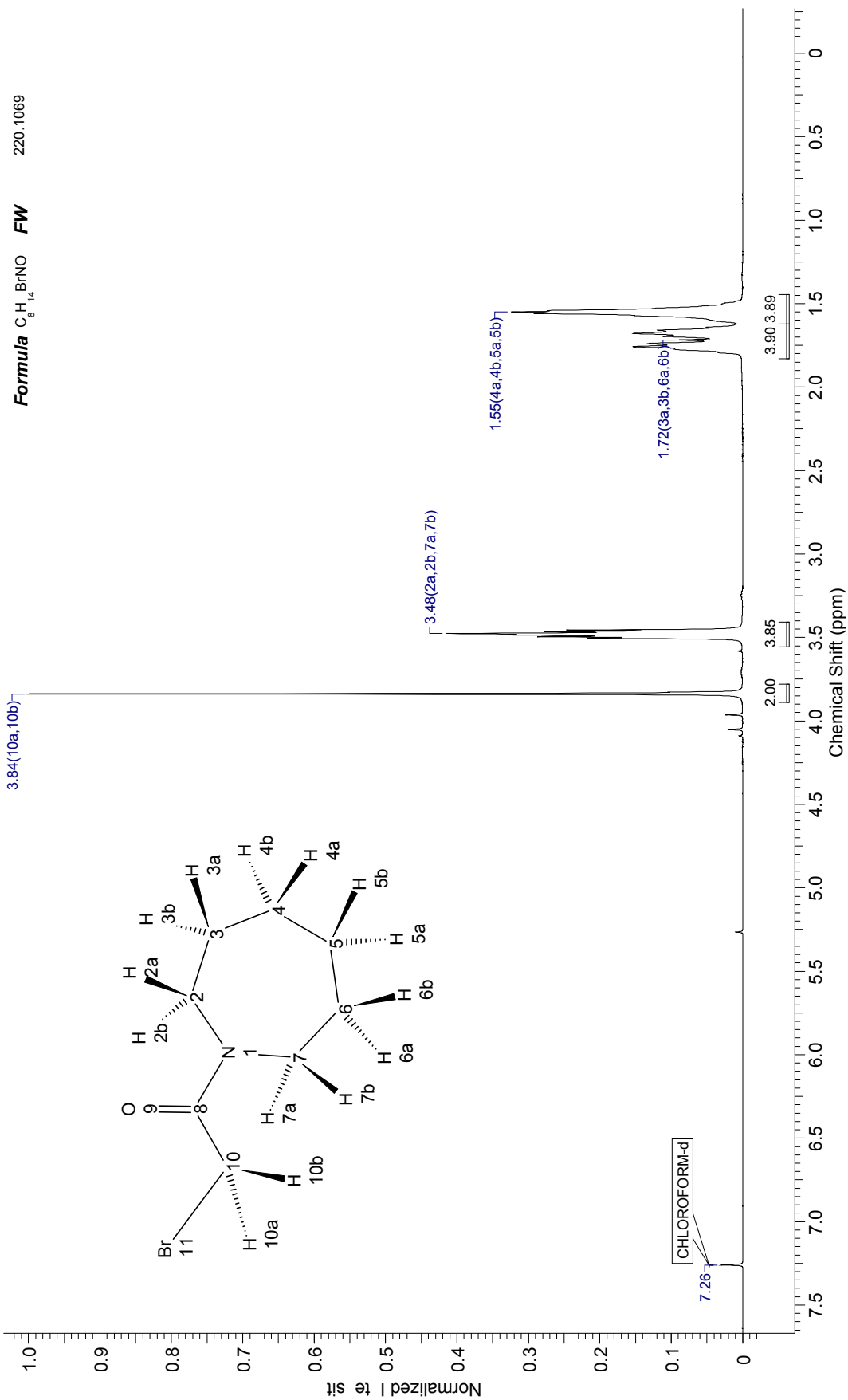


Acquisition Time (sec)	1.8219	Comment	C13DEPT135 CDCI3 D: (UIO)aasmuk) 51	Frequency (MHz)	75.48	Nucleus	13C
Number of Transients	256	Origin	DPX300	Original Points Count	32768	Points Count	32768
Receiver Gain	16384.00	SW(cyclical) (Hz)	17985.61	Solvent	CHLOROFORM-d	Spectrum Offset (Hz)	7539.9717
Spectrum Type	DEPT135	Sweep Width (Hz)	17985.06	Temperature (degree C)	25.160	Formula	C ₇ H ₁₂ BrNO FW 206.0803



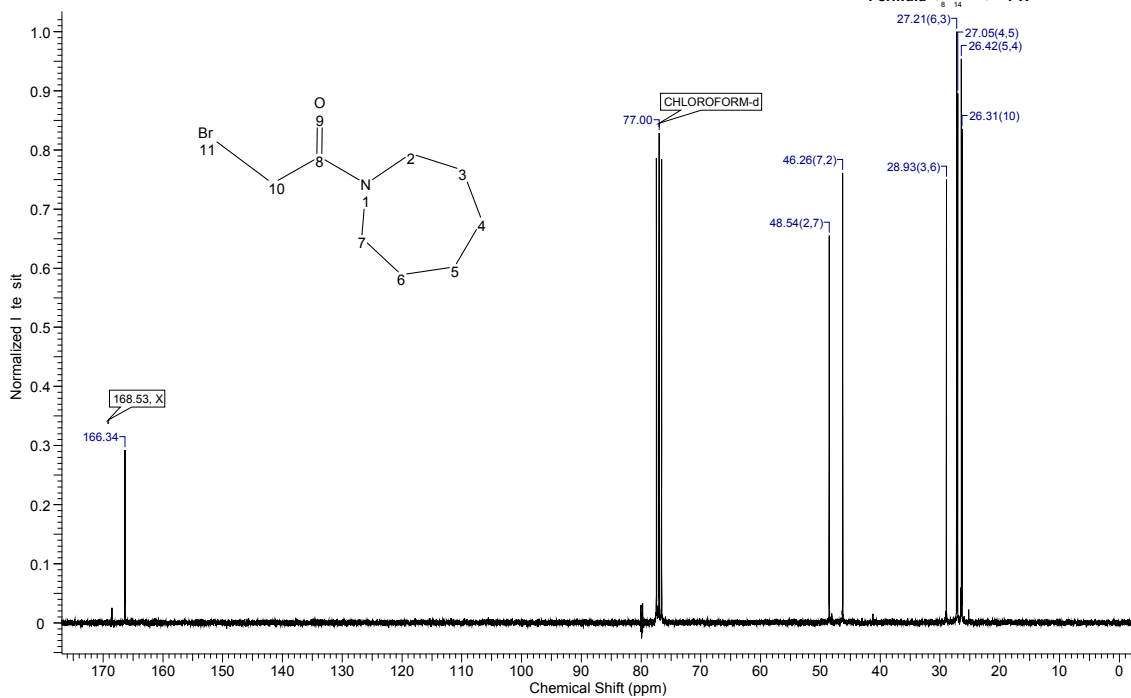
1-(azepan-1-yl)-2-bromoethanone – ¹H-NMR

Acquisition Time (sec)	5.3084	Comment	PROTON CDCl3 D: (UO\aaasmuk} 4	Frequency (MHz)	300.13	Nucleus	¹ H
Number of Transients	16	Origin	DPX300	Original Points Count	32768	Pulse Sequence	zg30
Receiver Gain	101.60	SW(cyclical) (Hz)	6172.84	Solvent	CHLOROFORM-d	Spectrum Offset (Hz)	1847.1124
Spectrum Type	STANDARD			Sweep Width (Hz)	6172.65	Temperature (degree C)	25.160

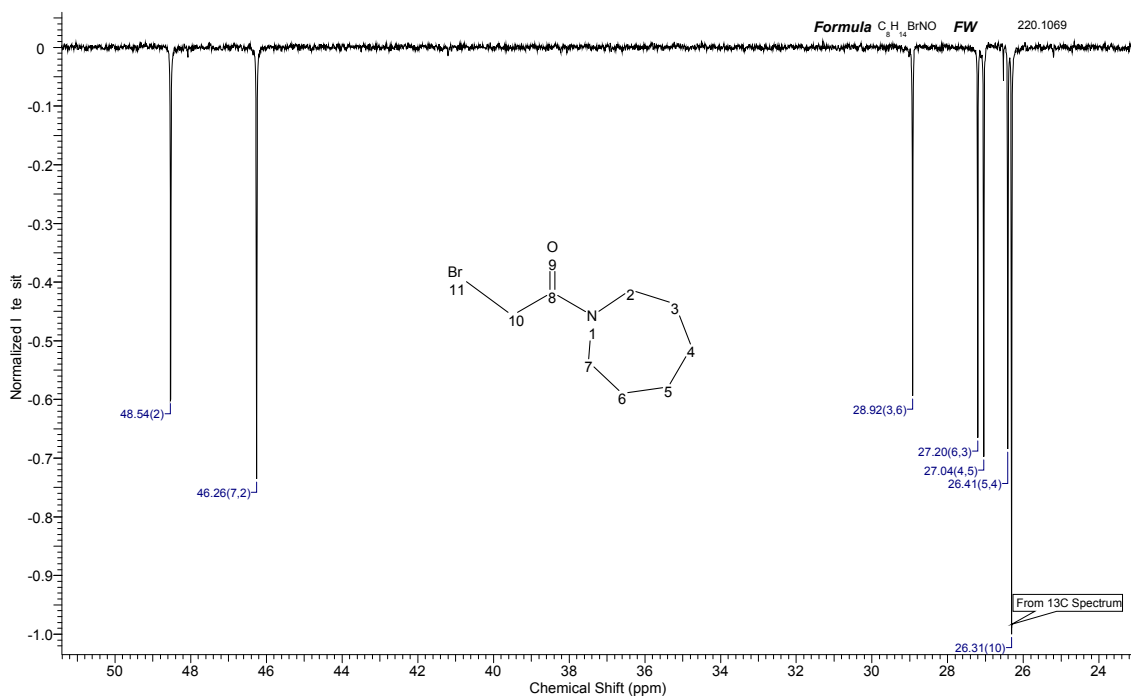


¹³C-NMR & DEPT-135 – 1-(azepan-1-yl)-2-bromoethanone

Acquisition Time (sec)	1.8219	Comment	C13CPD CDCI3 D: (UIO'aasmuk) 4	Frequency (MHz)	75.47	Nucleus	13C
Number of Transients	1024	Origin	DPX300	Original Points Count	32768	Points Count	32768
Receiver Gain	11585.20	SW(cyclical) (Hz)	17985.61	Solvent	CHLOROFORM-d	Spectrum Offset (Hz)	7536.9590
Spectrum Type	STANDARD	Sweep Width (Hz)	17985.06	Temperature (degree C)	25.160	Formula	C ₈ H ₁₄ BrNO FW 220.1069



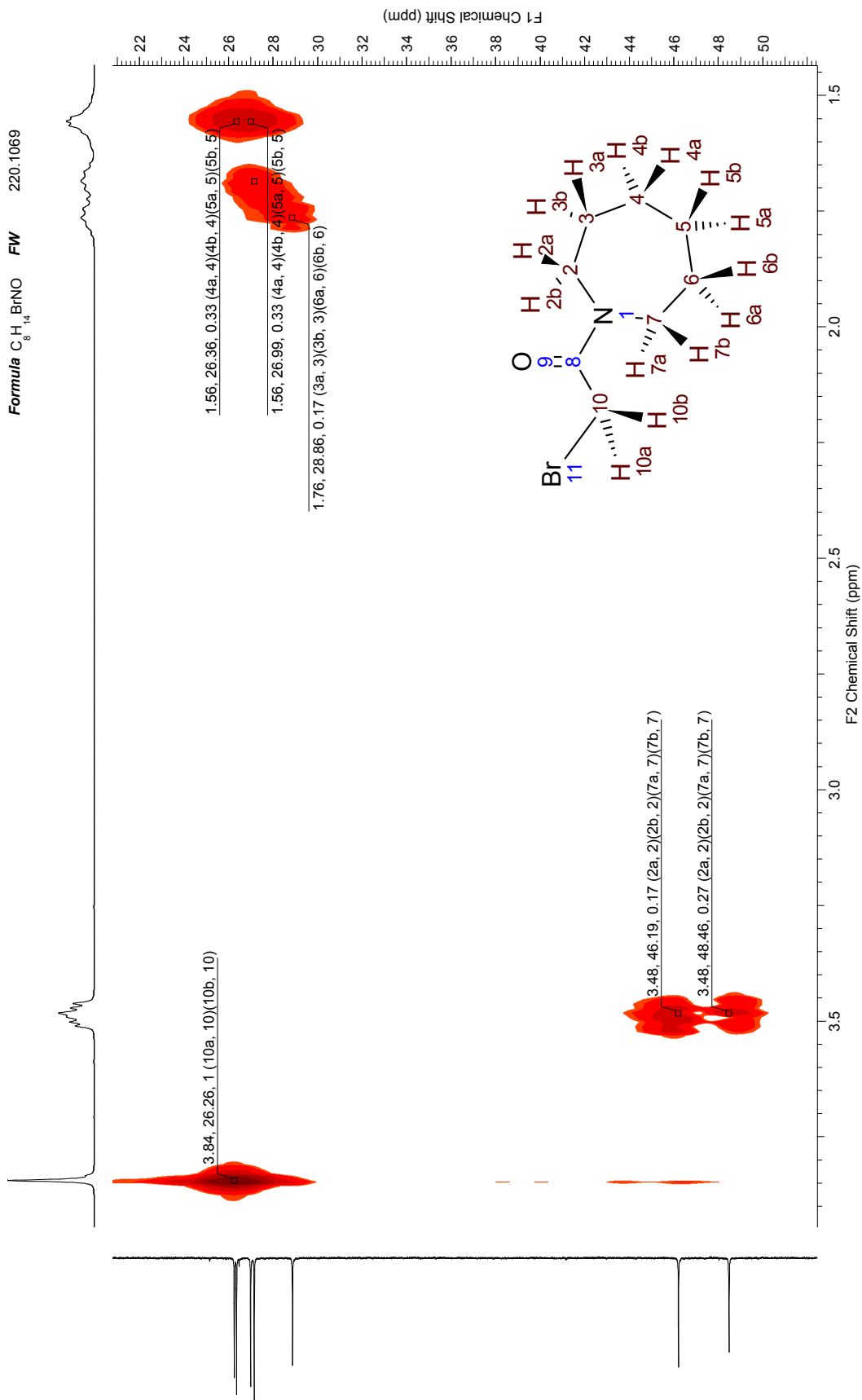
Acquisition Time (sec)	1.8219	Comment	C13DEPT135 CDCI3 D: (UIO'aasmuk) 4	Frequency (MHz)	75.47	Nucleus	13C
Number of Transients	256	Origin	DPX300	Original Points Count	32768	Points Count	32768
Receiver Gain	11585.20	SW(cyclical) (Hz)	17985.61	Solvent	CHLOROFORM-d	Spectrum Offset (Hz)	7536.6265
Spectrum Type	DEPT135	Sweep Width (Hz)	17985.06	Temperature (degree C)	25.160	Formula	C ₈ H ₁₄ BrNO FW 220.1069



1-(azepan-1-yl)-2-bromoethanone – HMQC ($^1J_{13C,1H}$)

Acquisition Time (sec) (0.5308, 0.0092)	Comment	5 mm QNP 1H/15N/13C/31P Z08011/0020	Frequency (MHz)	(300.13, 75.47)
Nucleus (1H, 13C)	Origin	DPX300	Points Count	(512, 1024)
Pulse Sequence hmqcqh	Solvent	CDCI3	Spectrum Type	HMQC
			Sweep Width (Hz)	(962.62, 13952.84)

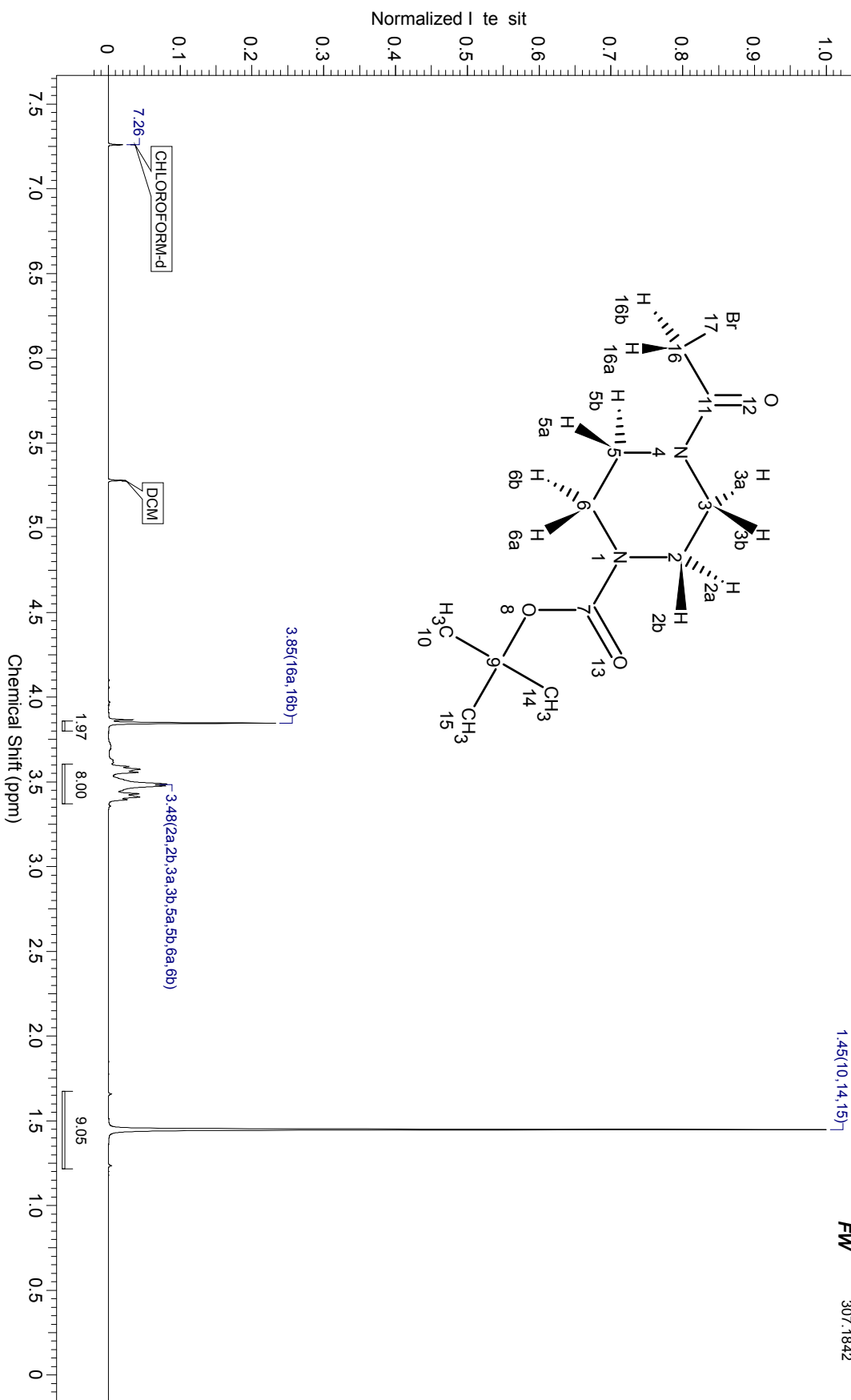
Formula $C_8H_{14}BrNO$ FW 220.1069



¹H-NMR – tert-butyl 4-(2-bromoacetyl)piperazine-1-carboxylate

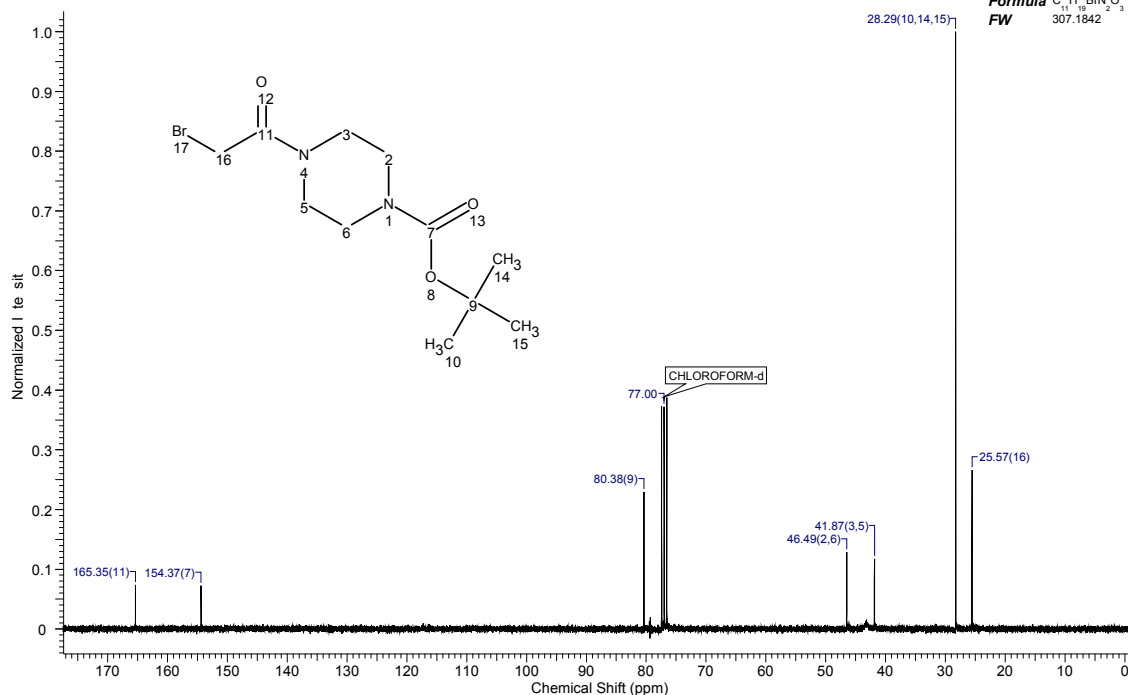
Acquisition Time (sec)	5.3084	Comment	PROTON CDCl3 D- (UO)aasmukj 46	Frequency (MHz)	300.13	Nucleus	¹ H
Number of Transients	128	Origin	DPX300	Points Count	32768	Pulse Sequence	zg30
Receiver Gain	161.30	SW(cyclical) (Hz)	6172.84	Solvent	CHLOROFORM-d	Spectrum Offset (Hz)	1847.1257
Spectrum Type	STANDARD	Sweep Width (Hz)	6172.65	Temperature (degree C)	25.160		

Formula C₁₁H₁₉BrN₂O₃
FW 307.1842

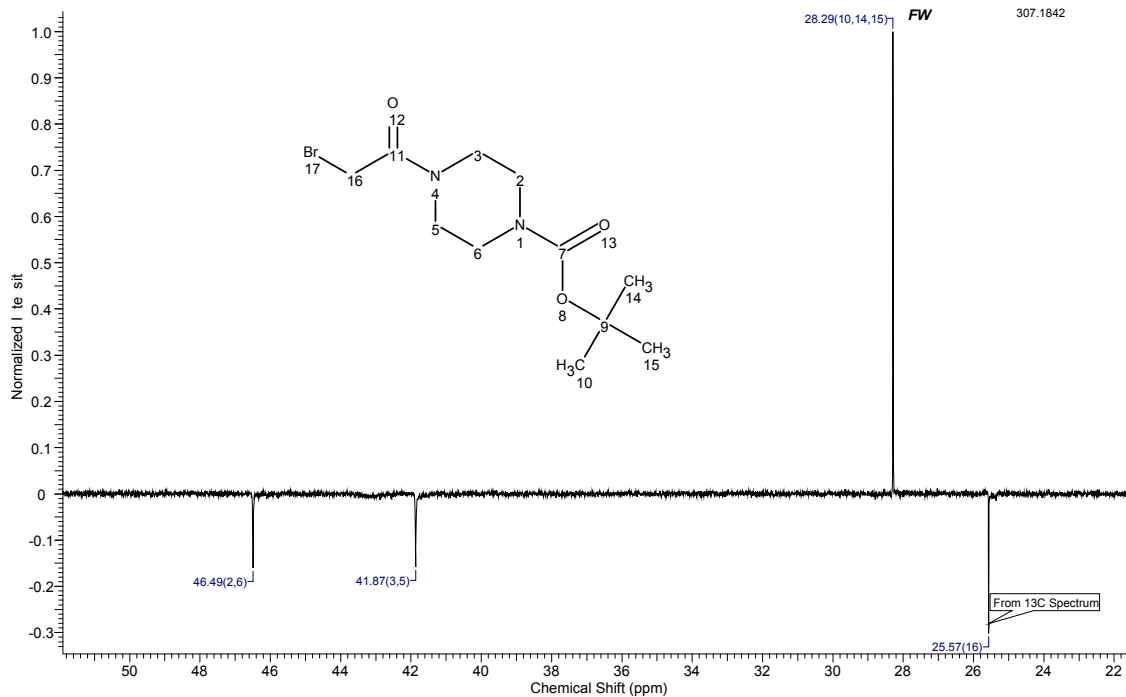


tert-butyl 4-(2-bromoacetyl)piperazine-1-carboxylate – ¹³C-NMR & DEPT-135

Acquisition Time (sec)	1.8219	Comment	C13CPD CDCl3 D: (UIOlaasmuk) 46	Frequency (MHz)	75.48	Nucleus	13C
Number of Transients	1024	Origin	DPX300	Original Points Count	32768	Points Count	32768
Receiver Gain	13004.00	SW(cyclical) (Hz)	17985.61	Solvent	CHLOROFORM-d	Spectrum Offset (Hz)	7541.9336
Spectrum Type	STANDARD			Sweep Width (Hz)	17985.06	Temperature (degree C)	25.160



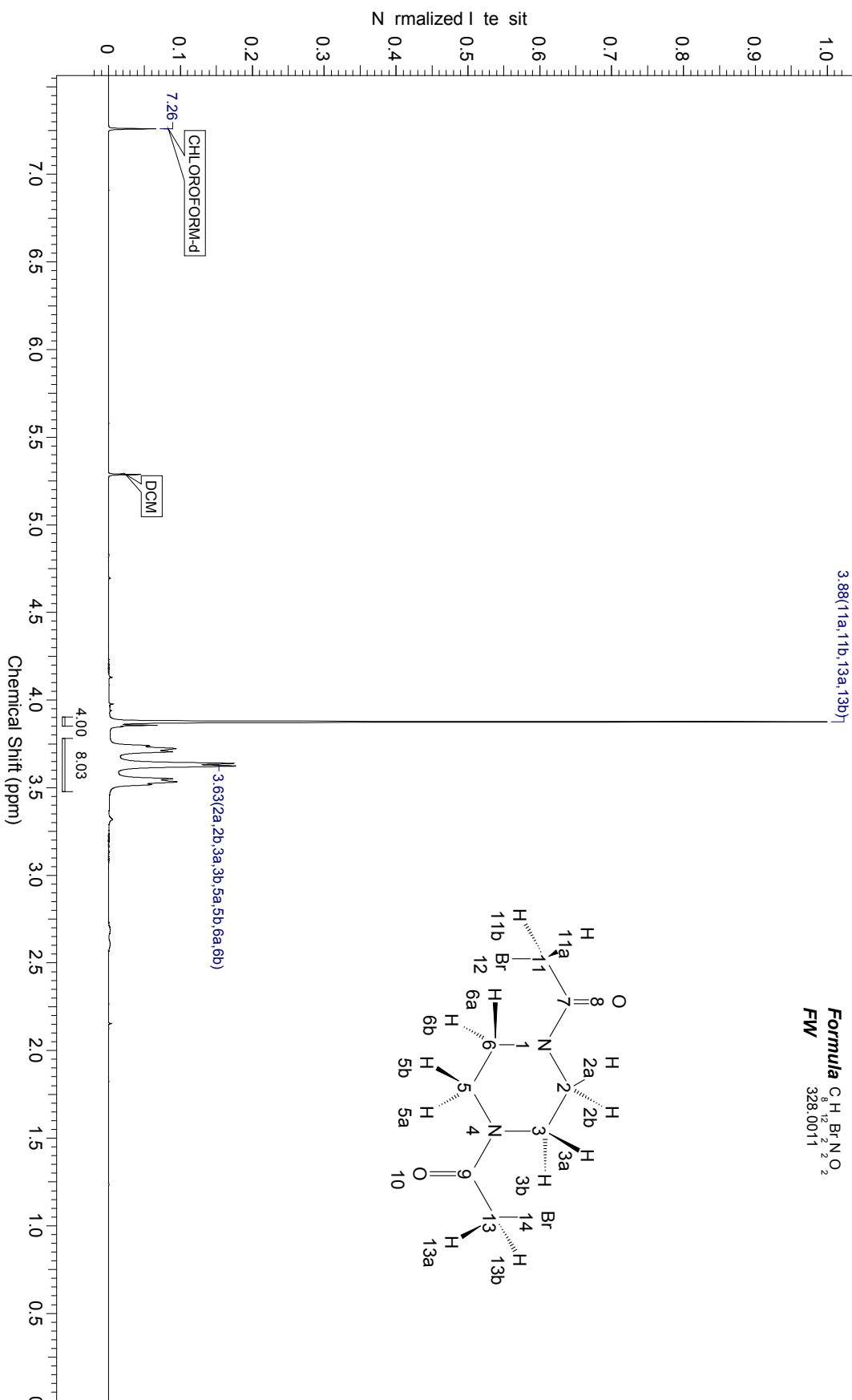
Acquisition Time (sec)	1.8219	Comment	C13DEPT135 CDCl3 D: (UIOlaasmuk) 46	Frequency (MHz)	75.48	Nucleus	13C
Number of Transients	256	Origin	DPX300	Original Points Count	32768	Points Count	32768
Receiver Gain	13004.00	SW(cyclical) (Hz)	17985.61	Solvent	CHLOROFORM-d	Spectrum Offset (Hz)	7541.8994
Spectrum Type	DEPT135	Sweep Width (Hz)	17985.06	Temperature (degree C)	25.160		



¹H-NMR – N,N'-bis(2-bromoacetyl)piperazine

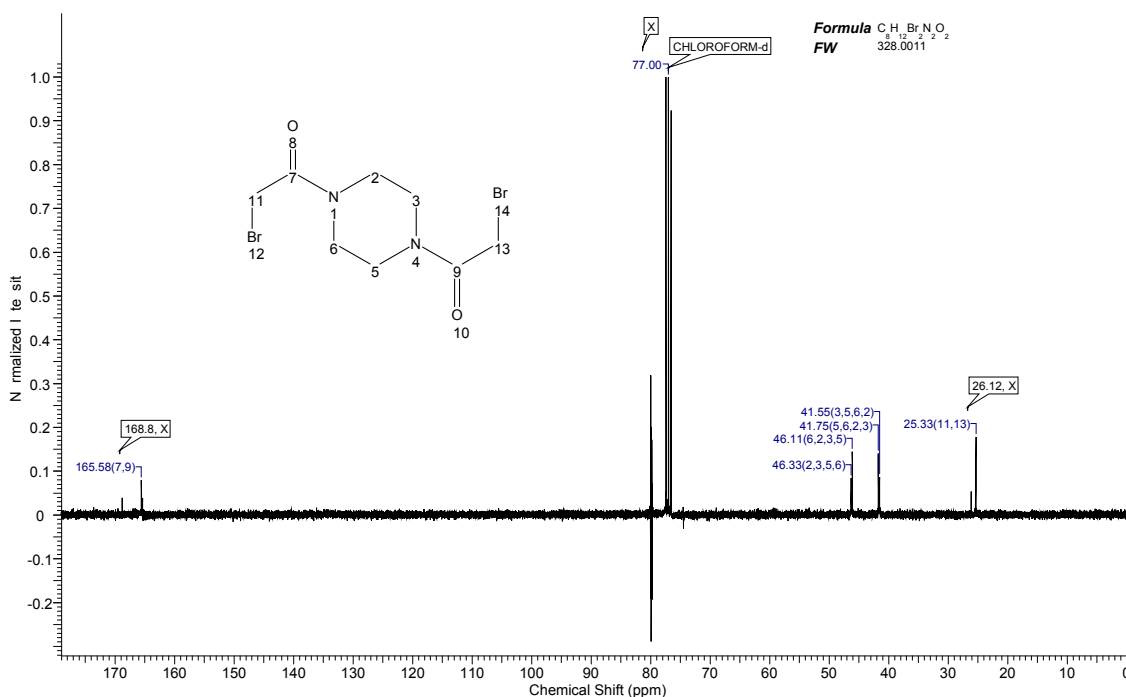
Acquisition Time (sec)	5.3084	Comment	PROTON CDCl3 D- (UO)aasmukj 20	Frequency (MHz)	300.13	Nucleus	¹ H
Number of Transients	128	Origin	DPX300	Points Count	32768	Pulse Sequence	zg30
Receiver Gain	406.40	SW(cyclical) (Hz)	6172.84	Solvent	CHLOROFORM-d	Spectrum Offset (Hz)	1846.9376
Spectrum Type	STANDARD	Sweep Width (Hz)	6172.65	Temperature (degree C)	25.160		

Formula C₈H₁₂Br₂N₂O₂
FW 328.0011

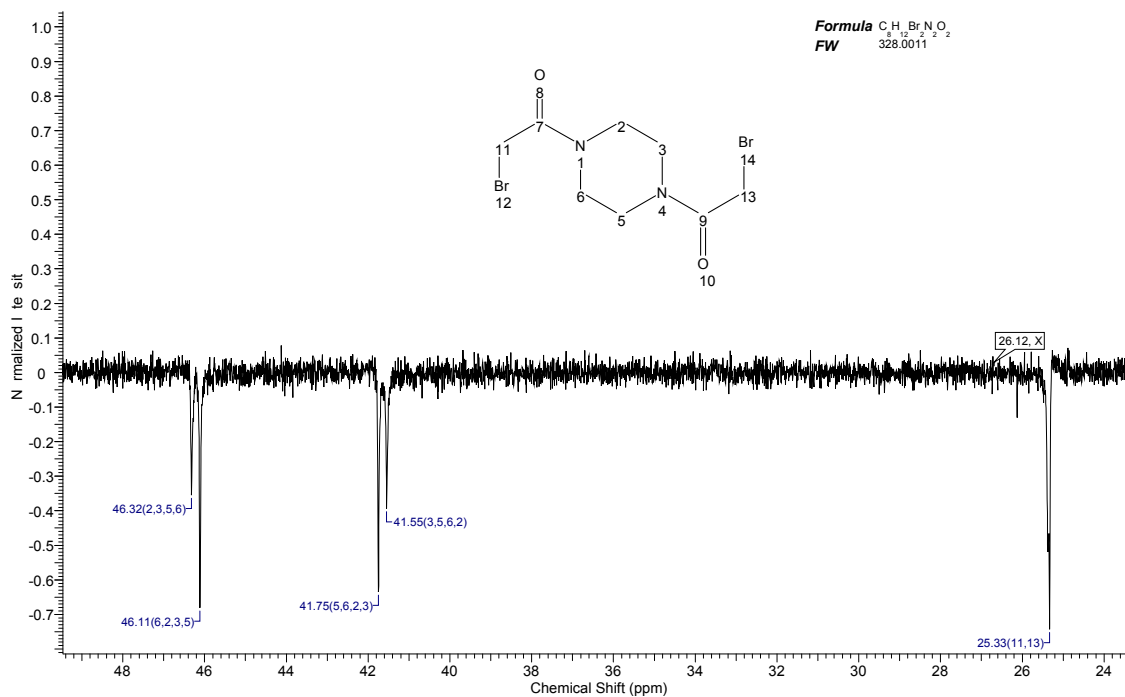


N,N'-bis(2-bromoacetyl)piperazine – ¹³C-NMR & DEPT-135

Acquisition Time (sec)	1.8219	Comment	C13CPD CDCl3 D: (UIOlaasmuk) 20	Frequency (MHz)	75.48	Nucleus	13C
Number of Transients	2048	Origin	DPX300	Original Points Count	32768	Points Count	32768
Receiver Gain	13004.00	SW(cyclical) (Hz)	17985.61	Solvent	CHLOROFORM-d	Spectrum Offset (Hz)	7541.9336
Spectrum Type	STANDARD	Sweep Width (Hz)	17985.06	Temperature (degree C)	25.160		



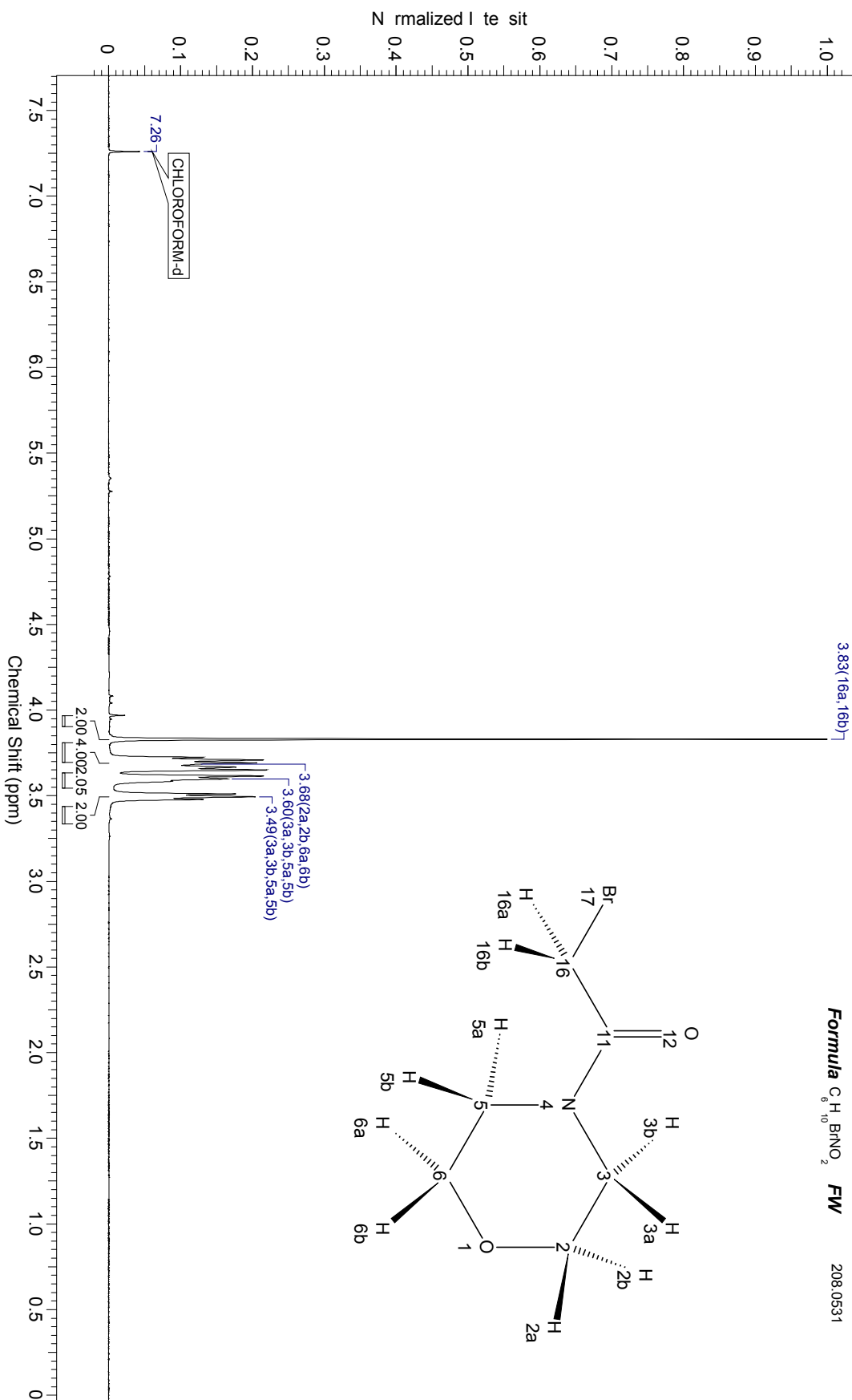
Acquisition Time (sec)	1.8219	Comment	C13DEPT135 CDCl3 D: (UIOlaasmuk) 20	Frequency (MHz)	75.48	Nucleus	13C
Number of Transients	512	Origin	DPX300	Original Points Count	32768	Points Count	32768
Receiver Gain	13004.00	SW(cyclical) (Hz)	17985.61	Solvent	CHLOROFORM-d	Spectrum Offset (Hz)	7541.8979
Spectrum Type	DEPT135	Sweep Width (Hz)	17985.06	Temperature (degree C)	25.160		



¹H-NMR – 2-bromo-1-morpholinoethanone

Acquisition Time (sec)	5.3084	Comment	PROTON CDCl3 D- (UO)aasmukj 52	Frequency (MHz)	300.13	Nucleus	¹ H
Number of Transients	128	Origin	DPX300	Points Count	32768	Pulse Sequence	zg30
Receiver Gain	161.30	SW(cyclical) (Hz)	6172.84	Solvent	CHLOROFORM-d	Spectrum Offset (Hz)	1847.1257
Spectrum Type	STANDARD	Sweep Width (Hz)	6172.65	Temperature (degree C)	25.160		

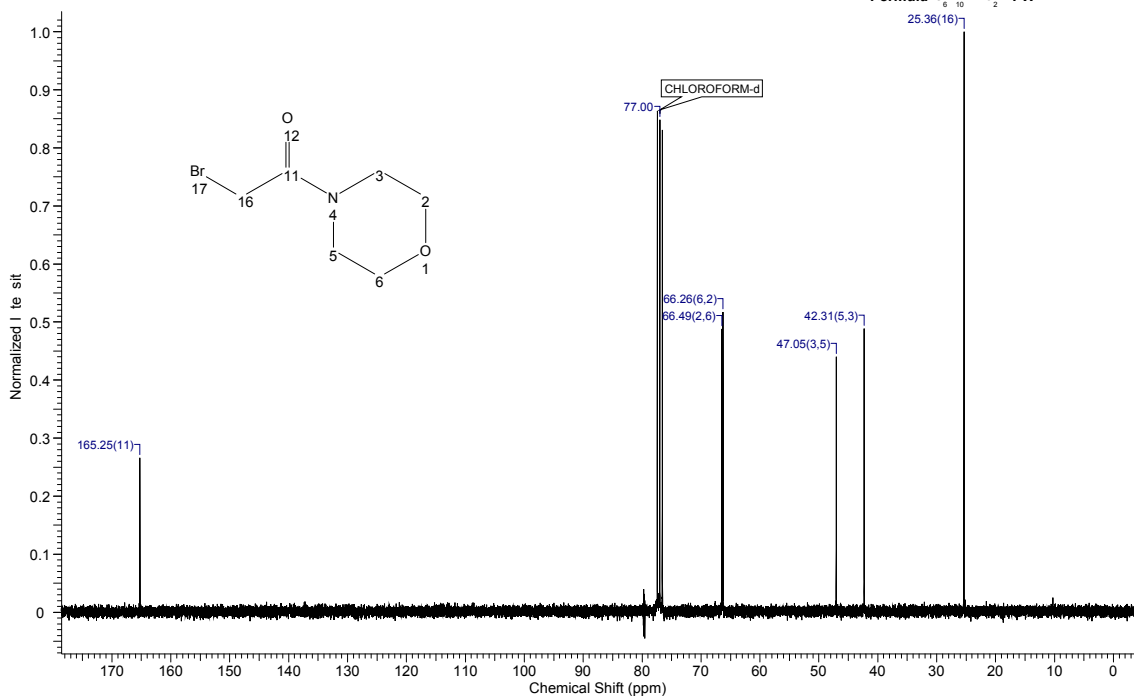
Formula C₆H₁₀BrNO₂ FW 208.0531



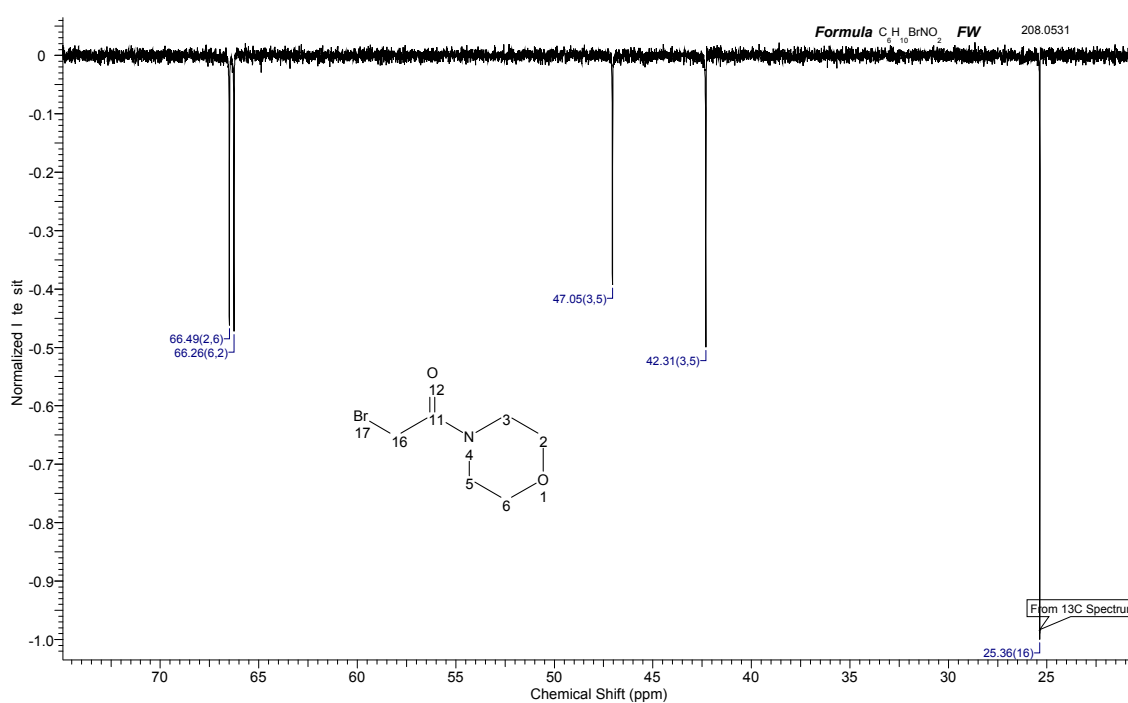
2-bromo-1-morpholinoethanone – ¹³C-NMR & DEPT-135

Acquisition Time (sec)	1.8219	Comment	C13CPD CDCI3 D: (UIOlaasmuk) 52	Frequency (MHz)	75.48	Nucleus	13C
Number of Transients	1024	Origin	DPX300	Original Points Count	32768	Points Count	32768
Receiver Gain	10321.30	SW(cyclical) (Hz)	17985.61	Solvent	CHLOROFORM-d	Spectrum Offset (Hz)	7539.7378
Spectrum Type	STANDARD			Sweep Width (Hz)	17985.06	Temperature (degree C)	25.160

Formula C₆H₁₀BrNO₂ FW 208.0531



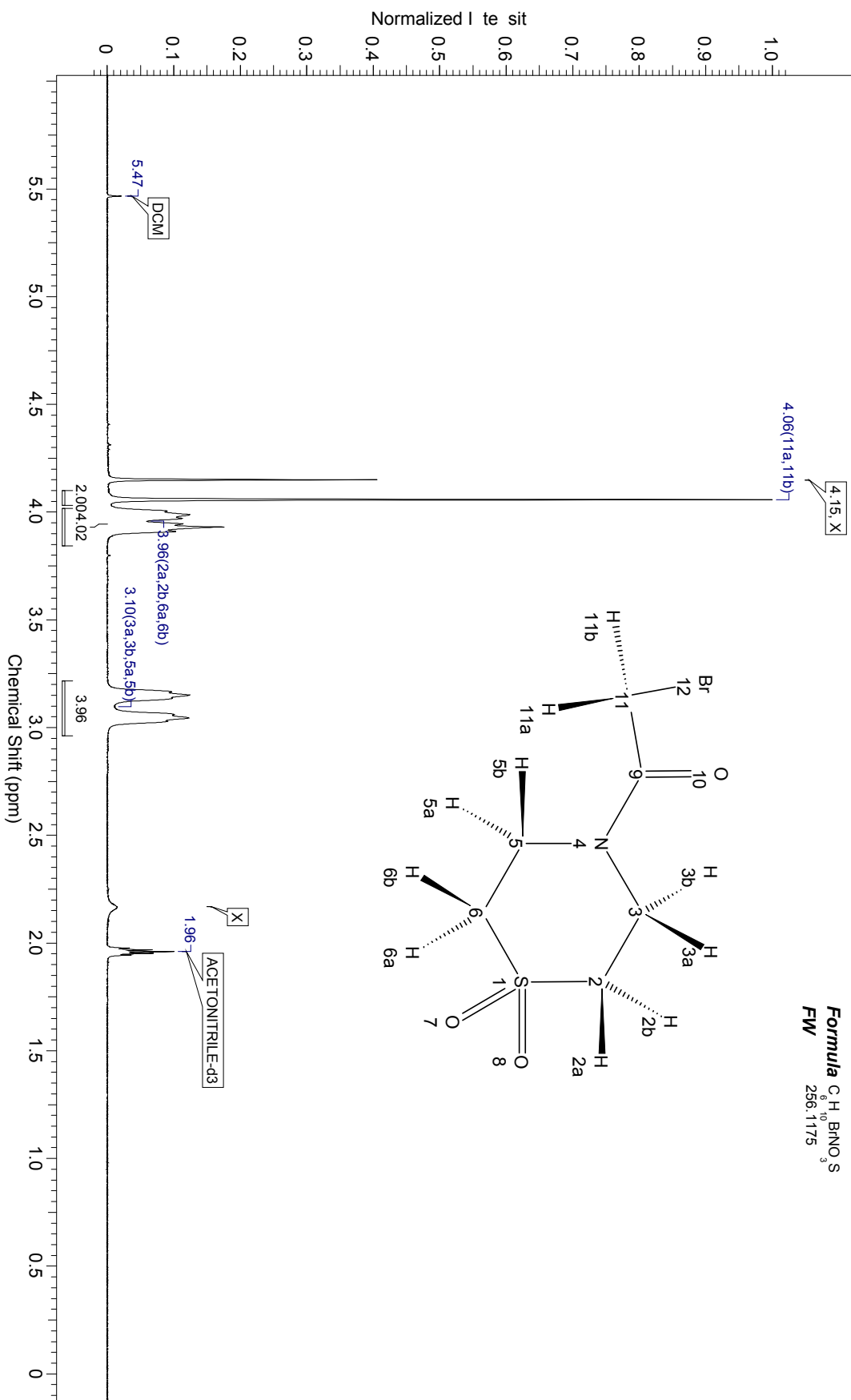
Acquisition Time (sec)	1.8219	Comment	C13DEPT135 CDCI3 D: (UIOlaasmuk) 52	Frequency (MHz)	75.48	Nucleus	13C
Number of Transients	256	Origin	DPX300	Original Points Count	32768	Points Count	32768
Receiver Gain	16384.00	SW(cyclical) (Hz)	17985.61	Solvent	CHLOROFORM-d	Spectrum Offset (Hz)	7539.7715
Spectrum Type	DEPT135			Sweep Width (Hz)	17985.06	Temperature (degree C)	25.160



¹H-NMR – 2-bromo-1-(1,1-dioxidothiomorpholino)ethanone

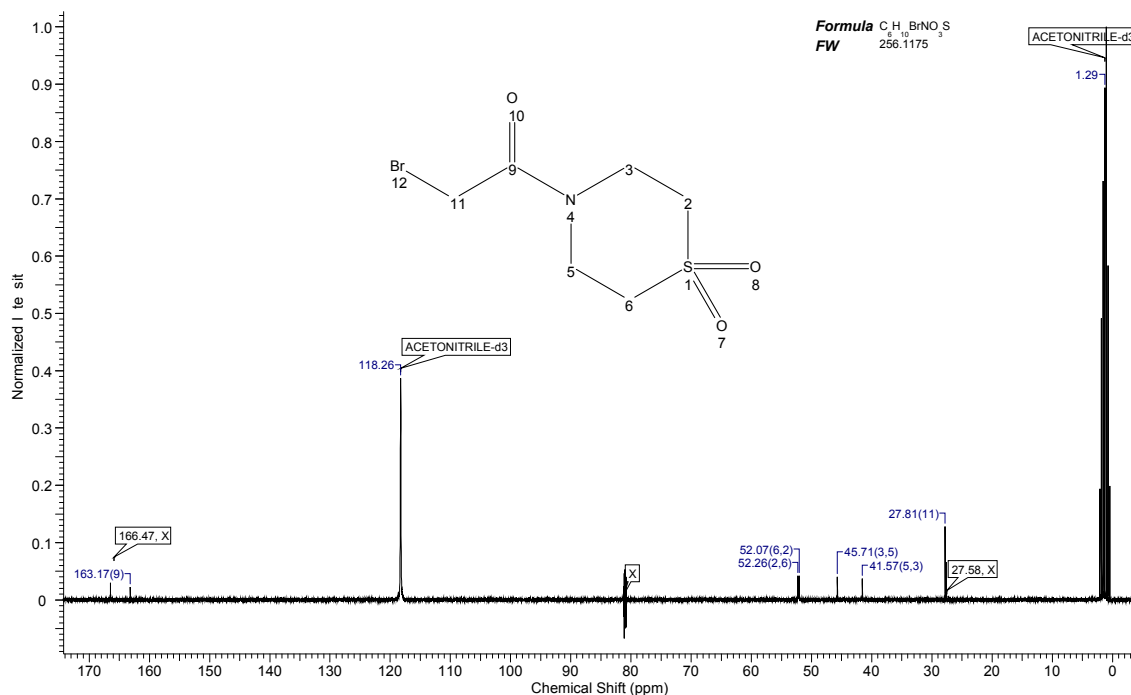
Acquisition Time (sec)	5.3084	Comment	PROTON CD3CN D: (U)O(aasmuk) 57	Frequency (MHz)	300.13	Nucleus	¹ H
Number of Transients	16	Origin	DPX300	Points Count	32768	Pulse Sequence	zg30
Receiver Gain	512.00	SW(cyclical) (Hz)	6172.84	Solvent	ACETONITRILE-d3	Spectrum Offset (Hz)	1851.8181
Spectrum Type	STANDARD	Sweep Width (Hz)	6172.65	Temperature (degree C)	25.160		

Formula C₆H₁₀BrNO₃S
FW 256.1775

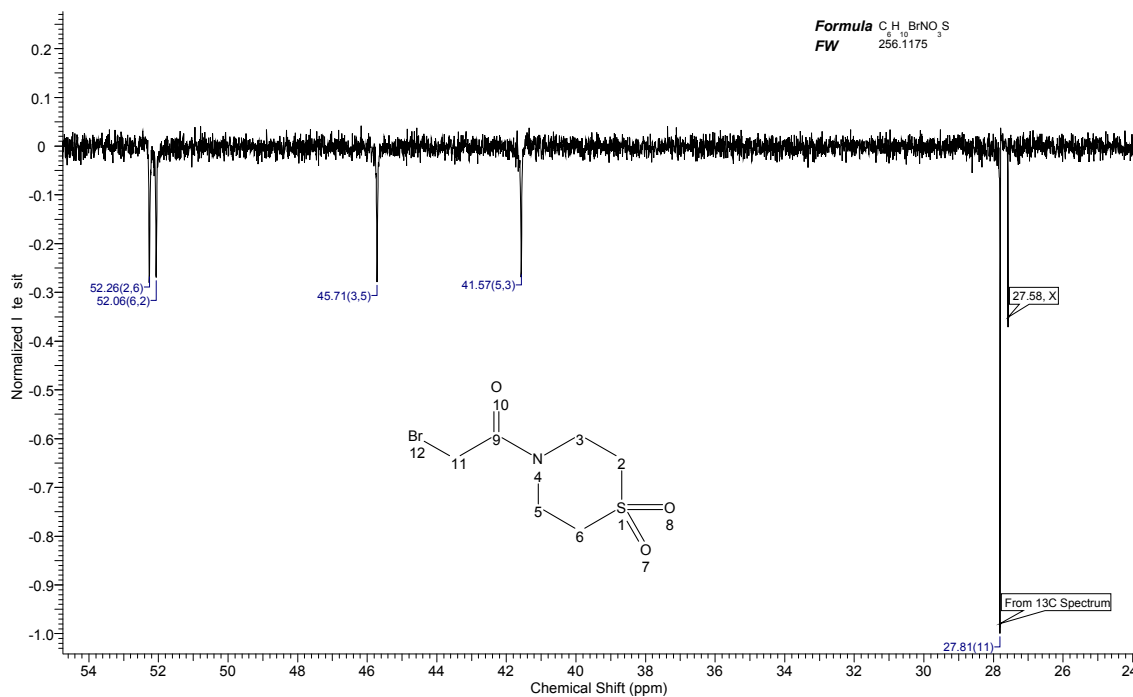


2-bromo-1-(1,1-dioxidothiomorpholino)ethanone – ^{13}C -NMR & DEPT-135

Acquisition Time (sec)	1.8219	Comment	C13CPD CD3CN D: (UIO)laasmuk) 57	Frequency (MHz)	75.48	Nucleus	^{13}C
Number of Transients	2048	Origin	DPX300	Original Points Count	32768	Points Count	32768
Receiver Gain	11585.20	SW(cyclical) (Hz)	17985.61	Solvent	ACETONITRILE-d3	Pulse Sequence	zgpg30
Spectrum Type	STANDARD	Sweep Width (Hz)	17985.06	Temperature (degree C)	25.160	Spectrum Offset (Hz)	7617.4600



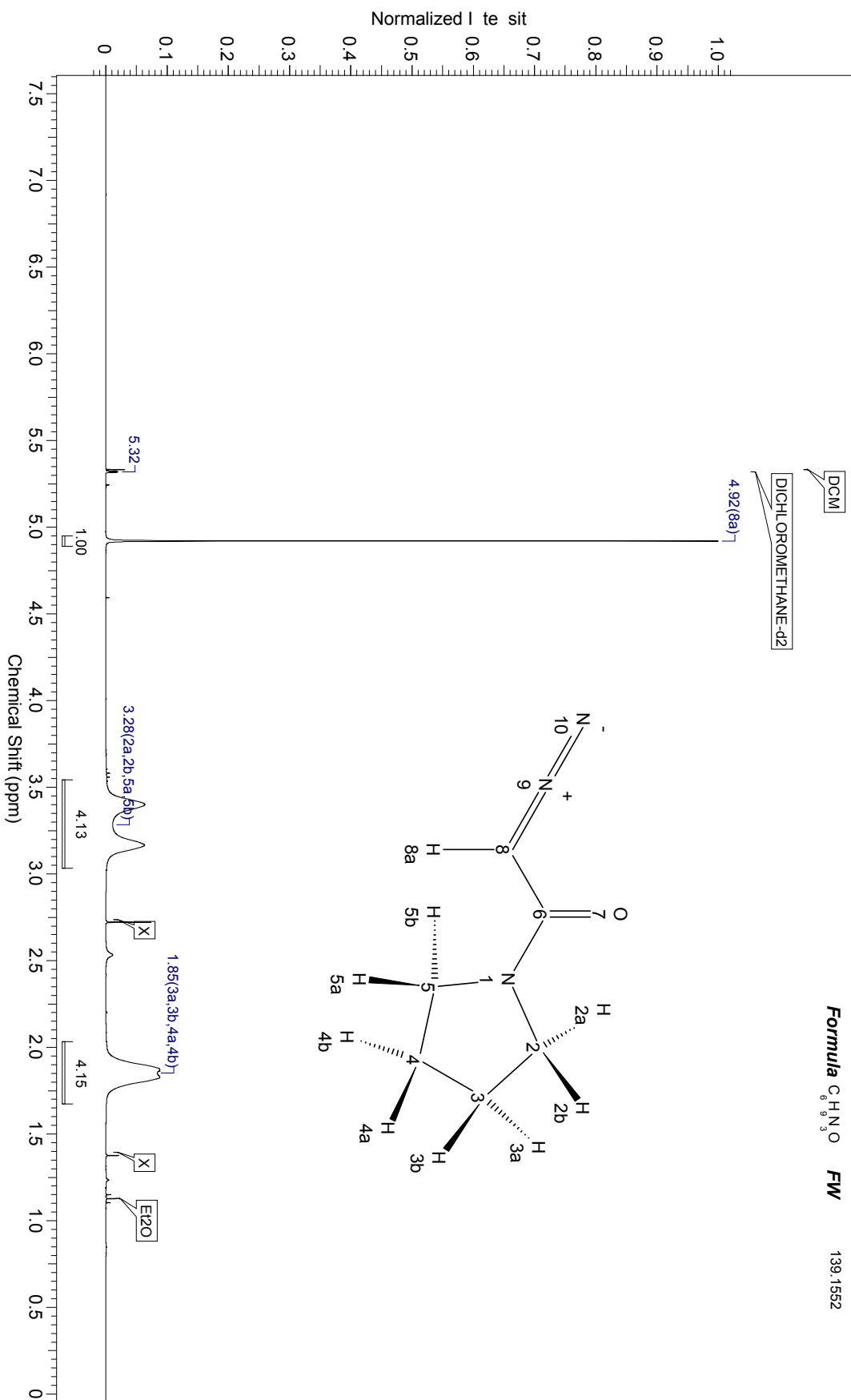
Acquisition Time (sec)	1.8219	Comment	C13DEPT135 CD3CN D: (UIO)laasmuk) 57	Frequency (MHz)	75.48	Nucleus	^{13}C
Number of Transients	512	Origin	DPX300	Original Points Count	32768	Points Count	32768
Receiver Gain	13004.00	SW(cyclical) (Hz)	17985.61	Solvent	ACETONITRILE-d3	Pulse Sequence	dept135
Spectrum Type	DEPT135	Sweep Width (Hz)	17985.06	Temperature (degree C)	25.160	Spectrum Offset (Hz)	7617.6548



¹H-NMR – 2-diazo-1-(pyrrolidin-1-yl)ethanone

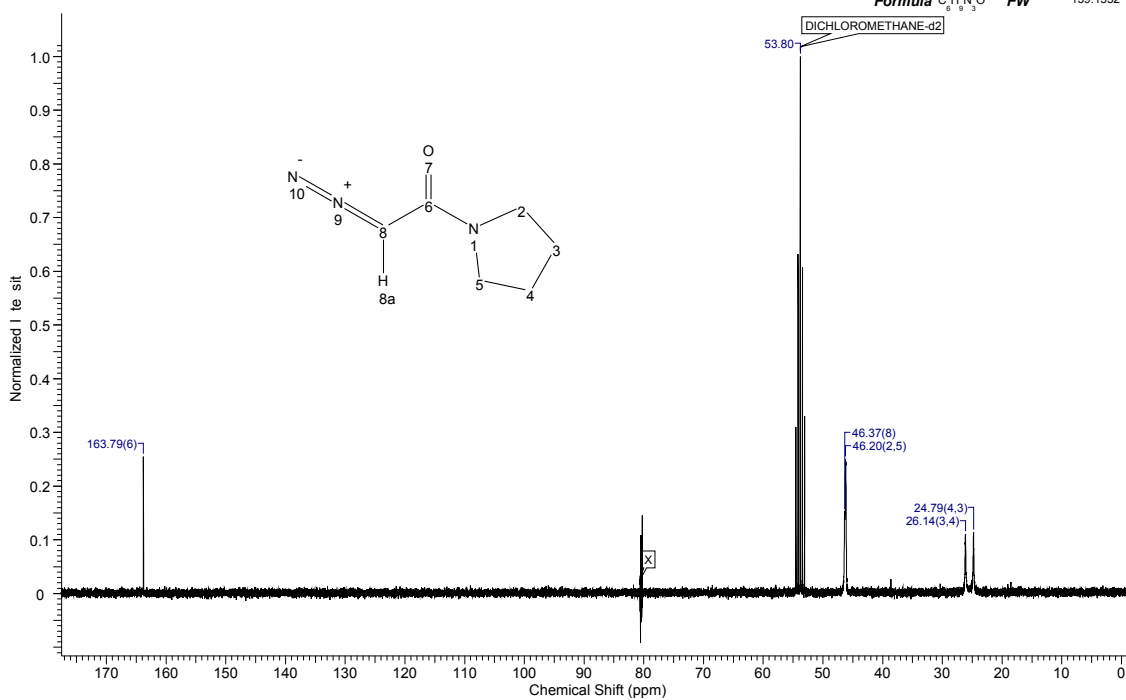
Acquisition Time (sec)	5.3084	Comment	5 mm QNP 1H/15N/13C/31P Z08011/0020	Frequency (MHz)	300.13	Nucleus	1H
Number of Transients	16	Origin	DPX300	Points Count	32768	Pulse Sequence	ZG30
Receiver Gain	71.80	SW(cyclical) (Hz)	6172.84	Solvent	DICHLOROMETHANE-d2	Spectrum Offset (Hz)	1842.9987
Spectrum Type	STANDARD	Sweep Width (Hz)	6172.65	Temperature (degree C)	26.160		

Formula C₆H₉N₃O FW 139.1552

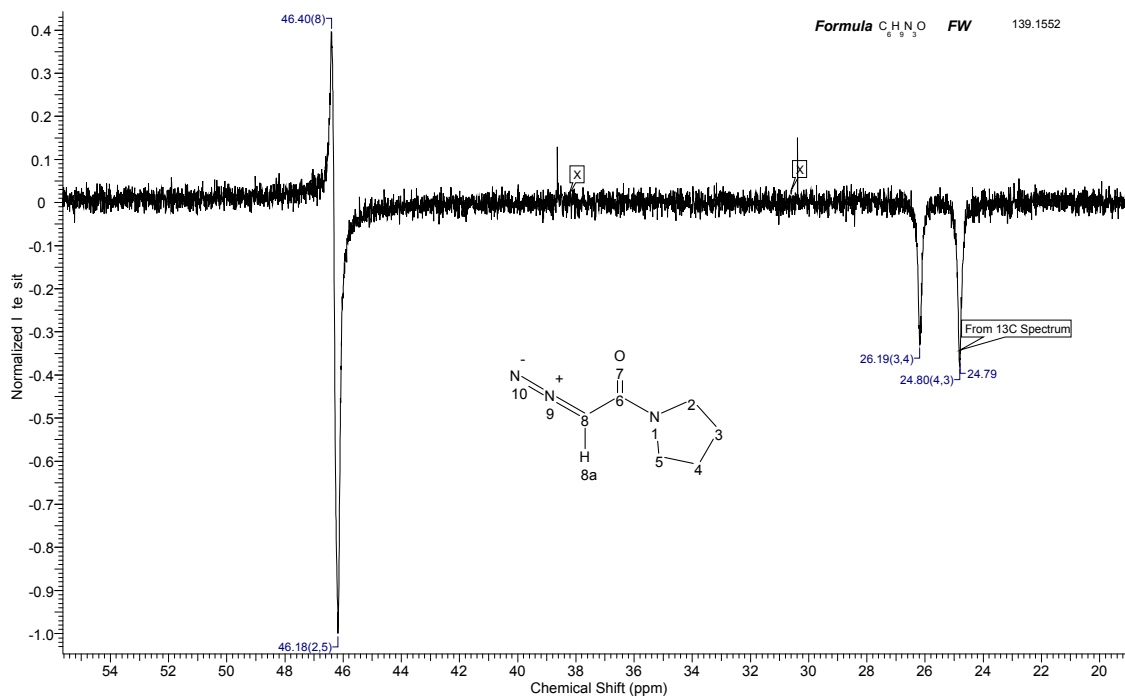


2-diazo-1-(pyrrolidin-1-yl)ethanone – ¹³C-NMR & DEPT-135

Acquisition Time (sec)	1.8219	Comment	C13CPD CD2Cl2 D: (UIO\laasmuk) 27	Frequency (MHz)	75.48	Nucleus	13C
Number of Transients	1024	Origin	DPX300	Original Points Count	32768	Pulse Sequence	zgpg30
Receiver Gain	11585.20	SW(cyclical) (Hz)	17985.61	Solvent	DICHLOROMETHANE-d2	Spectrum Offset (Hz)	7568.7197
Spectrum Type	STANDARD	Sweep Width (Hz)	17985.06	Temperature (degree C)	25.160		

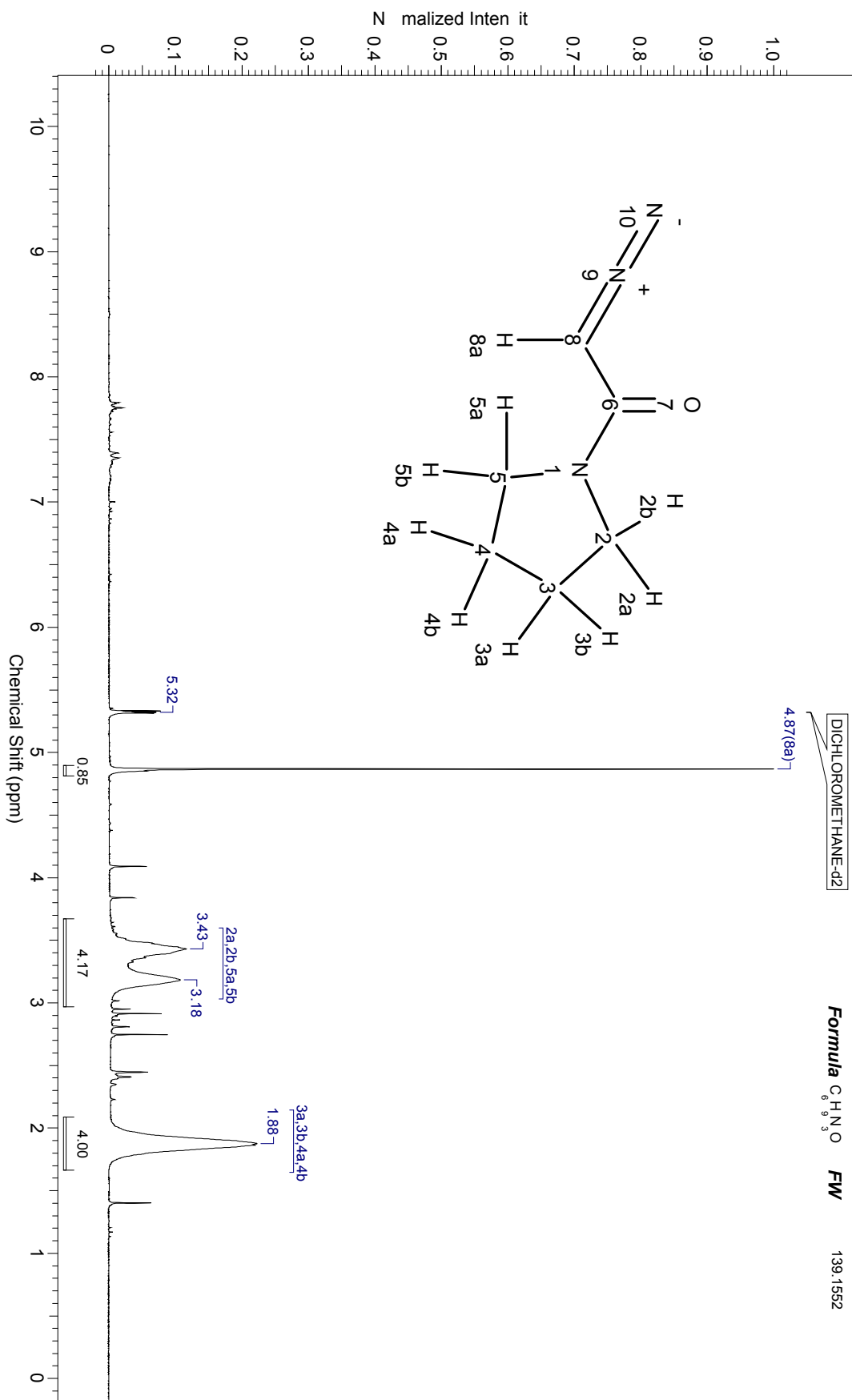


Acquisition Time (sec)	1.8219	Comment	C13DEPT135 CD2Cl2 D: (UIO\laasmuk) 27	Frequency (MHz)	75.48	Nucleus	13C
Number of Transients	1024	Origin	DPX300	Original Points Count	32768	Pulse Sequence	dept135
Receiver Gain	16384.00	SW(cyclical) (Hz)	17985.61	Solvent	DICHLOROMETHANE-d2	Spectrum Offset (Hz)	7570.8491
Spectrum Type	DEPT135	Sweep Width (Hz)	17985.06	Temperature (degree C)	25.160		



Crude ¹H-NMR – 2-diazo-1-(pyrrolidin-1-yl)ethanone

Acquisition Time (sec)	2.9999	Frequency (MHz)	200.13	Nucleus	¹ H	Number of Transients	16	Origin	DPX200
Original Points Count	12417	Points Count	16384	Pulse Sequence	zg30	Receiver Gain	574.70	SW(cyclical) (Hz)	4139.07
Solvent	DICHLOROMETHANE-d2		Spectrum Offset (Hz)	1224.4795	Spectrum Type	STANDARD			
Sweep Width (Hz)	4138.82	Temperature (degree C)	25.160						

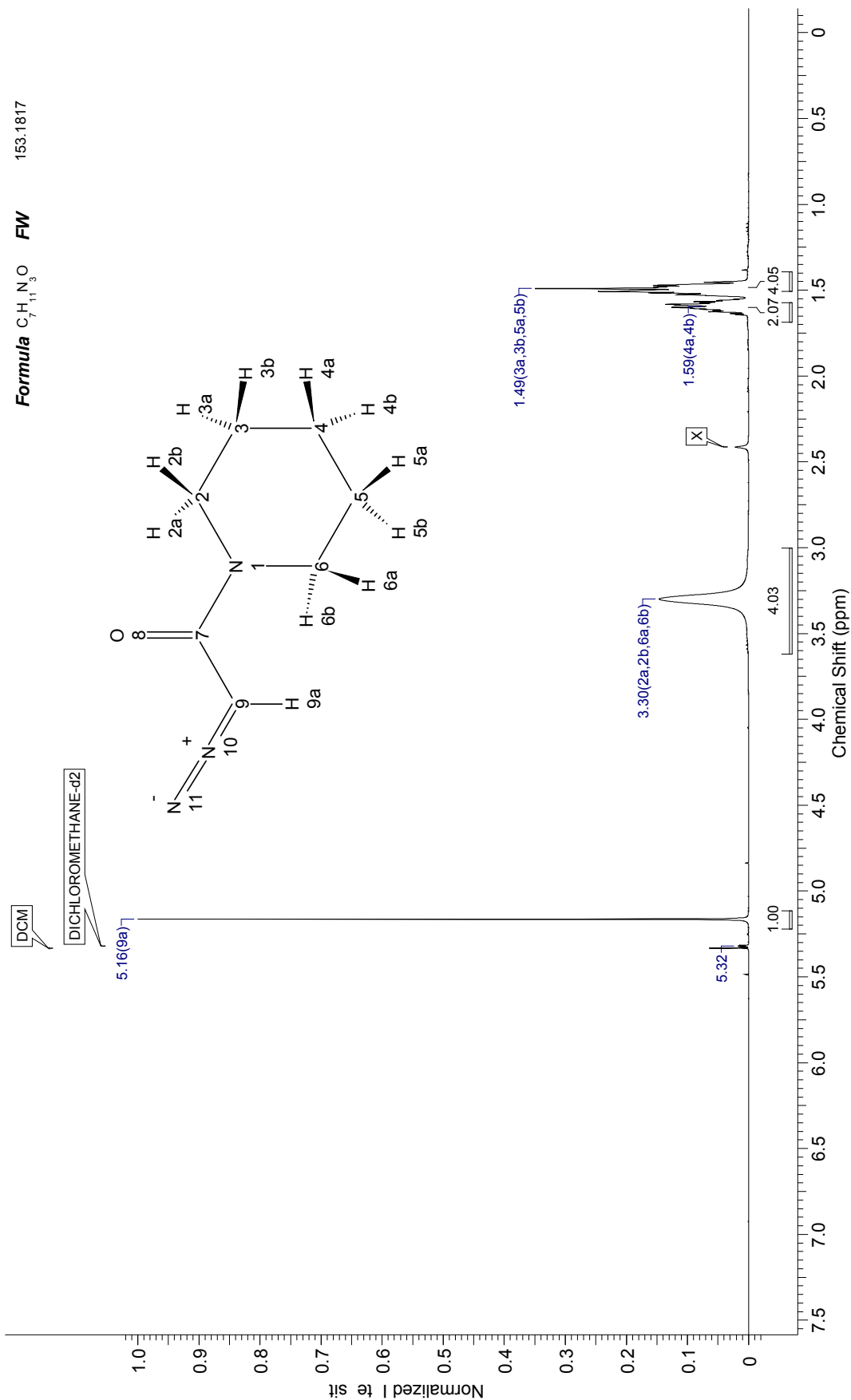


Formula C₅H₈N₂O FW 139.1552

2-diazo-1-(piperidin-1-yl)ethanone – ¹H-NMR

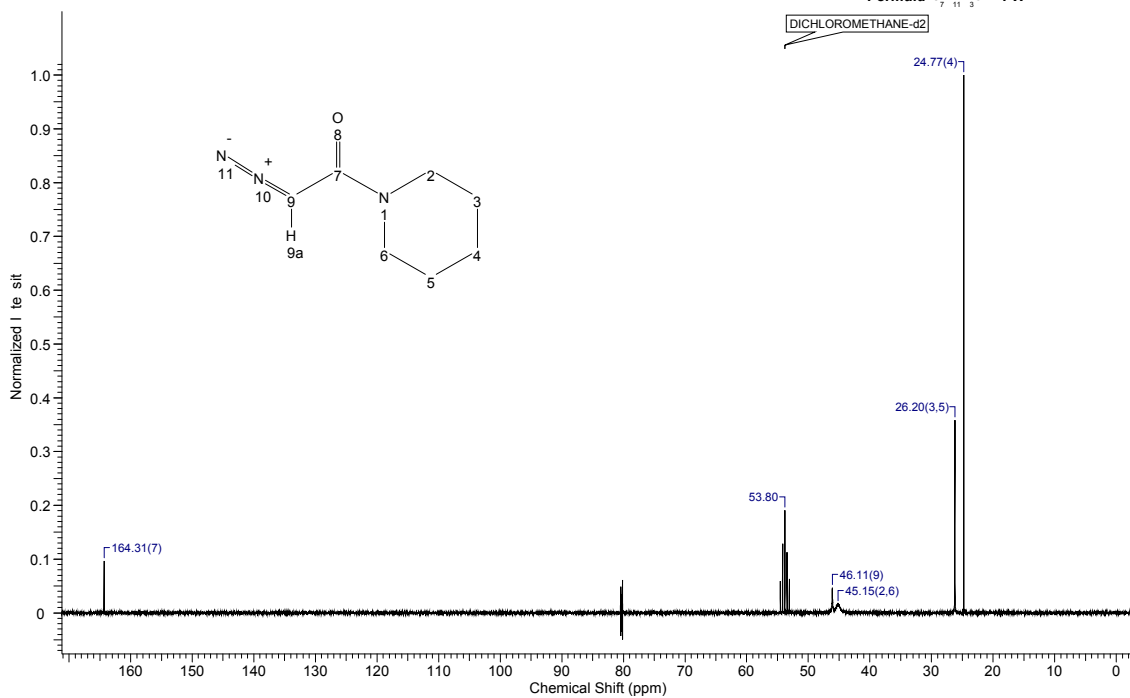
Acquisition Time (sec)	5.3084	Comment	5 mm QNP 1H/15N/13C/31P Z08011/0020	Frequency (MHz)	300.13	Nucleus	¹ H
Number of Transients	16	Origin	DPX300	Original Points Count	32768	Pulse Sequence	zg30
Receiver Gain	50.80	SW(cyclical) (Hz)	6172.84	Solvent	DICHLOROMETHANE-d2	Spectrum Offset (Hz)	1842.9887
Spectrum Type	STANDARD	Sweep Width (Hz)	6172.65	Temperature (degree C)	25.160		

Formula C₇H₁₁N₃ O FW 153.1817

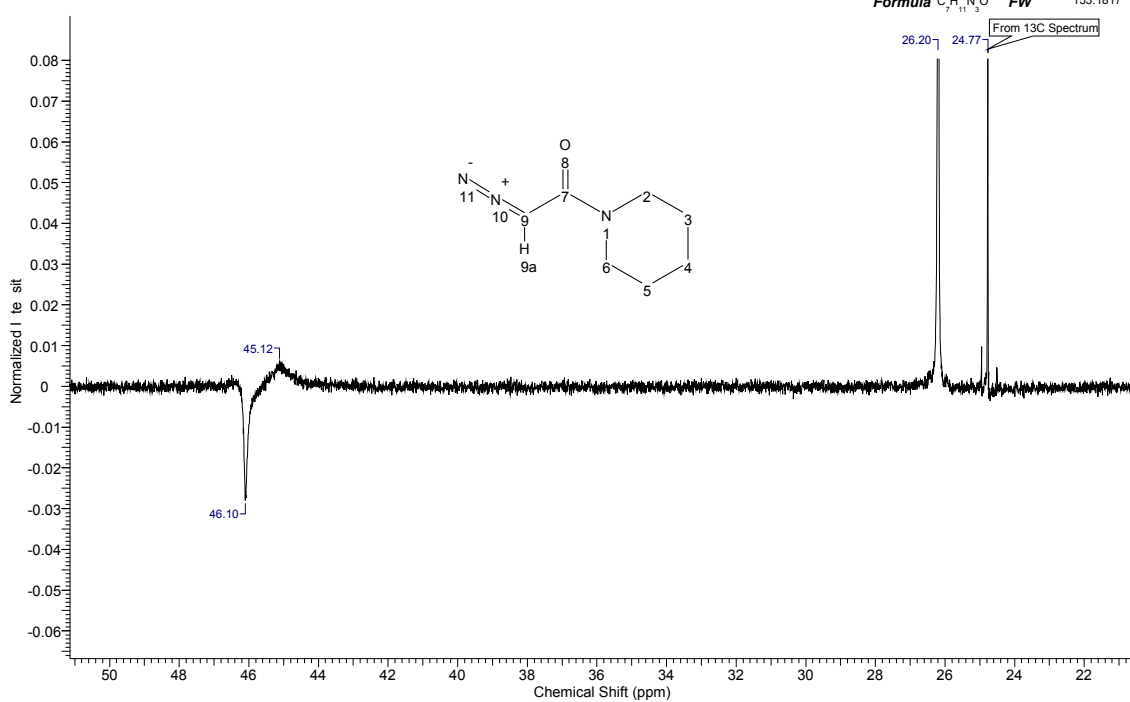


¹³C-NMR & DEPT-135 – 2-diazo-1-(piperidin-1-yl)ethanone

Acquisition Time (sec)	1.8219	Comment	C13CPD CD2Cl2 D: (UIO)aasmuk) 23	Frequency (MHz)	75.48	Nucleus	13C
Number of Transients	1024	Origin	DPX300	Original Points Count	32768	Points Count	32768
Receiver Gain	11585.20	SW(cyclical) (Hz)	17985.61	Solvent	DICHLOROMETHANE-d2	Spectrum Offset (Hz)	7568.1714
Spectrum Type	STANDARD	Sweep Width (Hz)	17985.06	Temperature (degree C)	25.160	Formula	C ₇ H ₁₁ N ₃ O FW 153.1817



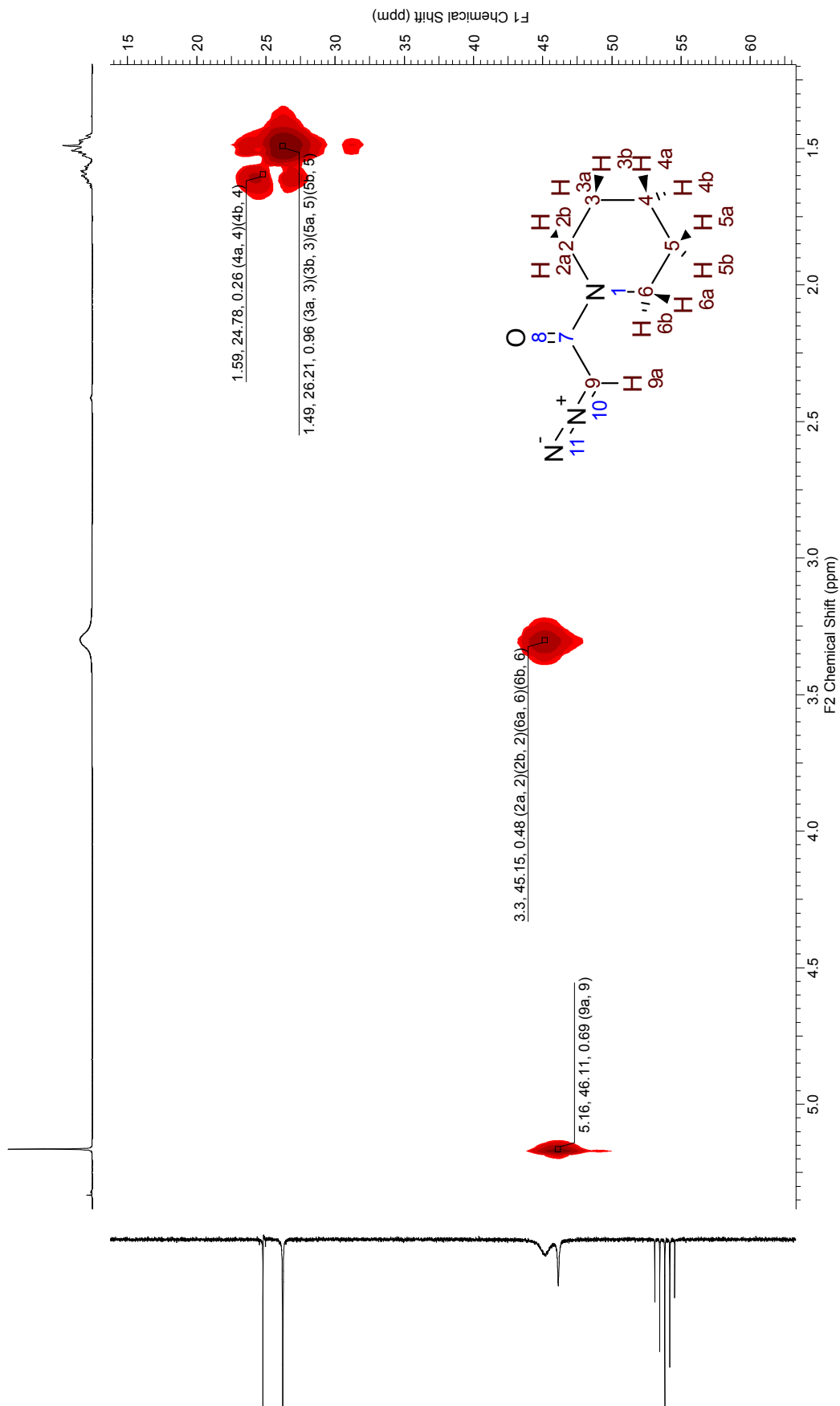
Acquisition Time (sec)	1.8219	Comment	C13DEPT135 CD2Cl2 D: (UIO)aasmuk) 23	Frequency (MHz)	75.48	Nucleus	13C
Number of Transients	1024	Origin	DPX300	Original Points Count	32768	Points Count	32768
Receiver Gain	11585.20	SW(cyclical) (Hz)	17985.61	Solvent	DICHLOROMETHANE-d2	Spectrum Offset (Hz)	7568.2417
Spectrum Type	DEPT135	Sweep Width (Hz)	17985.06	Temperature (degree C)	25.160	Formula	C ₇ H ₁₁ N ₃ O FW 153.1817



2-diazo-1-(piperidin-1-yl)ethanone – HMQC ($^1J_{13C,1H}$)

Acquisition Time (sec) (0.32111, 0.0092)	Comment	Frequency (MHz)	Points Count
Nucleus (1H, 13C)	5 mm QNP 1H/15N/13C/31P Z08011/0020	(300.13, 75.47)	(512, 1024)
Pulse Sequence hmqcqh	DPX300 CD2C/2	Sweep Width (Hz)	Spectrum Type
		(1591.27, 13952.84)	HMQC

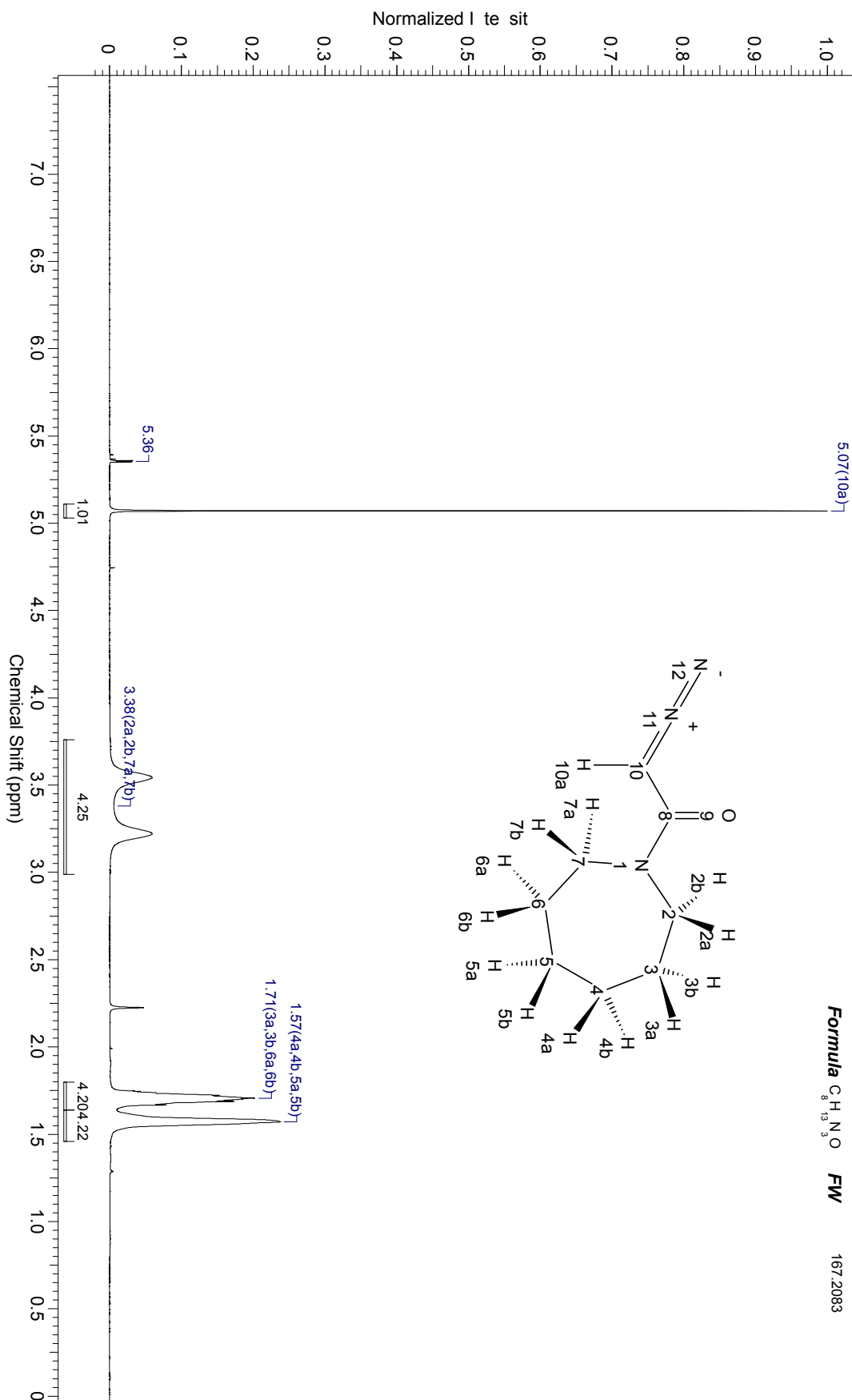
Formula $C_7H_{11}NO_3$ FW 153.1817



¹H-NMR – 1-(azepan-1-yl)-2-diazoethanone

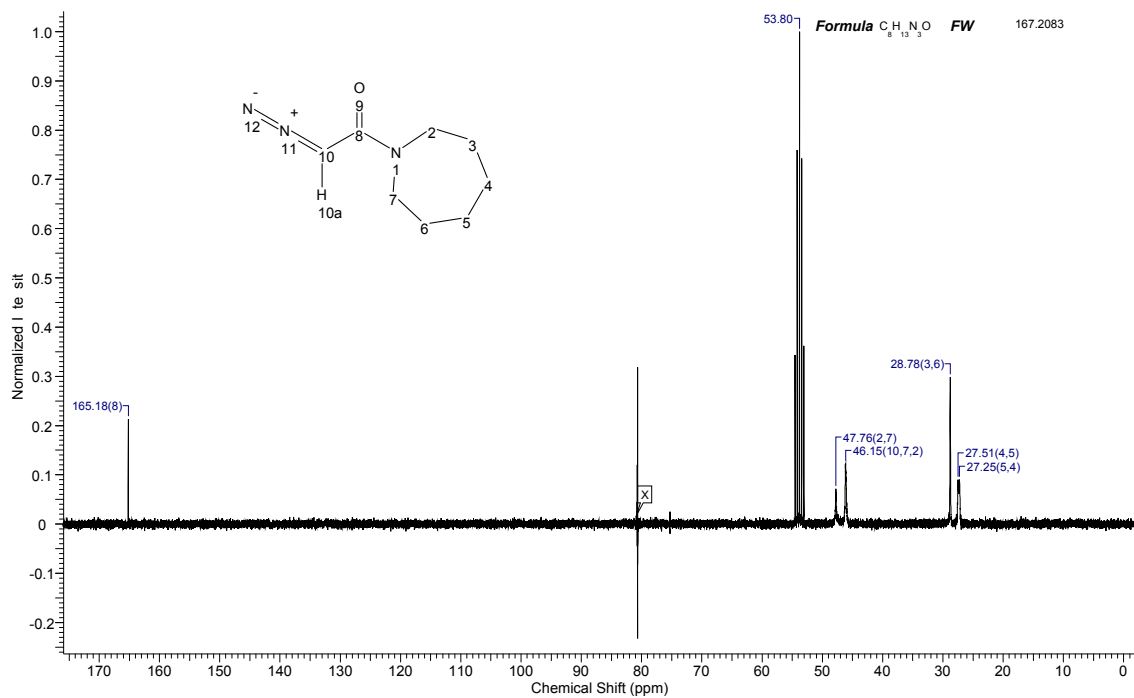
Acquisition Time (sec)	5.3084	Comment	5 mm QNP 1H/15N/13C/31P Z08011/0020	Frequency (MHz)	300.13	Nucleus	1H
Number of Transients	16	Origin	DPX300	Points Count	32768	Pulse Sequence	ZG30
Receiver Gain	80.60	SW(cyclical) (Hz)	6172.84	Solvent	DICHLOROMETHANE-d2	Spectrum Offset (Hz)	1853.4263
Spectrum Type	STANDARD	Sweep Width (Hz)	6172.65	Temperature (degree C)	25.160		

Formula C₈H₁₃N₃O FW 167.2083

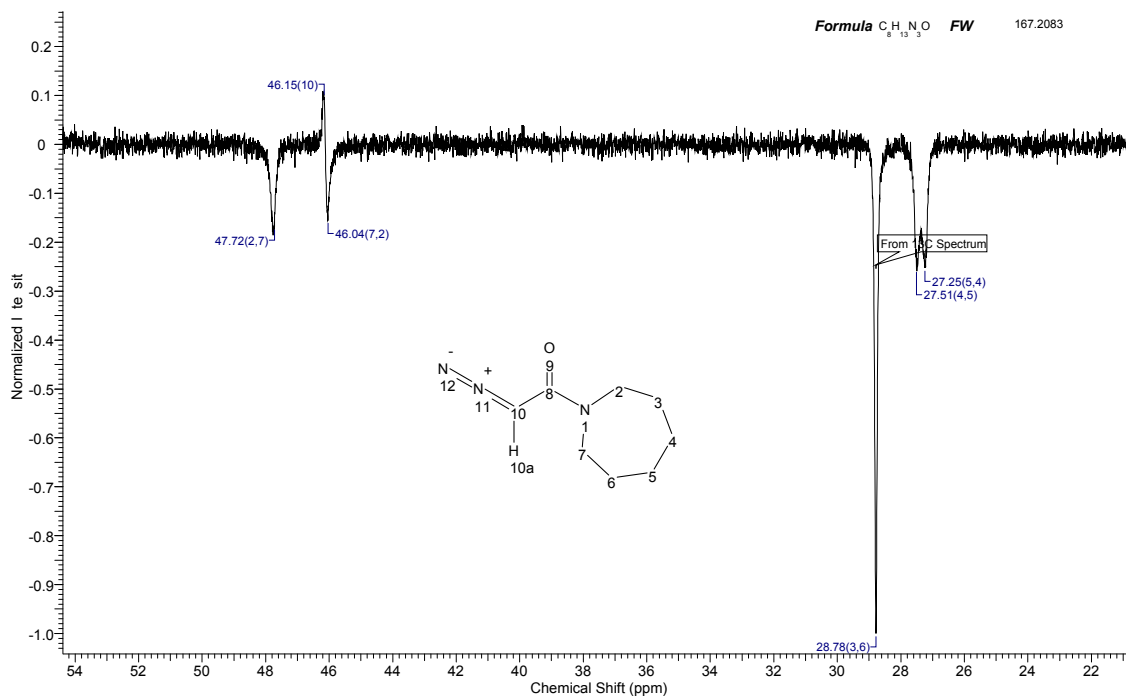


1-(azepan-1-yl)-2-diazoethanone – ¹³C-NMR & DEPT-135

Acquisition Time (sec)	1.8219	Comment	C13CPD CD2Cl2 D: (UIO)aasmuk} 59	Frequency (MHz)	75.48	Nucleus	13C
Number of Transients	1024	Origin	DPX300	Original Points Count	32768	Points Count	32768
Receiver Gain	10321.30	SW(cyclical) (Hz)	17985.61	Solvent	DICHLOROMETHANE-d2	Spectrum Offset (Hz)	7572.5620
Spectrum Type	STANDARD	Sweep Width (Hz)	17985.06	Temperature (degree C)	25.160		



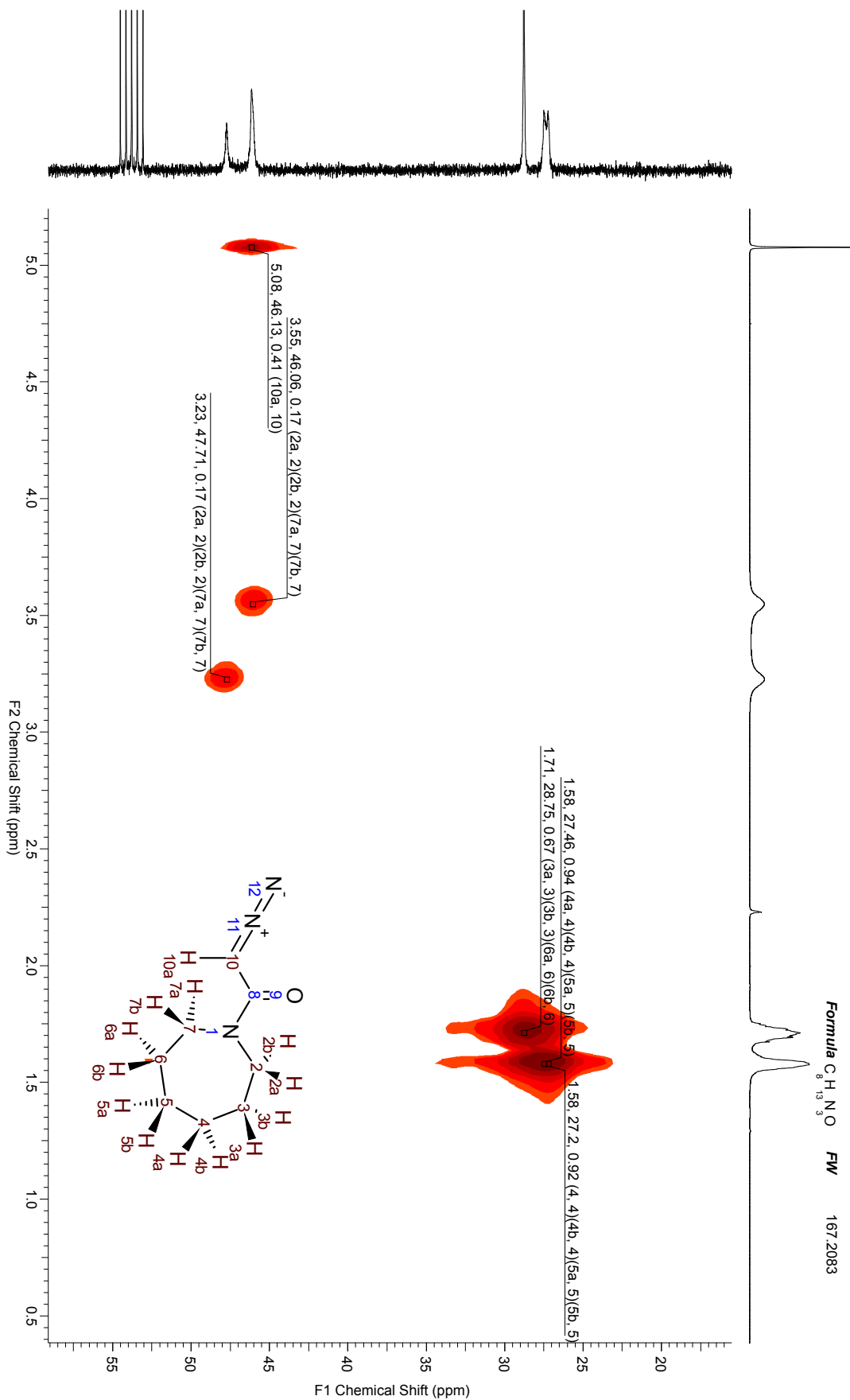
Acquisition Time (sec)	1.8219	Comment	C13DEPT135 CD2Cl2 D: (UIO)aasmuk} 28	Frequency (MHz)	75.48	Nucleus	13C
Number of Transients	1024	Origin	DPX300	Original Points Count	32768	Points Count	32768
Receiver Gain	11585.20	SW(cyclical) (Hz)	17985.61	Solvent	DICHLOROMETHANE-d2	Spectrum Offset (Hz)	7572.8574
Spectrum Type	DEPT135	Sweep Width (Hz)	17985.06	Temperature (degree C)	25.160		



HMQC ($^1J_{13C,1H}$) – 1-(azepan-1-yl)-2-diazoethanone

Acquisition Time (sec)	(0.3244, 0.0092)	Comment	5 mm QNP 1H/15N/13C/31P Z08011/0020	Frequency (MHz)	(300.13, 75.47)
Nucleus	(1H , ^{13}C)	Origin	DPX300	Points Count	(512, 1024)
Pulse Sequence	hmqcwf	Solvent	CD2Cl2	Spectrum Type	HMOC
				Sweep Width (Hz)	(1575.20, 13952.84)

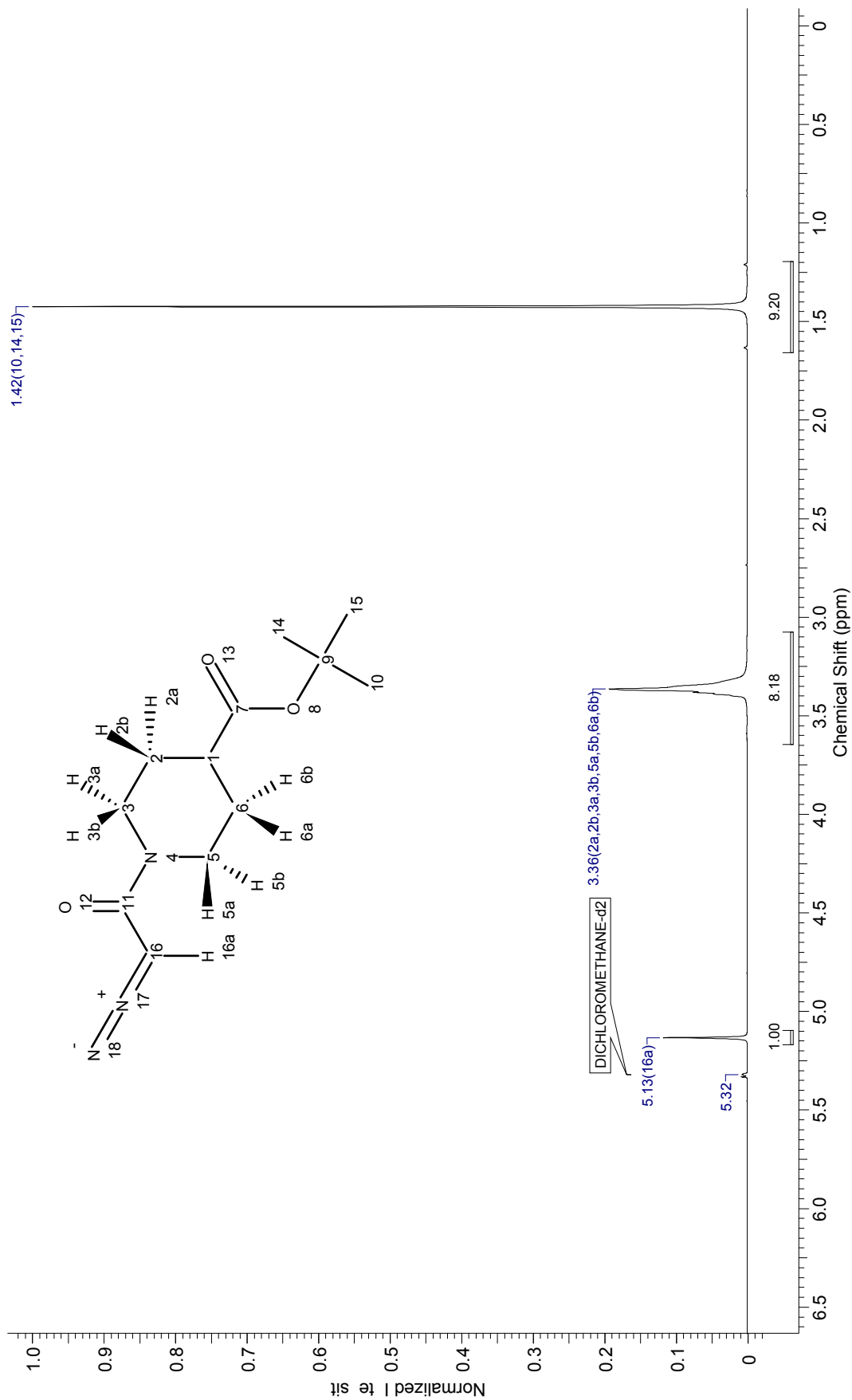
Formula $C_8H_{13}NO$ FW 167.2083



tert-butyl 4-(2-diazoacetyl)piperazine-1-carboxylate – ¹H-NMR

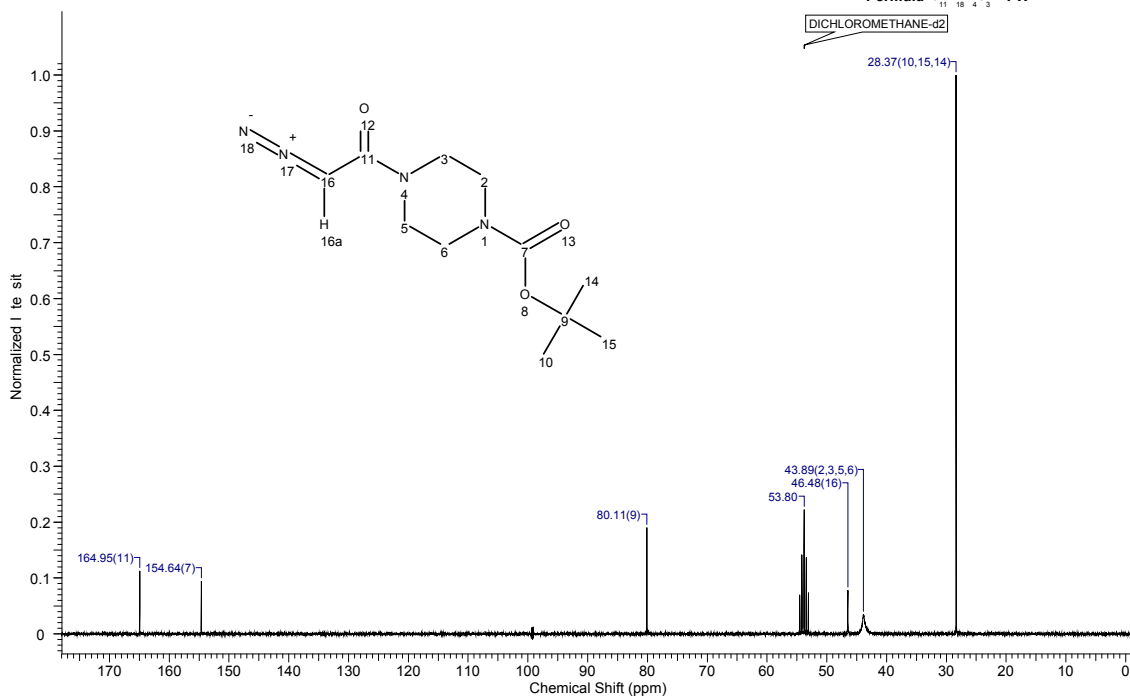
Acquisition Time (sec)	5.3084	Frequency (MHz)	300.13	Nucleus	¹ H	Origin	Bruker	Original Points Count	32768	Points Count	262144
Pulse Sequence	ZG30	Spectrum Offset (Hz)	1843.0216			Spectrum Type	STANDARD	Sweep Width (Hz)		Sweep Width (Hz)	6172.84

Formula C₁₂H₁₉N₃O₃ FW 253.2976

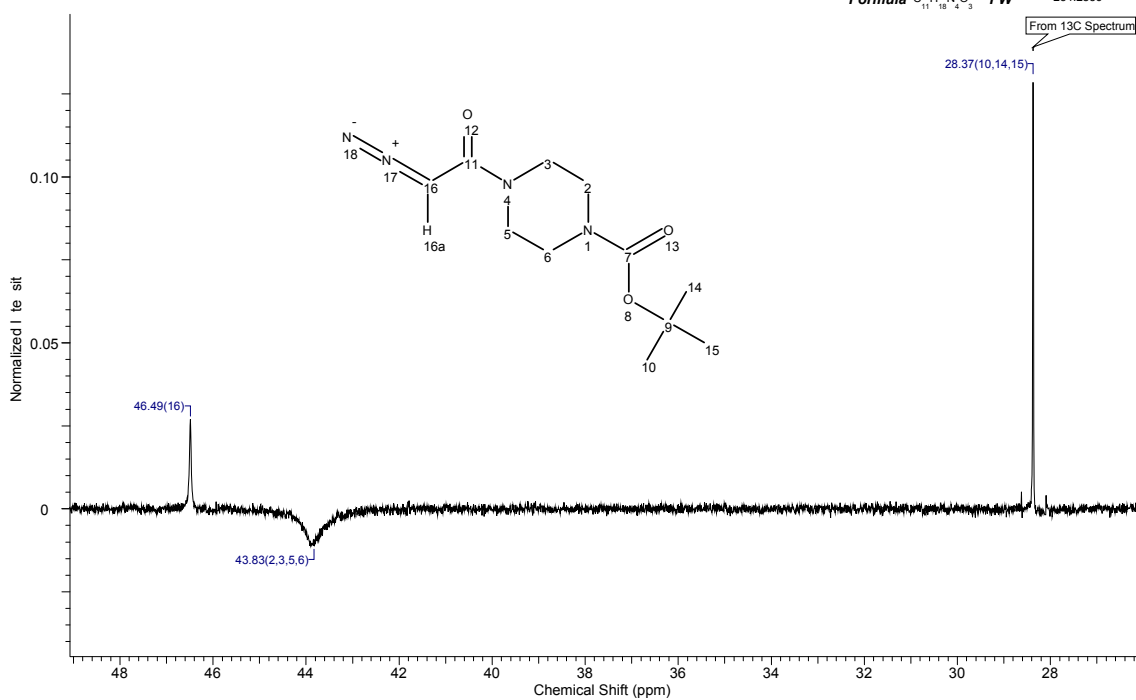


¹³C-NMR & DEPT-135 – tert-butyl 4-(2-diazoacetyl)piperazine-1-carboxylate

Acquisition Time (sec)	1.8219	Comment	C13CPD CD2Cl2 D: (UIO)aasmuk) 1	Frequency (MHz)	75.47	Nucleus	13C
Number of Transients	512	Origin	DPX300	Original Points Count	32768	Points Count	32768
Receiver Gain	10321.30	SW(cyclical) (Hz)	17985.61	Solvent	DICHLOROMETHANE-d2	Spectrum Offset (Hz)	7571.0566
Spectrum Type	STANDARD	Sweep Width (Hz)	17985.06	Temperature (degree C)	25.160	Formula	C ₁₁ H ₁₈ N ₄ O ₃ FW 254.2856

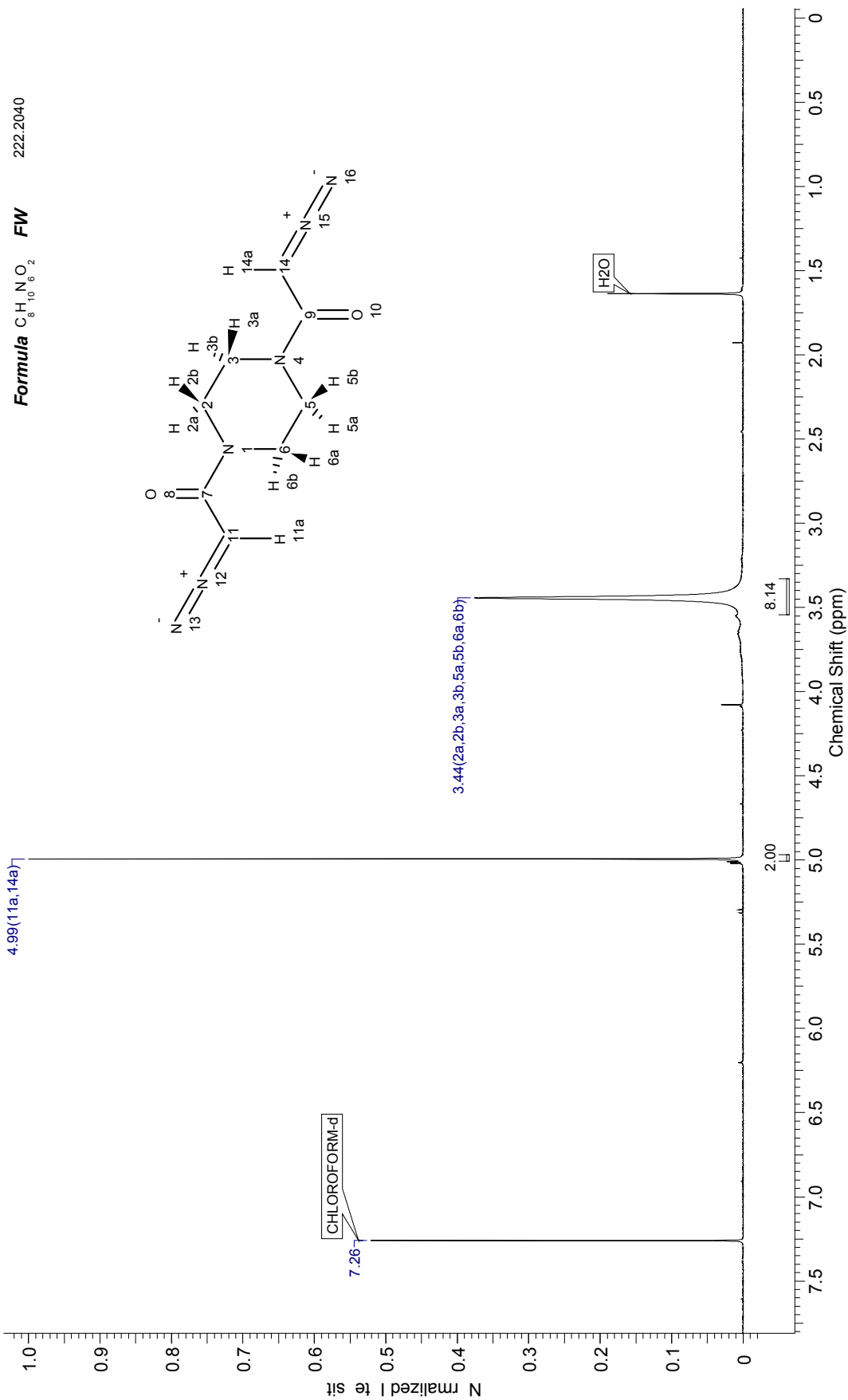


Acquisition Time (sec)	1.8219	Comment	C13DEPT135 CD2Cl2 D: (UIO)aasmuk) 1	Frequency (MHz)	75.48	Nucleus	13C
Number of Transients	256	Origin	DPX300	Original Points Count	32768	Points Count	32768
Receiver Gain	16384.00	SW(cyclical) (Hz)	17985.61	Solvent	DICHLOROMETHANE-d2	Spectrum Offset (Hz)	7571.5518
Spectrum Type	DEPT135	Sweep Width (Hz)	17985.06	Temperature (degree C)	25.160	Formula	C ₁₁ H ₁₈ N ₄ O ₃ FW 254.2856



N,N'-bis(2-diazoacetyl)piperazine – ¹H-NMR

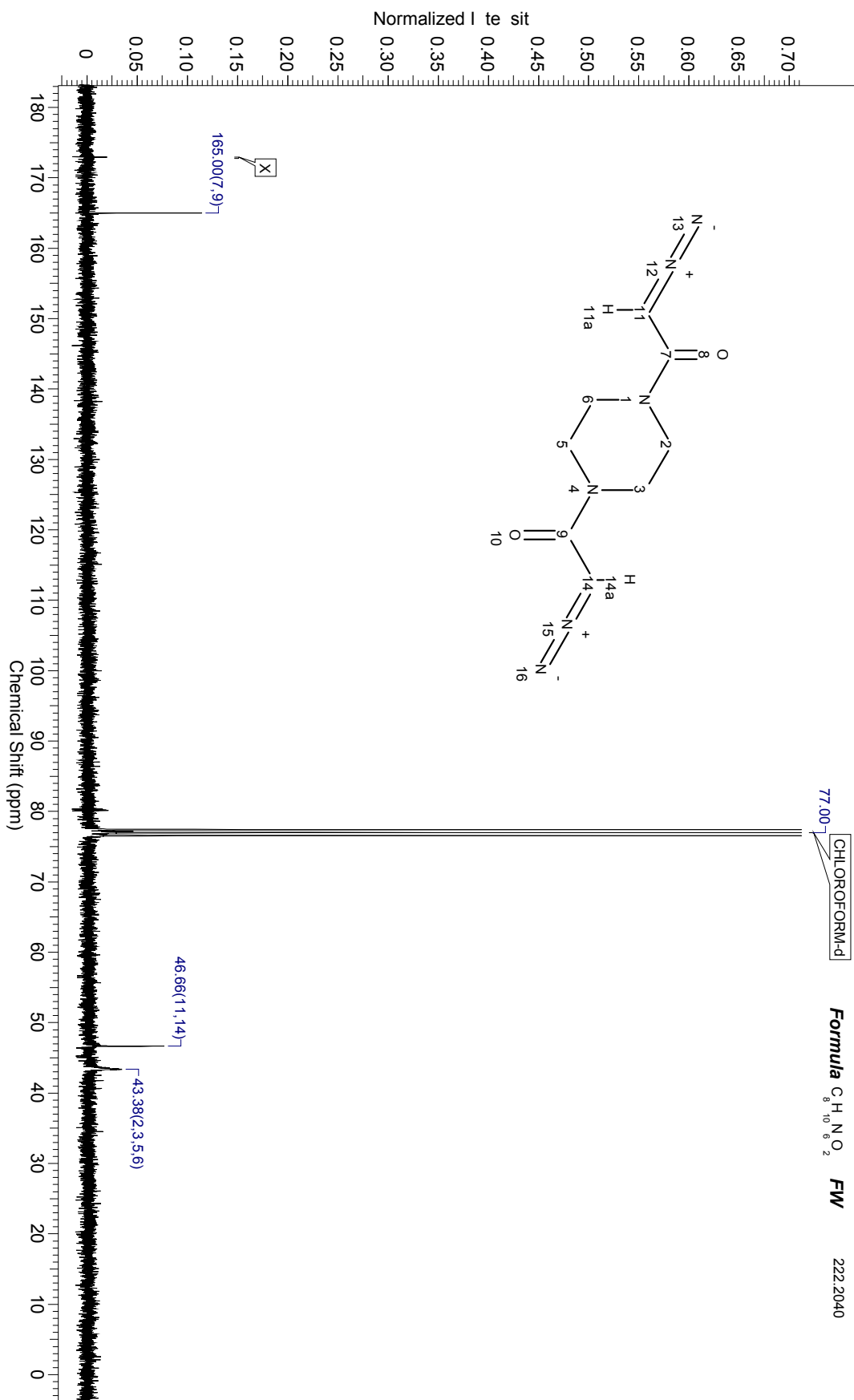
Acquisition Time (sec)	5.3084	Comment	5 mm QNP 1H/15N/13C/31P Z08011/0020	Frequency (MHz)	300.13	Nucleus	¹ H
Number of Transients	16	Origin	DPX300	Original Points Count	32768	Pulse Sequence	zg30
Receiver Gain	1290.20	SW(cyclical) (Hz)	6172.84	Solvent	CHLOROFORM-d	Spectrum Offset (Hz)	1847.1124
Spectrum Type	STANDARD			Sweep Width (Hz)	6172.65	Temperature (degree C)	25.160



¹³C-NMR – N,N'-bis(2-diazoacetyl)piperazine

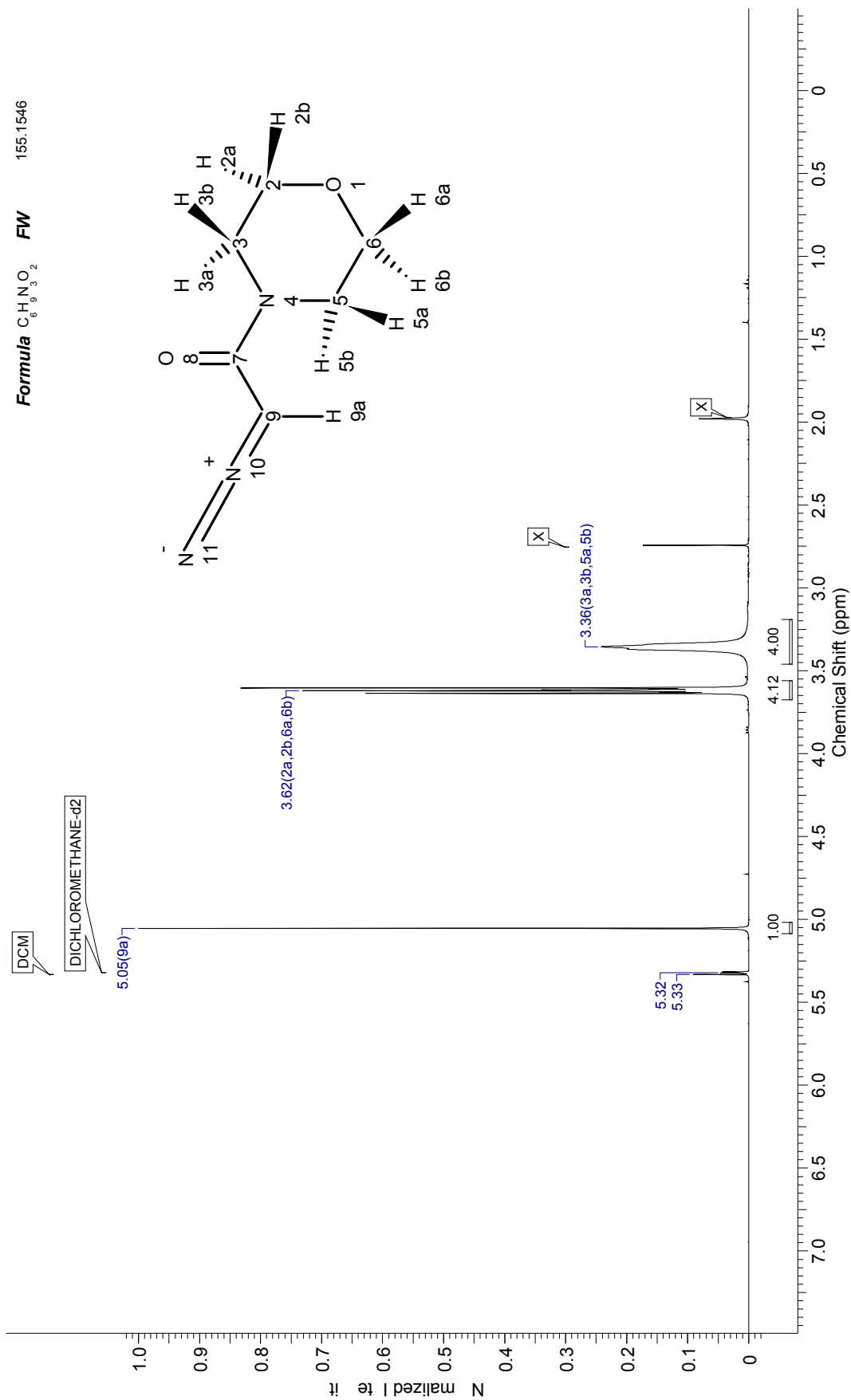
Acquisition Time (sec)	1.8219	Comment	13C	Frequency (MHz)	75.47	Nucleus	13C	Number of Transients	1024
Origin	DPX300	Original Points Count	32768	Points Count	32768	Pulse Sequence	zgpg30	Receiver Gain	11585.20
SW(cyclical) (Hz)	17985.61	Solvent	CHLOROFORM-d	Sweep Width (Hz)	17985.06	Spectrum Offset (Hz)	7544.0947	Temperature (degree C)	25.160
Spectrum Type	STANDARD								

77.00 CHLOROFORM-d Formula C₈H₁₀N₆O₂ FW 222.2040



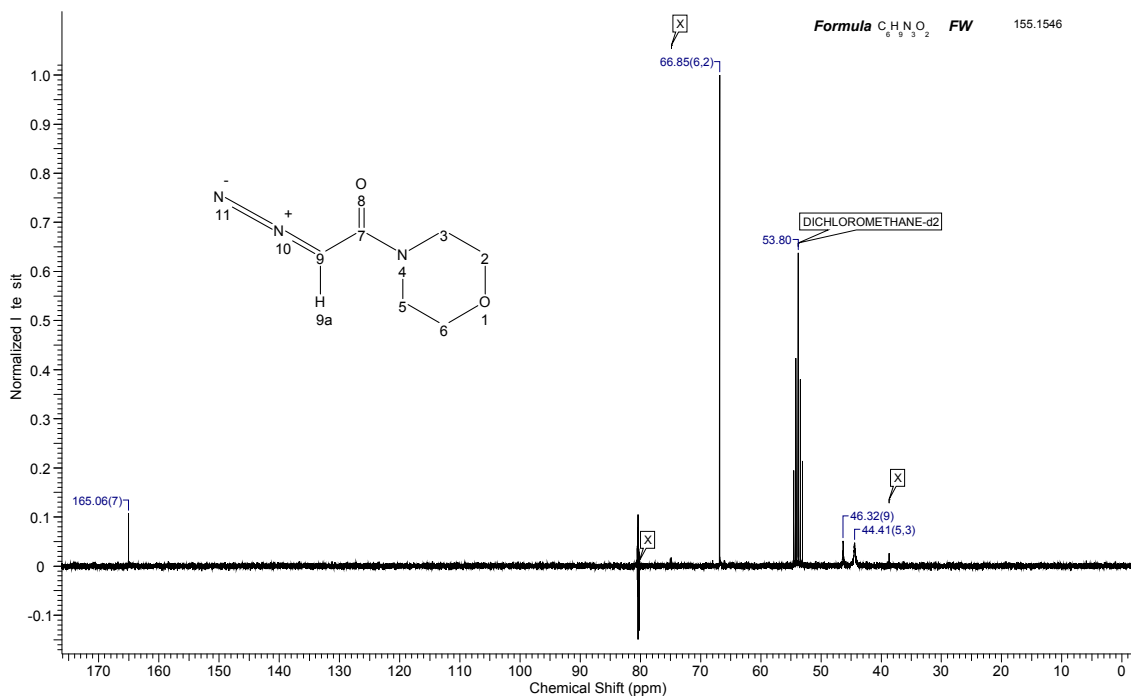
Acquisition Time (sec)	5.3084	Comment	5 mm QNP 1H/15N/13C/31P Z08011/0020	Frequency (MHz)	300.13	Nucleus	¹ H
Number of Transients	16	Origin	DPX300	Original Points Count	32768	Pulse Sequence	zg30
Receiver Gain	143.70	SW(cyclical) (Hz)	6172.84	Solvent	DICHLOROMETHANE-d2	Spectrum Offset (Hz)	1842.8103
Spectrum Type	STANDARD	Sweep Width (Hz)	6172.65	Temperature (degree C)	26.160		

Formula C₆H₉N₃O₂ FW 155.1546

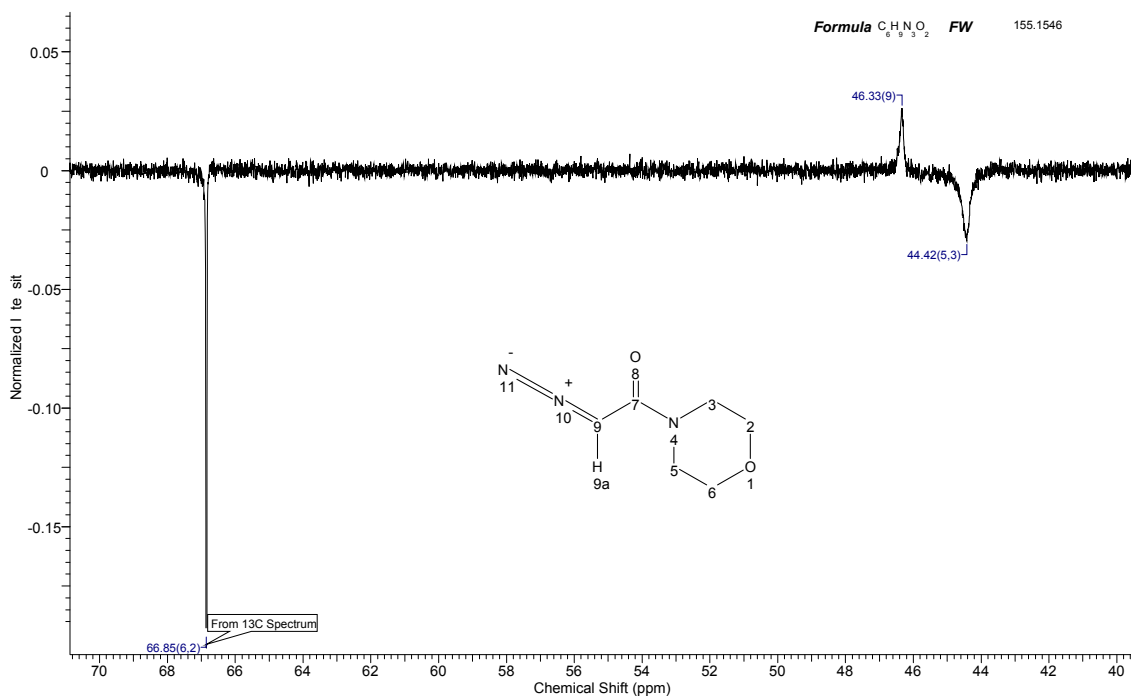


¹³C-NMR & DEPT-135 – 2-diazo-1-morpholinoethanone

Acquisition Time (sec)	1.8219	Comment	C13CPD CD2Cl2 D: (UIO)aasmuk) 19	Frequency (MHz)	75.48	Nucleus	13C
Number of Transients	1024	Origin	DPX300	Original Points Count	32768	Points Count	32768
Receiver Gain	11585.20	SW(cyclical) (Hz)	17985.61	Solvent	DICHLOROMETHANE-d2	Spectrum Offset (Hz)	7572.0137
Spectrum Type	STANDARD	Sweep Width (Hz)	17985.06	Temperature (degree C)	25.160		



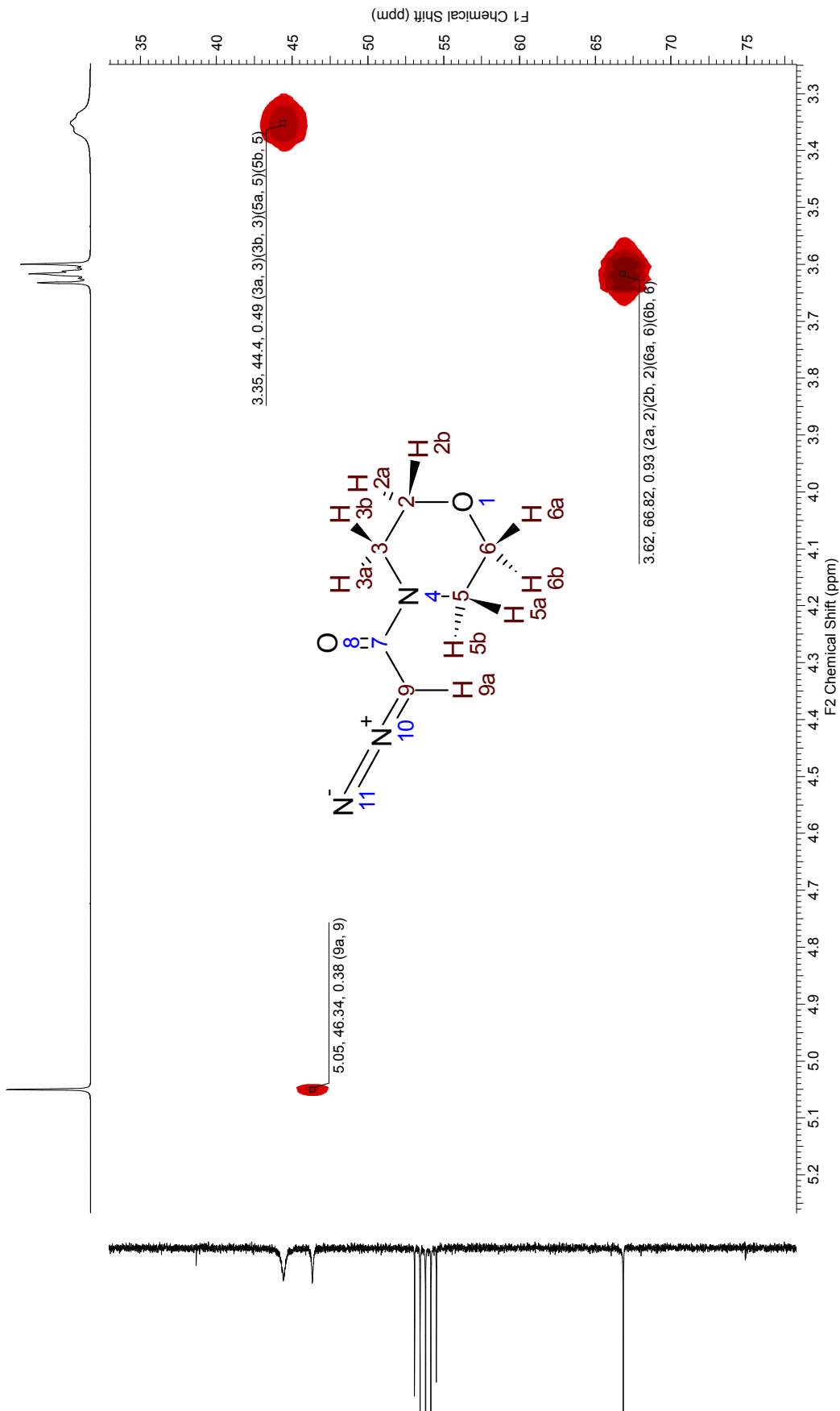
Acquisition Time (sec)	1.8219	Comment	C13DEPT135 CD2Cl2 D: (UIO)aasmuk) 19	Frequency (MHz)	75.48	Nucleus	13C
Number of Transients	1024	Origin	DPX300	Original Points Count	32768	Points Count	32768
Receiver Gain	16384.00	SW(cyclical) (Hz)	17985.61	Solvent	DICHLOROMETHANE-d2	Spectrum Offset (Hz)	7571.7314
Spectrum Type	DEPT135	Sweep Width (Hz)	17985.06	Temperature (degree C)	25.160		



2-diazo-1-morpholinoethanone – HMQC ($^1J_{13C,1H}$)

Acquisition Time (sec)	(0.4588, 0.0092)	Comment	5 mm QNP 1H/15N/13C/31P Z08011/0020	Frequency (MHz)	(300.13, 75.47)
Nucleus	(1H, 13C)	Origin	DPX300	Points Count	(512, 1024)
Pulse Sequence	hmqcqh	Solvent	CD2Cl2	Sweep Width (Hz)	(1113.89, 13952.84)

Formula $C_6H_9N_3O_2$ FW 155.1546

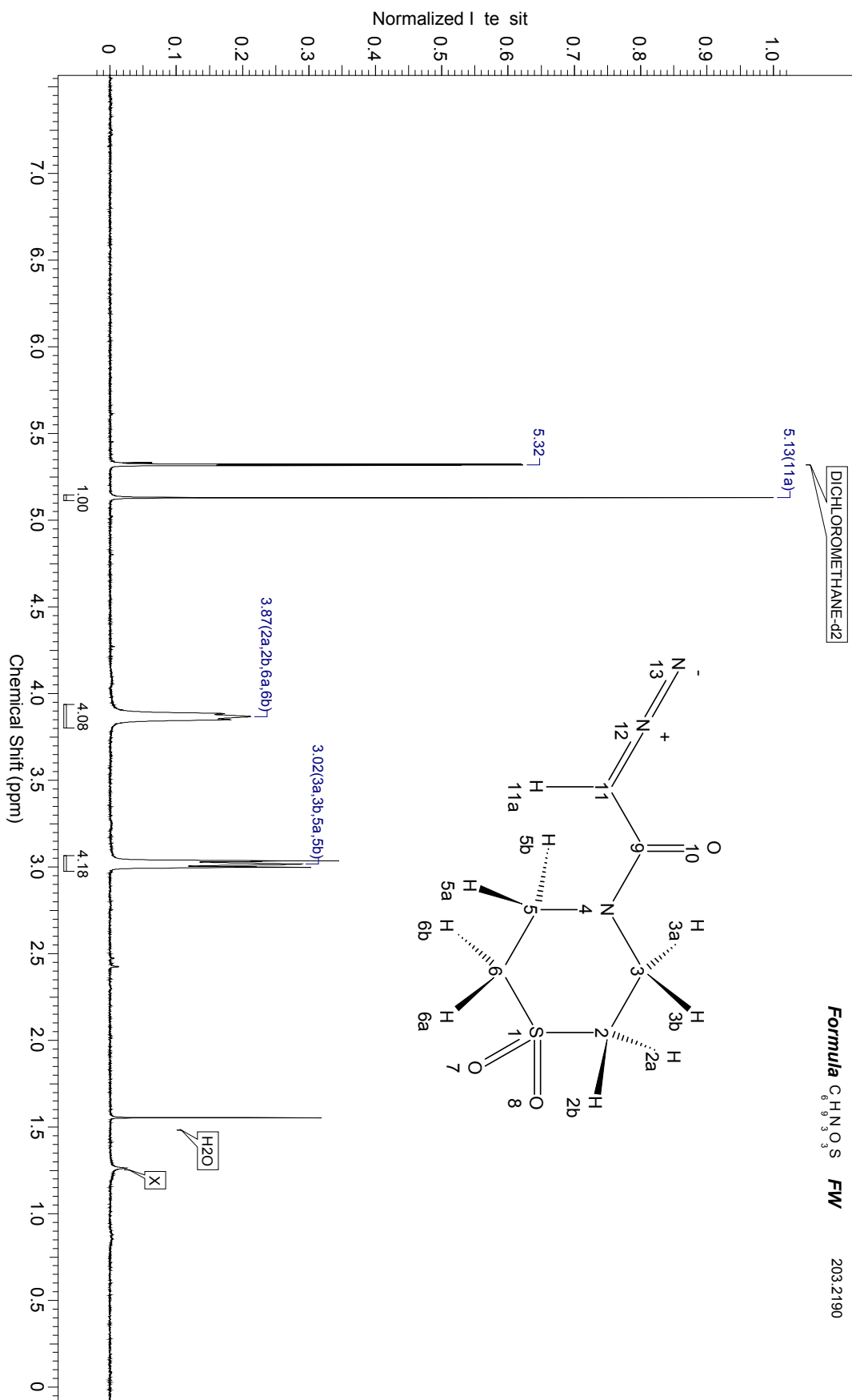
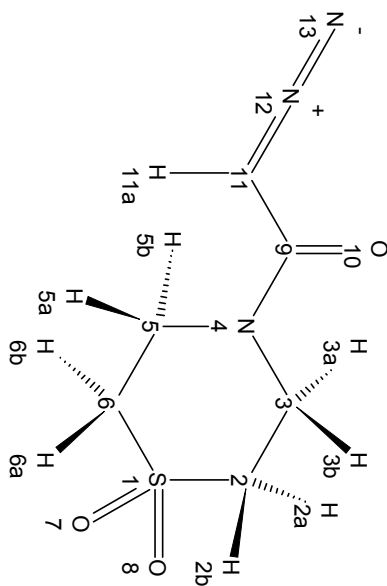


¹H-NMR – 2-diazo-1-(1,1-dioxido-4-thiomorpholinyl)ethanone

Acquisition Time (sec)	5.3084	Comment	PROTON CD2C12 D: (UOaasmuk) 1	Frequency (MHz)	300.13	Nucleus	¹ H
Number of Transients	16	Origin	DPX300	Points Count	32768	Pulse Sequence	zg30
Receiver Gain	1448.20	SW(cyclical) (Hz)	6172.84	Solvent	DICHLOROMETHANE-d2	Spectrum Offset (Hz)	1842.8202
Spectrum Type	STANDARD	Sweep Width (Hz)	6172.65	Temperature (degree C)	25.160		

DICHLOROMETHANE-d2

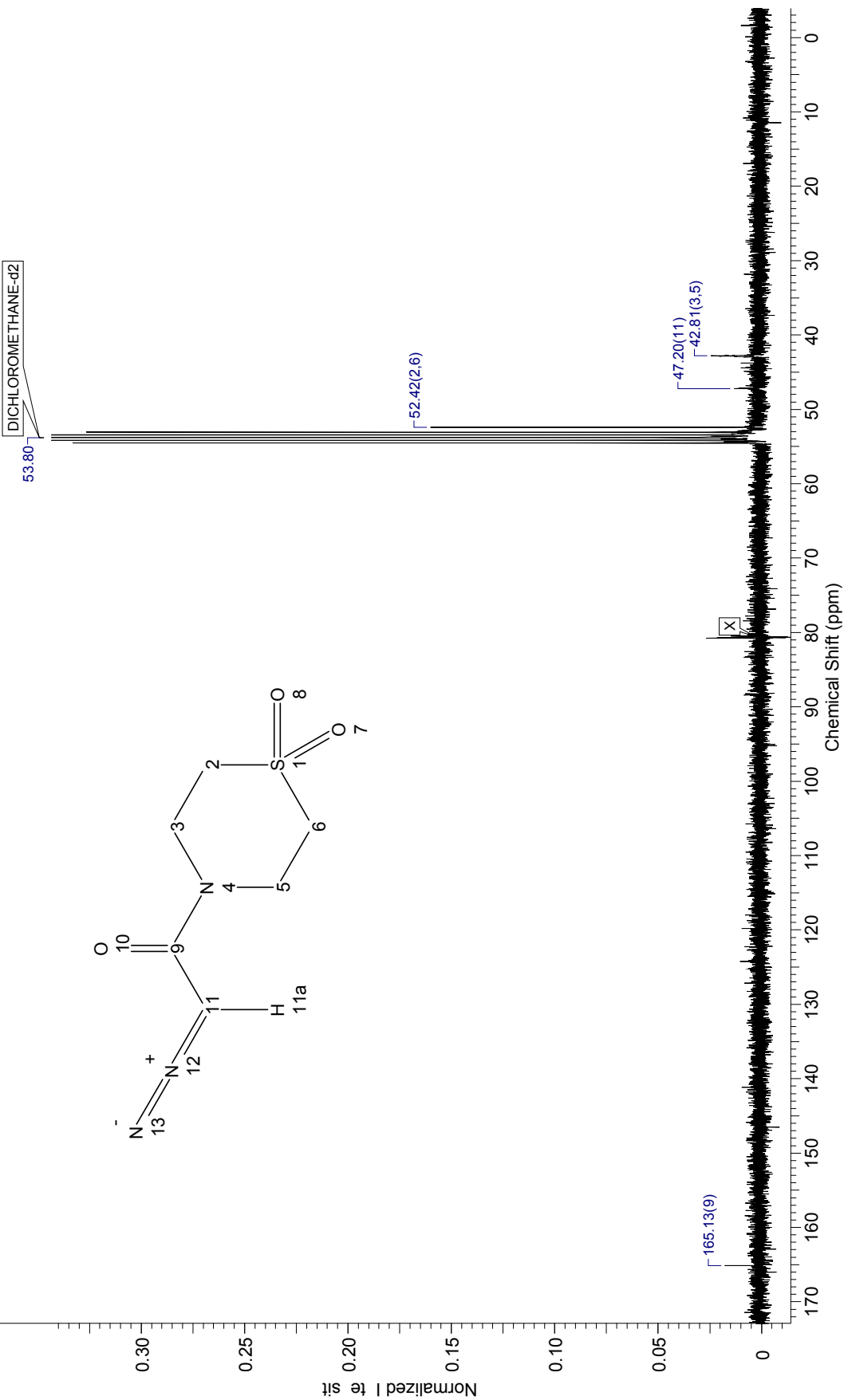
Formula C₆H₉N₃O₃S FW 203.2190



2-diazo-1-(1,1-dioxido-4-thiomorpholinyl)ethanone – ¹³C-NMR

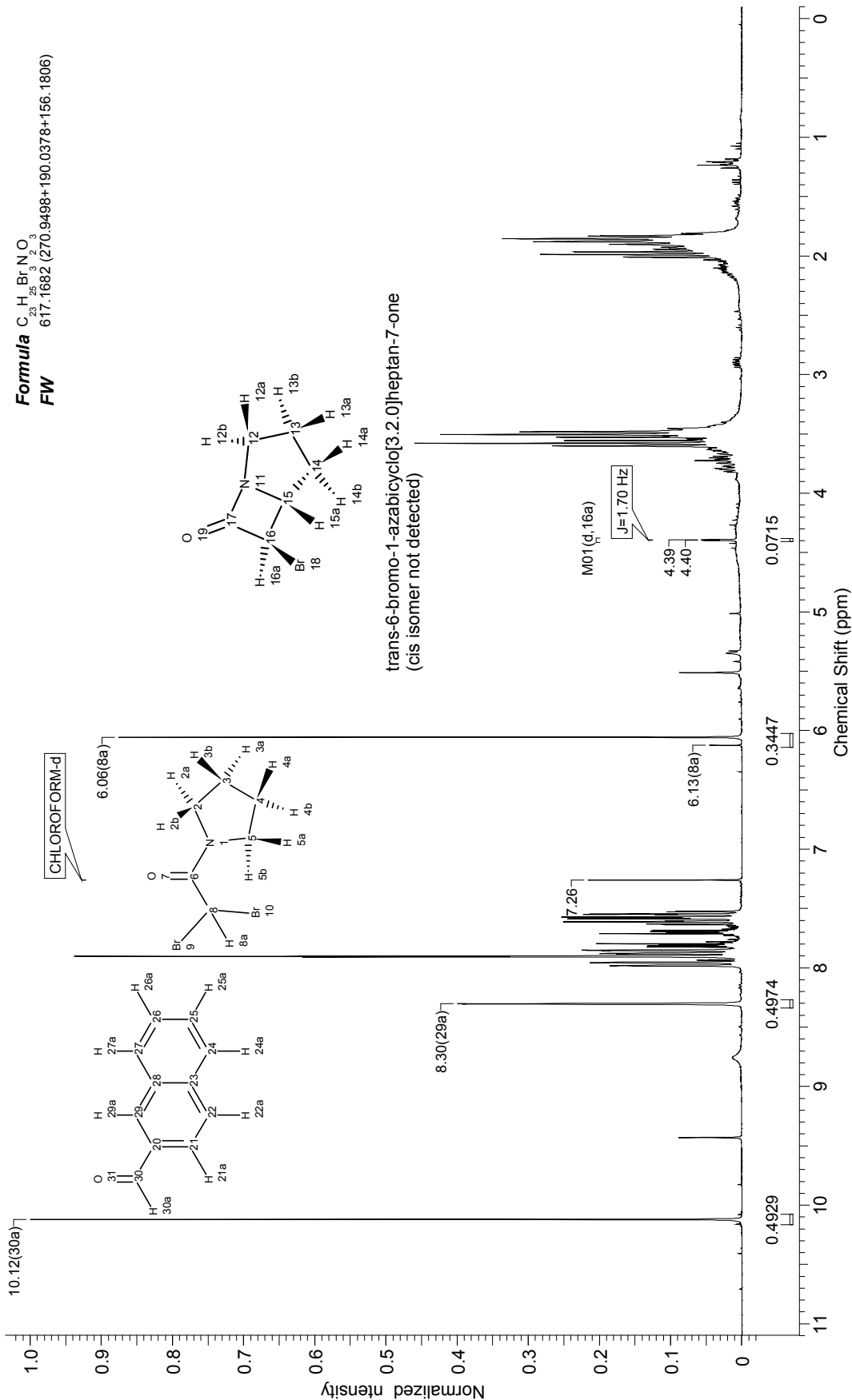
Acquisition Time (sec)	1.8219	Frequency (MHz)	75.47	Nucleus	¹³ C	Number of Transients	990	Origin	DPX300
Original Points Count	32768	Points Count	32768	Pulse Sequence	zgpg30	Receiver Gain	13004.00	SW(cyclical) (Hz)	17985.61
Solvent	DICHLOROMETHANE-d2	Temperature (degree C)	25.160	Spectrum Offset (Hz)	7574.8994	Spectrum Type	STANDARD		

Formula C₆H₉N₃O₃S FW 203.2190



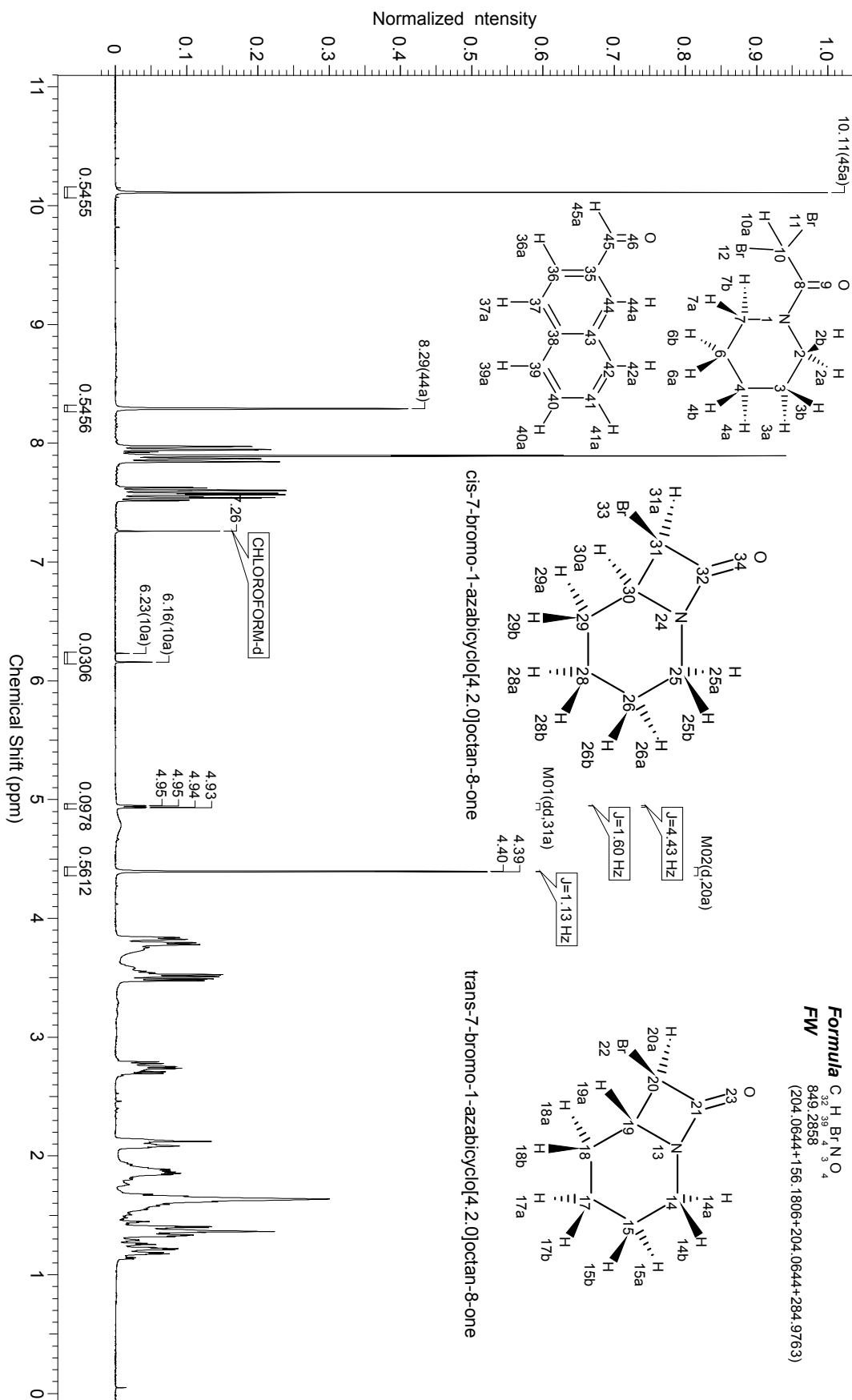
Crude 6-bromo-1-azabicyclo[3.2.0]heptan-7-one – ¹H-NMR

Acquisition Time (sec)	5.3084	Comment	5 mm QNP	¹ H/15N/13C/31P Z08011/0020	Frequency (MHz)	300.13	Nucleus	¹ H	
Number of Transients	16	Origin	DPX300	Original Points Count	32768	Points Count	32768	Pulse Sequence	zg30
Receiver Gain	128.00	SW(cyclical) (Hz)	6172.84	Solvent	CHLOROFORM-d	Spectrum Offset (Hz)	1847.3009	Spectrum Offset (Hz)	1847.3009
Spectrum Type	STANDARD	Sweep Width (Hz)	6172.65	Temperature (degree C)	25.160				



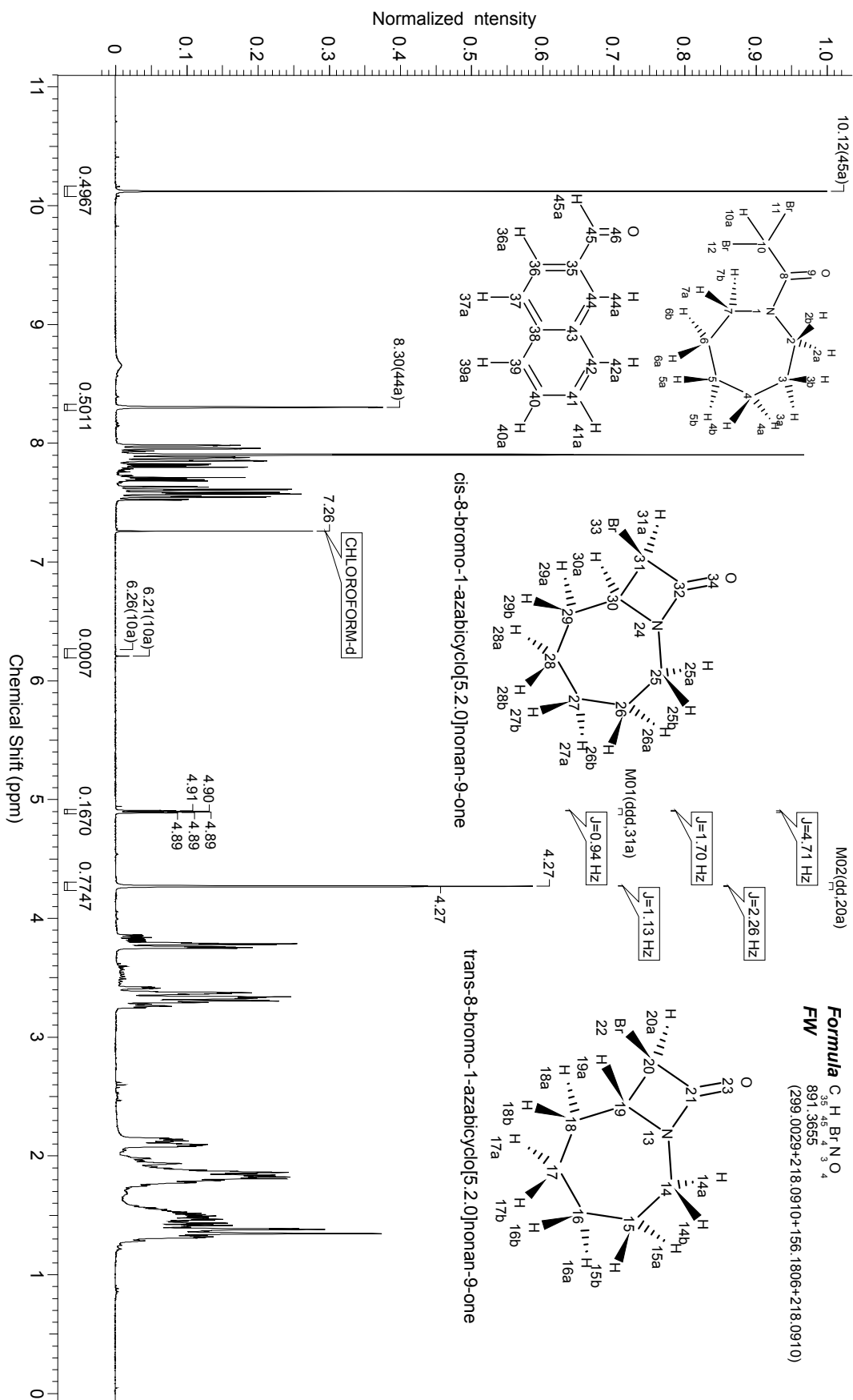
¹H-NMR – Crude 7-bromo-1-azabicyclo[4.2.0]octan-8-one - NBS

Acquisition Time (sec)	5.3084	Comment	5 mm NNP 1H/15N/13C/31P Z08011/0020	Frequency (MHz)	300.13	Nucleus	¹ H
Number of Transients	16	Origin	DPX300	Points Count	32768	Pulse Sequence	zg30
Receiver Gain	101.60	SW(cyclical) (Hz)	6172.84	Solvent	CHLOROFORM-d	Spectrum Offset (Hz)	1847.3009
Spectrum Type	STANDARD	Sweep Width (Hz)	6172.65	Temperature (degree C)	25.160		



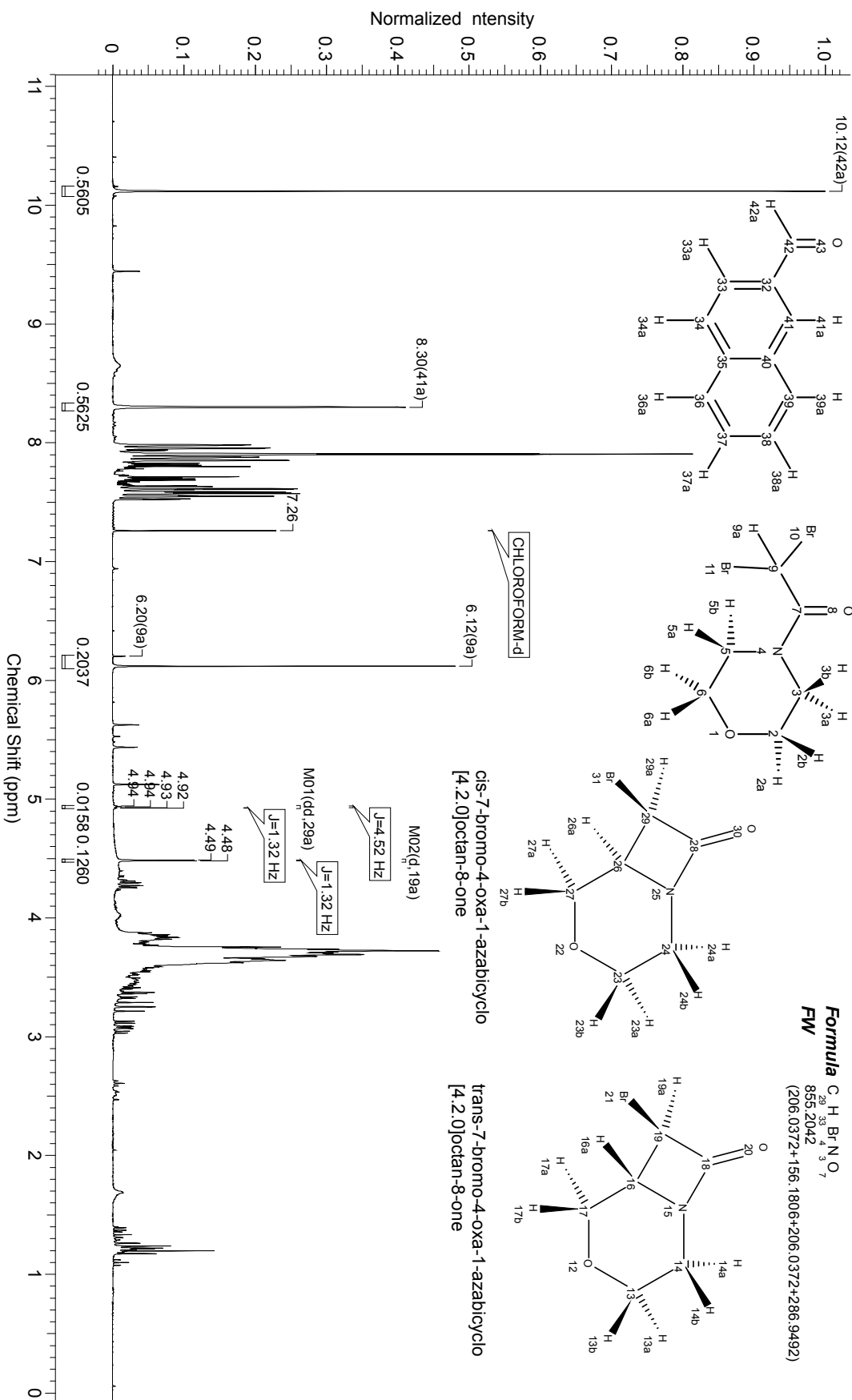
¹H-NMR – Crude 8-bromo-1-azabicyclo[5.2.0]nonan-9-one

Acquisition Time (sec)	5.3084	Comment	5 mm NNP 1H/15N/13C/31P Z08011/0020	Frequency (MHz)	300.13	Nucleus	¹ H
Number of Transients	16	Origin	DPX300	Points Count	32768	Pulse Sequence	zg30
Receiver Gain	114.00	SW(cyclical) (Hz)	6172.84	Solvent	CHLOROFORM-d	Spectrum Offset (Hz)	1847.3009
Spectrum Type	STANDARD	Sweep Width (Hz)	6172.65	Temperature (degree C)	25.160		

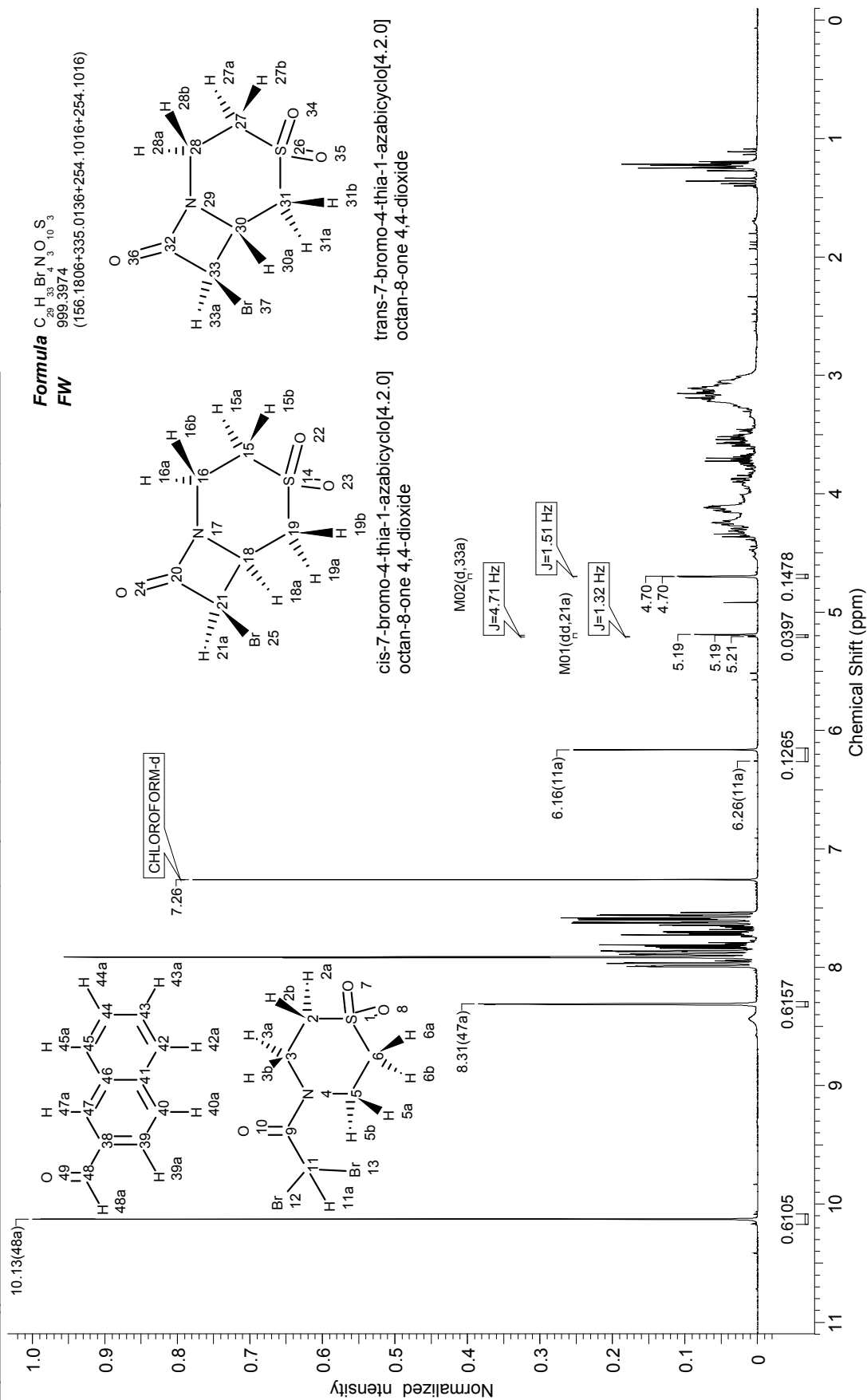


¹H-NMR – Crude 7-bromo-4-oxa-1-azabicyclo[4.2.0]octan-8-one

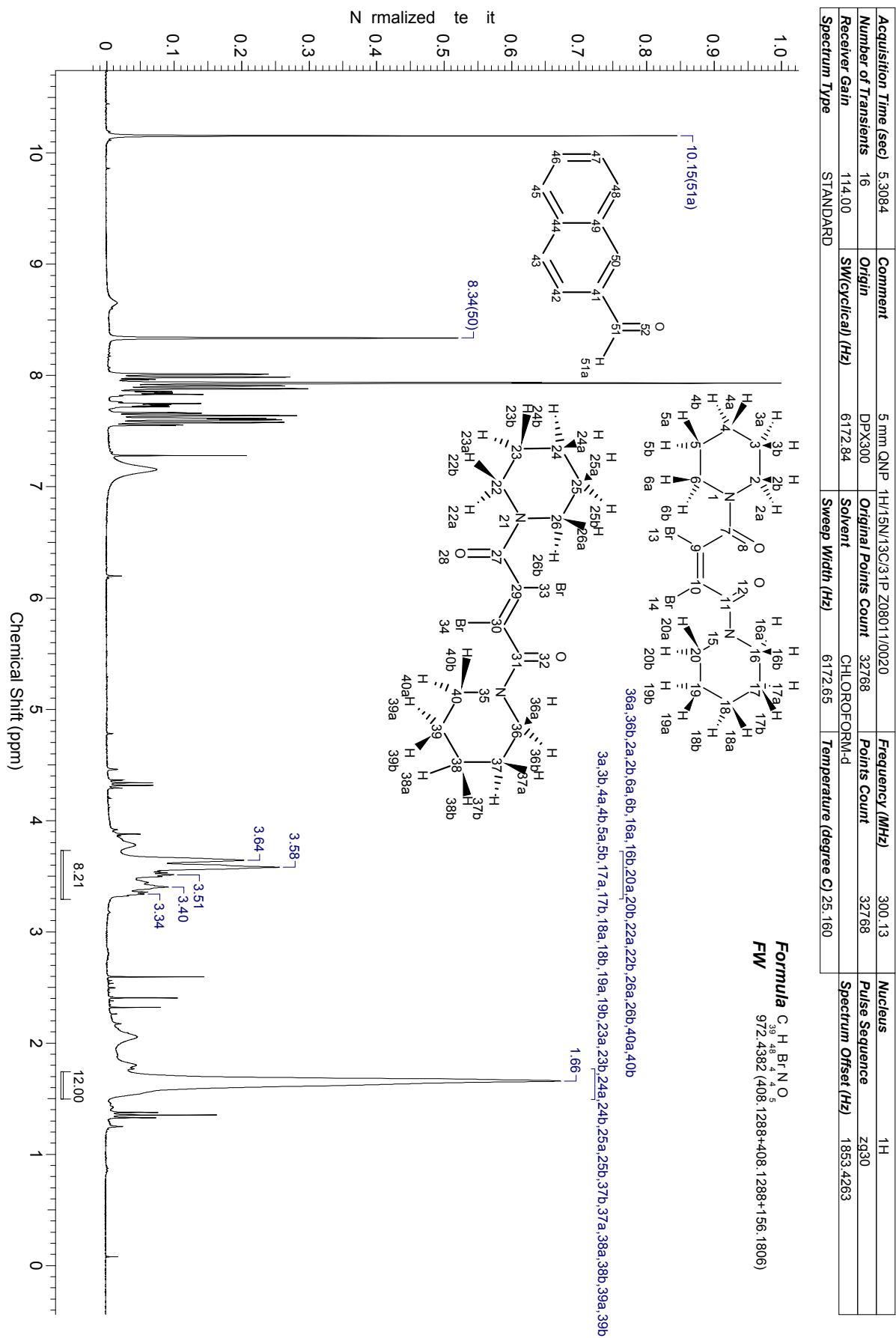
Acquisition Time (sec)	5.3084	Comment	5 mm NNP 1H/15N/13C/31P Z08011/0020	Frequency (MHz)	300.13	Nucleus	¹ H
Number of Transients	16	Origin	DPX300	Points Count	32768	Pulse Sequence	zg30
Receiver Gain	128.00	SW(cyclical) (Hz)	6172.84	Solvent	CHLOROFORM-d	Spectrum Offset (Hz)	1847.3009
Spectrum Type	STANDARD	Sweep Width (Hz)	6172.65	Temperature (degree C)	25.160		



Acquisition Time (sec)	5.3084	Comment	5 mm QNP	Frequency (MHz)	300.13	Nucleus	¹ H
Number of Transients	16	Origin	DPX300	Points Count	32768	Pulse Sequence	zg30
Receiver Gain	143.70	SW(cyclical) (Hz)	6172.84	Solvent	CHLOROFORM-d	Spectrum Offset (Hz)	1847.3009
Spectrum Type	STANDARD	Sweep Width (Hz)	6172.65	Temperature (degree C)	25.160		



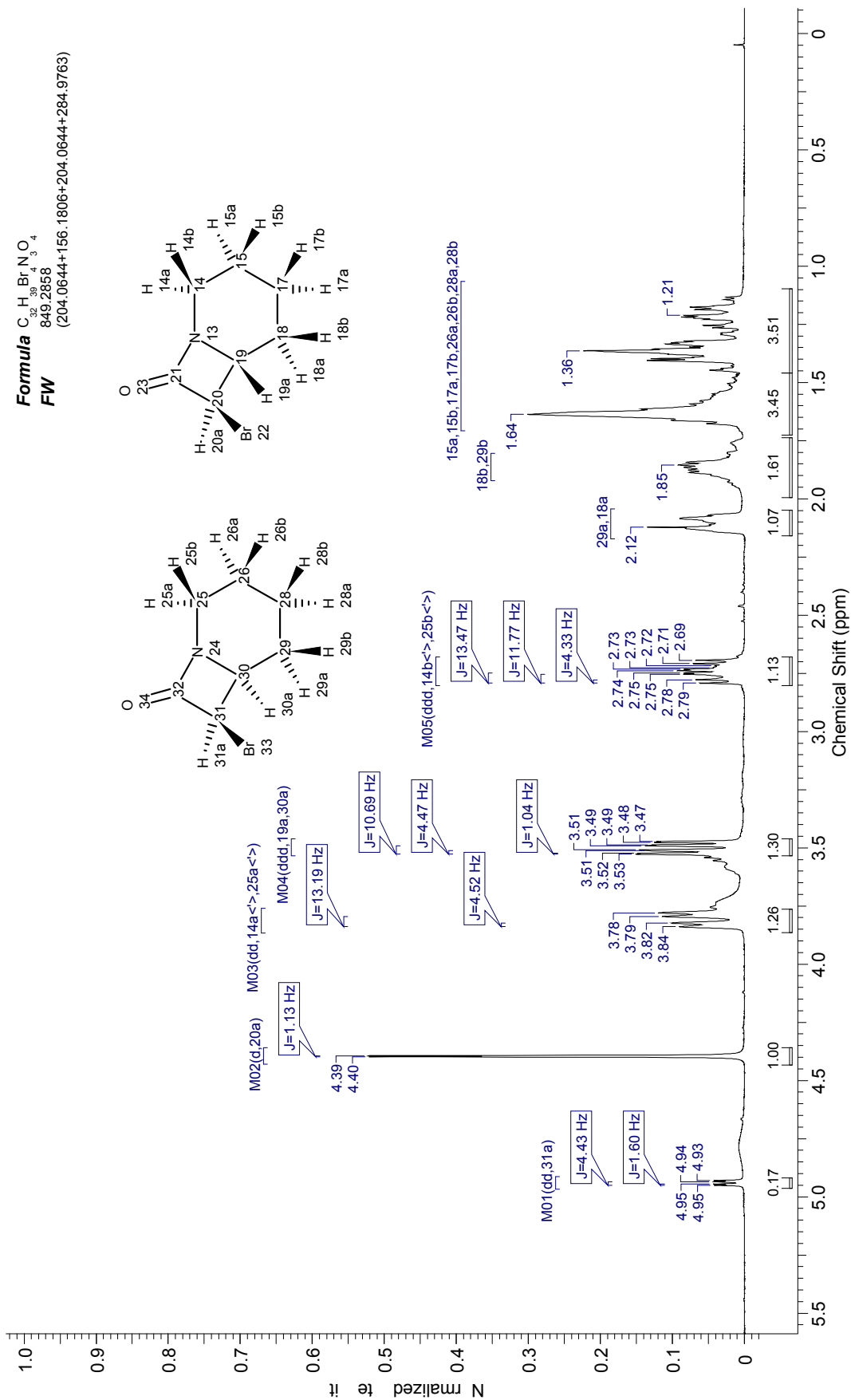
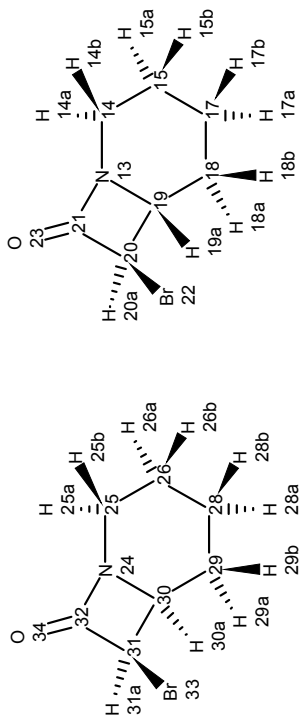
¹H-NMR – Crude; carbene dimer from catalytic decomposition of **2d** with Cu(acac)₂



7-bromo-1-azabicyclo[4.2.0]octan-8-one – ¹H-NMR

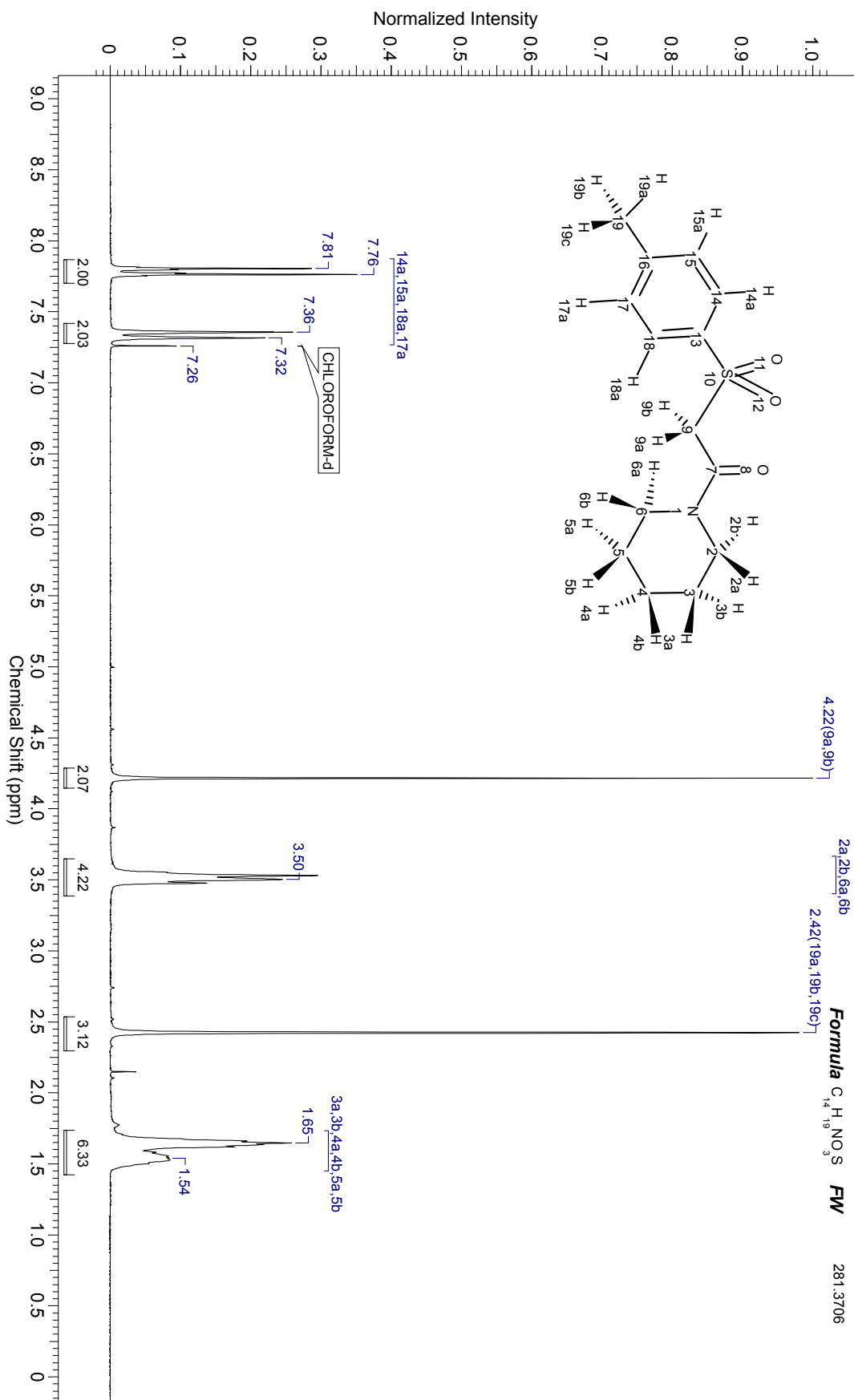
Acquisition Time (sec)	5.3084	Comment	5 mm QNP 1H/15N/13C/31P Z08011/0020	Frequency (MHz)	300.13	Nucleus	1H
Number of Transients	16	Origin	DPX300	Original Points Count	32768	Pulse Sequence	zg30
Receiver Gain	101.60	SW(cyclical) (Hz)	6172.84	Solvent	CHLOROFORM-d	Spectrum Offset (Hz)	1847.3009
Spectrum Type	STANDARD	Sweep Width (Hz)	6172.65	Temperature (degree C)	25.160		

Formula C₈H₁₀BrNO
 849.2858
 (204.0644+156.1806+204.0644+284.9763)
FW



¹H-NMR – 1-(piperidin-1-yl)-2-tosylethanone

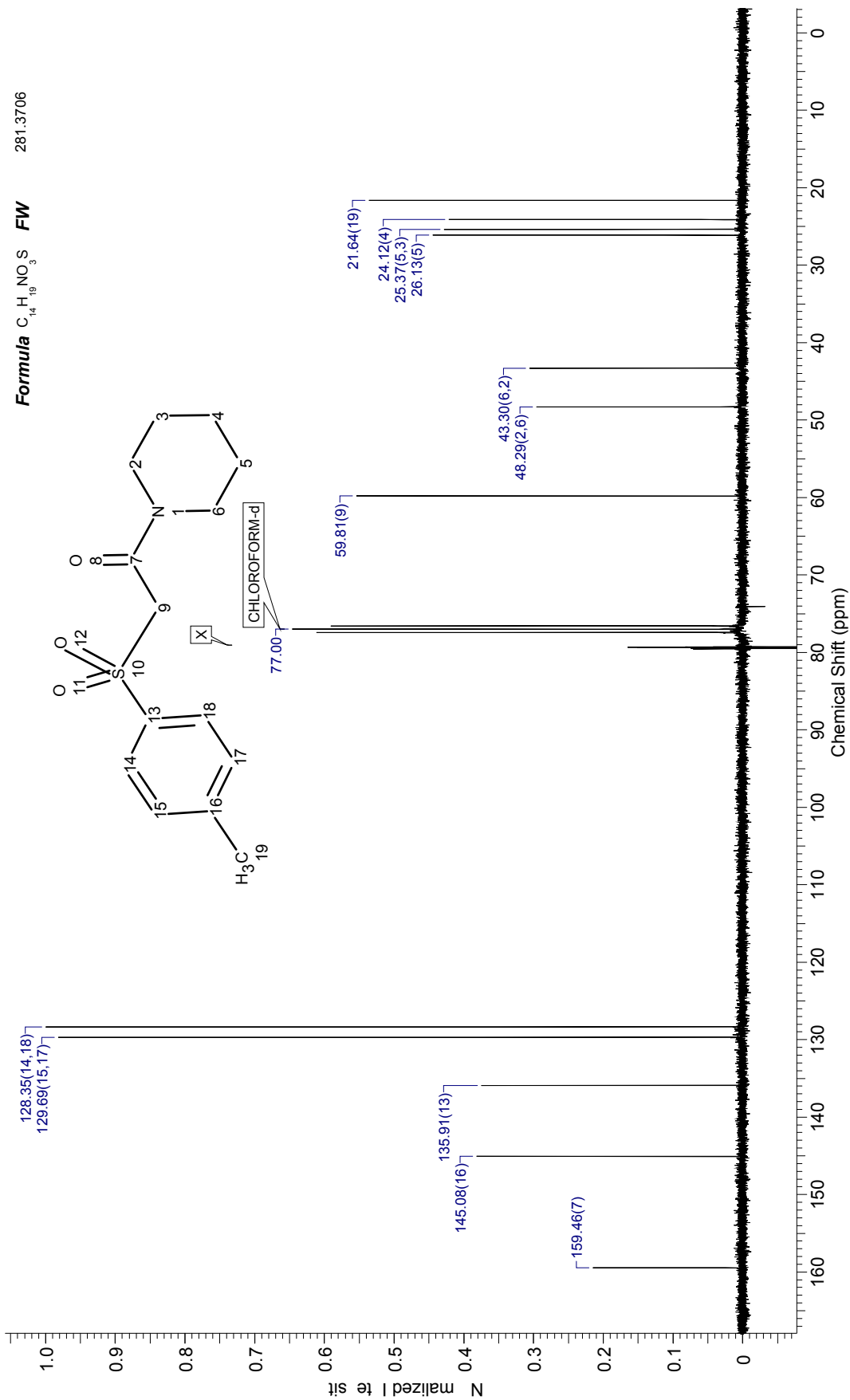
Acquisition Time (sec)	2.9999	Frequency (MHz)	200.13	Nucleus	¹ H	Number of Transients	16	Origin	DPX200
Original Points Count	12417	Points Count	16384	Pulse Sequence	ZG30	Receiver Gain	406.40	SW(Cyclical) (Hz)	4139.07
Solvent	CHLOROFORM-d	Spectrum Offset (Hz)	1227.4727	Temperature (degree C)	25.160	Spectrum Type	STANDARD		
Sweep Width (Hz)	4138.82								



1-(piperidin-1-yl)-2-tosylethanone – ¹³C-NMR

Acquisition Time (sec)	1.8219	Comment	C13CPD CDCI3 D: (UO\laasmuk)\24	Frequency (MHz)	75.48	Nucleus	¹³ C
Number of Transients	1024	Origin	DPX300	Points Count	32768	Pulse Sequence	zgpg30
Receiver Gain	10321.30	SW(cyclical) (Hz)	17985.61	Solvent	CHLOROFORM-d	Spectrum Offset (Hz)	7539.7378
Spectrum Type	STANDARD	Sweep Width (Hz)	17985.06	Temperature (degree C)	25.160		

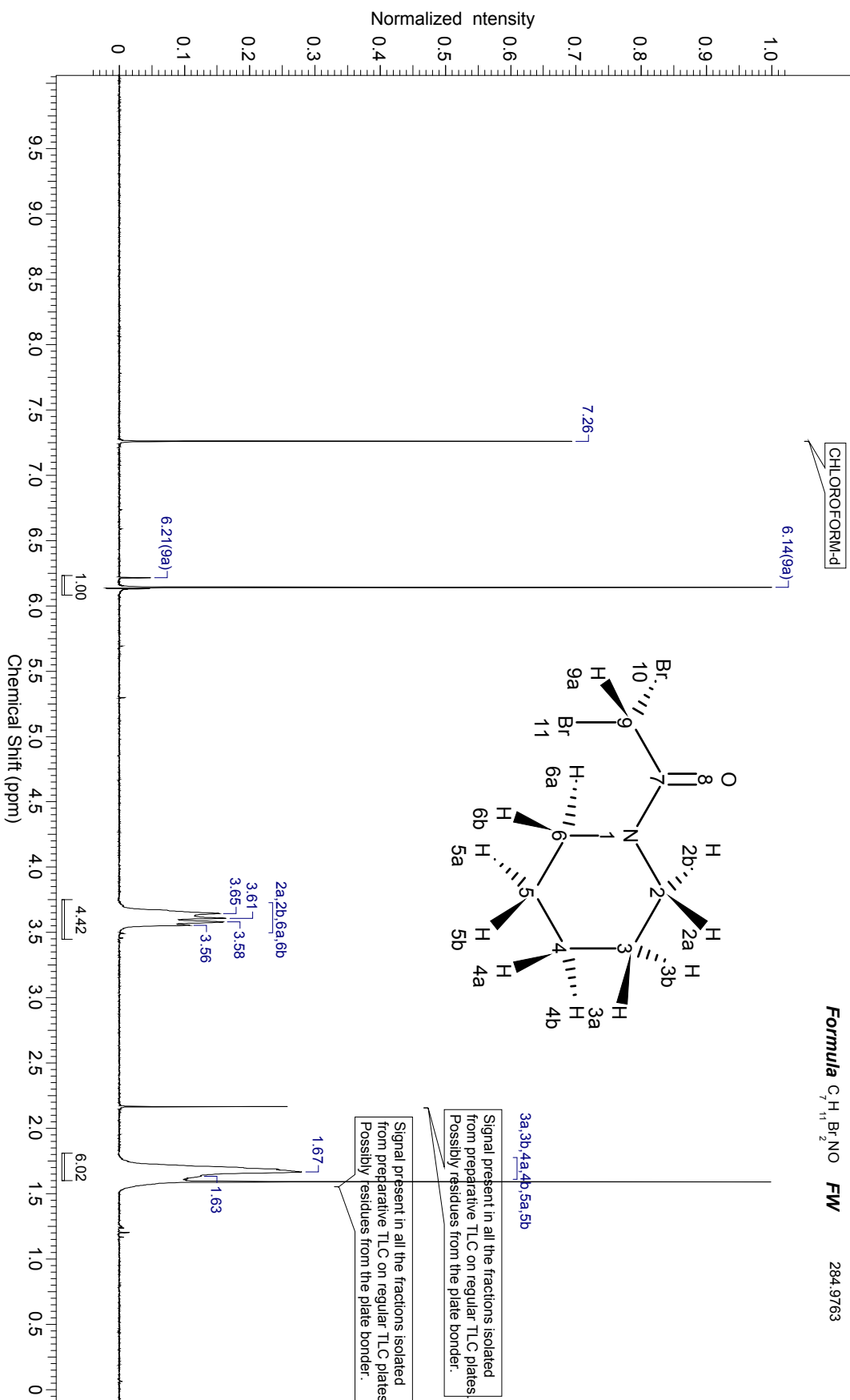
Formula C₁₄H₁₉NO₃ **FW** 281.3706

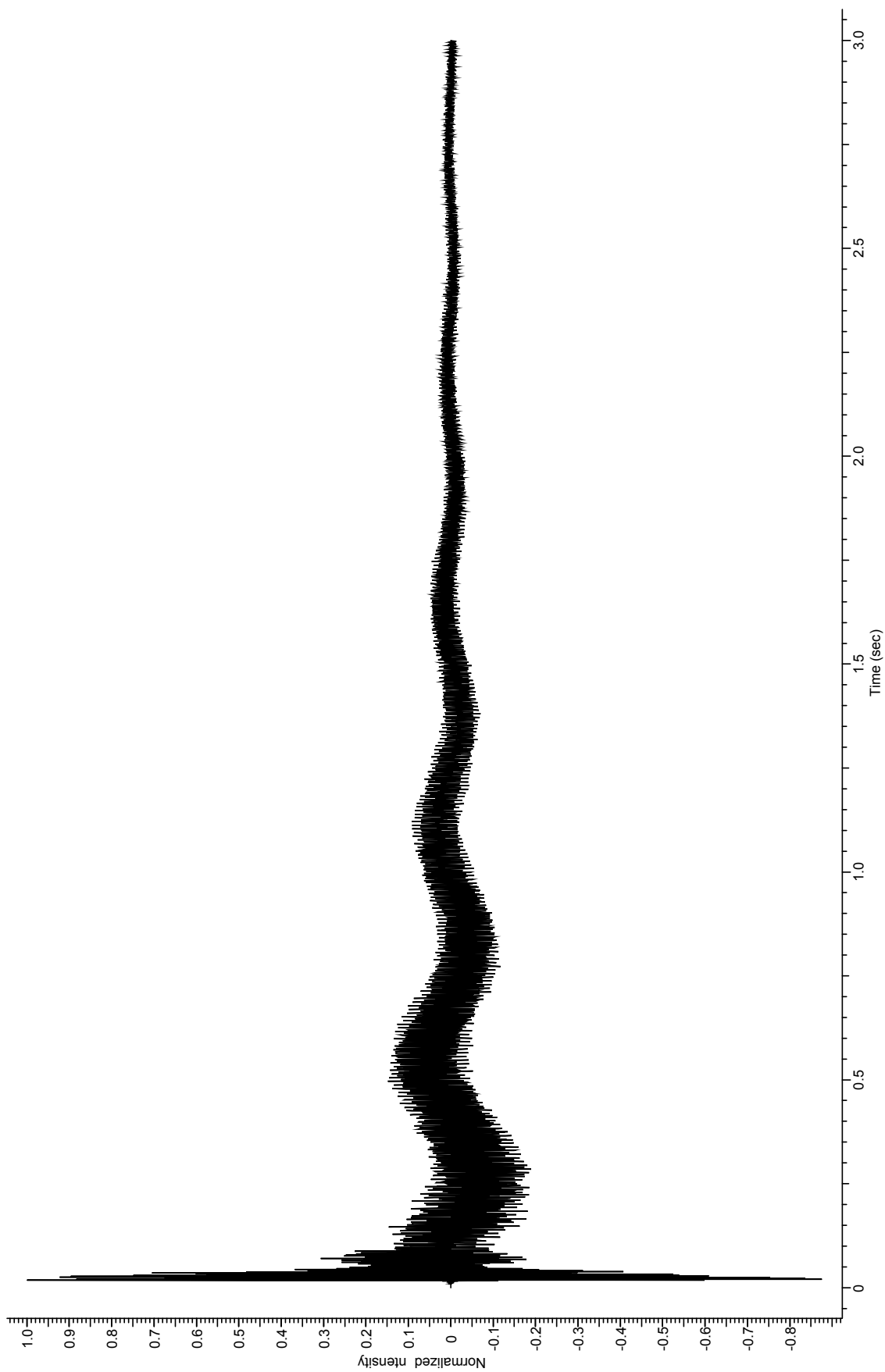


¹H-NMR – 2,2-dibromo-1-(piperidin-1-yl)ethanone

Acquisition Time (sec)	2.9999	Frequency (MHz)	200.13	Nucleus	¹ H	Number of Transients	16	Origin	DPX200
Original Points Count	12417	Points Count	16384	Pulse Sequence	zgpg30	Receiver Gain	2580.30	SW(cyclical) (Hz)	4139.07
Solvent	CHLOROFORM-d	Temperature (degree C)	25.160	Spectrum Offset (Hz)	1227.2200	Spectrum Type	STANDARD		
Sweep Width (Hz)	4138.82								

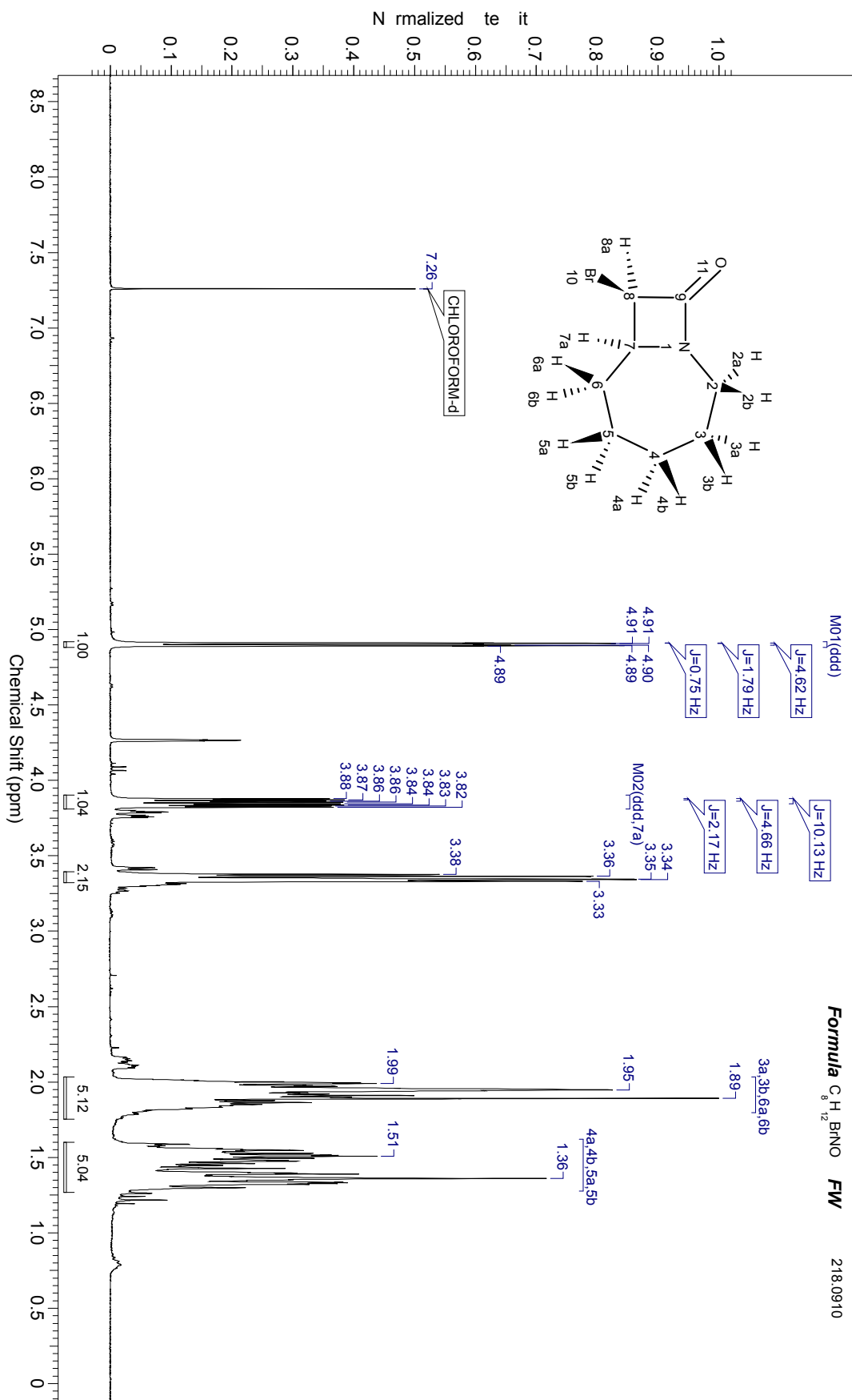
Formula C₇H₁₁Br₂NO FW 284.9763





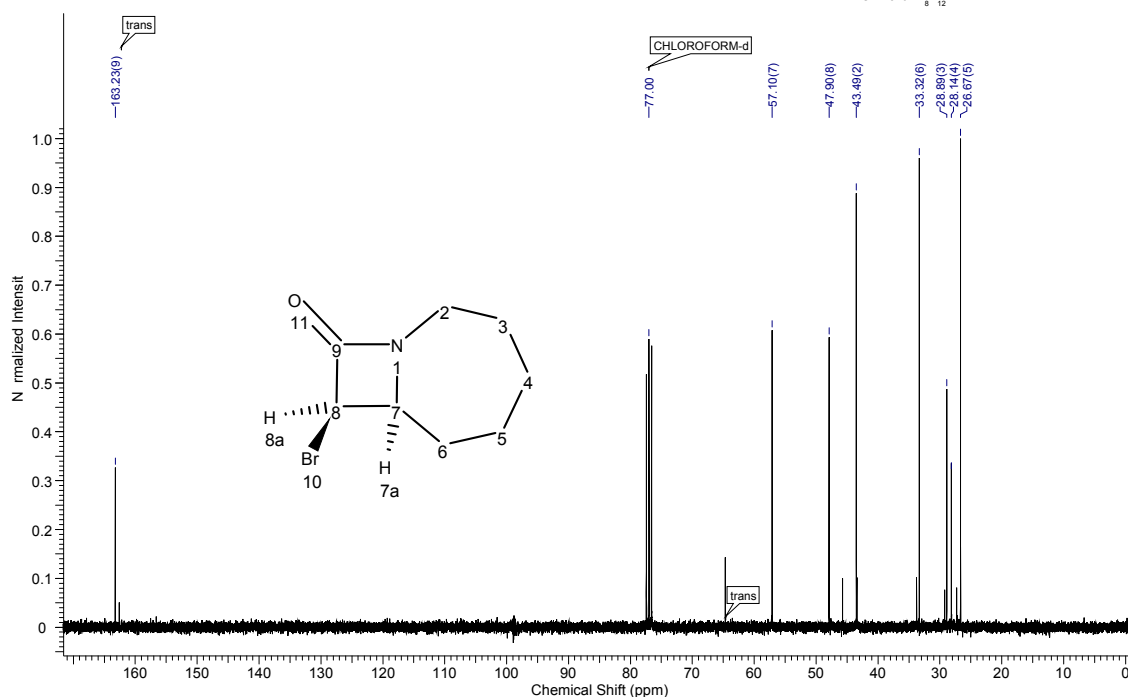
¹H-NMR – cis-8-bromo-1-azabicyclo[5.2.0]nonan-9-one

Acquisition Time (sec)	5.3084	Comment	5 mm QNP 1H/15N/13C/31P Z08011/0020	Frequency (MHz)	300.13	Nucleus	¹ H
Number of Transients	16	Origin	DPX300	Points Count	32768	Pulse Sequence	zg30
Receiver Gain	143.70	SW(cyclical) (Hz)	6172.84	Solvent	CHLOROFORM-d	Spectrum Offset (Hz)	1847.1124
Spectrum Type	STANDARD	Sweep Width (Hz)	6172.65	Temperature (degree C)	26.160		

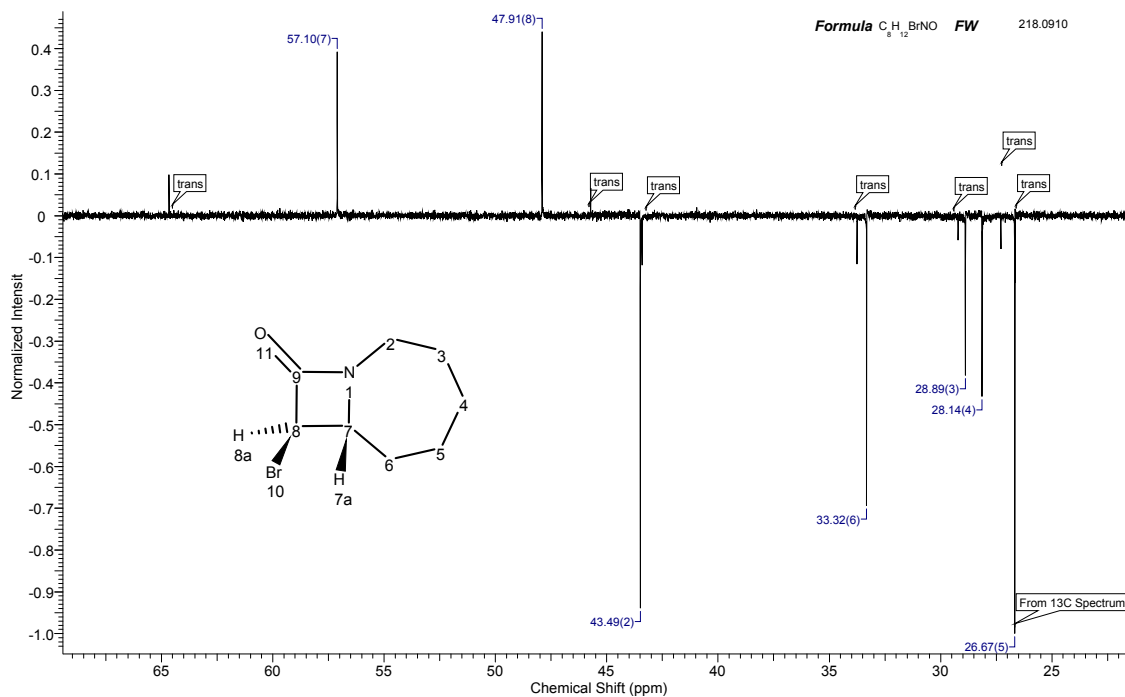


cis-8-bromo-1-azabicyclo[5.2.0]nonan-9-one – ¹³C-NMR & DEPT-135

Acquisition Time (sec)	1.8219	Comment	C13CPD CDC13 D: (UIOlaasmuk) 1	Frequency (MHz)	75.48	Nucleus	13C
Number of Transients	512	Origin	DPX300	Original Points Count	32768	Points Count	32768
Receiver Gain	10321.30	SW(cyclical) (Hz)	17985.61	Solvent	CHLOROFORM-d	Spectrum Offset (Hz)	7538.6401
Spectrum Type	STANDARD	Sweep Width (Hz)	17985.06	Temperature (degree C)	25.160	Formula	C ₈ H ₁₂ BrNO FW 218.0910



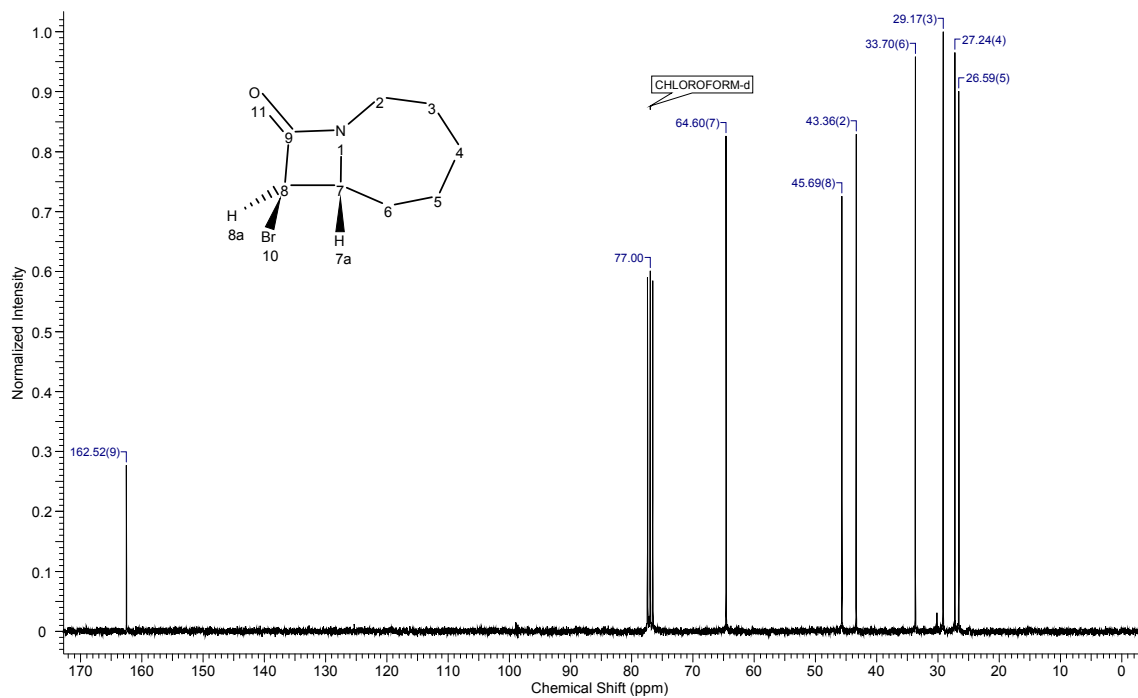
Acquisition Time (sec)	1.8219	Comment	C13DEPT135 CDC13 D: (UIOlaasmuk) 1	Frequency (MHz)	75.48	Nucleus	13C
Number of Transients	256	Origin	DPX300	Original Points Count	32768	Points Count	32768
Receiver Gain	16384.00	SW(cyclical) (Hz)	17985.61	Solvent	CHLOROFORM-d	Spectrum Offset (Hz)	7538.7485
Spectrum Type	DEPT135	Sweep Width (Hz)	17985.06	Temperature (degree C)	25.160	Formula	C ₈ H ₁₂ BrNO FW 218.0910



trans-8-bromo-1-azabicyclo[5.2.0]nonan-9-one – ^{13}C -NMR & DEPT-135

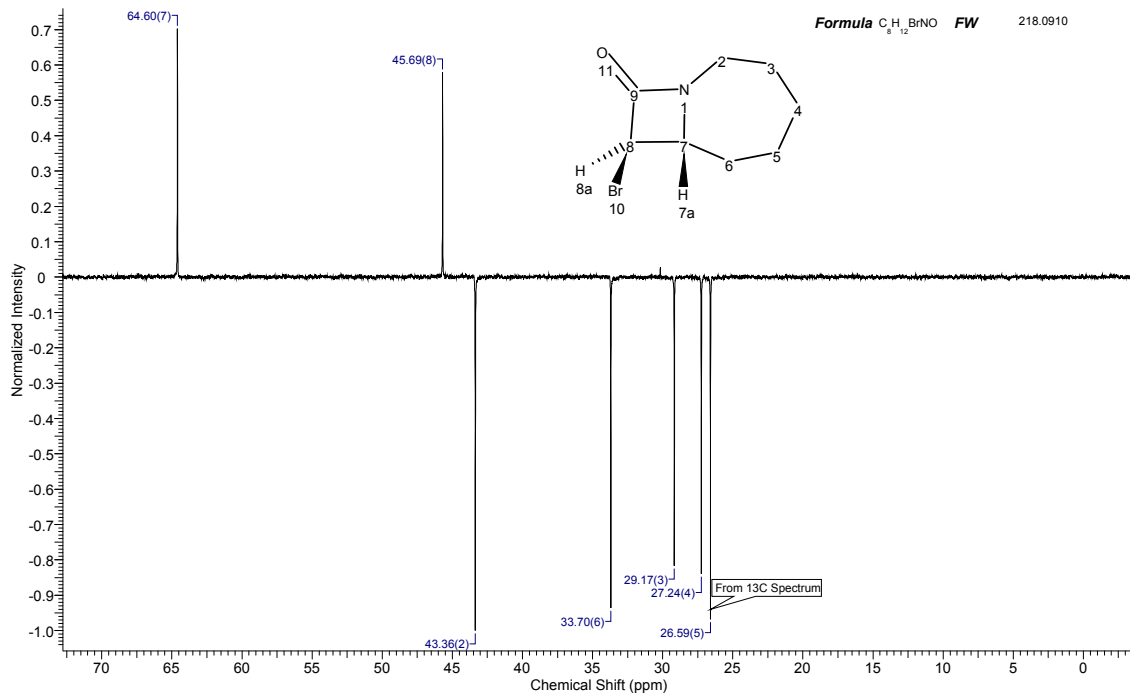
Acquisition Time (sec)	1.8219	Frequency (MHz)	75.48	Nucleus	^{13}C	Origin	Bruker	Original Points Count	32768	Points Count	65536
Pulse Sequence	ZGPG30	Spectrum Offset (Hz)	7536.3345	Spectrum Type	STANDARD			Sweep Width (Hz)	17985.61		

Formula $\text{C}_8\text{H}_{12}\text{BrNO}$ FW 218.0910



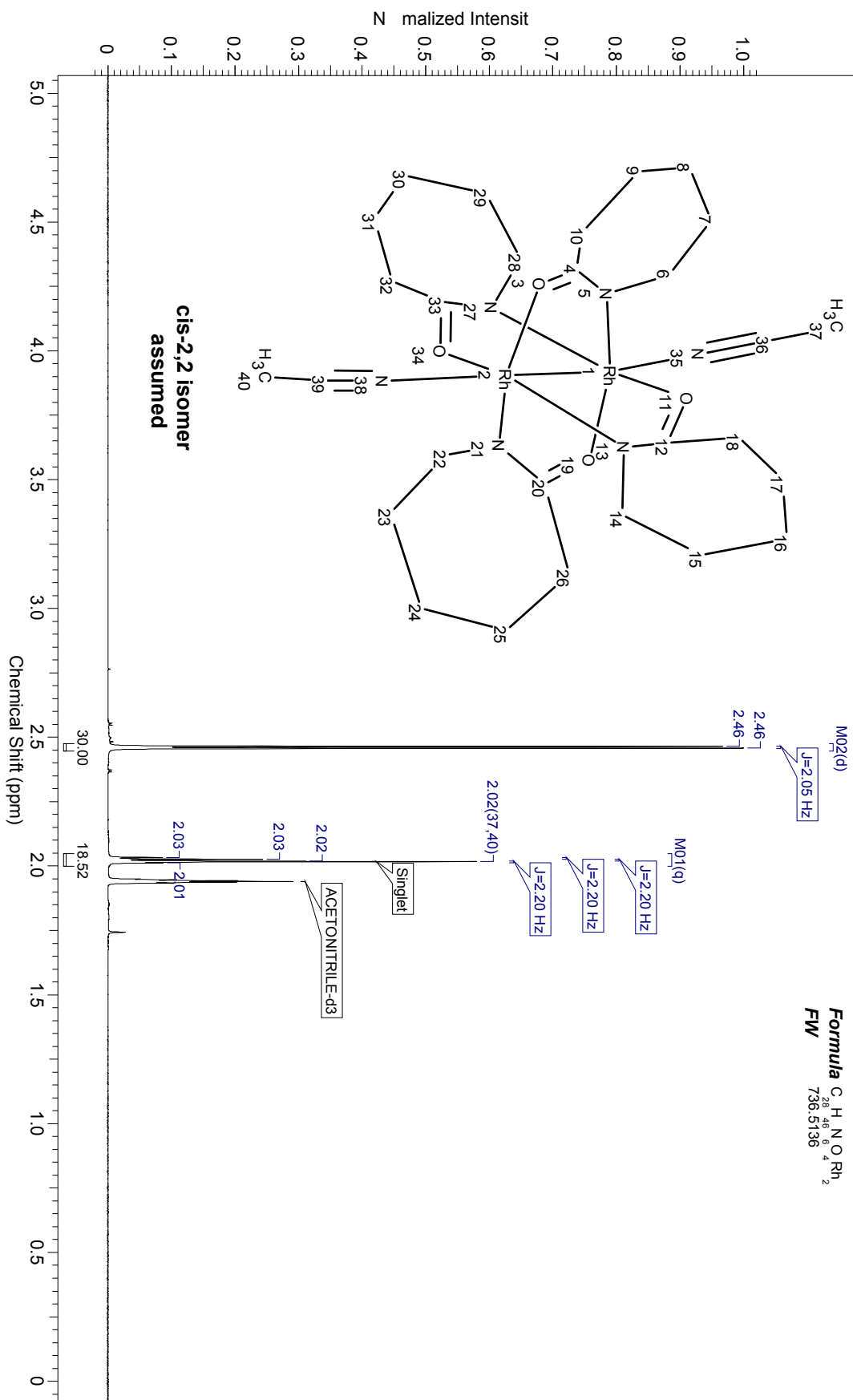
Acquisition Time (sec)	1.8219	Frequency (MHz)	75.48	Nucleus	^{13}C	Origin	Bruker	Original Points Count	32768	Points Count	65536
Pulse Sequence	DEPT135	Spectrum Offset (Hz)	7536.2251	Spectrum Type	DEPT135			Sweep Width (Hz)	17985.61		

Formula $\text{C}_8\text{H}_{12}\text{BrNO}$ FW 218.0910



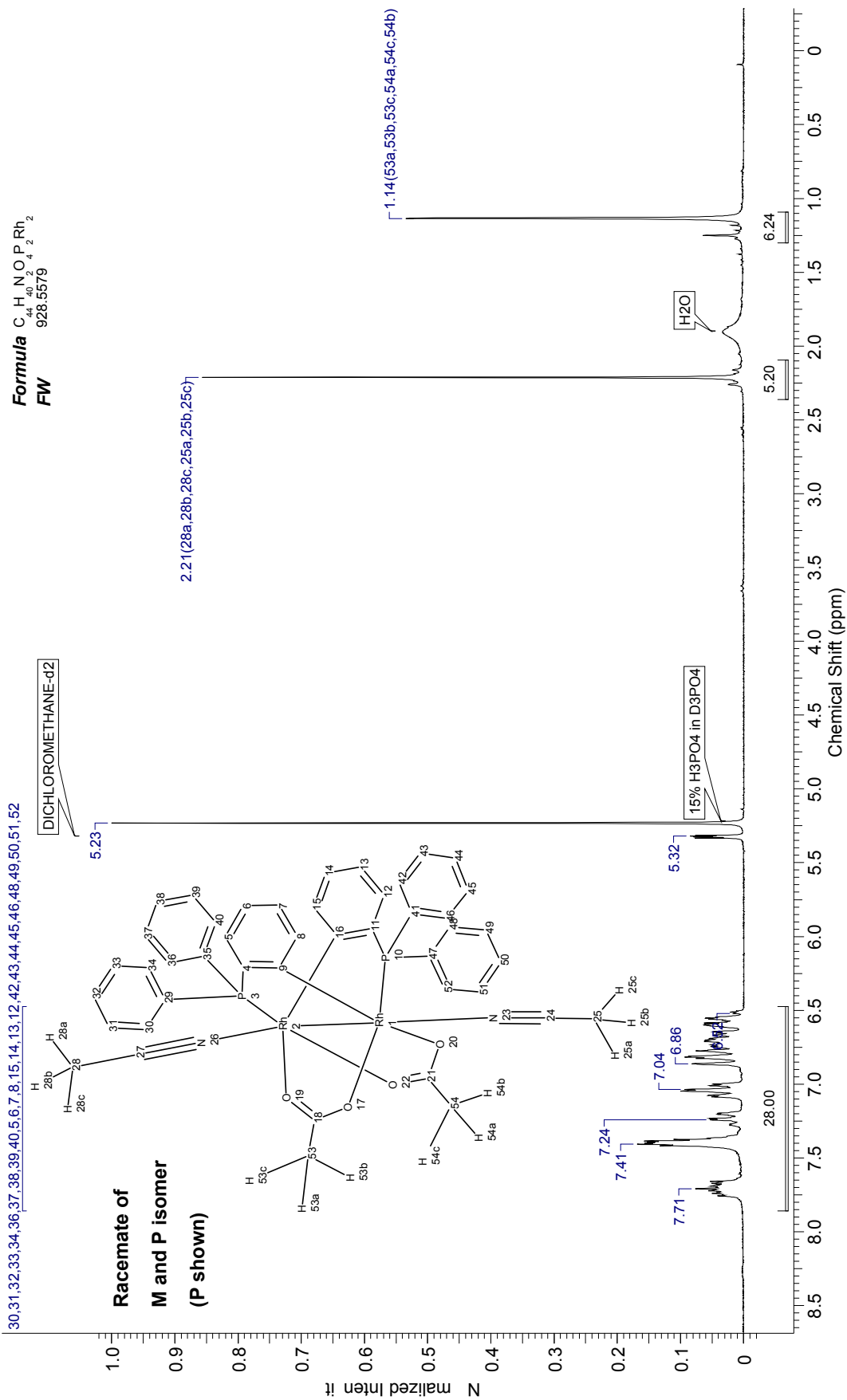
¹H-NMR – cis-2,2-Tetrakis μ-caprolactamato dirhodium(II)

Acquisition Time (sec)	13.6315	Comment	PROTON CD3CN D: {JUD\vaasmuk\21	Frequency (MHz)	300.13	Nucleus	¹ H
Number of Transients	256	Origin	DPX300	Points Count	32768	Pulse Sequence	zg30
Receiver Gain	1625.50	SW(cyclical) (Hz)	2403.85	Solvent	ACETONITRILE-d3	Spectrum Offset (Hz)	1074.3115
Spectrum Type	STANDARD	Sweep Width (Hz)	2403.77	Temperature (degree C)	25.160		

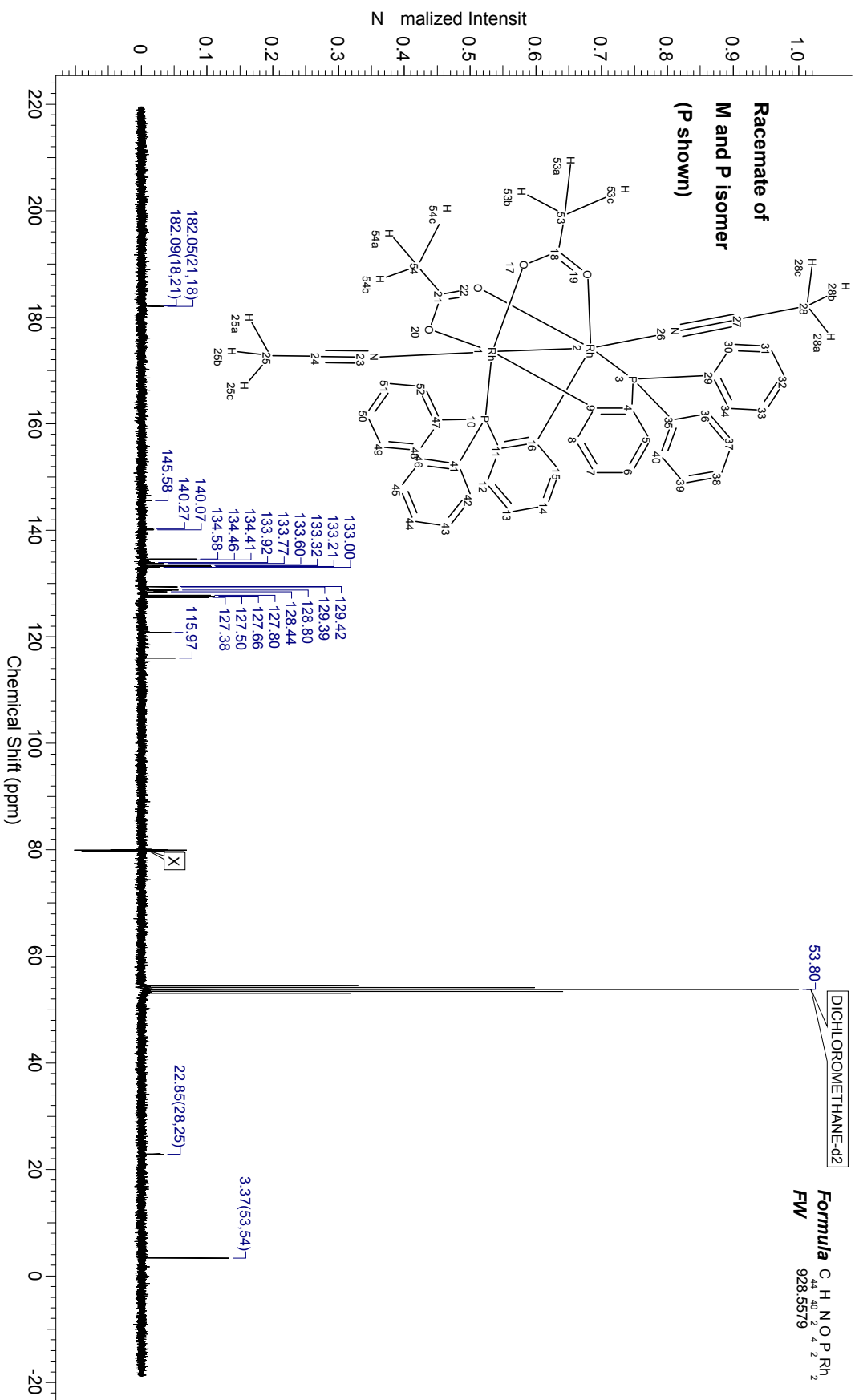


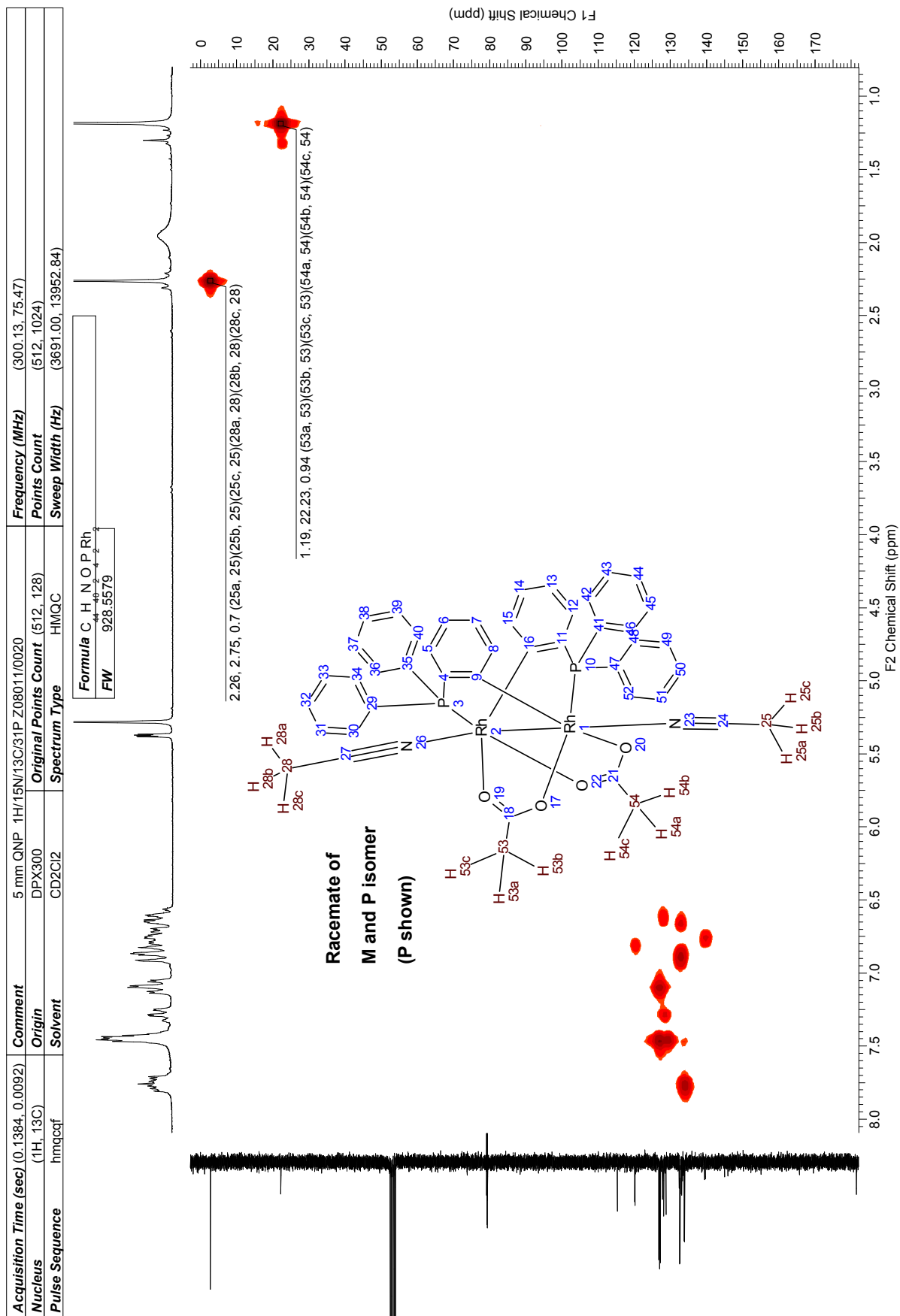
cis-M/P-Rh₂(μ-O₂CCH₃)₂[Ph₂P(C₆H₄)₂(CH₃CN)₂ - ¹H-NMR

Acquisition Time (sec)	2.9999	Frequency (MHz)	200.13	Nucleus	¹ H	Number of Transients	16	Origin	DPX200
Original Points Count	12417	Points Count	16384	Pulse Sequence	ZG30	Receiver Gain	724.10	SW(cyclical) (Hz)	4139.07
Solvent	DICHLOROMETHANE-d ₂		Spectrum Offset (Hz)		1224.4795	Spectrum Type		STANDARD	
Sweep Width (Hz)	4138.82	Temperature (degree C)	25.160						

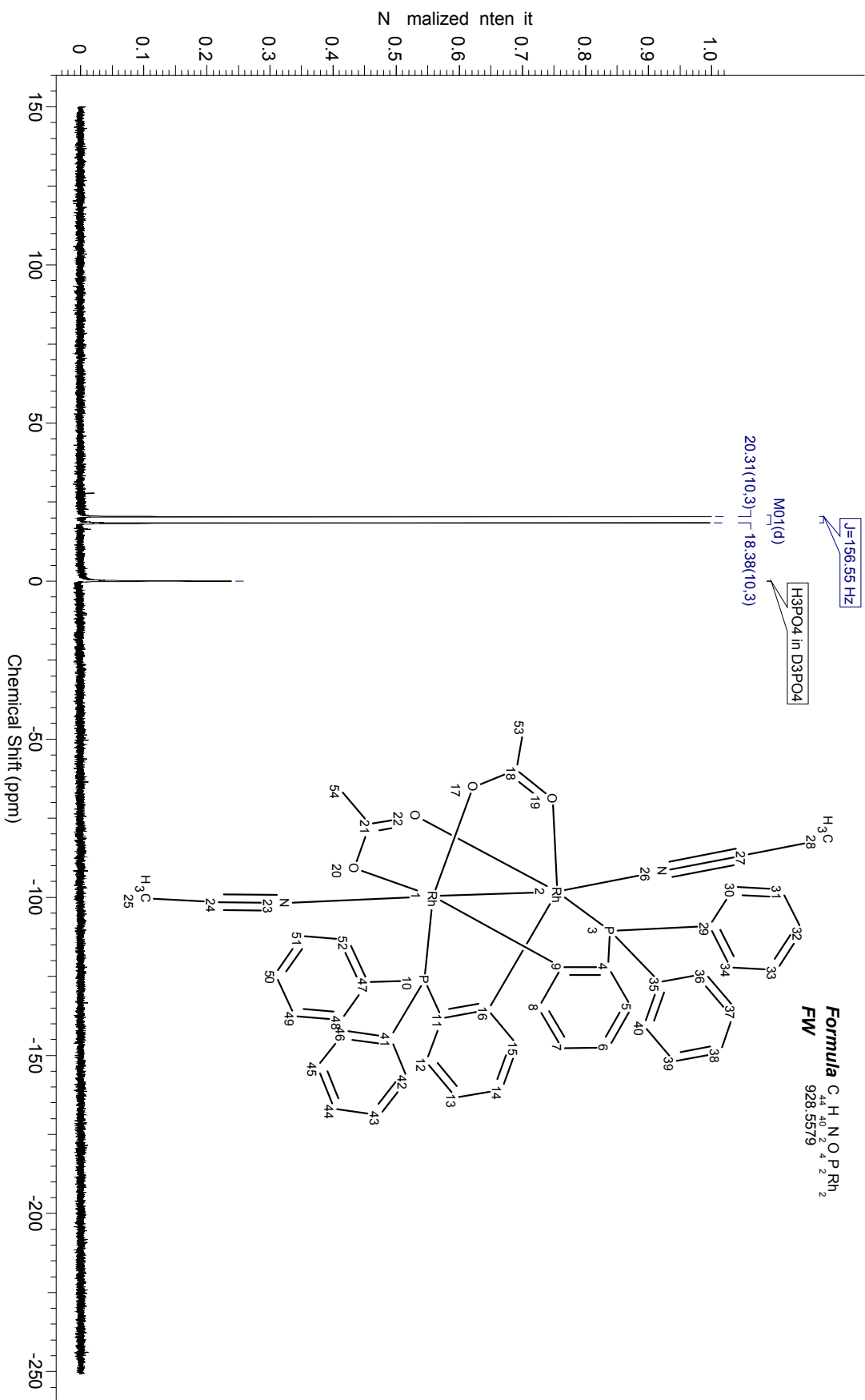


Acquisition Time (sec)	1.8219	Comment	C13CPD OD2C12.D: (UO)vaasmukl 5	Frequency (MHz)	75.48	Nucleus	¹³ C
Number of Transients	1024	Origin	DPX300	Points Count	32768	Pulse Sequence	zpgq30
Receiver Gain	9195.20	SW/cyclical (Hz)	17985.61	Solvent	DICHLOROMETHANE-d2	Spectrum Offset (Hz)	7573.6602
Spectrum Type	STANDARD	Sweep Width (Hz)	17985.06	Temperature (degree C)	25.160		



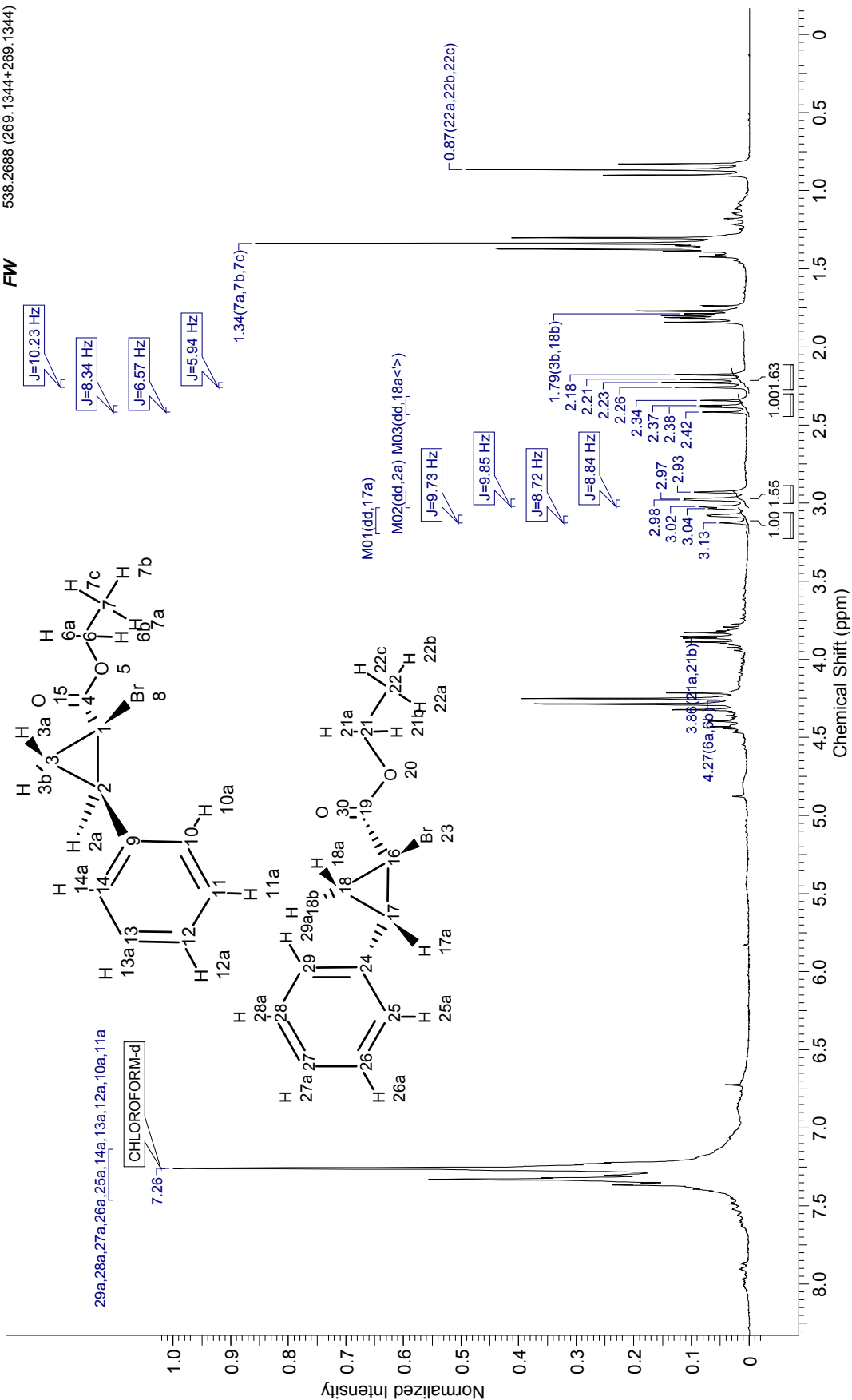


Acquisition Time (sec)	1.0093	Comment	5 mm QNP 1H/13C/31P/19F Z3183/0098	Frequency (MHz)	81.01	Nucleus	31P
Number of Transients	128	Origin	DPX200	Points Count	32768	Pulse Sequence	zgpg30
Receiver Gain	20642.50	SW/cyclical (Hz)	32467.53	Solvent	CHLOROFORM-d	Spectrum Offset (Hz)	-4075.7810
Spectrum Type	STANDARD	Sweep Width (Hz)	32466.54	Temperature (degree C)	25.160		

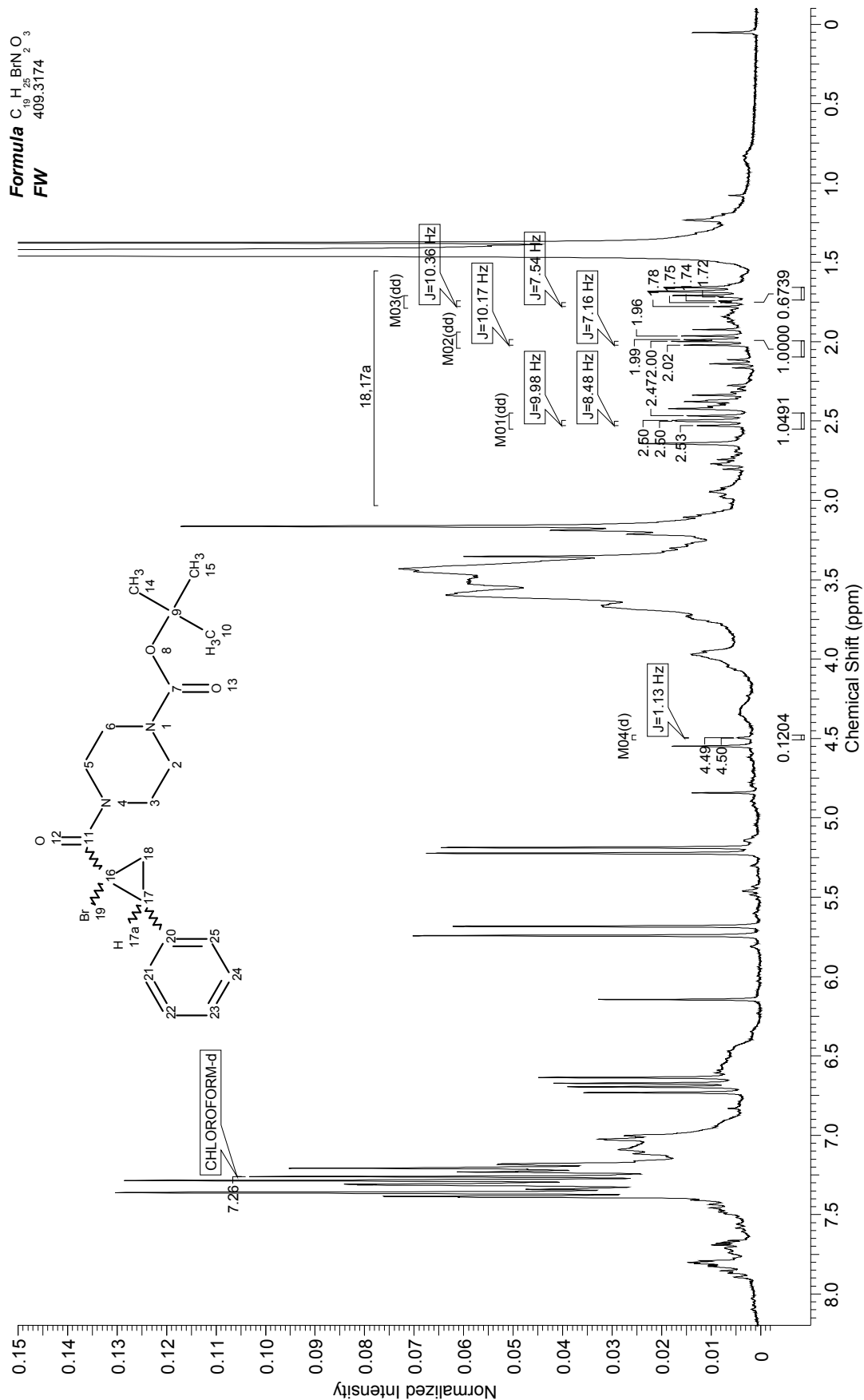


Acquisition Time (sec)	2.9999	Frequency (MHz)	200.13	Nucleus	^1H	Number of Transients	16	Origin	DPX200
Original Points Count	12417	Points Count	16384	Pulse Sequence	zg30	Receiver Gain	114.00	SW(cyclical) (Hz)	4139.07
Solvent	CHLOROFORM-d		Spectrum Offset (Hz)		1226.9673	Spectrum Type		STANDARD	
Sweep Width (Hz)	4138.82	Temperature (degree C)	25.160						

Formula $\text{C}_{24}\text{H}_{26}\text{O}_4$
FW 538.2688 (269.1344+269.1344)



Acquisition Time (sec)	5.3084	Comment	PROTON CDCl3 D: {JIO}aasmuk} 35	Frequency (MHz)	300.13	Nucleus	¹ H
Number of Transients	16	Origin	DPX300	Original Points Count	32768	Pulse Sequence	zg30
Receiver Gain	64.00	SW(cyclical) (Hz)	6172.84	Solvent	CHLOROFORM-d	Spectrum Offset (Hz)	1847.1257
Spectrum Type	STANDARD	Sweep Width (Hz)	6172.65	Temperature (degree C)	25.160		



15. X-ray Diffraction Data

***N,N*-bis(2-diazoacetyl)piperazine - 5c**

Bond precision: C-C = 0.0015 Å Wavelength=0.71073

Cell: a=4.0630(7) b=9.0941(15) c=13.231(2)
 alpha=90 beta=94.453(2) gamma=90

Temperature: 105 K

	Calculated	Reported
Volume	487.40(14)	487.38(14)
Space group	P 21/c	P 21/c
Hall group	-P 2ybc	-P 2ybc
Moiety formula	C8 H10 N6 O2	C8 H10 N6 O2
Sum formula	C8 H10 N6 O2	C8 H10 N6 O2
Mr	222.22	222.22
Dx,g cm-3	1.514	1.514
Z	2	2
Mu (mm-1)	0.115	0.115
F000	232.0	232.0
F000'	232.09	
h,k,lmax	5,12,17	5,11,17
Nref	1263	1190
Tmin,Tmax		
Tmin'		

Correction method= Not given

Data completeness= 0.942 Theta(max)= 28.660

R(reflections)= 0.0345(1013) wR2(reflections)= 0.0900(1190)

S = 1.052 Npar= 73

2-diazo-1-(1,1-dioxido-4-thiomorpholinyl)ethanone - 8c

Bond precision: C-C = 0.0020 Å Wavelength=0.71073

Cell: a=5.2729(3) b=20.1349(11) c=7.8683(4)
alpha=90 beta=95.171(2) gamma=90

Temperature: 105 K

	Calculated	Reported
Volume	831.97(8)	831.97(8)
Space group	P 21/n	P 21/n
Hall group	-P 2yn	-P 2yn
Moiety formula	C6 H9 N3 O3 S	C6 H9 N3 O3 S
Sum formula	C6 H9 N3 O3 S	C6 H9 N3 O3 S
Mr	203.23	203.22
Dx,g cm-3	1.622	1.622
Z	4	4
Mu (mm-1)	0.367	0.367
F000	424.0	424.0
F000'	424.68	
h,k,lmax	8,33,13	8,32,13
Nref	4152	3933
Tmin,Tmax		
Tmin'		

Correction method= Not given

Data completeness= 0.947

Theta(max)= 36.760

R(reflections)= 0.0570(3027)

wR2(reflections)= 0.1688(3933)

S = 1.115

Npar= 128

1,1,3,3-tetramethylguanidine *p*-toluenesulfinate

Bond precision: C-C = 0.0016 Å Wavelength=0.71073

Cell: a=11.0959(8) b=7.4038(5) c=17.1944(13)
alpha=90 beta=92.115(1) gamma=90

Temperature: 105 K

	Calculated	Reported
Volume	1411.59(18)	1411.59(18)
Space group	P 21/c	P 21/c
Hall group	-P 2ybc	-P 2ybc
Moiety formula	C5 H14 N3, C7 H7 O2 S	C5 H14 N3, C7 H7 O2 S
Sum formula	C12 H21 N3 O2 S	C12 H21 N3 O2 S
Mr	271.39	271.38
Dx, g cm ⁻³	1.277	1.277
Z	4	4
Mu (mm ⁻¹)	0.229	0.229
F000	584.0	584.0
F000'	584.70	
h,k,lmax	14,9,22	14,9,22
Nref	3492	3375
Tmin,Tmax		
Tmin'		
Correction method	Not given	

Data completeness= 0.966

Theta(max)= 28.250

R(reflections)= 0.0302(3026)

wR2(reflections)= 0.0852(3375)

S = 1.047

Npar= 174

1,1,3,3-tetramethylguanidine *p*-toluenesulfonate

Bond precision: C-C = 0.0066 Å Wavelength=0.71073

Cell: a=11.185(3) b=7.648(2) c=17.415(5)
alpha=90 beta=93.169(4) gamma=90

Temperature: 296 K

	Calculated	Reported
Volume	1487.5(7)	1487.5(8)
Space group	P 21/c	P 21/c
Hall group	-P 2ybc	-P 2ybc
Moiety formula	C5 H14 N3, C7 H7 O3 S	C5 H14 N3, C7 H7 O3 S
Sum formula	C12 H21 N3 O3 S	C12 H21 N3 O3 S
Mr	287.39	287.38
Dx, g cm ⁻³	1.283	1.283
Z	4	4
Mu (mm ⁻¹)	0.226	0.226
F000	616.0	616.0
F000'	616.74	
h,k,lmax	13,9,20	13,9,20
Nref	2624	2615
Tmin,Tmax		
Tmin'		
Correction method=	Not given	

Data completeness= 0.997

Theta(max)= 25.040

R(reflections)= 0.0669(1587)

wR2(reflections)= 0.1889(2615)

S = 1.087

Npar= 186

Acta Crystallographica Section E

Structure Reports

Online

ISSN 1600-5368

***tert*-Butyl 4-(2-diazoacetyl)piperazine-1-carboxylate**

Åsmund Kaupang, Carl Henrik Görbitz* and Tore Hansen

Department of Chemistry, University of Oslo, PO Box 1033 Blindern, N-0315 Oslo, Norway

Correspondence e-mail: c.h.gorbitz@kjemi.uio.no

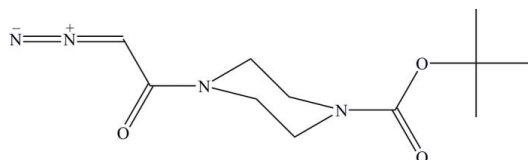
Received 22 April 2010; accepted 3 May 2010

Key indicators: single-crystal X-ray study; $T = 105$ K; mean $\sigma(\text{C}-\text{C}) = 0.002$ Å; R factor = 0.038; wR factor = 0.103; data-to-parameter ratio = 15.9.

The title crystal structure, $\text{C}_{11}\text{H}_{18}\text{N}_4\text{O}_3$, is the first diazoacetamide in which the diazoacetyl group is attached to an N atom. The piperazine ring is in a chair form and hence the molecule has an extended conformation. Both ring N atoms are bonded in an essentially planar configuration with the sum of the C–N–C angles being 359.8 (2) and 357.7 (2)°. In the crystal structure, the O atom of the diazoacetyl group accepts two H atoms from C–H donors, thus generating chains of weak hydrogen-bonded $R_2^1(7)$ rings.

Related literature

For the only other reported synthesis of a diazoacetamide in the Chemical Abstracts Service (CAS, American Chemical Society, 2008) with a 1,4-diaza six-membered ring, see: Mickelson *et al.* (1996). For other diazoacetamides, see: Ouhia *et al.* (1993). For related structures, see: Fenlon *et al.* (2007); Wang *et al.* (2006); Miller *et al.* (1991). For synthetic details, see: Kaupang (2010); Toma *et al.* (2007). For hydrogen-bond graph-set notation, see: Bernstein *et al.* (1995). For a description of the Cambridge Structural Database, see: Allen (2002).



Experimental

Crystal data

 $\text{C}_{11}\text{H}_{18}\text{N}_4\text{O}_3$
 $M_r = 254.29$

 Monoclinic, $P2_1/c$
 $a = 14.654$ (10) Å

 $b = 10.548$ (7) Å
 $c = 8.553$ (6) Å
 $\beta = 91.122$ (6)°
 $V = 1321.8$ (15) Å³
 $Z = 4$

 Mo $K\alpha$ radiation
 $\mu = 0.10$ mm⁻¹
 $T = 105$ K
 $0.55 \times 0.42 \times 0.08$ mm

Data collection

 Bruker APEXII CCD
 diffractometer
 Absorption correction: multi-scan
 (SADABS; Bruker, 2007)
 $T_{\min} = 0.870$, $T_{\max} = 0.992$

 7308 measured reflections
 2692 independent reflections
 2111 reflections with $I > 2\sigma(I)$
 $R_{\text{int}} = 0.041$

Refinement

 $R[F^2 > 2\sigma(F^2)] = 0.038$
 $wR(F^2) = 0.103$
 $S = 1.03$
 2692 reflections
 169 parameters

 H atoms treated by a mixture of
 independent and constrained
 refinement
 $\Delta\rho_{\max} = 0.17$ e Å⁻³
 $\Delta\rho_{\min} = -0.23$ e Å⁻³

Table 1

Hydrogen-bond geometry (Å, °).

$D-H\cdots A$	$D-H$	$H\cdots A$	$D\cdots A$	$D-H\cdots A$
$\text{C1}-\text{H1}\cdots\text{O1}^i$	0.946 (17)	2.313 (18)	3.250 (3)	170.6 (14)
$\text{C3}-\text{H32}\cdots\text{O1}^i$	0.99	2.36	3.327 (3)	164

Symmetry code: (i) $-x, y + \frac{1}{2}, -z + \frac{1}{2}$.

Data collection: APEX2 (Bruker, 2007); cell refinement: SAINT-Plus (Bruker, 2007); data reduction: SAINT-Plus; program(s) used to solve structure: SHELXTL (Sheldrick, 2008); program(s) used to refine structure: SHELXTL; molecular graphics: SHELXTL; software used to prepare material for publication: SHELXTL.

Supplementary data and figures for this paper are available from the IUCr electronic archives (Reference: LH5033).

References

- Allen, F. H. (2002). *Acta Cryst.* **B58**, 380–388.
 American Chemical Society (2008). Chemical Abstracts Service, American Chemical Society, Columbus, OH, USA; accessed Apr 27, 2010.
 Bernstein, J., Davis, R. E., Shimon, L. & Chang, N.-L. (1995). *Angew. Chem. Int. Ed. Engl.* **34**, 1555–1573.
 Bruker (2007). APEX2, SAINT-Plus and SADABS. Bruker AXS Inc., Madison, Wisconsin, USA.
 Fenlon, T. W., Schwaebisch, D., Mayweg, A. V. W., Lee, V., Adlington, R. M. & Baldwin, J. E. (2007). *Synlett*, pp. 2679–2682.
 Kaupang, Å. (2010). *Masters thesis, University of Oslo, Norway. Available at* <http://www.duo.uio.no/>.
 Mickelson, J. W., Jacobsen, E. J., Carter, D. B., Im, H. K., Im, W. B., Schreur, P. J. K. D., Sethy, V. H., Tang, A. H., McGee, J. E. & Petke, J. D. (1996). *J. Med. Chem.* **39**, 4654–4666.
 Miller, R. D., Theis, W., Heilig, G. & Kirchmeyer, S. (1991). *J. Org. Chem.* **56**, 1453–1463.
 Ouhia, A., Rene, L., Guilhem, J., Pascard, C. & Badet, B. (1993). *J. Org. Chem.* **58**, 1641–1642.
 Sheldrick, G. M. (2008). *Acta Cryst.* **A64**, 112–122.
 Toma, T., Shimokawa, J. & Fukuyama, T. (2007). *Org. Lett.* **9**, 3195–3197.
 Wang, J., Zeng, T., Li, M.-L., Duan, E.-H. & Li, J.-S. (2006). *Acta Cryst.* **E62**, o2912–o2913.

supplementary materials

Acta Cryst. (2010). E66, o1299 [doi:10.1107/S1600536810016211]

tert-Butyl 4-(2-diazoacetyl)piperazine-1-carboxylate

Å. Kaupang, C. H. Görbitz and T. Hansen

Comment

The tert-butyl 4-(2-diazoacetyl)piperazine-1-carboxylate (I) was prepared as part of a series of diazoacetamides, to be used in intramolecular C—H insertion reactions (Kaupang, 2010). It was synthesized from tert-butyl 4-(2-bromoacetyl)piperazine-1-carboxylate by a slight modification of the procedure reported by Toma *et al.* (2007), employing 1,1,3,3-tetramethylguanidine as the base instead of 1,8-diazabicyclo[5.4.0]undec-7-ene.

Diffraction data were first collected at ambient temperature, yielding a structure with a massively disordered six-membered ring. At 105 K the ring is completely ordered in a well defined chair conformation, Fig. 1.

The diazoacetyl moiety is not an uncommon functional group in organic molecules, however only 15 occurrences were found in the Cambridge Structural Database (Version 5.31 of November 2009; Allen, 2002), and none where, as here, the group is attached to a N atom. In only two structures the group sits on a non-aromatic ring (Miller *et al.*, 1991; Fenlon *et al.*, 2007).

In a model molecule like trimethylamine the N atom is located about 0.45 Å above the plane defined by the three C atoms. In the structure of (I) N3 is 0.125 (2) Å above the plane defined by C2, C3 and C4, while N4 is only 0.039 (2) Å above the plane defined by C5, C6 and C7, which essentially shows a planar configuration (sum of C—N—C angles 359.8 (2) °). This is due to the double bond character of the amidic N3—C2 and N4—C7 bonds measuring 1.3515 (18) and 1.3483 (18) Å, respectively. An example of a related structure is 1,4-di(chloroacetyl)piperazine (Wang *et al.*, 2006).

In the crystal structure, the O atom of the diazoacetyl group accepts two H atoms from C—H donors, thus generating chains of hydrogen-bonded R¹₂(7) rings (Bernstein *et al.*, 1995).

Experimental

A 2.5 ml vial containing tert-butyl 4-(2-diazoacetyl)piperazine-1-carboxylate (10.8 mg) and dichloromethane (1000 ml) was capped and a pinhole (0.5 mm) was made in the cap to allow for vapour diffusion of solvents. This vial was placed inside a 25 ml vial containing n-pentane (8 ml) that was subsequently capped and stored in the dark at ambient temperature for approximately 48 hours, affording bright yellow plate-shaped crystals.

Refinement

Coordinates were refined for H1 (bonded to C1), which is involved in the shortest intermolecular interaction. Other H atoms were positioned with idealized geometry and fixed C—H distances set to 0.98 Å (methyl) or 0.99 Å (methylene). Free rotation was permitted for the methyl groups. U_{iso} values were 1.2U_{eq} of the carrier atom or 1.5U_{eq} for methyl groups.

supplementary materials

Figures

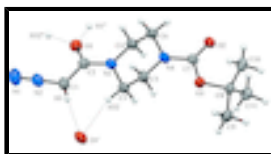


Fig. 1. The asymmetric unit of (I), with atomic numbering indicated, together with selected atoms of neighbouring molecules connected by weak hydrogen bonds shown as dotted lines (see Table 1, symmetry operations are $-x, 1/2+y, 1/2-z$ for O', $-x, -1/2+y, 1/2-z$ for H1'' and H32''). Displacement ellipsoids are shown at the 50% probability level with H atoms as spheres of arbitrary size.

tert-Butyl 4-(2-diazoacetyl)piperazine-1-carboxylate

Crystal data

$C_{11}H_{18}N_4O_3$

$M_r = 254.29$

Monoclinic, $P2_1/c$

$a = 14.654$ (10) Å

$b = 10.548$ (7) Å

$c = 8.553$ (6) Å

$\beta = 91.122$ (6)°

$V = 1321.8$ (15) Å³

$Z = 4$

$F(000) = 544$

$D_x = 1.278$ Mg m⁻³

Mo $K\alpha$ radiation, $\lambda = 0.71073$ Å

Cell parameters from 2404 reflections

$\theta = 2.4$ – 26.4 °

$\mu = 0.10$ mm⁻¹

$T = 105$ K

Plate, yellow

$0.55 \times 0.42 \times 0.08$ mm

Data collection

Bruker APEXII CCD
diffractometer

Radiation source: fine-focus sealed tube
graphite

Detector resolution: 8.3 pixels mm⁻¹

Three sets of frames each taken over 0.3° ω rotation
with 20 s exposure time. Detector set at $2\theta = 26^\circ$,
crystal-to-detector distance 6.00 cm. scans

Absorption correction: multi-scan
(SADABS; Bruker, 2007)

$T_{\min} = 0.870$, $T_{\max} = 0.992$

7308 measured reflections

2692 independent reflections

2111 reflections with $I > 2\sigma(I)$

$R_{\text{int}} = 0.041$

$\theta_{\max} = 26.4^\circ$, $\theta_{\min} = 2.4^\circ$

$h = -17 \rightarrow 18$

$k = -10 \rightarrow 13$

$l = -10 \rightarrow 10$

Refinement

Refinement on F^2

Least-squares matrix: full

$R[F^2 > 2\sigma(F^2)] = 0.038$

$wR(F^2) = 0.103$

$S = 1.03$

Primary atom site location: structure-invariant direct
methods

Secondary atom site location: difference Fourier map

Hydrogen site location: inferred from neighbouring
sites

H atoms treated by a mixture of independent and
constrained refinement

$w = 1/[\sigma^2(F_o^2) + (0.0463P)^2 + 0.1671P]$

where $P = (F_o^2 + 2F_c^2)/3$

2692 reflections	$(\Delta/\sigma)_{\max} = 0.001$
169 parameters	$\Delta\rho_{\max} = 0.17 \text{ e } \text{\AA}^{-3}$
0 restraints	$\Delta\rho_{\min} = -0.22 \text{ e } \text{\AA}^{-3}$

Special details

Experimental. Crystallized from dichloromethane and n-pentane.

Geometry. All esds (except the esd in the dihedral angle between two l.s. planes) are estimated using the full covariance matrix. The cell esds are taken into account individually in the estimation of esds in distances, angles and torsion angles; correlations between esds in cell parameters are only used when they are defined by crystal symmetry. An approximate (isotropic) treatment of cell esds is used for estimating esds involving l.s. planes.

Refinement. Refinement of F^2 against ALL reflections.

Fractional atomic coordinates and isotropic or equivalent isotropic displacement parameters (\AA^2)

	<i>x</i>	<i>y</i>	<i>z</i>	$U_{\text{iso}}^*/U_{\text{eq}}$
O1	0.02567 (7)	0.20344 (9)	0.19361 (12)	0.0353 (3)
O2	0.38950 (6)	0.35633 (9)	0.62995 (11)	0.0296 (2)
O3	0.33388 (6)	0.55670 (8)	0.64091 (11)	0.0294 (2)
N1	-0.14125 (10)	0.34028 (15)	-0.00383 (19)	0.0562 (4)
N2	-0.08817 (8)	0.37402 (12)	0.08229 (16)	0.0377 (3)
N3	0.10933 (7)	0.34931 (10)	0.32642 (14)	0.0293 (3)
N4	0.27460 (8)	0.42179 (11)	0.46913 (15)	0.0350 (3)
C1	-0.02502 (10)	0.41229 (14)	0.18201 (17)	0.0324 (3)
H1	-0.0254 (10)	0.4999 (17)	0.2058 (19)	0.039*
C2	0.03721 (9)	0.31392 (13)	0.23569 (16)	0.0276 (3)
C3	0.11676 (9)	0.47080 (12)	0.40835 (18)	0.0301 (3)
H31	0.0971	0.4604	0.5177	0.036*
H32	0.0760	0.5337	0.3568	0.036*
C4	0.17261 (10)	0.25284 (13)	0.38538 (18)	0.0317 (3)
H41	0.1681	0.1763	0.3188	0.038*
H42	0.1561	0.2287	0.4931	0.038*
C5	0.21342 (9)	0.51824 (13)	0.40729 (18)	0.0322 (3)
H51	0.2304	0.5397	0.2990	0.039*
H52	0.2188	0.5960	0.4717	0.039*
C6	0.26896 (10)	0.30251 (13)	0.38538 (19)	0.0349 (4)
H61	0.3104	0.2399	0.4357	0.042*
H62	0.2886	0.3150	0.2763	0.042*
C7	0.33775 (9)	0.43825 (12)	0.58409 (16)	0.0259 (3)
C8	0.39795 (9)	0.59837 (13)	0.76528 (15)	0.0275 (3)
C9	0.36780 (11)	0.73381 (14)	0.79087 (18)	0.0387 (4)
H91	0.3721	0.7811	0.6927	0.058*
H92	0.4073	0.7734	0.8707	0.058*
H93	0.3045	0.7346	0.8258	0.058*
C10	0.49473 (10)	0.59327 (15)	0.70952 (17)	0.0354 (4)
H101	0.4989	0.6386	0.6099	0.053*
H102	0.5129	0.5047	0.6951	0.053*

supplementary materials

H103	0.5354	0.6333	0.7873	0.053*
C11	0.38403 (10)	0.52052 (14)	0.91124 (17)	0.0351 (4)
H111	0.3190	0.5190	0.9358	0.053*
H112	0.4186	0.5583	0.9987	0.053*
H113	0.4055	0.4337	0.8939	0.053*

Atomic displacement parameters (\AA^2)

	U^{11}	U^{22}	U^{33}	U^{12}	U^{13}	U^{23}
O1	0.0331 (6)	0.0239 (5)	0.0487 (6)	-0.0044 (4)	-0.0025 (5)	-0.0072 (5)
O2	0.0298 (5)	0.0242 (5)	0.0348 (5)	0.0047 (4)	-0.0017 (4)	0.0004 (4)
O3	0.0326 (5)	0.0217 (5)	0.0336 (5)	0.0019 (4)	-0.0074 (4)	-0.0042 (4)
N1	0.0446 (8)	0.0565 (10)	0.0665 (10)	-0.0058 (7)	-0.0207 (8)	-0.0054 (8)
N2	0.0320 (7)	0.0341 (7)	0.0469 (8)	-0.0010 (5)	-0.0060 (6)	-0.0007 (6)
N3	0.0279 (6)	0.0200 (6)	0.0398 (7)	0.0018 (5)	-0.0042 (5)	-0.0041 (5)
N4	0.0304 (6)	0.0239 (6)	0.0503 (8)	0.0057 (5)	-0.0125 (6)	-0.0096 (5)
C1	0.0297 (8)	0.0281 (8)	0.0390 (8)	-0.0023 (6)	-0.0063 (6)	-0.0020 (6)
C2	0.0257 (7)	0.0241 (7)	0.0332 (7)	-0.0038 (5)	0.0042 (6)	-0.0018 (6)
C3	0.0324 (8)	0.0204 (7)	0.0373 (8)	0.0039 (6)	-0.0050 (6)	-0.0041 (6)
C4	0.0342 (8)	0.0202 (7)	0.0406 (8)	0.0031 (6)	-0.0035 (6)	-0.0040 (6)
C5	0.0341 (8)	0.0224 (7)	0.0396 (8)	-0.0002 (6)	-0.0089 (6)	-0.0014 (6)
C6	0.0325 (8)	0.0264 (7)	0.0455 (9)	0.0053 (6)	-0.0054 (7)	-0.0121 (6)
C7	0.0241 (7)	0.0237 (7)	0.0300 (7)	-0.0013 (5)	0.0030 (5)	-0.0008 (6)
C8	0.0314 (7)	0.0259 (7)	0.0249 (7)	-0.0041 (6)	-0.0037 (6)	-0.0013 (5)
C9	0.0523 (10)	0.0268 (8)	0.0367 (8)	-0.0006 (7)	-0.0048 (7)	-0.0049 (6)
C10	0.0346 (8)	0.0390 (8)	0.0325 (8)	-0.0078 (7)	-0.0006 (6)	0.0005 (6)
C11	0.0398 (8)	0.0354 (8)	0.0302 (8)	-0.0032 (7)	0.0025 (6)	0.0019 (6)

Geometric parameters (\AA , $^\circ$)

O1—C2	1.2303 (17)	C4—H41	0.9900
O2—C7	1.2099 (16)	C4—H42	0.9900
O3—C7	1.3422 (17)	C5—H51	0.9900
O3—C8	1.4722 (16)	C5—H52	0.9900
N1—N2	1.1189 (18)	C6—H61	0.9900
N2—C1	1.3099 (19)	C6—H62	0.9900
N3—C2	1.3515 (18)	C8—C10	1.506 (2)
N3—C4	1.4600 (18)	C8—C11	1.511 (2)
N3—C3	1.4635 (18)	C8—C9	1.513 (2)
N4—C7	1.3483 (18)	C9—H91	0.9800
N4—C5	1.4490 (18)	C9—H92	0.9800
N4—C6	1.4494 (19)	C9—H93	0.9800
C1—C2	1.450 (2)	C10—H101	0.9800
C1—H1	0.946 (17)	C10—H102	0.9800
C3—C5	1.503 (2)	C10—H103	0.9800
C3—H31	0.9900	C11—H111	0.9800
C3—H32	0.9900	C11—H112	0.9800
C4—C6	1.506 (2)	C11—H113	0.9800

supplementary materials

C7—O3—C8	120.57 (10)	N4—C6—H61	109.6
N1—N2—C1	179.04 (18)	C4—C6—H61	109.6
C2—N3—C4	119.35 (12)	N4—C6—H62	109.6
C2—N3—C3	124.53 (11)	C4—C6—H62	109.6
C4—N3—C3	113.83 (11)	H61—C6—H62	108.1
C7—N4—C5	125.93 (12)	O2—C7—O3	125.31 (12)
C7—N4—C6	120.26 (11)	O2—C7—N4	124.15 (13)
C5—N4—C6	113.59 (12)	O3—C7—N4	110.52 (11)
N2—C1—C2	114.68 (13)	O3—C8—C10	110.59 (12)
N2—C1—H1	115.7 (9)	O3—C8—C11	109.89 (11)
C2—C1—H1	129.6 (9)	C10—C8—C11	112.67 (12)
O1—C2—N3	122.08 (12)	O3—C8—C9	101.68 (11)
O1—C2—C1	120.21 (13)	C10—C8—C9	111.04 (12)
N3—C2—C1	117.64 (12)	C11—C8—C9	110.43 (13)
N3—C3—C5	110.49 (12)	C8—C9—H91	109.5
N3—C3—H31	109.6	C8—C9—H92	109.5
C5—C3—H31	109.6	H91—C9—H92	109.5
N3—C3—H32	109.6	C8—C9—H93	109.5
C5—C3—H32	109.6	H91—C9—H93	109.5
H31—C3—H32	108.1	H92—C9—H93	109.5
N3—C4—C6	110.29 (12)	C8—C10—H101	109.5
N3—C4—H41	109.6	C8—C10—H102	109.5
C6—C4—H41	109.6	H101—C10—H102	109.5
N3—C4—H42	109.6	C8—C10—H103	109.5
C6—C4—H42	109.6	H101—C10—H103	109.5
H41—C4—H42	108.1	H102—C10—H103	109.5
N4—C5—C3	109.92 (12)	C8—C11—H111	109.5
N4—C5—H51	109.7	C8—C11—H112	109.5
C3—C5—H51	109.7	H111—C11—H112	109.5
N4—C5—H52	109.7	C8—C11—H113	109.5
C3—C5—H52	109.7	H111—C11—H113	109.5
H51—C5—H52	108.2	H112—C11—H113	109.5
N4—C6—C4	110.27 (12)		
C4—N3—C2—O1	-4.1 (2)	C7—N4—C6—C4	128.14 (15)
C3—N3—C2—O1	-165.84 (14)	C5—N4—C6—C4	-57.04 (17)
C4—N3—C2—C1	178.83 (13)	N3—C4—C6—N4	53.39 (17)
C3—N3—C2—C1	17.1 (2)	C8—O3—C7—O2	2.4 (2)
N2—C1—C2—O1	-3.6 (2)	C8—O3—C7—N4	-178.51 (11)
N2—C1—C2—N3	173.55 (13)	C5—N4—C7—O2	-177.86 (14)
C2—N3—C3—C5	-143.07 (14)	C6—N4—C7—O2	-3.7 (2)
C4—N3—C3—C5	54.32 (16)	C5—N4—C7—O3	3.0 (2)
C2—N3—C4—C6	142.52 (13)	C6—N4—C7—O3	177.17 (13)
C3—N3—C4—C6	-53.89 (17)	C7—O3—C8—C10	62.39 (16)
C7—N4—C5—C3	-128.35 (15)	C7—O3—C8—C11	-62.62 (16)
C6—N4—C5—C3	57.18 (17)	C7—O3—C8—C9	-179.61 (12)
N3—C3—C5—N4	-53.86 (17)		

supplementary materials

Hydrogen-bond geometry (\AA , $^\circ$)

$D-H\cdots A$	$D-H$	$H\cdots A$	$D\cdots A$	$D-H\cdots A$
$C1-H1\cdots O1^i$	0.946 (17)	2.313 (18)	3.250 (3)	170.6 (14)
$C3-H32\cdots O1^i$	0.99	2.36	3.327 (3)	164

Symmetry codes: (i) $-x, y+1/2, -z+1/2$.

Fig. 1

